GLOBAL METHANE ASSESSMENT

Benefits and Costs of Mitigating Methane Emissions

ACKNOWLEDGEMENTS

CONTENTS

FOREWORD

Inger Andersen,
Under-Secretary-General of the United Nations and Executive Director of the UN Environment Programme

Today humanity is facing three systemic and escalating planetary crises: the climate crisis, the biodiversity and nature crisis, and the pollution and waste crisis. These crises are not independent but linked and often stem from the same sources and unsustainable models of consumption and production. These links provide an opportunity to identify and deploy solutions which deliver multiple-benefits and the ambitious emissions reductions needed to overcome these crises.

This *Global Methane Assessment* highlights one of the greatest opportunities available today to simultaneously address our interlinked planetary crises and make peace with nature. Methane is a powerful and short-lived climate pollutant which drives climate change and harms human and ecosystem health by contributing to the formation of ground-level ozone. Over the past decade, global methane emissions have risen at a rate faster than at any time in the last 30 years. While methane has both human and natural sources, recent increases are attributed to activity in three anthropogenic sectors, namely fossils fuels, waste and agriculture.

Current methane concentrations are well above those needed to achieve our 2° C target. According to the 2018 Intergovernmental Panel on Climate Change *Global Warming of 1.5° C* report, we cannot achieve the Paris Agreement targets without immediately reducing methane along with carbon dioxide and all other climate forcing emissions.

Fortunately, there are readily available targeted control measures that can reduce more than 30 per cent of projected anthropogenic methane emissions this decade. Most of these technical solutions are in the fossil fuels (oil, gas and coal) and waste sectors, and

can be deployed at low or negative cost. These measures must be implemented urgently and paired with increased efforts to find breakthroughs in agriculture and nature-based solutions. Additional measures that don't specifically target methane, like shifting to renewable energy, residential and commercial energy efficiency, and a reduction in food loss and waste, can reduce methane emissions by a further 15 per cent by 2030.

Readily achievable methane mitigation can deliver nearly 0.3° C of avoided warming over the next two decades while simultaneously reducing ground-level ozone concentrations. Such steps can avoid 255 000 premature deaths and help prevent more than half a million emergency room visits from asthma every year. And because ground level ozone also harms ecosystems and plants, the reduced methane concentrations could increase global crop yields by 26 million tonnes per year.

Fast and ambitious methane mitigation is one of the best strategies available today to deliver immediate and long-lasting multiple benefits for climate, agriculture, human and ecosystem health.

Since its founding in 2012, the Climate and Clean Air Coalition has led on global methane mitigation. As one of its founding partners, the UN Environment Programme (UNEP) has helped lead the Coalition's pioneering oil and gas work through the Oil and Gas Methane Partnership and the Global Methane Alliance. UNEP now hosts the International Methane Emissions Observatory an initiative that will integrate and reconcile methane emissions data, improve reporting and verification of information, and validate monitoring and measurement methodologies and techniques.

This year UNEP launched the UN Decade on Ecosystem Restoration. The next ten years will be paramount in the fight to avert climate change, the loss of nature and biodiversity, and the pollution and waste crisis. Nations, businesses, international organizations and individuals must commit to delivering methane mitigation consistent with the conclusions of this report to make progress towards restoring our degraded ecosystems and secure the future for humanity.

EXECUTIVE SUMMARY

Reducing human-caused methane emissions is one of the most cost-effective strategies to rapidly reduce the rate of warming and contribute significantly to global efforts to limit temperature rise to 1.5°C. Available targeted methane measures, together with additional measures that contribute to priority development goals, can simultaneously reduce human-caused methane emissions by as much as 45 per cent, or 180 million tonnes a year (Mt/yr) by 2030. This will avoid nearly 0.3°C of global warming by the 2040s and complement all long-term climate change mitigation efforts. It would also, each year, prevent 255 000 premature deaths, 775 000 asthma-related hospital visits, 73 billion hours of lost labour from extreme heat, and 26 million tonnes of crop losses globally (Figure ES1).

	Avoided warming (C) 2040-2070	Avoided deaths ozone (per year)	Avoided asthma-related ER visits (per year)	Avoided crop losses (Mt/yr)	Lost work hours avoided (billion hrs/yr)
AGRICULTURE	0.04	40 000	120 000	4	11
WASTE	0.05	45 000	135 000	5	13
FOSSIL FUELS	0.09	80 000	250 000	8	24
ADDITIONAL	0.10	90 000	270 000	9	25
TOTAL	0.28	255 000	775 000	26	73

Remaining global anthropogenic methane emissions

Range of methane mitigation consistent with the IPCC 1.5°C pathways

Figure ES1: Current and projected anthropogenic methane emissions and the identified sectoral mitigation potential in 2030 along with several benefits associated with sectoral-level methane emissions mitigation. Avoided warming occurs in the 2040s, other impacts are annual values beginning in 2030 that would continue thereafter.

The findings in this assessment are the result of modelling that uses five state-of-the art global composition-climate models to evaluate changes in the Earth's climate system and surface ozone concentrations from reductions in methane emissions. Results allow for rapid evaluation of impacts from methane emissions and the benefits from mitigation strategies to the climate and ground-level ozone formation and, air quality, public health, agricultural and other development benefits. The assessment results are also available in a web-based decision support tool[1] that allows users to input different methane emissions reduction goals to calculate the multiple benefits at a national level.

THE OPPORTUNITY

- **More than half of global methane emissions stem from human activities in three sectors: fossil fuels (35 per cent of human-caused emissions), waste (20 per cent) and agriculture (40 per cent).** In the fossil fuel sector, oil and gas extraction, processing and distribution account for 23 per cent, and coal mining accounts for 12 per cent of emissions. In the waste sector, landfills and wastewater make up about 20 per cent of global anthropogenic emissions. In the agricultural sector, livestock emissions from manure and enteric fermentation represent roughly 32 per cent, and rice cultivation 8 per cent of global anthropogenic emissions. (Sections 1, 2.1 and 4.1)

- **Currently available measures could reduce emissions from these major sectors by approximately 180 Mt/yr, or as much as 45 per cent, by 2030. This is a cost-effective step required to achieve the United Nations Framework Convention on Climate Change (UNFCCC) 1.5° C target**. According to scenarios analysed by the Intergovernmental Panel on Climate Change (IPCC), global methane emissions must be reduced by between 40–45 per cent by 2030 to achieve least cost-pathways that limit global warming to 1.5° C this century, alongside substantial simultaneous reductions of all climate forcers including carbon dioxide and short-lived climate pollutants. (Section 4.1)

- **There are readily available targeted measures that can reduce 2030 methane emissions by 30 per cent, around 120 Mt/yr**. Nearly half of these technologies are available to the fossil fuel sector in which it is relatively easy

1. http://shindellgroup.rc.duke.edu/apps/methane/

to reduce methane at the point of emission and along production/transmission lines. There are also available targeted solutions in the waste and agricultural sectors. Current targeted solutions alone, however, are not enough to achieve 1.5° C consistent mitigation by 2030. To achieve that, additional measures must be deployed, which could reduce 2030 methane emissions by another 15 per cent, about 60 Mt/yr. (Sections 4.1 and 4.2)

- **Roughly 60 per cent, around 75 Mt/yr, of available targeted measures have low mitigation costs[2], and just over 50 per cent of those have negative costs – the measures pay for themselves quickly by saving money** (Figure SDM2). Low-cost abatement potentials range from 60–80 per cent of the total for oil and gas, from 55–98 per cent for coal, and approximately 30–60 per cent in the waste sector. The greatest potential for negative cost abatement is in the oil and gas subsector where captured methane adds to revenue instead of being released to the atmosphere. (Section 4.2)

- **The mitigation potential in different sectors varies between countries and regions.** The largest potential in Europe and India is in the waste sector; in China from coal production followed by livestock; in Africa from livestock followed by oil and gas; in the Asia-Pacific region, excluding China and India, it is coal and waste; in the Middle East, North America and Russia/Former Soviet Union it is from oil and gas; and in Latin America it is from the livestock subsector. A majority of these major abatement potentials can be achieved at low cost, less than US$ 600 per tonne of methane, especially in the waste sector and the coal subsector in most regions and for the oil and gas subsector in North America. (Section 4)

- **Mitigation potential from all measures is expected to increase between 2030 and 2050, especially in the fossil fuel and waste sectors.** (Section 4.2)

- **The levels of methane mitigation needed to keep warming to 1.5° C will not be achieved by broader decarbonization strategies alone.** The structural changes that support a transformation to a zero-carbon society found in broader strategies will only achieve about 30 per cent of the methane reductions needed over the next 30 years. Focused strategies specifically targeting methane need to be implemented to achieve sufficient methane mitigation. At the same time, without relying on future massive-scale deployment of unproven carbon removal technologies, expansion of natural gas infrastructure and usage is incompatible with keeping warming to 1.5° C. (Sections 4.1, 4.2 and 4.3)

2. Less than US$ 600 per tonne of methane reduced, which would correspond to ~US$ 21 per tonne of carbon dioxide equivalent if converted using the IPCC Fifth Assessment Report's GWP100 value of 28 that excludes carbon-cycle feedbacks.

WHY ACT

- **Methane, a short-lived climate pollutant (SLCP) with an atmospheric lifetime of roughly a decade, is a potent greenhouse gas tens of times more powerful than carbon dioxide at warming the atmosphere.** Methane's atmospheric concentration has more than doubled since pre-industrial times and is second only to carbon dioxide in driving climate change during the industrial era. (Section 1.1)

- **Methane contributes to the formation of ground-level ozone, a dangerous air pollutant.** Ozone attributable to anthropogenic methane emissions causes approximately half a million premature deaths per year globally and harms ecosystems and crops by suppressing growth and diminishing production. (Section 1.1 and 3.3)

- **The atmospheric concentration of methane is increasing faster now than at any time since the 1980s.** In the absence of additional policies, methane emissions are projected to continue rising through at least 2040. Current concentrations are well above levels in the 2° C scenarios used in the IPCC's 2013 Assessment. The Paris Agreement's 1.5° C target cannot be achieved at a reasonable cost without reducing methane emissions by 40–45 per cent by 2030. (Sections 1.1 and 4.1)

- **The growing human-caused emissions come from all three sectors: fossil fuels, agriculture and waste.** (Section 1 and 4.1)

- **Methane's short atmospheric lifetime means taking action now can quickly reduce atmospheric concentrations and result in similarly rapid reductions in climate forcing and ozone pollution.** Lower methane concentrations would rapidly reduce the rate of warming, making methane mitigation one of the best ways of limiting warming in this and subsequent decades. Doing so would also help limit dangerous climate feedback loops, while simultaneously delivering important health and economic benefits from reducing ground-level ozone. (Sections 1.1 and 5)

- **This assessment found that every million tonnes (Mt) of methane reduced:**

  - **prevents approximately 1 430 annual premature deaths due to ozone globally.** Of those, 740 would have died from respiratory disease and 690 from cardiovascular disease. Every million tonnes of reduced methane emissions could also avoid approximately 4 000 asthma-related accident and emergency department visits and 90 hospitalizations per year. (Section 3.4)

  - **avoids losses of 145 000 tonnes of wheat, soybeans, maize and rice ozone exposure every year.** This is roughly equivalent to increased global yields of 55 000 tonnes of wheat, 17 000 tonnes of soybeans, 42 000 tonnes of maize, and 31 000 tonnes of rice annually for every million tonnes of methane reduced. (Section 3.5)

  - **avoids the annual loss of roughly 400 million hours of work, approximately 180 000 years, globally due to extreme heat[3].** Employment within those sectors of the economy that are affected by heat exposure varies between genders, leading to disparities in the impacts for men and women that differ across countries. (Section 3.4)

3. Labour impacts of heat exposure are the most dependent on the size of the methane emission changes, as well as background temperatures, and thus the linear scaling used here to obtain impacts per million tonnes is only approximate.

- **The global monetized benefits for all market and non-market impacts are approximately US\$ 4 300 per tonne of methane reduced[4].** When accounting for these benefits nearly 85 per cent of the targeted measures have benefits that outweigh the net costs. The benefits of the annually avoided premature deaths alone from a 1.5°C-consistent-methane mitigation strategy is approximately US\$ 450 billion per year. (Sections 3.5 and 3.6)

- **In addition to the benefits quantified here, methane reduction measures also contribute to multiple Sustainable Development Goals (SDGs),** including climate action (SDG13), zero hunger (SDG2), good health and well-being (SDG3). Additionally, they provide cost reductions and efficiency gains in the private sector, create jobs, and stimulate technological innovation. (Sections 1.1, 4.4 and 5)

	Avoided warming (C) 2040-2070	Avoided deaths ozone (per year)	Avoided asthma-related ER visits (per year)	Avoided crop losses (Mt/yr)	Lost work hours avoided (billion hrs/yr)
NEGATIVE COST	0.06	55 000	170 000	6	16
LOW COST	0.05	45 000	145 000	4	14
ALL COST	0.07	65 000	190 000	7	18
ADDITIONAL	0.10	90 000	270 000	9	25
TOTAL	0.28	255 000	775 000	26	73

Remaining global anthropogenic methane emissions

Range of methane mitigation consistent with the IPCC 1.5°C pathways

Figure ES2: Current and projected anthropogenic methane emissions and the identified mitigation potential in 2030 of targeted controls and their costs (low cost is greater than zero and less than 2018 US\$ 600 per tonne of methane) as well as a set of additional measures, such as energy efficiency and fuel switching, plus behavioural changes, such as reduced food waste, dietary modification and energy demand management, that are consistent with the 1.5° C long-term maximum warming target. The cost of implementation of all-cost measures is more than 2018 US\$ 600 per tonne of methane. Avoided warming is in 2040, other impacts are annual values beginning in 2030 that would continue thereafter.

4. Monetary values are in 2018 US\$. Fossil methane emissions are valued at ~\$4 400 per tonne of methane.

HOW TO DO IT

Trends in methane emissions need to be reversed to achieve a multitude of benefits by 2030. Targeted measures can be rapidly deployed to reduce methane emissions from the fossil fuel and waste sectors, with a majority at negative or low cost. To achieve targets consistent with keeping warming to 1.5° C, a combination of targeted measures and additional measures which reduce methane but do not primarily target it, are needed for all sectors, especially the agricultural one. There are many potential strategies that would facilitate the implementation of these measures including, for example, a price on emissions or an emissions reduction target. There are also barriers. These include addressing the lack of financing, enhancing awareness and improving education, changing production methods, developing new policies and regulations, and changes in consumption and consumer behaviour. Increased political will and private sector engagement and action are needed.

The specific measures include the following.

- **Oil, gas and coal:** the fossil fuel sector has the greatest potential for targeted mitigation by 2030. Readily available targeted measures could reduce emissions from the oil and gas sector by 29–57 Mt/yr and from the coal sector by 12–25 Mt/yr. Up to 80 per cent of oil and gas measures and up to 98 per cent of coal measures could be implemented at negative or low cost. (Section 4.2)

- **Waste:** existing targeted measures could reduce methane emissions from the waste sector by 29–36 Mt/yr by 2030. The greatest potential is in improved treatment and disposal of solid waste. As much as 60 per cent of waste-sector targeted measures have either negative or low cost. (Section 4.2)

- **Agriculture:** existing targeted measures could reduce methane emissions from the agricultural sector by around 30 Mt/yr by 2030. Methane emissions from rice cultivation could be reduced by 6–9 Mt/yr. The targeted mitigation potentials from livestock are less consistent, ranging from 4–42 Mt/yr. Average cost estimates vary across the available analyses. Behavioural change measures and innovative policies are particularly important to prevent emissions from agriculture, given the limited potential to address the sector's methane emissions through technological measures. Three behavioural changes, reducing food waste and loss, improving livestock management, and the adoption of healthy diets (vegetarian or with a lower meat and dairy content) could reduce methane emissions by 65–80 Mt/yr over the next few decades. (Sections 4.2 and 4.4)

- **Additional measures, which reduce methane emissions but do not primarily target methane, could substantially contribute to methane mitigation over the next few decades.** Examples include decarbonization measures – such as a transition to renewable energy and economy-wide energy efficiency improvements. Various implementation levers exist. Emissions pricing, for example, can be an effective policy which could incentivize substantial methane mitigation and support the broad application of methane reduction measures. A rising global tax on methane emissions starting at around US$ 800 per tonne could, for instance, reduce methane emissions by as much as 75 per cent by 2050. (Section 4.3)

- **Incomplete knowledge and monitoring of emissions in some sectors limits the potential for technical mitigation innovation and strategic decision making to efficiently reduce methane emissions.** While there is enough information to act now, addressing emissions at the scale and in the timeframe necessary to meet the 1.5° C target will require an improved understanding of methane emissions levels and sources. Continued and improved cooperation to create transparent and independently verifiable emissions data and mitigation analyses is needed. Such cooperative efforts would enable governments and other stakeholders to develop and assess methane emissions management policies and regulations, verify mitigation reporting and track emissions reductions. (Section 5)

- **Greater regional and global coordination and governance of methane mitigation would support the achievement of the 2030 abatement levels identified here.** While methane reductions are increasingly being addressed through local and national laws and under voluntary programmes, there are few international political agreements with specific targets for methane. The Climate and Clean Air Coalition (CCAC) leads global efforts to drive high-level ambition, and strengthens national actions, polices, planning, and regulations around methane mitigation. (Section 5)

AN INTEGRATED APPROACH

Urgent steps must be taken to reduce methane emissions this decade. Given the wide range of impacts from methane, the societal, economic, and environmental benefits of acting are numerous and far outweigh the costs. The existence of readily available, low-cost, targeted measures, and methane's short-lived atmospheric lifetime means significant climate and clean air benefits can be achieved by 2030. Targets and performance indicators to reduce methane must address the combined and multiple impacts methane has on climate, air quality, public health, agricultural production and ecosystem health. Assessment methodologies should be commonly agreed upon and transparent. An integrated approach to climate and air quality mitigation is required to put the benefits of methane reductions into context. To keep warming to 1.5° C, focused strategies specifically targeting methane emissions need to be implemented alongside substantial and simultaneous mitigation of all other climate pollutants including carbon dioxide and short-lived climate pollutants.

TARGETED MEASURES	
FOSSIL FUEL SECTOR (OIL, GAS, AND COAL)	**Upstream and downstream leak detection and repair**
	Recovery and utilization of vented gas: capture of associated gas from oil wells; blowdown capture; recovery and utilization of vented gas with vapor recovery units and well plungers; Installation of flares.
	Improved control of unintended fugitive emissions from the production of oil and natural gas: regular inspections (and repair) of sites using instruments to detect leaks and emissions due to improper operations; replace pressurized gas pumps and controllers with electric or air systems; replace gas-powered pneumatic devices and gasoline or diesel engines with electric motors; early replacement of devices with lower-release versions; replace compressor seals or rods; cap unused wells.
	Coal mine methane management: pre-mining degasification and recovery and oxidation of ventilation air methane; flooding abandoned coal mines.
WASTE SECTOR	**Solid waste management**: (residential) source separation with recycling/reuse; no landfill of organic waste; treatment with energy recovery or collection and flaring of landfill gas; (industrial) recycling or treatment with energy recovery; no landfill of organic waste.
	Wastewater treatment: (residential) upgrade to secondary/tertiary anaerobic treatment with biogas recovery and utilization; wastewater treatment plants instead of latrines and disposal; (industrial) upgrade to two-stage treatment, i.e., anaerobic treatment with biogas recovery followed by aerobic treatment.
AGRICULTURAL SECTOR	**Improve animal health and husbandry**: reduce enteric fermentation in cattle, sheep and other ruminants through: feed changes and supplements; selective breeding to improve productivity and animal health/fertility
	Livestock manure management: treatment in biogas digesters; decreased manure storage time; improve manure storage covering; improve housing systems and bedding; manure acidification.
	Rice paddies: improved water management or alternate flooding/drainage wetland rice; direct wet seeding; phosphogypsum and sulphate addition to inhibit methanogenesis; composting rice straw; use of alternative hybrids species.
	Agricultural crop residues: prevent burning of agricultural crop residues.
ADDITIONAL BENEFICIAL MEASURES	
FOSSIL FUEL SECTOR (OIL, GAS, AND COAL)	**Renewables for power generation:** use incentives to foster expanded use of wind, solar, and hydro power for electricity generation.
	Improved energy efficiency and energy demand management: (residential) use incentives to improve the energy efficiency of household appliances, buildings, lighting, heating and cooling, encourage rooftop solar installations; (industrial) introduce ambitious energy efficiency standards for industry; improve consumer awareness of cleaner energy options.
WASTE SECTOR	Reduced consumer waste and improved waste separation and recycling, improved sustainable consumption.
AGRICULTURAL SECTOR	**Reduced food waste and loss:** strengthen and expand food cold chains; consumer education campaigns; facilitate donation of unsold or excess food.
	Adoption of healthier diets: decrease intake where consumption of ruminant products is above recommended guidelines.

Table SDM1 Measures To Reduce Methane By 45 Per Cent By 2030

Note: The classification of measures as 'targeted' or 'additional' broadly reflects whether the measure's focus is on methane reductions or whether reductions occur largely as a co-benefit of measures with another primary purpose, but final categorization is governed by the underlying literature on mitigation.

1. INTRODUCTION

CHAPTER FINDINGS

- Methane amounts have risen rapidly over the past decade, reaching five-year average growth rates not seen since the 1980s.

- The increase in atmospheric methane during the 2010s has resulted in its amounts being well above those in the 2° C scenario used in the Intergovernmental Panel on Climate Change's (IPCC) 2013 Assessment.

- There is strong evidence that the increases in methane amounts during the 2010s were primarily attributable to increased emissions from fossil fuel-related, agricultural and waste sources, with fossil fuel-related activities contributing as much as agricultural and waste sources combined.

- Mitigation of methane is very likely the strategy with the greatest potential to decrease warming over the next 20 years.

1.1 IMPORTANCE OF METHANE

Methane (CH_4) is a powerful greenhouse gas, the atmospheric amount of which has more than doubled since pre-industrial times (Nisbet *et al*. 2019). It has been second only to carbon dioxide (CO_2) in driving climate change during the industrial era (Myhre *et al.* 2013). Methane is a short-lived climate pollutant (SLCP) with an atmospheric lifetime of roughly a decade (the perturbation lifetime, relevant for dealing with emission reductions, is 12 years). Methane contributes to the formation of tropospheric ozone (O_3), which, like methane, is a short-lived but powerful greenhouse gas and surface ozone is also an air pollutant with detrimental effects on people, ecosystems and crops.

Emissions of methane to the atmosphere are therefore harmful to society in multiple ways. While methane is not directly dangerous to human health, it does indirectly affect it and agricultural productivity through ozone and climate change. Recent studies have found evidence of these consequences to health and agricultural damage (Shindell *et al.* 2019) to be larger than previously believed. These new studies include the finding that tropospheric ozone may have much higher impacts on public health, particularly respiratory and cardiovascular deaths (Turner *et al.* 2016). In addition, understanding of methane's effect on radiative forcing has recently improved, leading to an upward revision since the Fifth Intergovernmental Panel on Climate Change

(IPCC) Assessment (Collins *et al.* 2018; Etminan *et al*. 2016). Taken together, improved understanding suggests that the overall societal impact of methane emissions is likely larger than indicated by prior estimates.

In large part, because of its impacts on public health and agriculture, the broad social cost of methane, that is the monetized societal damage, including climate and air quality related impacts, resulting from a tonne of emissions is 50–100 times greater, depending uon the preferred discount rate (Shindell et al. 2017), than the corresponding social cost of carbon dioxide, before taking into account the recent updates in knowledge.

The amounts of methane in the atmosphere have changed dramatically over the past four decades (Figure 1.1a). Amounts increased sharply in the 1980s but slowed to a near constant level between 2000 and 2005 when emissions and sinks were roughly balanced (Figure 1.2). However, atmospheric methane amounts have increased rapidly again over the past decade (Figure 1.1a). These observations demonstrate that it is crucial to change the trajectory of this greenhouse gas, which in 2020 exhibited the highest growth rate in NOAA's 37-year record (Figure 1.1b). They also shows that atmospheric methane responds quickly to reductions in emissions, as shown by the negative growth rates in the early 2000s (Figure 1.1b).
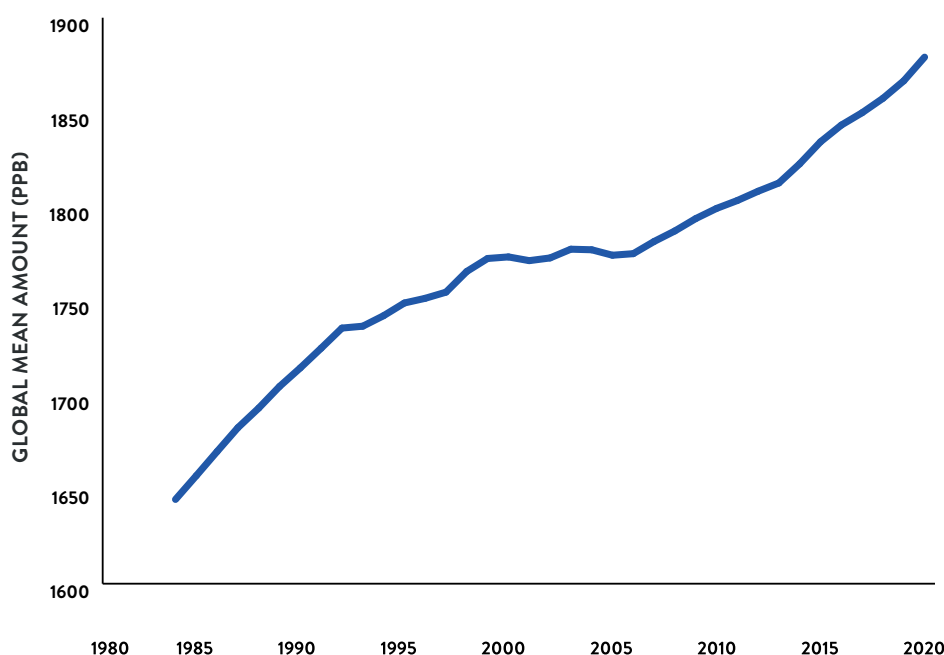
Figure 1.1a Global mean methane amount, 1984–2019, parts per billion

Source: Ed Dlugokencky, NOAA/ ESRL (www.esrl. noaa.gov/gmd/ccgg/ trends_ch4/)
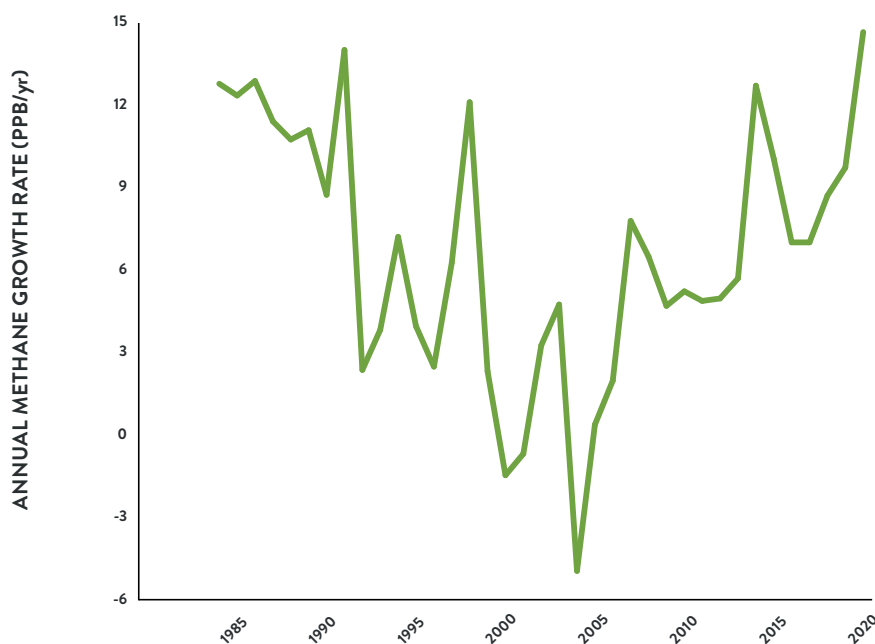
Figure 1.1b Global mean methane annual growth rate, 1984–2019, parts per billion per year

Source: Ed Dlugokencky, NOAA/ ESRL (www.esrl. noaa.gov/gmd/ ccgg/trends_ch4/ (accessed 6 February 2021)
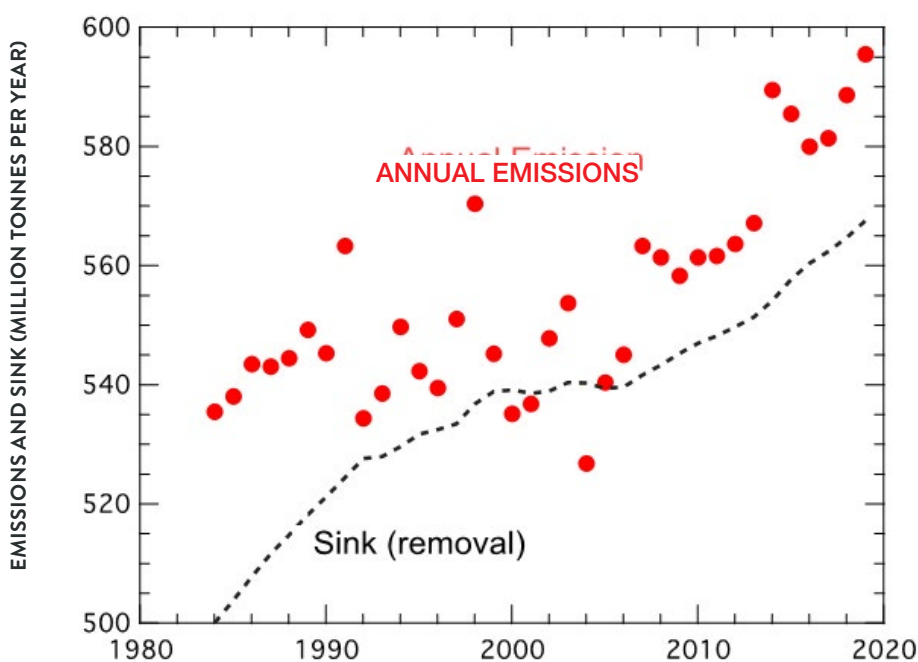
Figure 1.2 Estimated global methane emissions and sinks (removals), 1984–2019, million tonnes per year

Note: Estimated using an inversion from observed amounts based on a constant (time invariant) overall global lifetime of 9.1 years and mass balance (Section 2.1.3).

Source: Ed Dlugokencky, NOAA/ ESRL

The possible reasons for these trends have been discussed in a host of newly published papers (Jackson *et al.* 2020; Saunois *et al.* 2020). There is strong evidence that the increases in the abundance of atmospheric methane are due to growth in emissions rather than a slower atmospheric removal rate (Figure 1.2). It appears that increases are due to fossil fuel-related activities and the combined contribution from agricultural and waste sources in roughly equal parts (Jackson *et al.* 2020).

Methane is emitted from both natural and anthropogenic sources, as described more fully in Chapter 2. Humanity has the greatest leverage on anthropogenic sources, though human-induced climate change and land-use changes affect natural sources. Globally, anthropogenic methane emissions are expected to continue to increase. Under current policy scenarios, by 2030 anthropogenic methane emissions are expected to increase by more than 15 per cent over 2010 levels, reaching nearly 380 million tonnes per

year (Mt/yr), an 8 per cent increase on 2020 levels (Höglund-Isaksson *et al.* 2020). Significant emissions growth during the 2020s is expected from all three sectors – fossil fuels, agriculture and waste. The largest increases of about 13 Mt/yr are projected in the waste and wastewater sectors, driven in particular by expected strong growth in the population and income in regions that currently have poorly developed waste management systems. Emissions from the fossil-fuel sector are projected to grow by about 10 Mt/yr, with gas production and distribution being the largest source, followed by oil production whereas emissions related to coal mining are projected to decrease very slightly. The number of uncapped abandoned oil and gas wells and coal mines is increasing and could also continue to contribute to the growth in emissions. In the agriculture sector, continued growth in the number of ruminant animals, due to rising demand for meat from an increasing and increasingly affluent global population, will drive increases in emissions from enteric fermentation and manure management of around 6 Mt/yr. Emissions from rice cultivation are, however, likely to remain approximately constant.

For the 2015 United Nations (UN) Paris Agreement to succeed, reducing anthropogenic methane in addition to carbon dioxide is paramount. Currently the largest contributor to the departure from an idealized path to the 2° C target used in the IPCC's Fifth Assessment Report is the growth in methane amounts (Figure 1.3). Achieving the more stringent 1.5° C target requires even larger decreases in methane. The IPCC's 2018 Special Report concluded that reaching a sustainable mitigation pathway to 1.5° C can only be achieved with deep and simultaneous reductions of carbon dioxide and all non-carbon dioxide climate forcing emissions, including short-lived climate pollutants such as methane. In 1.5° C pathways, global anthropogenic methane emissions fall by an average of 45 per cent by 2040, with the full range showing decreases of 30–65 per cent relative to 2010 by this time. Such trajectories, which imply approximately a 2 per cent annual decrease in emissions over the next 20 years, are in sharp contrast to the current path which shows an increase in the order of 0.5 per cent per year and falls between methane abundance in idealized paths leading to approximately 3–5° C of warming in 2100 (Nisbet *et al*. 2020).
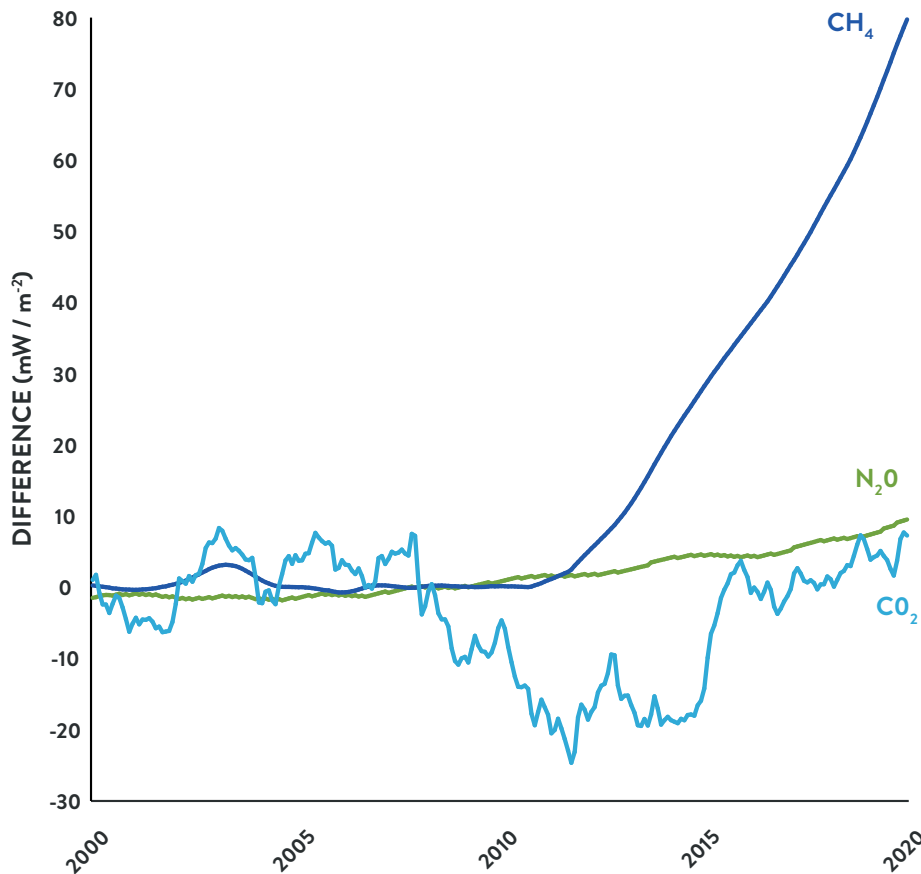
Figure 1.3 Values for the difference between actual global mean annual average radiative forcing from major greenhouse gases and values under Representative Concentration Pathway RCP2.6, 2000–2020, milliWatts per square metre

Note: Representative Concentration Pathway RCP2.6 (Collins et al., 2013) as used in IPCC's Fifth Assessment and consistent with the Paris Agreement.

Source: Nisbet et al. (2020), updated through 2020 courtesy M. Manning

The short lifetime of methane, and the quick response of methane abundance to reduced emissions described earlier, mean that any action taken to reduce emissions will have an immediate pay off for climate in addition to the current and near-future human health and agricultural production. Observations over the past few decades have shown that decreased emissions lead quickly to lower methane levels relative to those that could be expected in the absence of the decreases. That is, there are no mechanisms that offset the decreases even though there are significant natural sources. Simply put, natural emissions do not make up for the decrease in anthropogenic emission. Indeed, the expectation that a reduction in emissions will yield quick results, in the order of a decade, is confirmed and emphasizes the importance of methane.

Methane mitigation offer a way of rapidly reducing the rate of near-term warming. Also, mitigation of methane, along with non-fossil greenhouse gases including some hydroflurocarbons (HFCs) and black carbon-rich sources of particulate matter (PM), is the only plausible way of decreasing warming relative to a reference case with minimal changes in current policies over the next 20 years. This is because a realistically paced phase-out of fossil fuels, or even a rapid one under aggressive decarbonization, is likely to have minimal net impacts on near-term temperatures due to the removal of co-emitted aerosols (Shindell and Smith 2019). As methane is the most powerful driver of climate change among the short-lived substances (Myhre *et al*. 2013), mitigation of methane emissions is very likely to be the most powerful lever in reducing near-term warming. This is consistent with other assessments; for example, the Intergovernmental Panel on Climate Change Fifth Assessment Report (IPCC AR5) showed that methane controls implemented between 2010 and 2030 would lead to a larger reduction in 2040 warming than the difference between RCPs 2.6, 4.5 and 6.0 scenarios. (The noted IPCC AR5-era scenarios are called representative concentration pathways (RCPs, with the numerical value indicating the target radiative forcing in 2100 (Kirtman *et al*. 2013)).

Though decarbonization is essential to meeting long-term temperature goals, near-term impacts are also important. Climate changes over the next few decades will limit the ability of human and natural systems to adapt. This is especially problematic for the poorest and women, both groups are particularly vulnerable.

Additionally, impacts such as sea-level rise and glacier melting are influenced by cumulative heat uptake, and many impacts may be non-linear. Thus, there is a need for urgent action to reduce damage from ongoing climate change. A prior study (Shindell *et al*. 2017b) listed several reasons for urgency, including stating that early mitigation: *"(i) reduces damage due to climate change over the next few decades, including those dependent on the pace of climate change such as biodiversity losses; … (iii) reduces the risk of potential non-linear changes such as release of carbon from permafrost or ice sheet collapse; (iv) increases the probability of staying below 2° C through mid-century* (Shindell *et al*. 2012; Ramanathan and Xu 2010)*; (v) reduces long-term cumulative climate impacts; (vi) reduces costs of meeting temperature targets relative to late mitigation* (Hamsen *et al*. 2016)*; and (vii) stimulates progress toward the long-term 2° C target through achievement of near-term benefits* (Victor *et al*. 2016)"*. Reductions in methane emissions can thus provide near-term climate benefits while carbon dioxide emission reductions are implemented for long-term stabilization.

Reducing methane emissions provides an opportunity to rapidly change the environment, both through surface ozone pollution and climate change. Methane mitigation also has clear and immediate economic benefits including improved governance; cost reductions and efficiency in the private sector; job creation, particularly in relation to the leak detection and repair (LDAR) within industry; and technological innovation and entrepreneurship. Mitigating methane emissions directly contributes to the achievement of multiple Sustainable Development Goals (SDGs) (Haines *et al.* 2017), including:

- SDG2 Zero hunger by improving ecosystem health and agricultural yields, thereby helping to end hunger and achieve food security;

- SDG3 Good Health and well-being, SDG11 Sustainable cities and communities and SDG12 Responsible consumption and production by reducing indoor and outdoor air pollution, enabling sustainable food production and helping ensure healthy lives for people across the globe.

- SDG1 No poverty, SDG11 Sustainable cities and communities and SGD13 Climate action by helping reduce the exposure of vulnerable populations to climate-related extreme events.

All 17 SDGs are shown in the Figure 1.4 below:

Figure 1.4 The Sustainable Development Goals established by the United Nations in 2015

Source: United Nations

1.2 PURPOSE OF THIS ASSESSMENT

Despite the well-documented harms resulting from its emissions, efforts thus far to reduce methane have been inadequate given the rapid growth in observed atmospheric methane amounts. This is likely due in part to inadequate awareness of the multiple benefits of emission reductions. Additionally, a lack of adequate policies, institutional structures and governance play important roles. This assessment seeks to better characterize the impacts of methane reductions with state-of-the-art modelling, and to document the multiple benefits that could be realized through methane reductions with an examination of near-term targeted mitigation measures and additional measures which contribute to other development priority goals while also reducing methane emissions. The classification of measures as 'targeted' or 'additional' broadly reflects whether the measure's focus is on methane reductions or whether reductions occur largely as a co-benefit of measures with another primary purpose such as carbon dioxide reduction or health benefits. Such a classification is subjective, however, and the final categorization used in this assessment is governed by achieving consistency with the underlying literature on mitigation options. To better quantify the benefits of methane mitigation, and the uncertainties associated with such a quantification, this work looks at the response to emissions across a variety of impacts using a range of models. The impacts were chosen based on available evidence allowing specific endpoints to be reliably quantified along with an emphasis on links to the SDGs. Previous analyses have shown the multiple benefits of reducing methane emissions (Shindell *et al*. 2012; UNEP/WMO 2011). This assessment adds to those prior analyses by not only including more modelling to better characterize robustness and analyses of additional impacts, but also greatly extends the scope of the associated economic analysis.

In the troposphere, methane plays an important role in regulating both the oxidation capacity as a whole and the amount of ozone in particular. Methane's primary sink is oxidation through the hydroxyl radical. When nitrogen oxides (NO_x) and sunlight are present, this oxidation process leads to the production of ozone (O3). As ozone is also a greenhouse gas, the net impact of methane emissions on climate is larger than the direct impact of the increased methane – ozone adds about 38 per cent to the forcing associated with methane alone (Myhre *et al*. 2013). In addition to the warming caused by direct methane increases and indirect tropospheric ozone increases, there are smaller warming impacts from the oxidation of methane. These include:

1. an increase in carbon dioxide in the atmosphere;

2. an increase in water vapour in the stratosphere; and

3. changes in atmospheric hydroxide (OH) abundance that in turn affect concentrations of radiatively active gases such as HFCs and hydrochlorofluorocarbons.

These complexities mean that to obtain a detailed understanding of the influence of methane emissions requires the use of three-

dimensional composition-climate models capable of representing the most important of these processes, as is done in this assessment.

The physical system modelling examines the worldwide impact of methane emissions, which have virtually the same impact regardless of location (Fiore *et al*. 2008). This is because although methane is a short-lived climate pollutant, a class of pollutants with a lifetime of roughly fifteen years or less, it is a relatively longer-lived one and its atmospheric chemical lifetime of nearly a decade is long compared to atmospheric mixing timescales so that it is a well-mixed gas, in the sense that geographic variations in tropospheric concentrations are relatively small. Impacts of methane emissions include the responses of ozone, temperature and precipitation, as well as subsequent impacts of those changes on human health and crop yields. Full three-dimensional atmospheric composition-climate models are required to capture the response of ozone, which is quite inhomogeneous as it depends on the local availability of other ozone precursors and sunlight, as well as climate responses that are also inhomogeneous.

This new modelling of the composition-climate system is complemented by an analysis of the potential for methane mitigation. This includes both source specific analyses of the potential and cost of targeted methane emissions abatement as well as modelling with integrated assessment models (IAMs) that incorporate such potentials within their representation of the coupled energy-economy-land system. This assessment thus provides information on both the potential for the abatement of methane emissions and the impacts of such controls, both within this document and in an online web-based decision-support tool developed to support it. The potential is compared with reductions in methane emissions under scenarios consistent with avoiding dangerous anthropogenic interference in the climate system, the internationally agreed goal of climate policy. This information can help inform both large-scale efforts to set ambitious goals for the mitigation of methane emissions and detailed analyses of the most cost-effective ways of mitigating emissions at global and regional scales.

2. SOURCES OF METHANE

CHAPTER FINDINGS

- Anthropogenic emissions represent roughly 60 per cent of the total methane emissions.

- Anthropogenic methane emissions come primarily from three sectors: fossil fuels, ~35 per cent; agriculture, ~40 per cent; and waste, ~20 per cent.

- Emissions from livestock are the largest source of agricultural emissions with enteric fermentation the dominant process and cattle the dominant animal causing the emissions.

- The extraction, processing and distribution of the three main fossil fuels lead to comparable emissions: gas and oil each contribute ~34 per cent, followed by coal which contributes ~32 per cent of the fossil fuel methane emissions.

- Emissions vary greatly across regions, with the largest totals in China and South Asia, but there are significant contributions from all regions. Uncertainties in emissions are again largest for China but are also significant for the Americas.

- At subsectoral and regional levels, the largest emissions sources vary markedly. For fossil fuels, they are coal mining in China, ~24 Mt/yr; oil and gas extraction, processing and transport in West Asia, ~18 Mt/yr; in Russia, ~15 Mt/yr; and North America, ~14 Mt/yr. Livestock emissions are highest in Latin America, ~27 Mt/yr, followed by South Asia, ~22 Mt/yr. Emissions from rice cultivation are highest in Southeast Asia+the Republic of Korea+Japan, ~10 Mt/yr, closely followed by South Asia, ~8 Mt/yr, and China, ~8 Mt/yr. Emissions from the waste sector are much more evenly distributed around the world.

- Advances in technology, especially remote sensing, are opening up new opportunities to characterize emission sources more accurately, including high emitters, and highlight substantial biases in much reporting at the facility scale and even at a national scale.

- Changes in emissions from natural sources of methane are likely to create positive feedbacks as emissions increase in a warming climate.

Identifying and quantifying sources of methane is a complex but critical element in understanding atmospheric methane concentrations and their trends. Methane has both natural and anthropogenic sources that can be individually small and geographically dispersed. While most sources have been identified, their relative contributions to atmospheric methane levels remain uncertain. Estimates of global emissions come broadly from two methods:

1. bottom-up which traditionally use some type of activity data representative of the sector, multiplied by an appropriate emission factor;

AND

2. top-down which use atmospheric observations and models to indirectly infer emissions.

Both bottom-up and top-down estimates are discussed in this assessment.

The global methane budget is composed of many sources and a small number of sinks –atmospheric removal processes, primarily oxidation by hydroxyl along with a small contribution from uptake in soils (Table 2.1). This table is based on bottom-up estimates as these currently provide greater detail on specific sources than top-down ones. The sources and sinks are not currently in balance, and the greater emissions flux relative to the sinks drives the ongoing growth in atmospheric amounts.

The anthropogenic methane sources are the focus of this assessment, but natural sources are briefly described in Section 2.1.2 for completeness. Note that this assessment considers fires to be anthropogenic and wetland emissions to be natural although both sources are natural processes that are influenced by human activities. This assessment does not discuss the sinks in further detail as these are relatively well constrained by observations of the abundance of industrial trace gases whose only loss mechanism is oxidation by hydroxyl, the same loss process that dominates the methane sink (Prather *et al*., 2012), and any trends in methane sinks over recent decades are likely to have been very small (Saunois *et al*. 2020). It is noted, however, that there has been some work on the potential for the active removal of methane from the atmosphere in the future, though such studies are at very early stages and are their efficacy and economics remain to be demonstrated (Jackson *et al*. 2020b; Lackner 2020; Jackson *et al*. 2019; Stolaroff *et al*. 2012).

It is important to emphasize that as the atmospheric concentration of methane has been measured to a high degree of precision and the sinks and atmospheric residence time are constrained, the total emissions are also well constrained. This is because the atmospheric abundance times, the removal rate, plus any increase in concentrations, must balance the total emissions flux, allowing the quantification of emissions when the other factors are well-known. Hence, although many individual source strengths are not well known, any upward revision in estimates of the magnitude of one source would necessitate a downward revision in another. Thus, the uncertainty surrounding total emissions is substantially smaller than the sum of uncertainties of individual emissions would imply. Furthermore, isotopic data, in this case the ratio of methane molecules to carbon atoms containing seven neutrons and six protons (13C) to the more common value of six neutrons and six protons (12C)) constrain the apportionment of emissions to fossil and biogenic sources, so that the substantial uncertainties in many individual natural biogenic sources are largely independent from estimates of fluxes from fossil fuel sources.

NATURAL SOURCES	MAGNITUDE (MT/YR)	ANTHROPOGENIC SOURCES	MAGNITUDE (MT/YR)	SINKS	MAGNITUDE (MT/YR)
Wetlands	145 [100–183]	Coal mining	44 [31–63]	Soils	40 [37–47]
Termites	9 [3–15]	Oil and gas industry	84 [72–97]	Total chemical loss	531 [502–540]
Oceans	6 [4–10]	Landfill and waste	68 [64–71]	Total loss	571 [540–585]
Geological	45 [18–65]	Ruminants	115 [110–121]		
Wild animals	2 [1–3]	Rice cultivation	30 [24–40]		
Freshwaters	159 [117–212]	Biomass burning	16 [11–24]		
Permafrost soils	1 [0–1]	Industry	3 [0–8]		
		Biofuels	13 [10–14]		
		Transport	4 [1–13]		
Total natural	367 [243-489]	Total anthropogenic	380 [359–407]		
Total natural (top-down)	232 [194-267]	Total anthropogenic (top-down)	364 [340-381]		

Table 2.1 Estimated natural and anthropogenic sources and sinks of methane, 2017

Note: Values shown are best estimates based on bottom-up studies (except last row), with the minimum and maximum of the studies analyzed in that meta-analysis given in brackets. Natural sources are based on 2000–2006 data as the separation into individual sources was not reported for 2017. The total natural source was evaluated for 2017, however, and was identical to that for the 2000–2006 period. The last row shows natural and anthropogenic totals based on top-down constraints, highlighting how natural sources are substantially lower, based on top-down estimates, likely due to overlap between wetlands and freshwaters, whereas anthropogenic bottom-up and top-down estimates are more consistent.

Source: Jackson et al, (2020)

2.1 ANTHROPOGENIC SOURCES

Approximately 60 per cent of total global methane emissions come from anthropogenic sources. Of these, more than 90 per cent originate from three sectors: fossil fuels, ~35 per cent; agriculture, ~40 per cent; and waste, ~20 per cent.

Fossil fuels: release during oil and gas extraction, pumping and transport of fossil fuels accounts for roughly 23 per cent of all anthropogenic emissions, with emissions from coal mining contributing 12 per cent.

Waste: landfills and waste management represents the next largest component making up about 20 per cent of global anthropogenic emissions.

Agriculture: emissions from enteric fermentation and manure management represent roughly 32 per cent of global anthropogenic emissions. Rice cultivation adds another 8 per cent to anthropogenic emissions. Agricultural waste burning contributes about 1 per cent or less.

These three categories are referred to as sectors in this assessment, with further subdivisions within the three termed subsectors. Biomass burning, which has a mixture of anthropogenic and natural causes, and biofuels are relatively minor sources of methane emissions, as are industry and transport. Emissions from some subsectors show large uncertainties across the existing inventories, in particular for coal mining and rice cultivation (Table 2.1).

2.1.1 BOTTOM-UP ESTIMATES

So called bottom-up emissions inventories are created by compiling activity data and emission factors for individual sectors, with the product of these providing a total sectoral emissions estimate. An example of these is rice cultivation (hectare) for activity, and methane emissions per hectare of rice cultivation for the emission factor. These data are often estimated at the national level. National statistics are frequently used for activity estimates, whereas field and laboratory measurements are generally used as sources of data on emission factors.

Several groups of researchers have assembled global emission inventories for methane covering all sources, whereas other efforts have focused on emissions from specific sectors. A broad overview of available inventories for anthropogenic methane emissions has been assembled by the Global Carbon Project (Saunois *et al*. 2020), incorporating data from the Community Emissions Data System (CEDS) (Hoesly *et al*. 2018), the Emission Database for Global Atmospheric Research (EDGAR) (Janssens-Maenhout *et al*. 2019), the United States Environmental Protection Agency (US EPA) (US EPA 2012), and the Greenhouse Gas – Air Pollution Interactions and Synergies model (GAINS) (Höglund-Isaksson 2020) as well as several estimates for biomass burning emissions. It shows that for all inventories, the two largest sources are agriculture and waste together and fossil fuels, respectively (Figure 2.1).
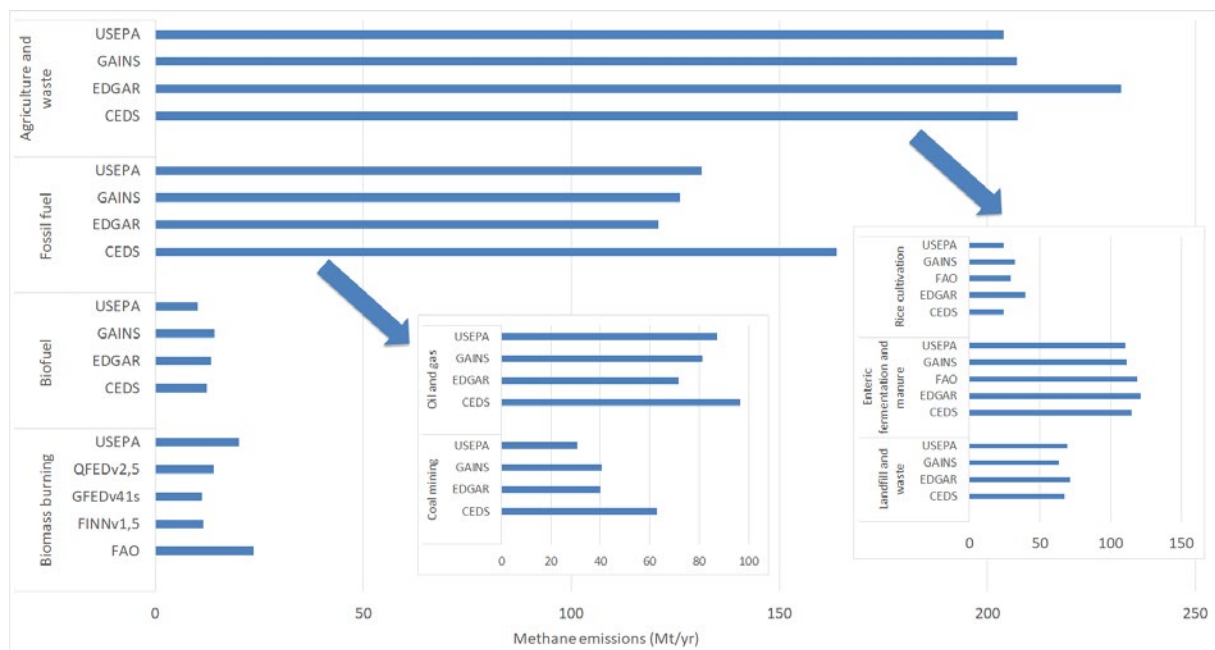
Source: Saunois et al. (2020). Emissions from EDGAR are the V4.3.2 version

Figure 2.1 Estimated anthropogenic methane emissions by sector from global inventories, 2017

Within the fossil fuel sector, the oil and gas subsector is the largest emitter, accounting for roughly two-thirds of the sector's total emissions, with emissions from coal mining making up most of the remainder. Emissions from industry and transport are small, totalling ~7 Mt/yr, less than 2 per cent of anthropogenic emissions, from both categories (averaged across the four inventories). Within the agriculture and waste sectors, emissions related to livestock are the largest source. These include emissions due to enteric fermentation, primarily from cattle, and emissions from manure. Landfills and waste represent the next largest component, followed by rice cultivation. In comparison, biomass burning, which has a mixture of anthropogenic and natural causes, and the use of biofuels are relatively minor sources of methane. Agricultural waste burning, included in the biofuels category in the US EPA inventory and in the agricultural sector in CEDS. GAINS, EDGAR and FAO estimates for this category but not included in Figure 2.1, range from 1 to 3 Mt/yr.

As noted, emissions for some subsectors show large uncertainties across the existing inventories, in particular for coal mining and rice cultivation. Total anthropogenic emissions, excluding biomass burning, are approximately 350–380 Mt/yr. For comparison, emissions from wetlands are estimated to be roughly 160–210 Mt/yr based on biogeochemical models. Hence approximately two-thirds of total emissions are anthropogenic.

The two largest sources are livestock and fossil fuels. Within the livestock subsector, enteric fermentation and manure management are the two processes generating emissions, with the former dominant and cattle the dominant animal (Figure 2.2). Within the manure category, pigs play the largest role though cattle are again important. Within the fossil fuel sector, extraction, processing and distribution of the three main fuels have comparable impacts, with emissions from oil and gas each contributing 34 per cent followed by coal with 32 per cent of sectoral emissions in 2020 (Höglund-Isaksson 2020). Emissions from the coal subsector are entirely from mining-related activities, including both active and abandoned facilities. Within oil and gas, methane emissions associated with onshore conventional extraction along with downstream gas usage are the largest sources

(Figure 2.3). Venting, the deliberate release of unwanted gas, is the primary cause of emissions during onshore conventional extraction, whereas fugitive emissions, the inadvertent release or escape of gas from fossil fuel systems, dominate downstream gas emissions. Within the fossil fuel sector, at the national level, emissions from the oil subsector in Russia and the coal subsector in China appear to be far larger than any other national level subsectors (Scarpelli *et al*. 2020). While these types of data based on national inventories are useful, it is important to note that many local measurements show large differences and often substantially higher emissions than conventional reporting, in many cases due to the presence of a small number of super-emitters, and imply these estimates may be too low (Zhang *et al*. 2020; Duren *et al*. 2019; Varon *et al*., 2019; Zavala-Araiza *et al*. 2018). These emissions give a sense of mitigation opportunities by region and sector, which is explored in Chapter 4.

Though some biomass burning is natural, current burning results largely from anthropogenic activities. Large amounts of biomass are burned in the tropics in human induced fires related to shifting cultivation, deforestation, burning of agricultural wastes and the use of biofuels (Dlugokencky and Houweling 2015). Biomass burning remains a relatively small source of methane and it accounts for approximately 5 per cent of global methane emissions, an estimated 10–25 Mt/yr (Figure 2.1) (Saunois *et al*. 2020).

While rice cultivation feeds up to a third of the world's population, rice fields are a significant source of methane (Mbow *et al*. 2019; Dlugokencky and Houweling 2015). Methane is produced through anaerobic decomposition of organic material in flooded rice fields which are responsible for approximately 8–11 per cent of global anthropogenic methane emissions (Saunois *et al*. 2020; Mbow *et al*. 2019).

As noted, there are substantial differences in sector-specific bottom-up methane emissions estimates created by different groups (Figure 2.1). This difference indicates that these estimates could be improved by additional work to better quantify activity levels for each source, and by improved quantification of source-specific emission factors which may vary substantially both between and within nations.
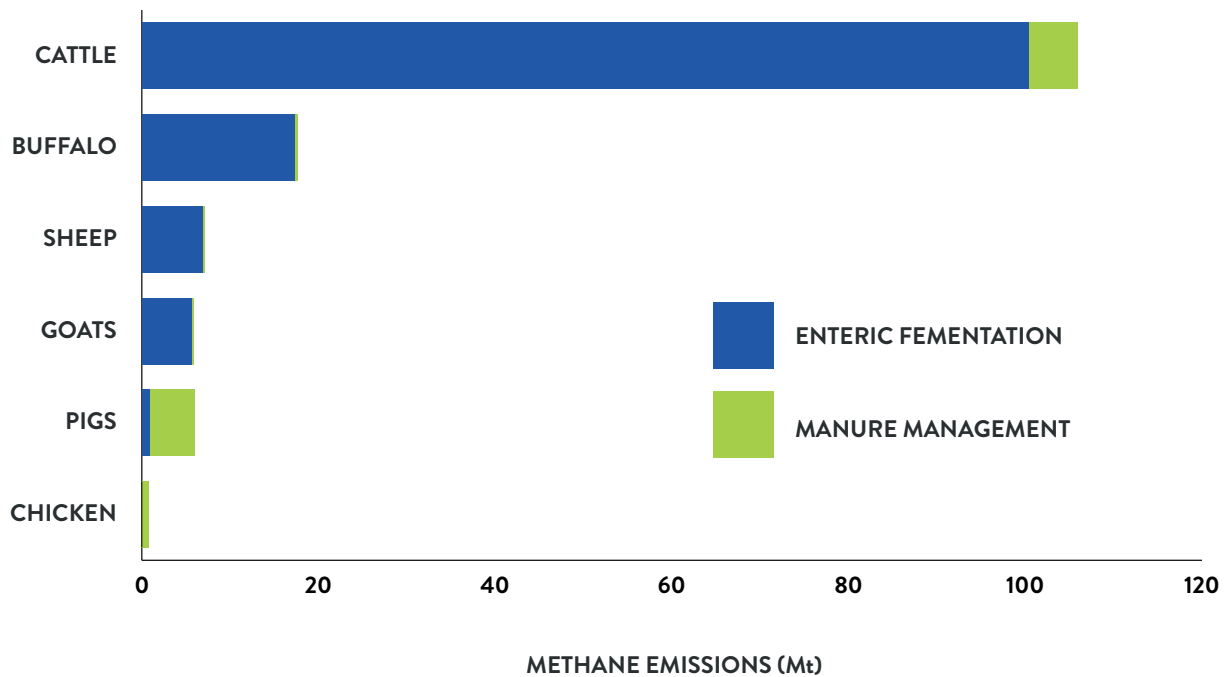
Figure 2.2 Annual livestock methane emissions , million tonnes

Source: FAO (2013; 2017)
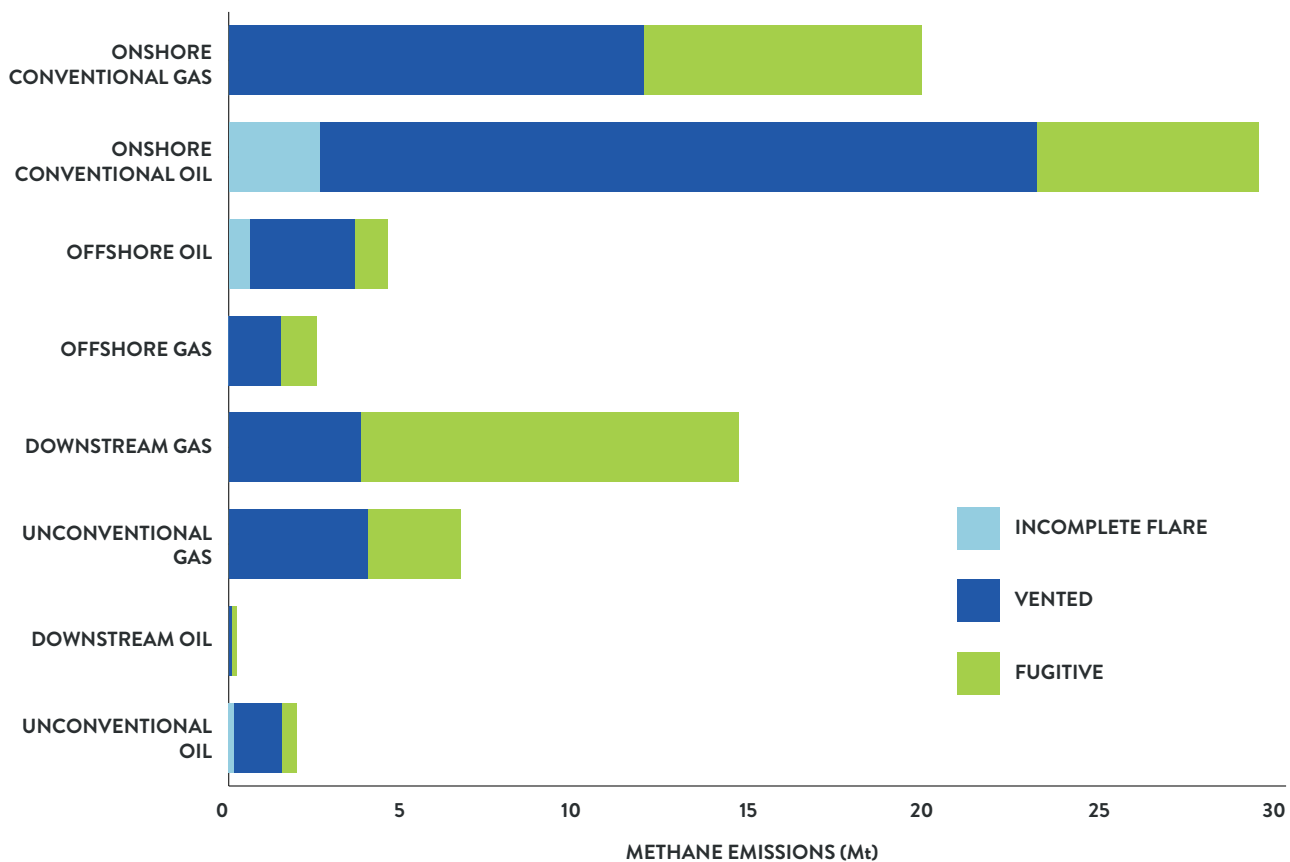
Figure 2.3 Annual oil and gas sector methane emissions by production type and reason, million tonnes

Source IEA (2020)

2.1.2 REGIONAL DIFFERENCES IN BOTTOM-UP ESTIMATES OF EMISSION SOURCES

Across multiple bottom-up inventories, emissions are largest in China, ~46–74 Mt/yr, and South Asia, ~35–50 Mt/yr, but large totals are also emitted from North America, ~35–50 Mt/yr; Latin America, ~50-60 Mt/yr; Southeast Asia+the Republic of Korea+Japan, ~25–35 Mt/yr; Africa, ~45–50 Mt/yr; Russia, ~20–25 Mt/yr; West Asia, ~23–29 Mt/yr; and Europe, ~22–26 Mt/yr (Figure 2.4). Uncertainties about emissions from China are particularly large, but there are also substantial uncertainties about North and Latin America.
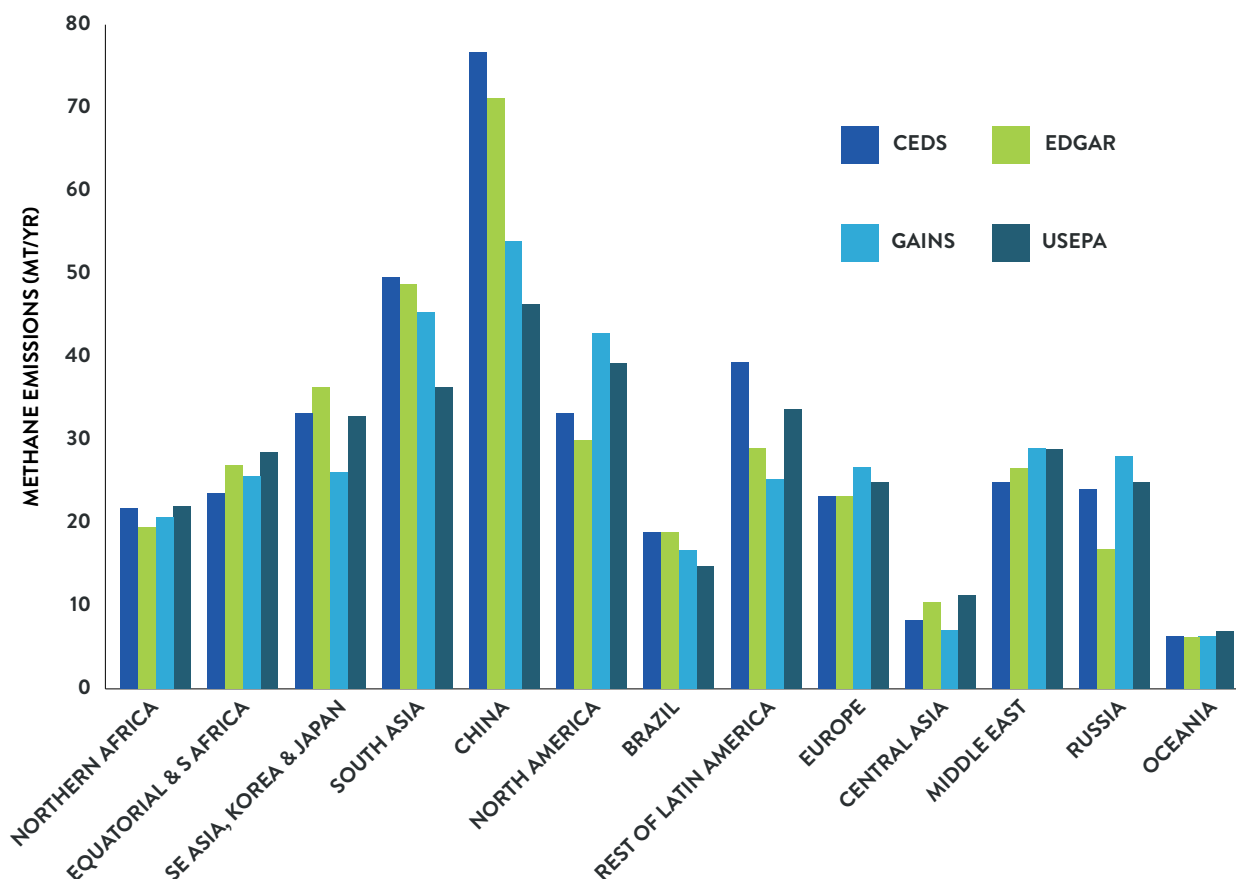
Figure 2.4 Estimated anthropogenic methane emissions by region from global inventories, excluding biomass burning, 2017, million tonnes

Source: Saunois et al. (2020)

While all sources of methane emissions are important in every region, there are some significant regional differences. Emissions from the coal and rice subsectors are particularly important in Asia. Fossil fuel-related emissions are generally a large share of regional emissions throughout the northern hemisphere. Solid waste separation and treatment offers opportunities across all regions. Figure 2.5 shows the global methane emissions for the year 2012 as reported by the EDGARv4.3.2 database, with sector specific shares and total emissions for major world regions.
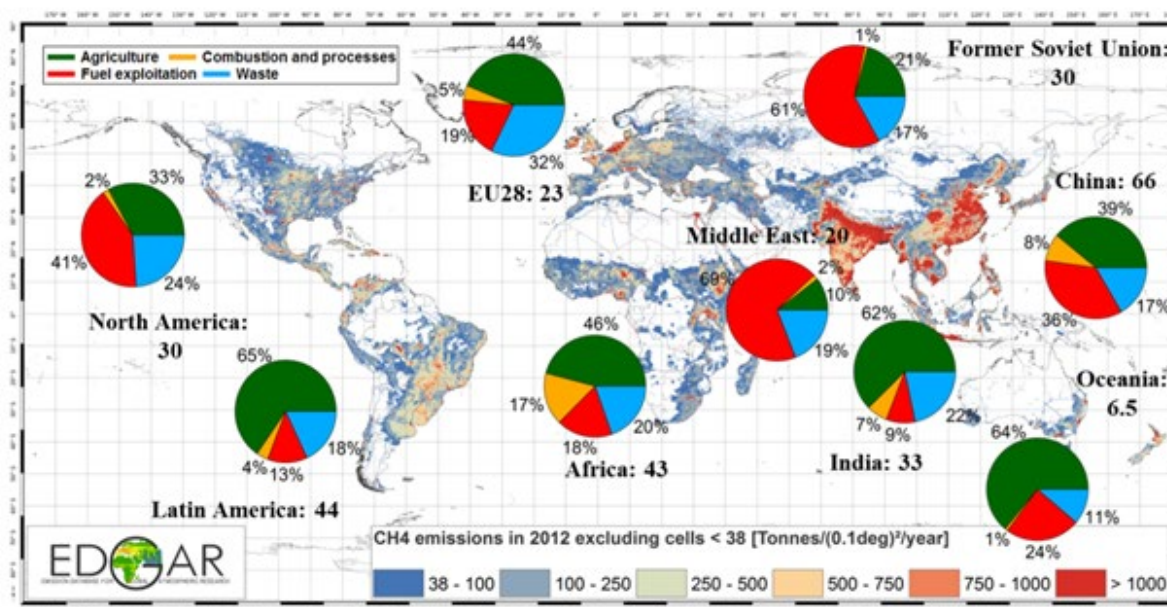
Figure 2.5 Global methane emissions for major world regions, 2012, million tonnes

Source: EDGARv4.3.2

The regional contribution to emissions from individual sectors varies markedly. Within fossil fuels, China is by far the largest source of coal-mining related methane emissions at ~24 Mt/yr; whereas for oil and gas the largest contributions come from West Asia, ~18 Mt/yr; Russia, ~15 Mt/yr; and North America, ~14 Mt/yr (Figure 2.6). Examining emissions related to livestock, the largest contributions comes from Latin America, ~27 Mt/yr, roughly half of which is from Brazil; and South Asia, ~22 Mt/yr; followed by nearly equal contributions from China, Equatorial and Southern Africa; Europe, North Africa and North America, each with 8–11 Mt/yr.

Emissions from rice cultivation are dominated by Southeast Asia+the Republic of Korea+Japan, ~10 Mt/yr; South Asia, ~8 Mt/yr; and China, ~8 Mt/yr, which together account for about 85 per cent of worldwide emissions. In contrast, emissions from landfills and waste are much more evenly distributed across the world. These emissions give a sense of mitigation opportunities by region and sector, which is explored in Chapter 4.
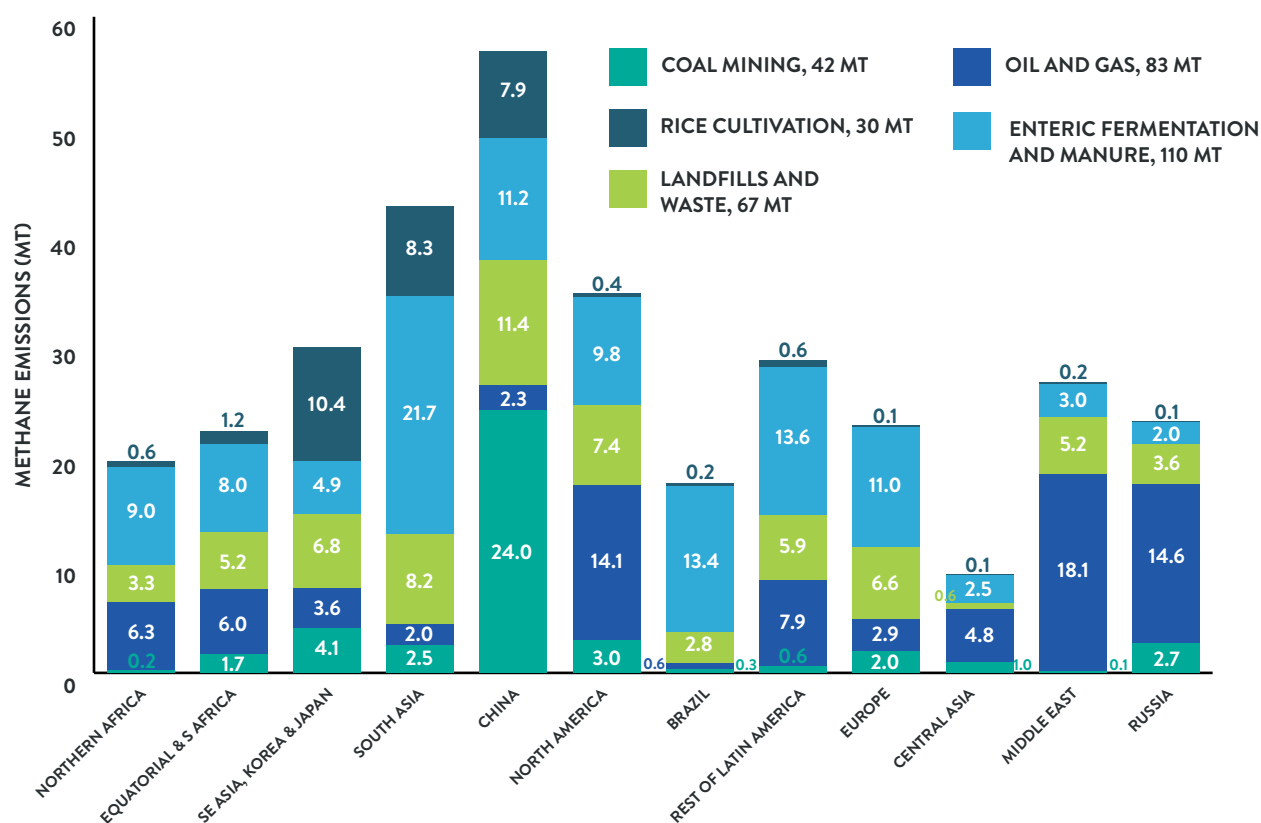
Figure 2.6 Estimated annual sectoral methane emissions by region and global sector totals, excluding Oceania, 2017, million tonnes

Source: Saunois et al. (2020).

2.1.3 ESTIMATING EMISSIONS USING TOP-DOWN METHODS FROM OBSERVED METHANE AMOUNTS

To evaluate bottom-up inventories and obtain a good quantitative understanding of methane sources and sinks, it is critical to monitor and quantify historic and current methane amounts. This section gives a brief description of the different ways of measuring methane amounts and producing emissions estimates, and Table A4 in the Annex gives a summary of each measurement technique available as well as its advantages and disadvantages. Ground-based measurements, ice core data, observations from aircraft, forward and inverse modelling and satellite data are all discussed. Results from such top-down methods generally compare reasonably well with bottom-up estimates such as those shown in Table 2.1 (Jackson *et al*. 2020; Saunois *et al*. 2020).

Ground-based data is highly accurate and now fairly common. The first accurate *in situ* measurements of methane were made in 1978 (Blake *et al*. 1982). In 1983, measurement stations from the National Oceanic and Atmospheric Administration (NOAA/ESRL)[5] and Advanced Global Atmospheric Gases Experiment (AGAGE) (Prinn et al., 2000)[6] had global coverage. As shown in Figure 1.1a, these networks show the amount of methane and its change over time. The latter is proportional to the imbalance between emission sources and sinks. The globally averaged amount, for example, stabilized at approximately 1 770 parts per billion (ppb) around the year 2000, indicating that at that time sources and sinks were equal (Figure 1.1).

To extend the record of methane amounts back in time before ground-based measurements became available, several studies (Bock *et*

5. www.esrl.noaa.gov/gmd/ccgg/trends_ch4/ (accessed 18 February 2021)
6. https://agage.mit.edu/ (accessed 18 February 2021)

al. 2017; Chappellaz et al. 2000; Bender et al. 1997; Chappellaz et al. 1990; Stauffer et al. 1985) have been published on atmospheric methane amounts reconstructed from polar ice cores. These records provide further and strong evidence of the predominant role of anthropogenic sources of methane emissions in causing the observed increases over the industrial era. Another important contribution of the evidence from ice cores is the range of emissions during the Holocene[7], which further demonstrates the current rise is well outside natural variability. These measurements significantly improve the quantitative understanding of historic and current changes in the global methane budget. Ice core records published by Etheridge et al. (1998), for example, showed that atmospheric methane levels have almost tripled since 1800.

Understanding methane abundances in the atmosphere can help constrain emissions from particular sources. Several studies (Gasbarra et al. 2019; Vaughn et al. 2018; Lavoie et al. 2017; Robertson et al. 2017; Sweeney et al. 2015; Karion et al. 2013) have used aircraft-based measurements to estimate methane emissions from individual facilities including landfills or natural gas production regions, or specific regions such as North America. One typical approach includes transects at multiple altitudes around a source while continuously measuring methane concentrations, and wind speed and direction. Figure 2.7 shows an example of a network that contains measurements from aircraft.

As discussed in the National Academy of Sciences report Methane Emission Measurement and Monitoring Methods (2018), following in situ sampling, the emission rates are estimated using a mass balance approach in which the concentration differences between the upwind and downwind sections of the flight paths are multiplied by the ventilation rate for the volume enclosed by the flight paths to arrive at the emission estimate (Conley et al. 2017; Gvakharia et al. 2017).

While these techniques have been applied with success to a variety of methane sources in urban areas (Mehrotra et al. 2017; Cambaliza et al. 2015) they have limitations and restrictions that need to be further investigated – this approach, for example, can only detect emissions that are encountered at flight elevations at the flight radial distance.

Very recently, remote sensing from aircraft has been used to quantify emissions from specific sources with relatively high accuracy, based on flights of independent instruments on different aircraft (Gorchov Negron et al. 2020; Duren et al. 2019; Baray et al. 2018; Johnson et al. 2017; Frankenberg et al. 2016; Karion et al. 2013). These data have shown that many bottom-up estimates are incorrect. Measurements in California, for example, revealed that multiple landfills that had reported emission rates in the range of 400–800 kilograms (kg) methane per hour in fact had emission rates of ~1 200–2 200 kg methane per hour (Duren et al. 2019). Similarly, measurements near offshore drilling platforms in the Gulf of Mexico show that emission rates were roughly double those in standard US EPA inventories (Gorchov Negron et al. 2020). These datasets also reveal that a few super-emitting sources typically play an outsized role in the total emissions from a specific source sub-sector. Ground-based studies similarly show that many bottom-up inventories underestimate methane emissions relative to observations (Chen et al. 2020; Alvarez et al. 2018; Brandt et al. 2014). Though valuable, such ground-based and aircraft data are currently available for only a very small area as they require expensive field and flight campaigns.

In addition to aircraft measurements, high altitude platforms can be used to measure methane. High altitude platforms are developmental vehicles typically situated between 20 and 100 kilometres. These platforms combine many of the advantages of satellites and ground-based systems, providing a flexible potential solution to many communications challenges (Wang and Shao 2013).

7. the current geological epoch, which began approximately 11,650 years before present, after the last glacial period

Cooperative Measurement Programs
NOAA GML Carbon Cycle
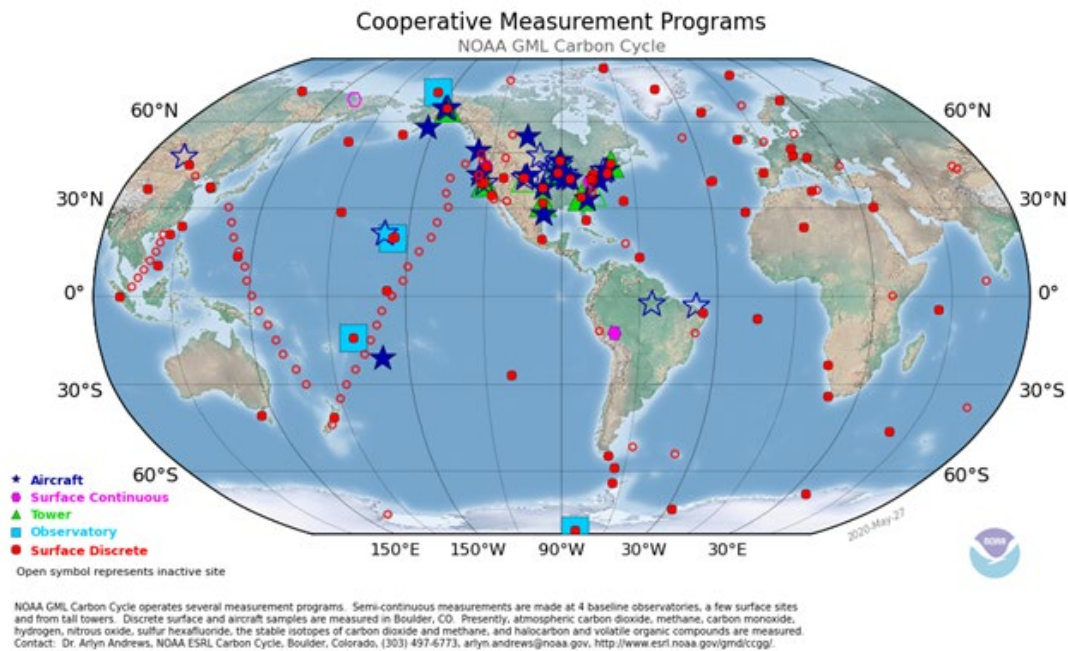
Figure 2.7 Global Monitoring Laboratory network, 2020

Source: NOAA

To understand and quantify global and regional budgets of methane and relate tropospheric measurements to individual sources, forward and inverse modelling can be used. Forward modelling converts an emission source with a certain quantity released per time into atmospheric abundance in specific locations using bottom-up estimates of emissions and sinks, as described in Section 2.1.1, along with an atmospheric transport model to simulate atmospheric methane that can be compared with observations.

Inverse modelling does the reverse where measurements of atmospheric abundance are used to calculate the location of an emission source as well as the emission rate. An inversion is a method that can be used to estimate emissions of a gas at the surface of a domain from atmospheric measurements of these gases usually in mole fractions. Most inverse models are based on Bayesian inference, in which observations are combined with bottom-up estimates (prior) resulting in estimated emissions (posterior). By using inverse modelling to evaluate bottom-up models of emissions, improvements can be made to the bottom-up models.

Though most methane data through the end of the 20th century comes from networks of ground-based and airborne *in-situ* measurements, these ways of measuring methane are generally labour intensive and, in the case of most aircraft data, because of their spatiotemporal scale, can only provide snapshots of emissions. Another limitation of these types of data is the limited spatial coverage. There is great interest in and calls for more satellite measurements of methane to overcome some of these limitations.

Though still a relatively new data source, satellite measurements of atmospheric methane have already been used to detect emission hotspots (Buchwitz *et al*. 2017; Kort *et al*. 2014; Marais *et al*. 2014; Worden *et al*. 2012), to estimate emission trends (Turner *et al*. 2016; Schneising *et al*. 2014) and to derive emissions of large basins with oil and gas extraction activities (Schneising *et al*. 2020; Zhang *et al*. 2020). They have been used in global inverse analyses to estimate emissions on regional scales (Miller *et al*. 2019; Maasakkers *et al*. 2019; Alexe *et al*. 2015; Wecht *et al*. 2014; Bergamaschi *et al*. 2013, 2009, 2007; Monteil *et al*. 2013). In December 2019, satellite data were used to quantify methane emissions from a gas well blowout in Ohio, United States in February– March 2018 (Pandey *et al*. 2019). That study, using data from the Tropospheric Monitoring Instrument (TROPOMI), demonstrated how strong and effective satellite measurements can be in detecting and quantifying methane emissions from unpredictable events. Satellite data from GHGSat and TROPOMI was also used to detect a major continuous methane leak in central Asia which had gone unnoticed (Varon *et al*. 2019).

Table 2.2 lists the types of instruments that have been used to measure methane from satellites in the recent past, along with those proposed for the coming years. Satellite missions tend to be of two types, global monitoring such as SCIAMACHY, GOSAT and TROPOMI, or mission-focused ones including GHGSat and MethaneSAT. The former have very broad spatial coverage at relatively low resolution whereas the latter are at higher resolution but are targeted at specific locations to monitor facility-scale amounts. With the rapid advancements in the ability to monitor methane emissions from space, several commercial enterprises provide or intend to provide facility-scale methane emissions information based on satellite data, either using their own instruments, such as GHGSat, Bluefield Technologies, or combining data from government-launched satellites with bottom-up information to better identify sources, Kayrros, for example.

The overall understanding of methane emissions by source is informed by both bottom-up studies and top-down inversions based on measurements. These provide complementary constraints on the methane budget and are in fairly good agreement for anthropogenic sources though bottom-up estimates for natural sources are generally much larger than top-down values (Jackson *et al*., 2020; Saunois *et al*. 2020).

INSTRUMENT OR SATELLITE	AGENCY	DATA PERIOD	REFERENCE
SCIAMACHY	ESA	2003–2012	Frankenberg *et al.* (2006)
GOSAT	JAXA	2009+	Kuze *et al.* (2016)
TROPOMI	ESA, NSO	2017+	Butz *et al.* (2012)
GHGSat	GHGSat, Inc.	2016+	Varon *et al.* (2018)
GOSAT-2	JAXA	2018+	Glumb *et al.* (2014)
geoCARB	NASA	(2022)	Polonsky *et al.* (2014)
MethaneSAT	EDF	(2022)	Benmergui (2019)
CO2M	ESA	(2025)	Meijer *et al.* (2019)
MERLIN	DLR and CNES	(2021/2022)	
Bluefield	Bluefield Technologies	(2023)	
Sentinel-5	ESA, NSO	(2023, 2030, 2037)	

Table 2.2 Satellite instruments for measuring tropospheric methane

Source: Updated from Jacob et al. (2016). Dates in parentheses are intended launches.

2.2 NATURAL SOURCES

Natural sources of methane include gas hydrates, freshwater bodies, oceans, termites and wetlands as well as other sources such as wildfires. Values for each of these are presented in Table 2.1.

Wetlands are defined as ecosystems in which soils or peats are water saturated or where surface inundation, whether permanent or not, dominates the soil biogeochemistry and determines the ecosystem species composition (US EPA 2012). Examples of wetlands are bogs, fens, marshes, muskegs, peatlands and swamps. Globally, wetlands are the largest natural source of methane with emissions, estimated at 102–200 Mt/yr on average over 2008–2017 (Jackson et al. 2020; Saunois et al. 2020) which is approximately one quarter of global methane emissions. As can be seen from the range of emissions estimates, however, there is significant uncertainty surrounding methane emissions from wetlands. Key to understanding methane emissions from wetlands are three factors that influence its production which are the spatial and temporal extent of anoxia, linked to water saturation; temperature; and substrate availability (Saunois et al. 2020; Wania et al. 2010; Whalen 2005; Valentine et al. 1994). Wetlands are critical to the current and future global methane budget, but currently significant gaps remain in the understanding of them (Sjögersten et al. 2020). Freshwaters are another significant natural source of methane, and in many cases these are similar to wetlands and, as a result, double-counting is a significant issue (Saunois et al. 2020).

Geological methane emissions from Earth's degassing are a major source to the atmosphere. These emissions are from gas-oil seeps, microseepage, mud volcanoes and submarine seepage in sedimentary petroleum-bearing basins and geothermal and volcanic manifestations (Etiope and Schwietzke 2019). Bottom-up estimates range from 27–63 Mt/yr, accounting for ~8 per cent of total methane sources, and most top-down estimates are consistent with this range. More recently, however, using an ice core record of the isotopic composition of methane extending back to preindustrial times, it was shown that geological sources were likely to be much lower, in the range of 1–6 Mt/yr (Hmiel et al. 2020). This suggests that this source may have been considerably overestimated and that anthropogenic fossil methane sources may be underestimated by a similar amount, given the relatively good constraints on the total emissions of fossil methane.

Termites are a significant source of methane and are responsible for approximately 1–3 per cent of global methane – symbiotic micro-organisms in their digestive parts of termites are responsible for this. Methane emissions from termites in studies conducted between 1982 and 2013 have, however, varied from 0.9 to 150 Mt/yr (Nauer et al. 2018) with the most recently reported value being 9 Mt/yr (range [3–15] Mt/yr) (Jackson et al. 2020; Saunois et al. 2020). This significant uncertainty could be due to several reasons, but the most prominent ones are:

a. lack of data on termite biomass required to upscale (Nauer et al. 2018); and

b. a poor understanding of methane turnover in the arboreal, epigeal or hypogeal nests (mounds) of termite colonies (Kirschke et al. 2013; Brune et al. 2010; Bignell et al. 1997).

As discussed in Sjögersten et al. (2020), research conducted in 2006–2019 by different groups provides evidence that trees may be an underestimated source of methane. Keppler et al. (2006) suggested that plants produce methane in aerobic conditions, and that the fluxes were 62–236 Mt/yr, or approximately 11–46 per cent of the total global methane budget (Nisbet et al., 2009; Keppler et al., 2006). It is argued that the contribution of vegetation to the methane budget is perhaps the least understood and more recent estimates give a range of methane emissions of 32–143 Mt/yr, approximately 22 per cent of the total annual methane flux (Carmichael et al., 2014). Significant uncertainties still remain however, in particular, much of the flux from trees occurs in wetland areas and so is already accounted for in their estimated methane flux.

The ocean is a highly uncertain but small contributor to the global methane budget, emitting 5–25 Mt/yr or 1–13 per cent of natural emissions (Saunois et al. 2020; Weber et al. 2019). Possible sources of oceanic methane include:

1. leaks from geological marine seepage;

2. production from sediments or thawing sub-sea permafrost;

3. emissions from the destabilization of marine hydrates, crystal water structures that trap methane in sediments deposited on the ocean floor;

4. in situ production in the water column, especially in coastal areas because of submarine groundwater discharge (Sharke et al. 2014; Saunois et al. 2012).

Venting from the seabed usually does not release methane to the atmosphere since it dissolves in the ocean before reaching the surface. There are,
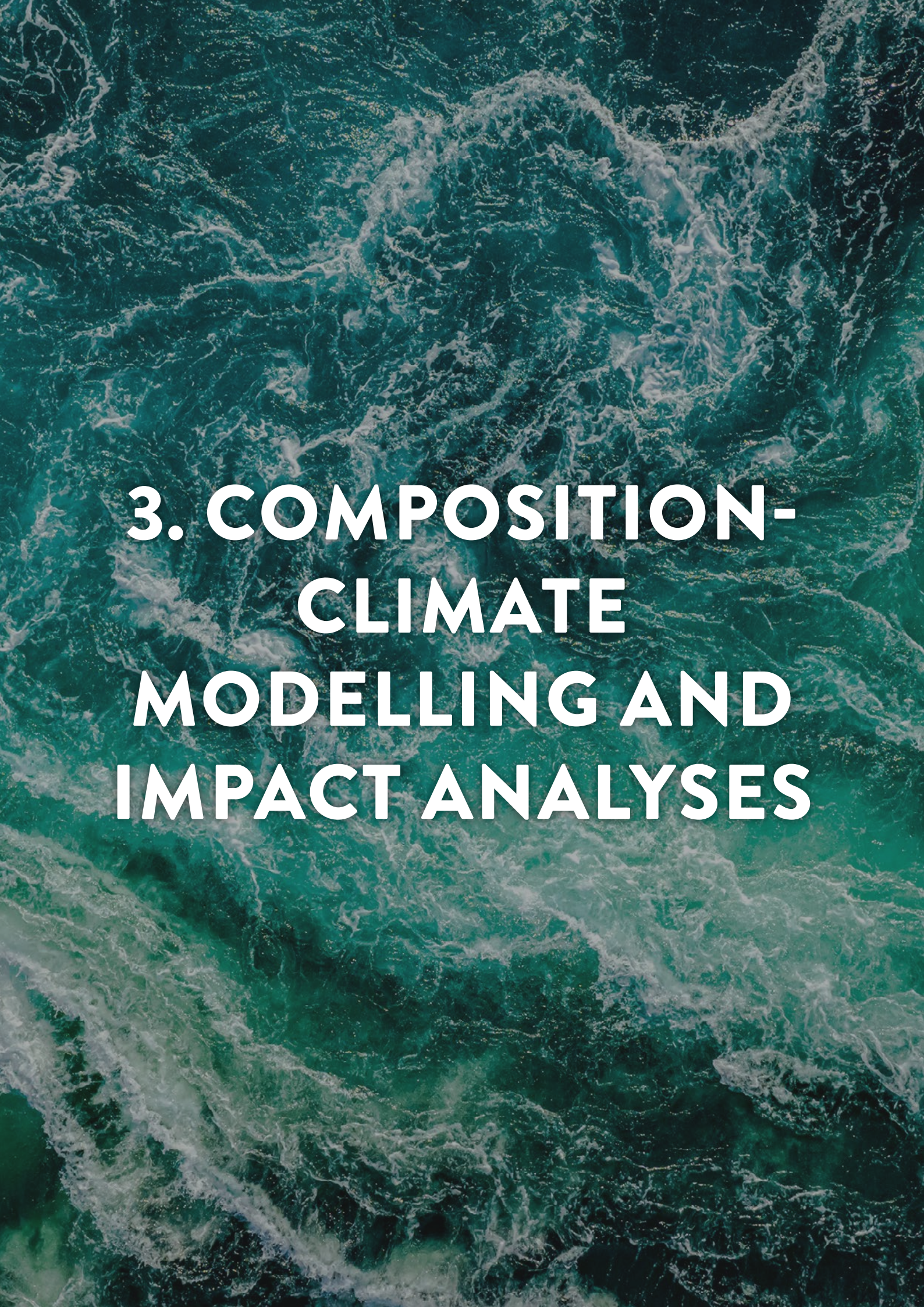
however, two well-known processes that emit methane from the ocean into the atmosphere – diffusive gas transfer and ebullition or bubbling across the air–sea interface (Reeburgh 2007). Further pathways have been identified that may produce methane in the surface ocean mixed layer, providing a more direct pathway for methane to be emitted to the atmosphere (Weber et al. 2019; Lenhart et al. 2016; Karl et al. 2008).

As noted above, several of the natural methane sources potentially overlap with one another, especially freshwaters and wetlands. Presumably because of this, the total from adding up each individual source based on bottom-up estimates is in fact much larger than the total value estimated using top-down methods (Table 2.1). As such, this Assessment relies upon the top-down constraint for the total natural methane emissions, which leads to relative source strengths for anthropogenic and natural methane emissions of ~60 and 40 per cent, respectively. Taking into account the recent findings of Hmiel et al. (2020) discussed previously, the balance may be closer to two thirds and one third, however.

Natural sources can also respond to climate change, in which case a portion of the natural flux is indirectly attributable to humans. Examples include increased emissions from wetlands under a warming climate (Shindell et al. 2013; Gedney et al. 2004) and increased emissions from thawing permafrost (Oh et al. 2020; Dean et al. 2018; Cooper et al. 2017; Zhang et al. 2017; Schuur et al. 2015). Identified responses of natural methane emissions to climate change overwhelmingly represent positive feedbacks and may be non-linear. An example is evidence that the release of methane from thawing permafrost occurs faster as a result of abrupt rather than gradual thawing (Anthony et al. 2018). These feedbacks cannot be mitigated directly but can instead be reduced by the mitigation of anthropogenic methane emissions and emissions of other drivers of warming. It should also be noted that increases in emissions due to these feedbacks would increase methane's lifetime, so that the impact of each tonne of anthropogenic methane would increase slightly. Similarly, potential reductions in emissions of nitrogen oxides, offset in part by reductions in emissions of volatile organic compounds (VOCs), would also increase methane's lifetime. In either case, the benefits of each tonne of methane mitigation would be larger than those analyzed here for current conditions.

3. COMPOSITION-CLIMATE MODELLING AND IMPACT ANALYSES

CHAPTER FINDINGS

- Coordinated modelling of both composition and climate responses to methane changes was carried out for this assessment by five teams using the models developed by the National Center for Atmospheric Research (NCAR; CESM2; US); the Met Office and academia (UKESM1; UK); the National Oceanic Atmospheric Administration Geophysical Fluid Dynamics Laboratory (NOAA GFDL) (ESM4.1; US); the National Institute for Environmental Studies (NIES), University of Tokyo and the Japan Agency for Marine-Earth Science and Technology (JAMSTEC) (MIROC: Japan); and the National Aeronautics and Space Administration (NASA) (GISS E2.1; US). This provides improved characterization of responses of ozone and climate and their uncertainties.

- Based upon recently updated epidemiological results, the new modelling indicates that there are 1 430 (670–2 110; 95 per cent confidence interval) premature deaths due to ozone in response to each million tonne of methane emitted, a value considerably higher than prior estimates. Of those, 740 (460–990; 95 per cent confidence interval) are caused by respiratory problems 690 (210–1 120; 95 per cent confidence interval) by cardiovascular ones.

- Roughly 30 per cent of these premature deaths are of people aged less than 70, and just more than 10 per cent of those aged less than 60.

- At the national level, the largest total numbers of premature deaths are in India, China, the US, Russia, and Japan, whereas the largest per person impacts are in Ukraine, Lesotho, Egypt, Georgia and the Democratic People's Republic of Korea.

- There are ~125 (60–185; 95 per cent confidence interval) premature deaths due to heat exposure in China and the United States together per million tonnes of methane emitted, and perhaps ~500 worldwide, though confidence is low for the global values.

- There are approximately 4 000 asthma-related accident and emergency department (A&E) visits and 90 hospitalizations per million tonnes of methane emitted.

- Roughly 300 (210–390; per cent confidence interval) million hours of work are lost globally due to heat per million tonnes of methane emitted.

- 145 (90–200) kilotonnes (kt) of wheat, soybeans, maize and rice are lost per million tonnes of methane emitted. The largest impacts are in Brazil, China, India and the US.

- Mortality impacts are valued at ~US$ 3 200 per tonne of methane using an income elasticity of 1.0 across countries and ~US$ 6 700 using an elasticity of 0.4, both undiscounted.

- Quantified market costs are comparatively small at ~US$ 122/tonne and stem predominantly from agricultural yield changes, and labour and forestry losses.

- The total valuation per tonne of methane is ~US$ 4 300 using a cross-nation income elasticity of 1.0 and US$ 7 900 using an elasticity of 0.4. Valuation is dominated by the effects of ozone, which are only weakly sensitive to discounting, and thus the total valuation does not strongly depend upon the relative weighting of impacts occurring at different times in the future.

- Uncertainties in health- or agriculture-related ozone metrics are roughly 25 per cent (95 per cent confidence interval) at the global level whereas for surface temperature response they are ~55 per cent. Responses are nearly linearly proportional to the methane change.

Modelling was undertaken using five state-of-the art global composition-climate models that evaluate both the changes in surface ozone concentrations and in the Earth's climate system in response to methane reductions. This coordinated comparison allows the investigation of the potential of reducing warming and the impacts associated with ozone formation by decreasing methane emissions, and the characterization of the robustness of these responses.

3.1 EXPERIMENTAL SETUP

The modelling focused on the response to 50 per cent reductions in the anthropogenic increase in methane amounts. A 50 per cent value was chosen as it is large enough to give a clear signal over meteorological noise in the models and is similar in magnitude to what the worldwide application of existing best targeted practices could potentially achieve (Chapter 4). Based on observations reported by NOAA's Earth System Research Laboratory, the 2015 mixing ratio of methane was 1 834 parts per billion by volume (ppbv). Ice core data indicate that the value in 1750 was about 722 ppbv, hence the anthropogenic increase is 1 112 ppbv. A 50 per cent reduction in that increase would therefore lower amounts by 556 ppbv, so that the atmospheric abundance would then be 1 278 ppbv.

The response is evaluated under present day (2015) conditions and for two sets of 2050 emissions following a reference SSP3-7.0 and short-lived climate pollutant control scenarios developed previously by the Asia-Pacific Integrated Model (AIM) group for other pollutants that affect oxidation capacity (Table 3.1; simulations 1–6). The latter cases follow the harmonized Shared Socio-economic Pathway 3 (SSP3) markerscenarios for the baseline (SSP3-7.0) and short-lived climate pollutant controls (SSP3-7.0_lowNTCF) (Fujimori *et al*. 2017). These 2050 cases, with high and low emissions of the non-methane ozone precursors nitrogen oxides, carbon monoxide (CO) and non-methane volatile organic compounds (NMVOCs) (Figure 3.1), are designed to provide information about the sensitivity of the response to methane under most conditions that are likely to be encountered over the next few decades, potentially allowing interpolation of methane responses to any given set of emissions projections. Note that biomass burning emissions were not changed in these simulations.

Aerosol and aerosol precursor emissions increase under the reference SSP3-7.0 case in 2050, but these are unlikely to substantially affect methane. One model performed additional simulations with a 25 per cent decrease and 50 per cent increase in methane to test the linearity of the response (Table 3.1; simulations 7 and 8). Anthropogenic and biomass burning emissions are from the SSP3 dataset produced in support of CMIP6 and the IPCC AR6 cycle assessments. For consistency with 2050 projections, 2015 emissions are taken from the same SSP dataset which has been harmonized to 2015 historical emissions reported by the Community Emissions Data System (CEDS) project (v2017-05-08).

Five state-of-the-art composition-climate models participated in the assessment: the CESM2(WACCM6) model developed at the National Center for Atmospheric Research (NCAR) in Boulder, Colorado, US (Danabasoglu *et al*. 2020; Gettelman *et al*. 2020); the GFDL AM4.1/ESM4.1 (Horowitz *et al*. 2020; Dunne *et al*. 2019) model developed by NOAA in Princeton, New Jersey, US; the Goddard Institute of Space Studies (GISS) E2.1/E2.1-G model developed by the NASA in New York, New York, US (Gillet *et al*. 2021; Kelley *et al*. 2020); the MIROC-CHASER model developed jointly by the Atmosphere and Ocean Research Institute, the University of Tokyo, Kashiwa, the National Institute for Environmental Studies (NIES), Tsukuba, the Japan Agency for Marine-Earth Science and Technology, Yokohama, and Nagoya University, Nagoya, Japan (Sekiya *et al*., 2018; Watanabe *et al*. 2011; Sudo *et al*. 2002); and the UKESM1 model developed jointly by the Met Office, Exeter, UK, and the United Kingdom's academic community (Archibald *et al*. 2019; Sellar *et al*. 2019).

To reduce the burden imposed by running these very computationally expensive models, only a single pair of simulations were run with coupled (i.e. responsive) ocean and sea-ice (denoted C1 and C2, with the C indicating coupled). Those runs of 40–45 years length are used to assess climate response to methane reductions. Other runs examining the sensitivity of the ozone response to methane changes were performed in a configuration with fixed ocean boundary conditions and, in most models, with fixed meteorology and were therefore only run from 1–7 years. These shorter simulations include a repeat of the base C1 and C2 simulations in this configuration to assess the impacts of the different experimental setup. Again, for the sake of reduced computational expense, the simulations were amount-driven, with conversion to per million tonne emissions performed afterwards (Section 4.1).

SIMULATION #	METHANE [PPB]	MODELS	CONFIGURATION	ANTHROPOGENIC EMISSIONS	
				CO, NO$_x$, NMVOC [year]	BC, OC, NH$_3$, SO$_2$ [year]
1	1 834	CESM2, GFDL AM4.1, GISS E2.1, MI-ROC-CHASER, UKESM1	Fixed sea surface Temperatures/sea ice, fixed meteo-rology	2015	2015
2	1 278			2015	2015
3	1 834			SSP3-7.0 2050	SSP3-7.0 2050
4	1 278			SSP3-7.0 2050	SSP3-7.0 2050
5	1 834			SSP3-7.0_lowNTCF 2050	SSP3-7.0 2050
6	1 278			SSP3-7.0_lowNTCF 2050	SSP3-7.0 2050
7	1 556	GISS E2.1		2015	2015
8	2 390			2015	2015
C1	1 834	CESM2, GFDL ESM4.1, GISS E2.1-G	Coupled ocean and sea ice	2015	2015
C2	1 278			2015	2015

Table 3.1 Simulations performed for this assessment
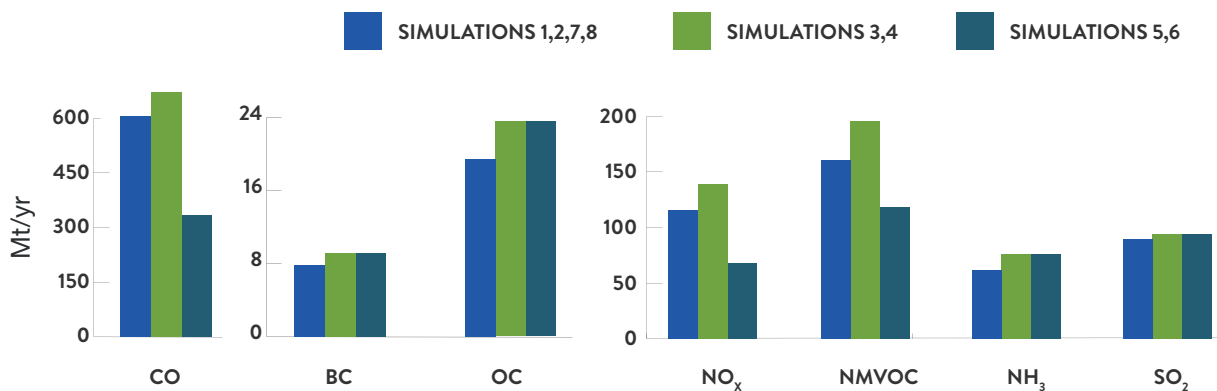
Figure 3.1 Global anthropogenic emissions used in this analysis, million tonnes per year

Note: Simulations C1 and C2 used the emissions shown here for simulations 1 and 2, respectively. Emissions for simulations 1, 2, 7 and 8 are from 2015; emissions for simulations 3 and 4 are from SSP3-7.0 for 2050; and emissions for simulations 5 and 6 are from SSP3-7.0_lowNTCF for ozone precursors and SSP3-7.0 for aerosols, both for 2050 (Table 3.1).

Source: UNEP and CCAC based on Fujimori et al. 2017.

3.2 MODELLED OZONE RESPONSE TO METHANE EMISSIONS CHANGES

Initially, the ozone response under present-day (2015) atmospheric conditions (simulations 1 and 2) was examined. Reducing anthropogenic concentrations by 50 per cent in this case led to a reduction in the global area-weighted annual average surface ozone of ~1.5–2 ppbv. Though a small number, the reduction is larger in the northern than the southern hemisphere and tends to be greatest over land areas where methane catalyzes ozone production more efficiently than over the oceans owing to the presence of anthropogenic nitrogen oxides. Hence the global population-weighted exposure change is ~2–2.5 ppbv. More relevant to human health is the maximum daily 8-hour exposure averaged over the year (MDA8), which is the metric most closely linked to increases in premature deaths from ozone in one of the largest epidemiological studies to date (Turner *et al*. 2016). Changes in this metric have been calculated for all individual models as well as for the multi-model mean (MMM) (Figure 3.2). Changes in this metric are between 2–5 ppbv over much of the northern hemisphere tropical and sub-tropical latitudes. The GFDL AM4.1, GISS E2.1 and CESM2 models are generally quite similar to one another, with the UKESM1 model showing substantially larger responses than those three and the MIROC-CHASER model showing substantially weaker responses.
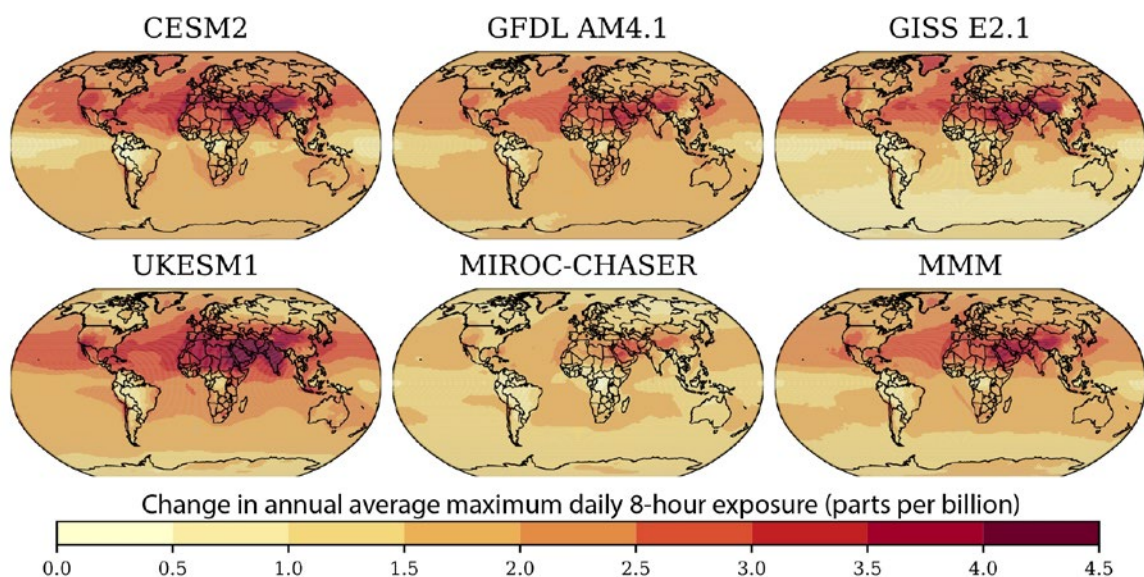
Figure 3.2 Change in annual average maximum daily 8-hour ozone exposure between the present day (2015) and half anthropogenic methane simulations in various models and the multi-model mean (MMM)

Source: UNEP and CCAC

Exploring the sensitivity of the ozone response to the background loading of other pollutants (simulations 1–6), there is a clear dependence of the response on the loading of nitrogen oxides. Throughout the world, the ozone response is larger when methane is altered within a background atmosphere containing higher levels of nitrogen oxides. The sensitivity varies substantially from place to place depending on other factors influencing ozone photochemistry, including the availability of sunlight and of other hydrocarbons or carbon monoxide that can play the same role as methane. Despite the complexity, it appears that this dependence can be represented by a fairly simple logarithmic equation that captures ozone sensitivity to background nitrogen oxide conditions (Figure 3.3). Sensitivity to other pollutants is markedly weaker. This indicates that the dependence of ozone's response to methane on background nitrogen oxides can readily be captured in policy-support tools to allow the estimation of the impacts of changes in methane emissions in any plausible near-future condition. This should provide accurate results for fairly large nations, for which domestic methane emissions dominate nitrogen oxides, and of course requires projected nitrogen oxides emissions levels.
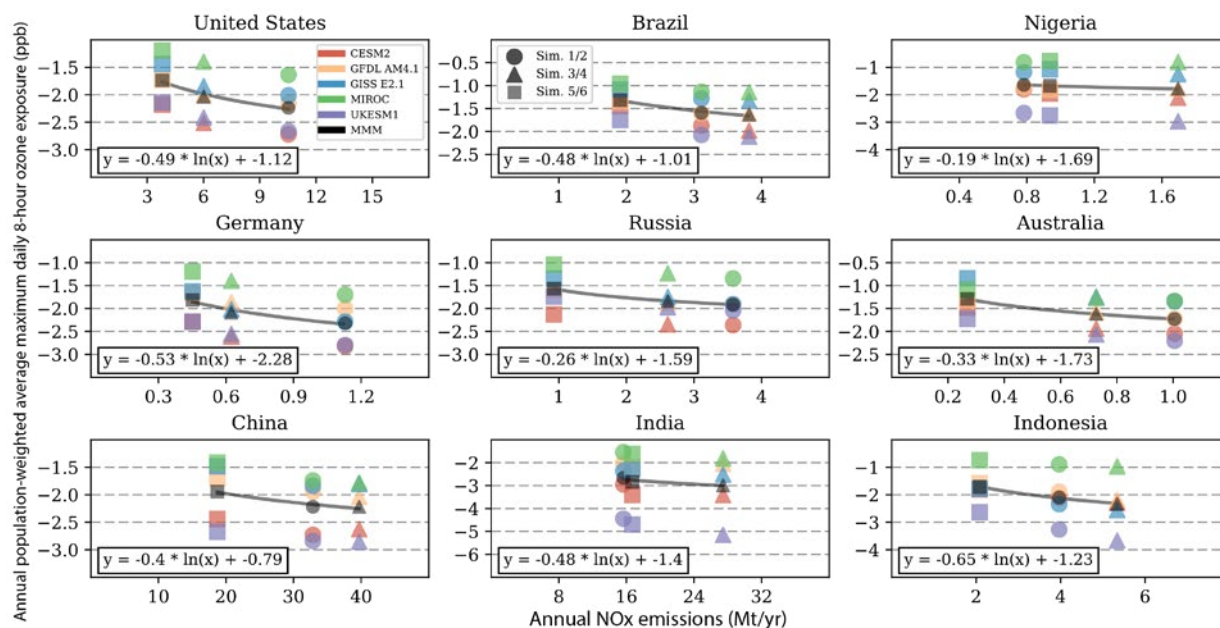
Figure 3.3 Country specific response of annual population-weighted average maximum daily 8-hour ozone exposure due to a 50 per cent reduction in global methane concentrations, parts per billion

Note: The x axis is the country specific anthropogenic land emissions of nitrogen oxides from each simulation pairing. The line is a logarithmic function for the multi-model mean, with the country specific equation displayed in each panel.

Source: UNEP and CCAC

Next, the linearity of the response to different magnitudes of methane concentration change was examined. At the national level, population-weighted ozone changes are extremely linear across a range of methane increases and decreases (Figure 3.4). Though the response itself varies from country to country (i.e. the slopes are different), the ozone change at the national level is directly proportional to the methane concentration change regardless of the ozone metric chosen. This result is consistent with prior studies which also indicate that the ozone/methane relationship is approximately linear (Fiore *et al*. 2008) but its magnitude depends on the local availability of nitrogen oxides, and, through nitrogen oxides, of hydroxyl (West *et al*. 2006; Wang and Jacob 1998).
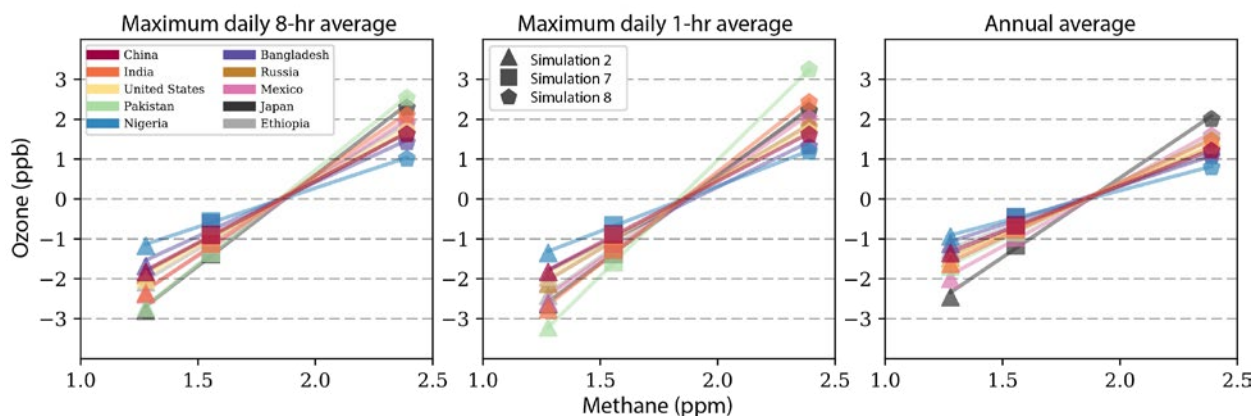
Figure 3.4 Relationship between changing global methane concentrations and the country-level population-weighted ozone metric (parts per billion), with non-methane ozone precursor emissions (carbon dioxide non-methane volatile organic compounds and nitrogen oxides held at 2015 levels (simulations 1, 2, 7 and 8 in Table 3.1)

Note: All results are from the GISS E2.1 model and are plotted as ozone changes relative to the metric values from simulation 1 ([methane] = 1.834 parts per million). The selected countries are the 10 most populous in the northern hemisphere.

Source: UNEP and CCAC

Given that the ozone response to methane concentrations changes is quite linear with the change in methane itself, the response of ozone was converted into the response per unit of methane emission change. For this analysis, the response of methane concentrations per unit methane emission change was first calculated, using the relationship between methane concentrations and emissions derived in prior work (Fiore *et al*., 2008):

$$\frac{C'}{C} = \left(\frac{E'}{E}\right)^f$$

where C and C' are initial and perturbed concentrations, E and E' are initial and perturbed emissions, and f is the feedback factor defined as the ratio of the perturbation lifetime to the total atmospheric lifetime. As in Myhre *et al*. (2013), f=1.34 was used and set total present-day annual methane emissions at 568 Mt (Saunois *et al*. 2016). Based on the simulations using values of 1 834 and 1 278 for C and C', E' is found to be 434 Mt/yr. Hence the concentration change between simulations 1 and 2 corresponds to emissions changes of 134 Mt/yr, so that the methane response to emissions changes is 4.1 ppb CH_4/Mt CH_4. Note that using total present-day methane emissions from another estimate would modestly affect this result. For example, using the 550 Mt/yr estimate of Kirschke *et al*. (2013) would lead to emissions changes of 130 Mt/yr in simulations 1 versus 2.

The interannual variability of national and global population-weighted annual MDA8 differences were evaluated between runs 1 and 2 over three years of simulation for the four models with multiple years of simulations, except MIROC-CHASER. At the global level, the standard deviation based on interannual variability driven by year-to-year differences in meteorology for these ozone responses were 8.8, 5.3, 1.0 and 7.6 per cent respectively for CESM2, GFDL AM4.1, GISS E2.1, and UKESM1. Values were even smaller for MDA1. In comparison, the 95 per cent confidence interval, based on the variation across models in the global population-weighted MDA8, was 24 per cent. Values at the national scale showed a similar range, except for some small countries, and were still small in comparison with national level variations between modes. Hence it appears that variability within a model in the fixed Sea Surface Temperature/meteorology setup is relatively small, and hereafter only model-to-model variability is incorporated along with uncertainty in the exposure-response functions

in the uncertainty analysis as this provides a good representation of the total. This analysis also supports the inclusion of the MIROC-CHASER single year simulations in this multi-model assessment.

The effect of the model setup on the ozone response was also examined by comparing the changes in the coupled model simulations with those in the simulations with fixed boundary conditions – sea surface temperatures and sea ice, along with meteorology in some models. Again, examining the global population-weighted annual MDA8, the differences between the 50 per cent anthropogenic methane reduction runs including climate (C1 and C2) were found to be very similar to those for the analogous runs without a climate response (simulations 1 and 2). Specifically, responses in the coupled model version were 3 per cent smaller for GFDL, 7 per cent smaller for GISS, and 1 per cent larger for CESM. As in the previous analysis, variability in CESM is largest, but overall there was minimal difference in the response over time in these long simulations. For example, differences in ozone responses over the last 10 years of those simulations were typically within 3 per cent of those in the first 10 years. Variations in response due to setup, as with interannual variability, were similar at the national scale except for some small countries.

3.3 MODELLED CLIMATE RESPONSE TO METHANE EMISSIONS CHANGES

Three of the five participating models were able to complete the long climate simulations, C1 and C2 described in Section 3.1. The response of these three were evaluated separately and for the multi-model mean. Statistical significance was assessed at the grid-point level by evaluating the standard deviation across individual years of model output – years 11–40 in each model's simulation. Temporal autocorrelation was accounted for at each grid point by reducing the sample size to represent an effective number of independent data points, based on the lag-1 autocorrelation (Zwiers and Von Storch 1995). For the multi-model mean, this measure thus includes both variations across the three models and internal variability within the physical climate system as represented by each individual model and has been shown to give reliable statistical ranges for sample sizes larger than about 50, well below the sample size used of 90 (Conley et al., 2018). For zonal and global mean values, statistical significance was assessed

by examining the variability between models in the long-term average surface temperature response. Though atmospheric composition will have largely equilibrated to the perturbed methane within a decade in these experiments, the climate system takes much longer to fully respond. These results thus represent a partial adjustment, as noted averaged over one to three decades following the methane change. To explore this topic further, the GISS E2.1 simulations C1 and C2 were extended by an additional 40 years. Whereas the global mean surface temperature response during years 11–40 was 0.20 ± 0.05° C, the response during the next 40 years was 35 per cent larger with a value of 0.27 ± 0.04° C (total response over years 41–80). This suggests that the evaluation of temperature responses provides a good indication of the near-term impact of methane changes, but that the longer-term changes would be on the order of 35 per cent larger, consistent with the slow response time of the ocean. It is noted also that none of these simulations include either the effect of carbon dioxide produced from methane oxidation or the response of the carbon cycle to methane-induced warming. The former is estimated to add ~2 per cent to the total radiative forcing from methane (Myhre et al. 2013). The latter occurs as the warming induced by methane emissions suppresses carbon uptake, further enhancing the temperature change attributable to methane by ~10 per cent and extending its impact at long timescales (Fu et al. 2020; Gasser et al. 2017).

The results for surface temperature show that methane emissions, which lead to increases in methane, tropospheric ozone and stratospheric water vapour, cause clear and consistent zonal mean, averaged over longitudes, warming over most of the Earth during most seasons (Table 3.2 and Figure 3.5). Impacts are particularly large over the mid-latitudes of the northern hemisphere and especially over the Arctic. The models were most consistent in the response in the tropics. There is substantial variation across the models in the annual mean surface temperature response in the southern hemisphere extratropics, however, especially over the Southern Ocean, and even in parts of the northern hemisphere – eastern Siberia/Alaska and parts of eastern Europe – when looking at the regional scale. It was noted that the sample size was very small in this analysis with just three models participating, and hence the uncertainty in a quantity, such as the annual global mean surface temperature change over the 11–40-year period following emissions

changes, is likely smaller than a broader sampling of models would yield for at least some globally or zonally averaged results. In particular, the 95 per cent confidence interval in climate sensitivity is estimated to be approximately ±34 per cent (Sherwood et al., 2020), which translates into a 95 per cent confidence interval for the global mean annual average surface temperature response to a methane change of ±0.06° C (34 per cent of 0.18° C) rather than the ±0.02° C in this analysis. It is recommended the larger uncertainty range, ~34 per cent relative uncertainty, is used in impact calculations going forward.

Within the tropics, 30° S–30° N, the models give very similar zonal mean responses (Table 3.2 and Figure 3.5). All suggest that warming over the Pacific is less uniform than warming over the Atlantic or especially the Indian Ocean basins (Figure 3.6). Warming over tropical land areas shows fairly good agreement across models except over southernmost Africa. In contrast, the consistently enhanced warming in the Arctic is distributed differently in the three models. It thus becomes difficult to precisely quantify climate responses at national or even continental scales over many parts of the world.

At seasonal timescales, the models are less consistent over northern hemisphere mid-latitude continental areas during boreal winter than other seasons, as expected due to the greater influence of dynamic relative to thermodynamic response in that season (Table 3.2 and Figure 3.7). In the Arctic, however, the models show both stronger and more consistent responses during boreal winter/spring than summer/autumn. Responses in the tropics and southern hemisphere mid-latitudes are quite similar across all seasons. In the Antarctic, there is a high degree of variation across the models in both austral autumn and winter seasons. Seasonal values are often more variable at smaller spatial scales but are nonetheless robust for many large nations such as the Australia, Brazil or the United States, or for some seasons (Figure A1). There is little robust response in precipitation at the local scale (Figure A2) or at the zonal mean scale.

A large body of prior literature has shown that the global mean surface temperature response to well-mixed greenhouse gases scales fairly linearly with the applied forcing (Collins *et al*. 2013; Hansen et al., 2005). Although the response to methane emissions is not exclusively driven by the well-mixed gas methane, roughly three quarters of the forcing comes from non-ozone quasi-uniform forcing, due to methane,

stratospheric water and carbon dioxide; all well-mixed greenhouse gases, and hence it is assumed hereafter that it is a reasonable approximation to scale climate impacts by the methane emission change in a given case relative to that applied in this analysis' modelling.

Although changes in methane forcing are also not perfectly linear with changes in emissions or concentrations, these non-linearities are relatively weak. Furthermore, the non-linearity of forcing relative to concentrations tends to offset the non-linearity in the concentration response to emissions, so that the response of forcing to emissions is closer to linear than either of those

relationships. A reduction of one quarter in the concentration, for example, causes 48 per cent as much forcing as reducing the concentration by half rather than the 50 per cent one would obtain with a linear change. Similarly, a reduction in emissions of half the value used in simulations 1 versus 2 yields a concentration change, using the equation given in Section 3.2, that is 51 per cent as large as that in the simulations, again close to the linear value of 50 per cent. Combining these, a reduction in emissions of half the value used in the simulations hence leads to almost exactly half the forcing used in the simulations.

AREA	ANNUAL	DEC-FEB	MAR-MAY	JUN-AUG	SEP-NOV
Global	0.18 (0.02)	0.19 (0.02)	0.18 (0.04)	0.17 (0.03)	0.17 (0.03)
60° N–90° N	0.28 (0.05)	0.56 (0.08)	0.31 (0.22)	0.07 (0.01)	0.19 (0.19)
30° N–60° N	0.22 (0.10)	0.19 (0.09)	0.19 (0.15)	0.25 (0.09)	0.26 (0.07)
30° S–30° N	0.16 (0.02)	0.16 (0.02)	0.16 (0.03)	0.16 (0.03)	0.18 (0.04)
60° S–30° S	0.12 (0.12)	0.13 (0.11)	0.12 (0.02)	0.11 (0.13)	0.12 (0.09)
90° S–60° S	0.19 (0.11)	0.20 (0.09)	0.29 (0.12)	0.24 (0.24)	0.05 (0.22)

Table 3.2. Multi-model mean area-weighted zonal mean temperature response (°C) to the methane increase from one-half present methane to present value, along with the ozone and stratospheric water vapour responses to that methane increase.

Note: values in parentheses are the 95 per cent confidence interval based on the model-to-model variations, with results in bold statistically significant. These values are responses averaged over one to three decades after emissions changes. Values over the subsequent four decades are ~35 per cent larger and values including carbon cycles feedbacks are ~10 per cent larger, as discussed.
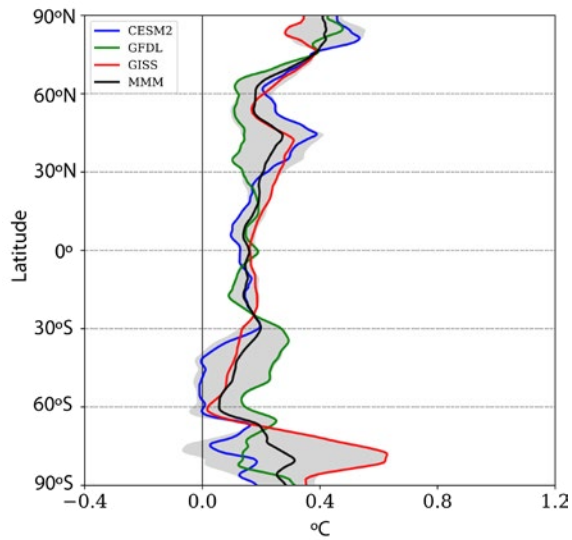
Figure 3.5 Zonal mean annual average temperature response to methane increases from one-half present methane to present value, along with the ozone and stratospheric water vapour responses to that methane increase, degrees centigrade

Note: Shaded area indicated 95 per cent confidence interval based on the three models.

Source: UNEP and CCAC
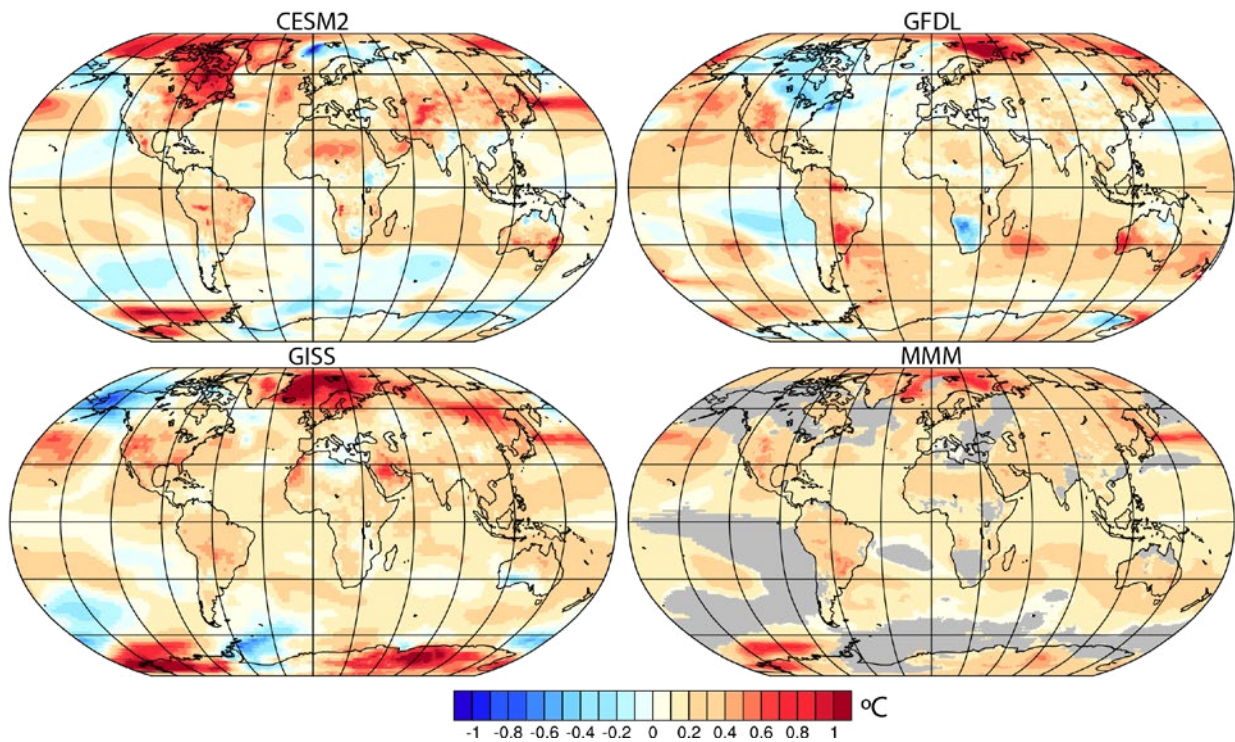
Figure 3.6 Annual average temperature response to methane increases from one-half present methane to present value along with the ozone and stratospheric water vapor responses to that methane increase, degrees centigrade

Note: The multi-model mean (lower right) only includes values for areas in which the value is statistically significant. Non-statistically significant areas are shown in grey.

Source: UNEP and CCAC
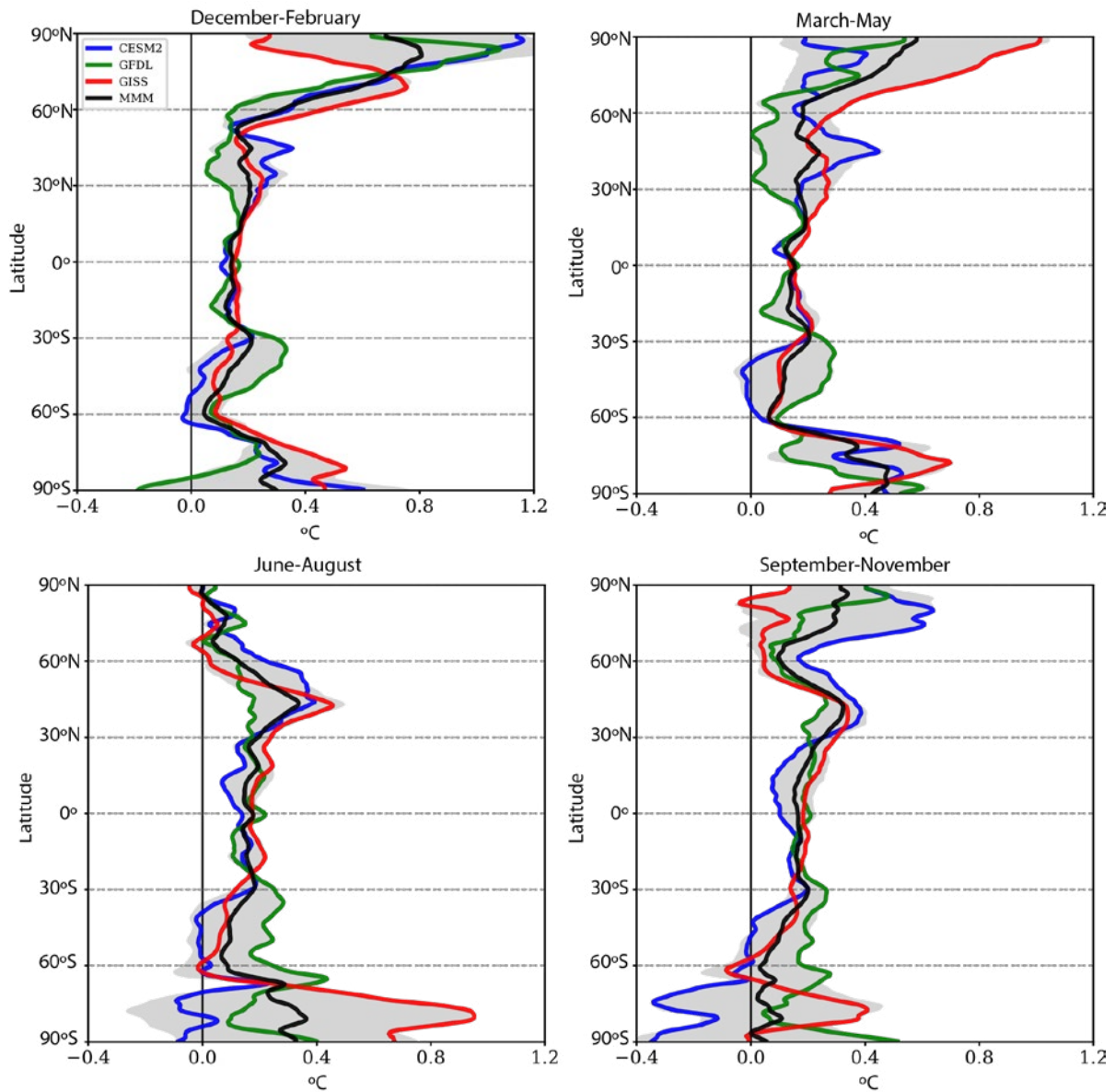
Figure 3.7 Seasonal zonal mean annual average temperature response to methane increases from one-half present methane to present value, along with the ozone and stratospheric water vapor responses to that methane increase, degrees centigrade

Note: Shaded area indicated 95 per cent confidence interval based on the three models.

Source: UNEP and CCAC

3.4 HUMAN HEALTH IMPACTS: METHODS AND RESULTS

Both climate and ozone responses to methane can affect human health through multiple pathways. The relationship between ozone exposure and respiratory mortality and morbidity is well-established. Cardiovascular impacts from ozone exposure have also been identified. Climate change can affect human health in many ways, including the spread of vector- and water-borne diseases, undernutrition and food safety and security-related illnesses, and exposure to weather extremes such as heatwaves, floods and storms. The focus here is on the current impacts and projected risks of changing exposure to high ambient temperatures as this is the best quantified climate-related health impact.

In addition to the ozone and surface temperature related impacts on human health quantified here, other impacts from changes in methane emissions are likely to exist but are not analyzed in this assessment. Changes in stratospheric ozone attributable to methane emissions, for example, could affect human and ecosystem health by altering the flux of ultraviolet (UV) radiation reaching the surface. Policy changes that affect methane emissions could also have indirect effects on well-being. Fuel switching away from natural gas, for example, could reduce injuries related to pipelines. From January 2010 to November 2018, fossil fuel pipelines in the United States are estimated to have resulted in more than 5 500 accidents, with effects including 800 fires, 300 explosions, 600 injuries and 125 fatalities according to an analysis of data from the Pipeline and Hazardous Materials Safety Administration (Kelso 2018). Other potential ways of reducing methane emissions, such as transitioning to healthier diets in areas where consumption of cattle-based products is above recommended guidelines, could have profound health benefits (Springmann *et al*. 2016). Hence the effects reported here are likely to represent a conservative estimate of the overall health impacts of methane emissions or policy/behavioural changes that could lead to methane emissions reductions.

3.4.1 OZONE-RELATED MORTALITY

What are the impacts of ozone and heat exposure on human mortality? Long-term exposure to ozone can cause inflammation and allergic responses leading to respiratory mortality, as well as the development of a systemic oxidative, proinflammatory environment that can increase

the risk of cardiovascular diseases. This analysis of the impacts of ozone exposure on premature death is based on the responses reported in one of the largest studies to date that uses the American Cancer Society Cancer Prevention Study-II (ACS CPS-II) cohort (Turner *et al*. 2016). which calculated cause-specific deaths attributable to incremental changes in MDA8 using a version of this cohort that spans 22 years of follow-up and included 669 046 subjects of whom 237 201 died. Here these results are used globally, implicitly assuming that these long-term ozone exposure-response relationships are homogeneous across populations. While there is evidence from other cohort studies in Canada (Crouse et al. 2015) and in the United States, including a cohort of ~61 million elderly people (Di et al. 2017), showing a significant relationship between long-term, seasonal to annual, ozone exposure and premature mortality, none of the smaller cohort studies conducted in European countries have reported a statistically significant relationship between ozone and mortality (Bentayeb et al. 2015; Carey et al. 2013,). This may be due to differences in study design, for example, the study of the French cohort (Bentayeb et al. 2015) has a 95 per cent confidence interval that is more than an order of magnitude larger than other studies, such as exposure estimation methods, length of follow-up and number of events (Jerrett et al. 2013). No studies are available for Africa, Asia, Australia or South America.

Premature mortality attributable to long-term ozone exposure is calculated using well-established methods (Malley *et al*. 2017; Anenberg *et al*. 2010), as described in the equations below.

$$\Delta X = \begin{cases} O & if\,[O_3] \le TMREL \\ [O_3] - TMREL & if\,[O_3] > TMREL \end{cases}$$

$$AF = 1 - exp^{-\beta \Delta X}$$

$$\Delta Mort = y_0 \times AF \times Population$$

where TMREL is the theoretical minimum risk exposure level (i.e. the counterfactual) in parts per billion by volume, ΔX is the ozone exposure in a particular grid box above the TMREL, β is the exposure-response function – i.e. the slope of the log-linear relationship between the change in exposure and mortality from the epidemiological study, AF is the attributable fraction of the disease burden related to long-term ozone exposure, y0 is the cause-specific baseline mortality rate, population is the population count in a particular grid box of people aged

30 years or older, and ΔMort is the estimated number of premature, cause-specific mortalities attributable to exposure to ozone levels above TMREL. Note that TMREL is set simply as the minimum ozone exposure reported in the epidemiological study, in this case 26.7 ppbv for the annual maximum daily 8-hour average. There is no compelling evidence that exposure to levels lower than those at which data is available is safe, however. Hence this aspect of the method is a conservative one.

Though the exposure-response function is uniform worldwide, geographic variation in age-binned values of both population and baseline mortality rates is included. Population statistics from the United Nations Population Division for each country[8] for the year 2015 are distributed to grids using population density data from the Gridded Population of the World (GPW) version 4 (CIESIN 2016). Baseline mortality rates, which are the ratio of total deaths within a particular age bin due to a particular cause, such as respiratory deaths, to the total population in a particular age bin, were derived by the Global Burden of Disease (GBD) project (GBD 2017) for each country of the world and the values for 2015 were used for consistency with the population dataset. Global Burden of Disease baseline mortality rates were mapped to best match the current International Classification of Diseases (ICD) codes for respiratory and cardiovascular disease related deaths (respectively ICD-10 Codes: J00-J98; GBD Codes: B.3, A.2.3, A.2.4, and ICD-10 Codes: I20-I25, I30-I51, I60-I69, I70; GBD Codes: B.2.2, B.2.3, B.2.8, B.2.9, B.2.10) for which significant impacts were found in the epidemiological study (Turner *et al*., 2016). In addition to this primary analysis based upon 2015 population and baseline mortality, an analysis focused on the year 2030 was also performed to explore how the benefits of future policies might compare to those from changes in the recent past or present. Projections for 2030 baseline mortality rates are obtained from the International Futures project version 7.53 (International Futures 2020) for respiratory and cardiovascular deaths by age group. Population projections for 2030 were taken from SSP2 though these are fairly similar across the shared socioeconomic pathways at this date (KC and Lutz 2017). The geographic distribution of population is unchanged in the 2030 analysis, so too is the age distribution of the population – only population totals are projected under the shared socioeconomic pathways.

8. https://esa.un.org/unpd/wpp/DataQuery

Note that a statistically significant impact on deaths associated with diabetes was also reported but resulted in few total deaths and is not included here. Cause-specific risk increases per 10 ppbv were 1.12 (1.08–1.16; 95 per cent confidence interval) for respiratory diseases and 1.03 (1.01–1.05; 95 per cent confidence interval) for cardiovascular diseases based on the two-pollutant model, accounting for exposure to fine particulate matter, of the epidemiological study (Turner *et al*. 2016). All impacts reported here are based on ozone responses to sustained (rather than pulse) methane emission changes.

Overall, in the primary analysis for 2015 conditions, the 50 per cent reduction in methane leads to 99 000 (62 000–132 000; 95 per cent confidence interval) fewer premature respiratory and 92 000 (28 000–150 000; 95 per cent confidence interval) fewer cardiovascular deaths due to ozone exposure, which corresponds to ~1 400 fewer total deaths per million tonnes of methane emission reductions. Of these, a similar fraction is attributable to respiratory and cardiovascular related deaths, respectively 740 (460–990; 95 per cent confidence interval), and 690 (210–1120; 95 per cent confidence interval), with the uncertainty range on the latter markedly larger. At the national scale, this leads to the largest total impacts occurring in countries with large populations, namely China, India, Japan, Russia and the United States (Figure 3.8). On a per person basis, however, impacts maximize in lower latitude regions where ozone responses are largest and especially in those nations where baseline health conditions are relatively poor. Per person impacts are greatest in Ukraine, Lesotho, Egypt, Georgia, the Democratic People's Republic of Korea, Afghanistan, Bulgaria, Serbia, Uzbekistan and Eritrea (in that order). The United Kingdom, at 13th, is the highest impacted on a per person basis of Organisation for Economic Co-operation and Development (OECD) countries.

In the analysis using 2030 population and baseline mortality, the 50 per cent reduction in methane leads to 105 000 (66 000–140,000; 95 per cent confidence interval) fewer premature respiratory deaths and 81 000 (25 000–132 000; 95 per cent confidence interval) fewer cardiovascular deaths due to ozone exposure. Respiratory-related deaths hence increase by 6 000 relative to the 2015 analysis, due to increases in, for example, India, 1400; the United States, 600; Indonesia, 300; Mexico, 200, and many countries in Western Europe

that are partially offset by decreases in China, -600, and many countries in Eastern Europe. In contrast, cardiovascular-related deaths for 2030 are 11 000 fewer than those in the 2015 analysis due to decreases in, for example, China, -6 000; Russia -1000; Germany, -400; India, -500; Indonesia, -400; Japan, -400; and the United States, -400, that are offset by increases in some other nations such as Pakistan, +200. There is a divergence in response between respiratory and cardiovascular deaths due to differences in projected changes in baseline mortality rates. In China, for example, mortality rates for cardiovascular disease are projected to decrease across all age groups whereas mortality rates for respiratory disease are projected to drop only for those aged 45–70 and rise for both younger and older populations. In the United States, mortality rates for cardiovascular disease are again projected to decrease across all age groups whereas mortality rates for respiratory disease are projected to drop for those aged less than 80 while rising for the 80+ age group, with a decrease in mortality rates in some younger populations, such as those aged 75–80, being outpaced by the projected growth in the population within that age bin. Similar trends are at work in other nations, for example, in India population is projected to increase by 17 per cent but this is outweighed for cardiovascular deaths by projected reductions in baseline cardiovascular mortality rates which is not the case for respiratory health. Given the generally modest differences between these results, only the primary 2015 analysis is reported hereafter but it should be noted that, in particular for analyses focused only on the better-constrained respiratory-related deaths, the 2030 global impacts are likely to be ~6 per cent larger.

Globally, roughly 40 per cent of avoided respiratory-related premature deaths are in those aged 80+, with about 28 per cent for people in their 70s and 18 per cent for those in their 60s. These values vary substantially, however, at the national level. Two thirds to three quarters of avoided deaths are for 80+ year-olds in many European countries, including France, Sweden, Switzerland and the United Kingdom, whereas that age group experiences less than one third of the total impact in several populous developing countries such as India, Indonesia and Pakistan, which instead see larger effects on populations

in their 70s and sometimes in their 60s. Values are similarly distributed for cardiovascular deaths. At the global level, for example, 36 per cent of avoided premature cardiovascular-related deaths are people aged 80+, 36 per cent for those in their 70s and 20 per cent for people in their 60s. Unlike age, current epidemiological studies do not report whether there are gender differences in exposure-response functions.

As shown in Figure 3.4, the ozone exposure metrics respond nearly linearly to methane changes. Using the methods described to calculate premature mortality attributable to long-term ozone exposure, the linearity of this impact to changes in methane were investigated. It was assumed, based on Figure 3.4, that the MDA8 ozone responds linearly to methane changes and so this test examines the linearity of the exposure-response function. Over a wide range of methane emission reductions, national-level responses are highly linear (Figure 3.9). This is because the national average MDA8 ozone changes in response to methane are fairly small, ranging from a 1 to 4 ppbv decrease in response to half anthropogenic emissions reductions –134 Mt. Such small changes in methane do not induce substantial non-linearity through the exposure-response exponential function, nor do they cause national exposures to pass the TMREL threshold. The threshold is not passed as countries in the Northern Hemisphere are typically well above the 26.3 ppbv threshold used here, whereas the few nations with very low exposures, such as New Zealand or Papua New Guinea are already below the threshold. A few countries, including Australia, Colombia and Uruguay, have national exposures within a few parts per billion by volume of the threshold and hence could easily see non-linear behaviour were methane to be reduced in concert with other pollution changes, but with methane changes alone only a few island countries cross the TMREL threshold. These results hold for both respiratory and cardiovascular premature deaths. It can thus be concluded that the modelled response to a 134 Mt change in methane emissions can be linearly scaled to yield a highly accurate estimate of per million tonne responses. Scaled results for the countries most affected are given in Table 3.3 and a full list is given in the Annex.
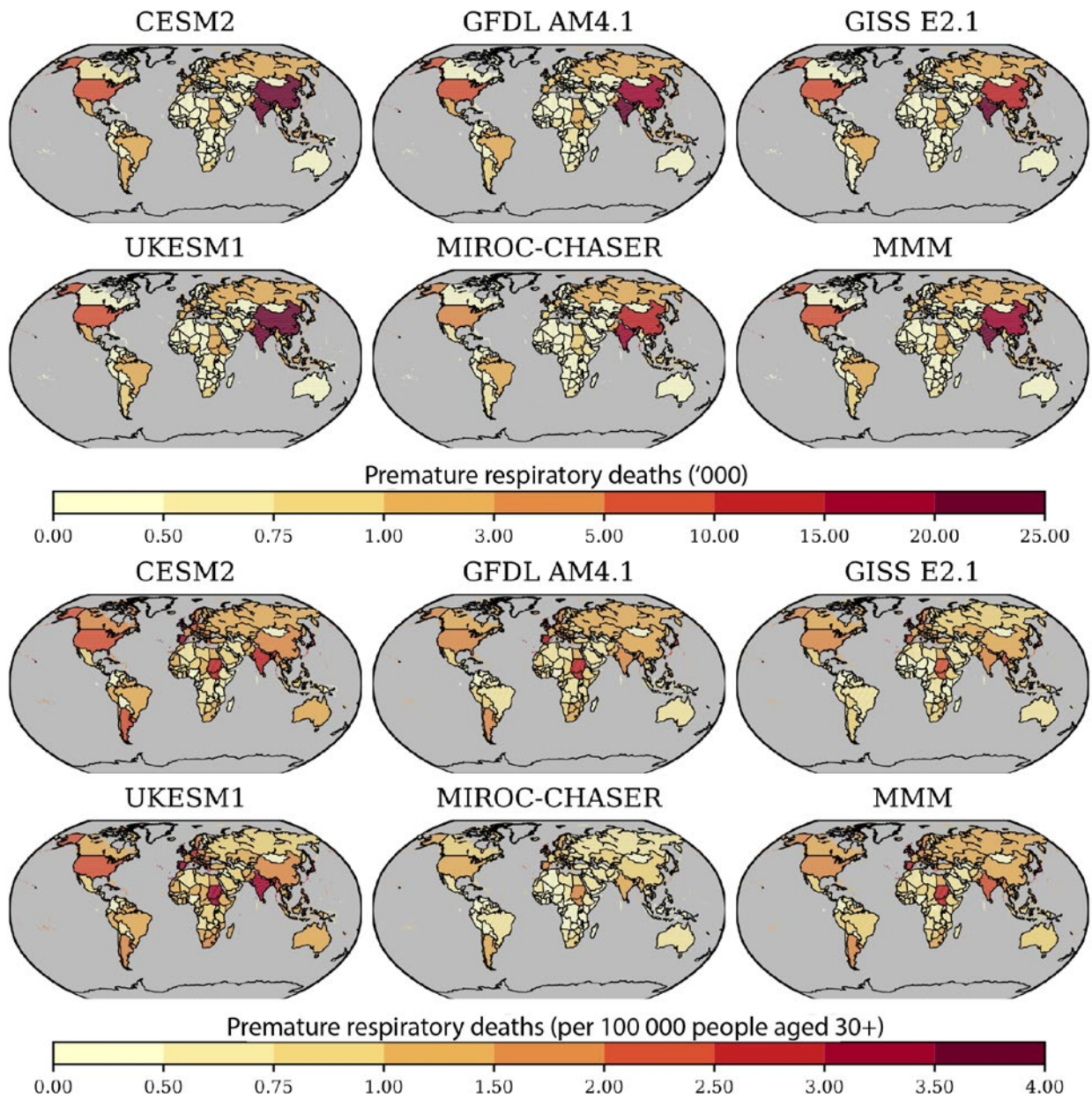
Figure 3.8 National total premature respiratory death changes between present-day (2015) and one-half anthropogenic methane simulations in five different models and the multi-model mean

Note: Values are given as totals and per 100 000 people aged 30 or over.

Source: UNEP and CCAC
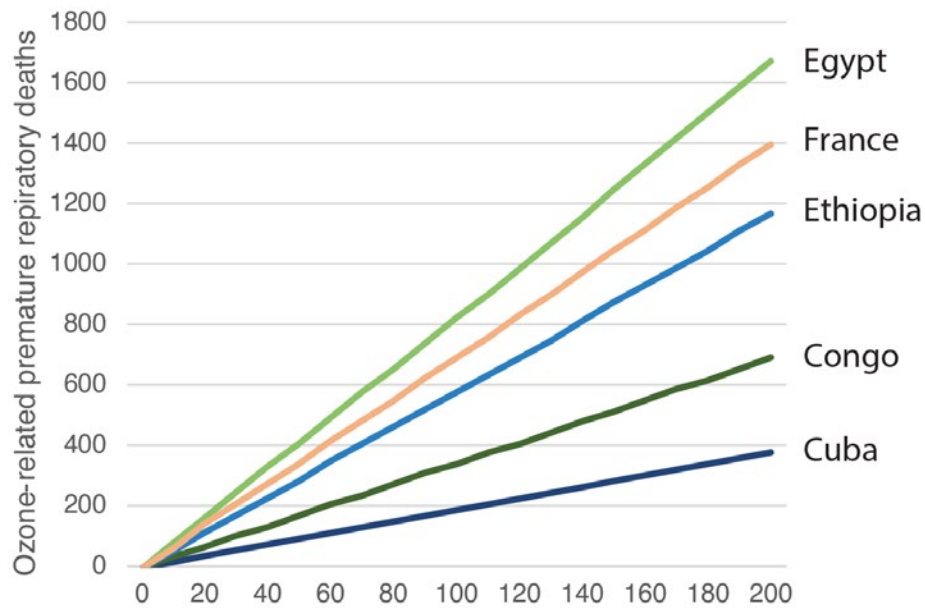
Figure 3.9 National-level reductions in ozone-related premature respiratory deaths associated with the given decrease in methane emissions, 5 selected countries

Note: Developed using the exposure-response function described in the text and assuming a linear response of the maximum daily eight-hour average ozone to methane change.

Source: UNEP and CCAC

Table 3.3 Modelled total deaths and per million people aged 30+ per 10 Mt methane, 10 highest countries

RESPIRATORY							
COUNTRY	TOTAL	LOW	HIGH	COUNTRY	PER MILLION	LOW	HIGH
India	2 045	1 169	2 863	Lesotho	5.1	3.5	6.5
China	1 419	948	1 831	Korea Dem. People's Rep.	4.5	3.2	5.7
United States	428	287	553	Eritrea	4.1	2.5	5.6
Japan	251	176	316	United Kingdom	3.8	2.5	5.0
Brazil	160	100	216	India	3.5	2.0	4.9
Pakistan	159	98	215	Portugal	3.2	2.1	4.2
United Kingdom	157	102	207	São Tomé and Principe	3.2	2.0	4.3
Indonesia	154	86	219	Guinea-Bissau	3.1	1.6	4.6
Germany	121	79	160	Zimbabwe	3.1	2.0	4.1
Russia	109	71	143	Denmark	3.1	2.1	4.0
CARDIOVASCULAR							
COUNTRY	TOTAL	LOW	HIGH	COUNTRY	PER MILLION	LOW	HIGH
China	1 566	502	2 522	Ukraine	6.5	2.1	10.8
India	1 122	297	1 844	Georgia	5.4	1.8	8.7
Russia	379	122	624	Uzbekistan	5.3	1.8	8.4
United States	333	108	540	Bulgaria	5.3	1.7	8.6
Pakistan	225	65	365	Egypt	5.1	1.7	8.2
Indonesia	219	57	368	Serbia and Montenegro	4.9	1.6	8.0
Egypt	194	64	310	Belarus	4.8	1.5	7.9
Ukraine	193	61	3`18	Lithuania	4.7	1.5	7.7
Japan	148	50	236	Latvia	4.3	1.4	7.2
Germany	133	42	218	Afghanistan	4.3	1.5	6.9
RESPIRATORY + CARDIOVASCULAR							
COUNTRY	TOTAL	LOW	HIGH	COUNTRY	PER MILLION	LOW	HIGH
India	3 167	472	5 567	Ukraine	7.6	1.7	13.2
China	2 984	729	5 003	Lesotho	7.5	2.0	12.6
United States	761	189	1 284	Egypt	7.3	1.9	12.1
Russian	488	117	839	Georgia	7.2	1.9	12.1
Japan	399	108	659	Korea Dem. People's Rep.	6.9	1.9	11.4
Pakistan	384	74	659	Afghanistan	6.8	1.9	11.1
Indonesia	373	52	671	Bulgaria	6.7	1.6	11.5
Egypt	276	72	457	Serbia and Montenegro	6.4	1.5	11.0
Brazil	255	54	447	Uzbekistan	6.3	1.7	10.4
Germany	254	60	436	Eritrea	6.1	1.2	10.8

In prior modelling (Shindell *et al*. 2012; UNEP/WMO 2011), each million tonne of methane was estimated to lead to 340 premature deaths per year due to ozone (220–490; central 66 per cent confidence interval). The new value of ~1 400 is roughly four times greater. In large part, the increase in the estimated impact stems from the use of the updated epidemiology based on the extended ACS CPS-II cohort relative to the epidemiology based on the earlier version of this same cohort (Jerrett *et al*. 2009). The newer analysis of this cohort includes not only a greater impact of ozone on respiratory mortality but also the addition of the impact of ozone on cardiovascular mortality. Additional studies on the links between ozone exposure and cardiovascular mortality would be useful as the evidence base for this outcome is less robust than that for respiratory mortality. For example, the US Environmental Protection Agency recently published an *Integrated Science Assessment for Ozone* in which it noted that a limited number of epidemiologic and animal toxicological studies contribute new evidence characterizing the relationship between long-term ozone exposure and cardiovascular health effects. That evidence includes epidemiologic evidence that long-term ozone exposure may be associated with blood pressure changes or hypertension among different life stages or those with pre-existing disease, as well as toxicological evidence of inflammation, oxidative stress, and impaired cardiac contractility in rodents following long-term ozone exposure. Their assessment concluded that the evidence of the relationship between long-term ozone exposure and cardiovascular health effects is suggestive of a causal relationship, but not more definitive. Given the differences in their evidence bases, this assessment presents the results for respiratory and cardiovascular impacts separately.

Additionally, the newer epidemiology uses the metric of the maximum daily 8-hour average over the entire year whereas the older one was based on the warm-season maximum daily 8-hour average. As methane is particularly important during winter months, the response to methane is virtually certain to have been enhanced by the change in the metric. We note that the relationship between ozone exposure and premature death, including exposure timing and ozone-attributable risk, is still an active area of scientific investigation. Total deaths per million tonnes of methane attributable solely to respiratory impacts are, as noted, 740 (460–990; 95 per cent confidence interval). Hence the results here for respiratory impacts are roughly double those found in the earlier work. Previous analyses found a 32–50 per cent increase in respiratory only impacts using the larger, extended cohort relative to the older risk estimates (Seltzer *et al*. 2018) based on observed ozone rather than the response to methane. This suggests that much of the increase may be related to the metric change, with an additional portion potentially due to the use of newer models of atmospheric chemistry and new emissions datasets for non-methane species that affect ozone.

It should be noted that the larger impact of ozone on health has been reported in several previous studies. Malley *et al.* (2017) used the new health exposure relationships (Turner *et al*. 2016) along with modelled ozone distributions, and found a 125 per cent increase in respiratory deaths attributable to ozone exposure in 2010 compared to previous estimates – 1.04–1.23 million deaths compared to 0.40–0.55 million. Using observed ozone data for the China, Europe and the United States, where coverage is fairly complete combined with statistical infilling of missing data, another recent study showed that by including both respiratory and cardiovascular impacts of ozone based on the Turner *et al*. (2016) epidemiology impacts were 153 per cent larger across the three regions than the values with the prior epidemiology, which included respiratory effects only (Seltzer *et al*. 2018). Hence the larger impacts are robust despite the tendency of models to overestimate surface ozone concentrations. Further to this, a bias-adjusted model recently reported total worldwide ozone-related premature deaths of 1.0 ± 0.3 million (Shindell *et al*. 2018). The value for respiratory-related premature deaths due to ozone was 0.6 ± 0.2 million for 2010, and 1.0 ± 0.3 million without bias adjustment, the latter being consistent with the value reported by Malley *et al*. (2017).

3.4.2 HEAT-RELATED MORTALITY

Exposure to heat, even at temperatures that are moderately hot, can compromise the body's ability to regulate its internal temperature, potentially resulting in heat exhaustion, hyperthermia, worsening of chronic conditions and heatstroke, leading to temperature-related deaths

(Sarofim *et al*. 2016; Gasparrini *et al*. 2015; Lee *et al*. 2014). Small temperature changes at mild or moderate temperatures can have larger health impacts than changes at extreme levels, such as during heatwaves or cold snaps, since they occur more frequently (Wellenius *et al*. 2017; Sarofim *et al*. 2016; Gasparrini *et al*.

2015). Heat exposure is currently the primary weather-related illness in the United States, with millions affected annually (Luber and McGeehin 2008). Cold-related mortality is not addressed here given its complexities and uncertainties. In particular, it is unclear to what extent empirically derived cold-related impacts are likely to reflect causal mechanisms given that other confounding affects such as influenza occur with a similar seasonality. Exposure to both heat and high humidity contribute to health impacts (Buzan and Huber 2020; Li *et al*. 2020). Though humidity changes are not explicitly accounted for here, since the epidemiological exposure–response relationships are based on temperature alone, they are implicitly included to some extent as humidity changes are highly correlated with global-scale surface air temperature changes that are included in the long-term epidemiological studies. Epidemiological studies have also reported that despite the known impacts of high humidity on health, there is little evidence that using heat indices that account for both temperature and humidity provides a better fit to the observed mortality data (Armstrong *et al*. 2019).

In the case of premature deaths owing to heat exposure, impacts based on the climate response simulations (C1 and C2) are analyzed here. The analyses are focused on China and the United States as detailed generalized exposure–response relationships have been derived for these two nations from a substantial body of local epidemiological evidence. Most prior studies have relied on city-specific epidemiological studies that created local exposure response functions for the influence of heat exposure on human health (Weinberger *et al*. 2017; Schwartz *et al*. 2015; Honda *et al*. 2014). Based on the available city-specific exposure–response functions for the United States, generalized functions that were shown to be applicable nationwide were recently developed (Shindell *et al*. 2020). These capture the geographic variation in the observed epidemiological functions by including a dependence on local climatic conditions, which may also incorporate at least a portion of localized differences in humidity.

As climate responses are evaluated for one to three decades after emissions reductions take place, the generalized exposure–response functions to the 2030 population were applied together with baseline mortality data using the sources described above for ozone-related deaths. In this instance, based on the underlying epidemiological studies, impacts of heat were applied as an altered all-cause risk rather than

cause-specific as for ozone. Hence all-cause all-age mortality projections were used along with projected population changes, again with the geographic distribution of population unchanged. Based on results described in Ma *et al*. (2014), generalized equations have been created for China analogous to those developed previously for the United States (Shindell *et al*. 2020). Briefly, using data from 15 cities in China, relative-risk curves were created from the epidemiological exposure–response functions using a second-order polynomial following the equation $RR = 1 + aT^2 + bT$. The relationship between the coefficients a and b and the local city mean summer temperature (MST) was then derived by linear regression to create a generalized exposure–response function that captured the sensitivity of this function to local climatic conditions, as done for the United States. The result is a generalized polynomial function with the equation:

$$RR = 1 + a_s \times (MST - a_i)T^2 + b_s \times (MST - b_i)T$$

where as and bs were the slopes of the linearly regressed coefficients versus mean summer temperature and ai and bi were the intercepts of the same regressions. The mean summer temperature is unique for each city, and T is the temperature in degrees centigrade above the optimum temperature defined as the value at which relative risk is equal to 1 – set to the 84th percentile of temperatures at a given location.

For the United States, the coefficients are:

$$a_s = -0.0014, \ a_i = 30.9, \ b_s = 0.005, \ b_i = 26.7.$$

For China, the coefficients are:

$$a_s = 0.0037, \ a_i = 21.0, \ b_s = -0.0045, \ b_i = 23.8.$$

Averaged over all available cities, the generalized equations yield results for current conditions (~2010) that are relatively close to those obtained using the local epidemiological results, with values 9 per cent higher for the 15 Chinese cities and 7 per cent lower for the 10 cities in the United States. Hence these generalized equations appear to provide valuable insights into national level impacts of heat exposure. In the analysis conducted for this assessment, the above generalized function at the grid cell level across the China and the United States were applied. As was the case for ozone-related

deaths, epidemiological studies do not provide distinct results according to gender. In the primary calculations, adaptation is not included. In a sensitivity study, the value for the mean summer temperature was allowed to change between the C1 and C2 simulations in order to represent human adaptation to long-term seasonal temperature changes. In a warming climate, for example, United States' cities in cooler regions take on more of the character of warmer cities, becoming less sensitive to heat extremes. In contrast, the optimum temperature is kept fixed at the value from simulation C1 to represent the influence of short-term temperature excursions (see Shindell *et al*., 2020 for additional discussion of adaptation).

It was found that the 50 per cent reduction in methane leads to 2 800 (1 700–3 800; 95 per cent confidence interval) fewer annual heat-related deaths in the United States and 14 000 (6 000–21 000; 95 per cent confidence interval) fewer in China based on the climate response averaged over one to three decades following emissions reductions and accounting for the uncertainty in that national level climate response. For comparison, the total annual ozone-related deaths in these countries are 10 200 for the United States and 40 100 for China. Hence ozone-related reductions in deaths are roughly factors of 3–4 larger. As the ozone-related reductions begin immediately rather than a decade later, they have a larger overall impact on mortality rates in these two countries. Nonetheless, this analysis, especially the results for China, suggests that the human health benefits attributable to reduced climate change are also substantial and that they could contribute a large fraction of total health benefits, in particular in countries with low ozone pollution levels. Based just on these two countries for which data are available, each million tonne of methane emissions mitigation leads to about 125 fewer premature heat-related deaths. The ozone-related deaths in these two countries make up about one quarter of the global total, suggesting that the global total might be roughly 500 fewer premature heat-related deaths per million tonnes of methane if the ratio of China+United States to global heat-related deaths is similar to that for ozone-related deaths.

Potential impacts of adaptation by accounting for the change in summer mean temperatures, as described above, were examined. This led to a reduction in the United States annual heat-related deaths of ~100, or about 2 per cent (0–5 per cent across models). This suggests only weak effects for at least this type of

adjustment to mean climatological changes. Warmer cities in the United States experience less increase in the risk of heat-related mortality per degree warming than cooler cities, so that acclimatization to warmer temperatures leads to reduced risk. In China, however, the opposite is true in that warmer cities experience greater risk per degree of warming. Hence this method of accounting for adaptation was not applied to China. Presumably, the difference between these countries is related to the greater wealth in the United States that allows nearly complete use of air conditioning in warm climates, making them better adapted to heat extremes than cooler climates, whereas air conditioning ownership in China has only expanded rapidly very recently, after the epidemiological studies on which the generalized equation for China is based were performed. Given the minimal changes in the United States and lack of an adequate method for China, hereafter only the values without accounting for possible adaptation are reported, though it is noted that a broader exploration of potential adaptation found that it might reduce impacts roughly by half (Shindell *et al*. 2020; Anderson *et al*. 2018; US EPA 2017).

An additional estimate of wider scale heat-related mortality impacts is based on the national-level responses to national average warm-season temperature changes reported in a recent study (Lee *et al*. 2019). This study reported an increase in national level risk for heat-related mortality as a function of national level warming based on averaging across available local datasets, typically from several urban areas within each country. Regional averages were also provided for most parts of the world, with the significant exceptions of Africa and South Asia. The responses were examined using this much rougher relationship with the results from our spatially explicit response to the distribution of daily temperature values in China and the United States. The national-average seasonal-mean method produced an impact that was 55–57 per cent of that found in the more detailed analyses of China and the United States. Based on the consistency across those countries, and assuming the more spatially and temporally explicit method was the more accurate, all national results from the other method were normalized by dividing by 0.56.

Using this normalized national-average seasonal-mean method, the total across regions with data is 53 000 (39 000–74 000 across the three models). This corresponds to about 390 avoided heat-related deaths per million tonnes of methane emissions reduction.

Given the exclusion of Africa, except for Egypt, which is included as part of the Middle East in this analysis, South Asia and this value appears to be fairly consistent with the estimate of 500 deaths per million tonne of methane from the extrapolation of China and the United States results based on the ratio of the ozone-related impacts in those two countries to the global total. More specifically, the World Health Organization estimated worldwide mortality effects of heat exposure, based on data from Japan alone, and reported that 37 per cent of premature deaths due to heat were projected for 2030 in Africa and South Asia (WHO 2014). Applying this same ratio to the results in this analysis would imply ~600 deaths per million tonne of methane.

Though both large-scale estimates are relatively crude and thus confidence in the precise values is low, they provide an indication of a plausible level of worldwide heat-related mortality impacts, adding to a growing body of evidence for such widespread effects (Carleton *et al*. 2020; Lee *et al*. 2019; WHO 2014). It should also be noted that the Lee *et al*. (2019) study reported that impacts were fairly linear with warming, so that the scaling approach used throughout this assessment appears reasonable for this impact as well, although due to data limitations that specifically could not be examined in this analysis. These results suggest that there are, very roughly, three times more ozone-related deaths than heat-related ones. Additionally, ozone-related deaths would decrease immediately in response to reductions in methane emissions, with ozone-related deaths evolving rapidly over time following the ~12 year adjustment time for methane, whereas heat-related deaths would change more slowly as climate responds, with the values estimated here occurring one to three decades after emissions changes.

3.4.3 MORBIDITY AND LABOUR PRODUCTIVITY

The effect of methane emissions reductions is examined here on two non-fatal health impacts in many countries:

1. hospital admissions due to respiratory illness resulting from ozone exposure; and

2. visits accident and emergency departments due to asthma resulting from ozone exposure.

The change in hours of lost labour due to extreme heat is also quantified, but only in the United States due to data limitations.

3.4.3.1 MORBIDITY AND LABOUR PRODUCTIVITY METHODS

Changes in respiratory hospital admission are evaluated for the population aged 65+ based on decreases in ozone exposure in response to methane emissions reductions. Estimates are based on the epidemiological studies of three groups of investigators, in Canada, Europe and the United States, covering 149 cities globally under the Air Pollution and Health: a European and North American Approach (APHENA) project (Katsouyanni *et al*. 2009). Hospital admissions data were collected from medical records for all respiratory diseases, conditions or infections (International Classification of Diseases, Ninth Revision (ICD-9) codes 460–519). This global effort showed a robust relationship between ozone exposures and respiratory hospital admissions for this age group, without distinguishable geographical difference. This relationship was therefore applied worldwide. As with mortality, the epidemiology does not clearly indicate whether there is any differentiation in risk by gender.

A well-established approach (Fann *et al*. 2018; Heroux *et al*. 2015; WHO 2013) was used to estimate respiratory hospital admissions.

$$AF = 1 - exp^{-\beta\Delta[O_3]}$$

$$\Delta Hospital\ admissions = y_0 \times AF \times Population$$

where β is the exposure-response function, that is the slope of the log-linear relationship between unit change in exposure and respiratory hospital admission, developed from APHENA, AF is the attributable fraction of hospital admissions associated with ozone exposure, y_0 is the baseline hospitalization rate of respiratory diseases among the 65+ age group, and population is the count of 65+ year-olds at each 0.5° x 0.5° grid box. This approach is similar to the method used to calculate mortality, except that no lower exposure threshold is applied for morbidity. Given the short-term nature of the link between respiratory hospital admission and ozone exposure, responses in hospital admissions on a daily basis were estimated and the total summed over a year.

National-level variations result from the uneven distribution of ozone changes, country-specific hospitalization admission or discharge rates for those aged 65+ hospitalized due to respiratory diseases, and population distributions of 65+ year-olds. The exposure–response functions studied in APHENA have used both penalized

spline and natural spline models. For this analysis the average of the two exposure–response functions was calculated, and a relative risk of 1.006 (0.0008–1.012) used for per 10 ppbv of ozone maximum daily 8-hour average (i.e. β is 0.00063 (0.000087–0.0012)). Data on the post-65 population were again from GPW version 4 (CIESIN, 2016), the same dataset used for mortality estimation. Baseline hospital admission data are compiled from multiple datasets. Efforts were made to include all the available datasets representing a baseline level of respiratory hospitalization. The baseline rate of respiratory hospital admissions for the United States was obtained from Environmental Benefits Mapping and Analysis Program – Community Edition (BenMAP-CE) (US EPA 2015), which calculated the baseline respiratory hospital admission rate by age-groups from the Healthcare Cost and Utilization Project (HCUP) 2014. This is also the only available dataset that reports age-specific rates. The all-age rate for respiratory hospital admissions for China was obtained from China's *2016 Health and Family Planning Statistics Yearbook* (NHFPC, 2016) while the all-age hospital discharge rate for respiratory diseases for European countries came from Eurostat (Eurostat, 2016). Hospital discharge rates here, which are virtually the same as the hospital admission rates, include "*finalisation of treatment, signing out against medical advice, transfer to another healthcare institution, or because of death*". To transform the all-age rate to the 65+ rate in China and Europe, a ratio of 3.30:1 was applied, which was the average ratio of hospital admissions between those aged 65+ and all-age groups that was calculated from the United States dataset. Finally, the annual hospital admission rates were divided by 365 to obtain a daily average hospitalization rate. Given the limited availability of data, this compiled dataset of 35 countries from multiple sources was not ideal and may have introduced heterogeneity. In particular, it assumes the ratio between those aged 65+ and all-age groups in China and Europe is the same as that in the United States. It also assumes that there are no seasonal variations in respiratory hospital admissions over the year. The impacts of these heterogeneity and assumptions are, however, likely to be significantly lower than the uncertainty associated with the exposure–response function. Ozone responses are based upon the modelling in simulations 1 and 2.

Asthma-related accident and emergency department visit changes were evaluated for the entire population based upon decreases in ozone exposure in response to methane emissions reductions. Results are based upon the average of epidemiological relationships across three meta-analyses of existing literature that reviewed 22, 26 and 50 studies (Orellano et al. 2017; Zhang *et al*. 2016; Zheng *et al*. 2015). These reviews cover studies in the Asia, Europe and the United States. The approach developed in Anenberg *et al.* (2018) was used to estimate the global asthma accident and emergency department visits due to ozone exposure.

$$AF = 1 - exp^{-\beta \Delta [O_3]}$$

$$\Delta Hospital\ admissions = y_0 \times A\&EV \times AF \times Population$$

where, again, β is the exposure–response function, that is the slope of the log-linear relationship between unit change in ozone exposure and asthma emergency room visits, AF is the attributable fraction, y_0 is the country-specific baseline prevalence rate of asthma for the all-age population, accident and emergency department visits (A&EV) is the fraction of individuals with asthma visiting accident and emergency departments in each country, and population is the all-age population count in each grid box. Note that although accident and emergency department visits are a short-term morbidity impact, estimation is usually based on the relationship with an annual change of ozone exposure. As such, an annual average of ozone exposure changes was calculated using annual maximum daily 8-hour average and the above method applied.

Exposure response functions were applied from the three meta-analyses respectively: Orellano *et al*. (2017): 1.03 (1.01–1.06); Zhang *et al*. (2016): 1.05 (1.04–1.07) and Zheng *et al*. (2015): 1.02 (1.01–1.02). An average of the three results for estimated asthma-related accident and emergency department visits was then calculated. Annual country-specific baseline asthma prevalence rate for the all-age group was collected from the GBD 2018 (Global Burden of Disease Collaborative Network, 2018). The A&EV for available countries compiled by Anenberg *et al*. (2018) was used, which includes multiple national data sources. The final results here are for 56 countries and territories, due to data availability in A&EV . The gridded all-age population was again from GPW version 4 (CIESIN 2016). Ozone responses were again based on the modelling in simulations 1 and 2. As both ozone morbidity impacts are based upon the maximum daily 8-hour average, and prior studies have shown that a sum of daily maximum daily 8-hour averages is very close

to the annual maximum daily 8-hour average (Anenberg *et al*. 2018), the analysis presented previously regarding the linearity of the annual maximum daily 8-hour average (Figure 4.3) applies to these endpoints as well and hence hereafter it is assumed these impacts can be represented by a linear scaling from the results explicitly modelled in this assessment.

Labour losses due to exposure to extreme heat are evaluated using two distinct methods. The first is based on an empirically established exposure–response function for the United States (Graff Zivin and Neidell 2014). To evaluate this exposure–response relationship, nationally representative survey data from 2003–2006 and daily weather observations from roughly 8 000 weather stations were used to investigate how Americans allocate their work and leisure time as a function of ambient temperatures. The authors found a statistically significant approximately linear decrease in the time allocated to labour with increasing temperatures above a threshold of about 29° C for high-risk sectors. This relationship has been used in several recent studies of the United States (Hsiang *et al*. 2017; USGCRP 2018). In the calculations for this assessment, the value of time lost is calculated using county-level annual employment, covering 15–64 year-olds, and annual average weekly wages from the Quarterly Census of Employment and Wages, U.S. Bureau of Labor Statistics. The North American Industry Classification System was used to determine the number of workers in high-risk industries/sectors – largely those that cannot readily be air-conditioned: agriculture, forestry, fishing and hunting; construction; manufacturing; mining; transportation: and utilities. The 2016 fraction of workers in high-risk industries was used for each county. The analysis covers the contiguous United States, that is, excluding Alaska and Hawaii. Surface temperature changes in response to methane emissions reductions are based upon the daily temperature values modelled in simulations C1 and C2. Ninety years of data were used, years 11–40 from each of the three models that performed the C1 and C2 simulations, giving adequate data to establish a clear signal despite the noise inherent in daily temperatures.

The second method is based on a publication (Knittel *et al*. 2020) that appeared after the modelling to support this assessment was already largely completed. The relationship between heat and labour productivity in this study has

the advantage of being applicable globally, but it relates productivity to relative humidity as well as temperature and daily humidity data was only available from an extension of the simulations performed for 20 years with one model as the need for this output had not been anticipated (thought the study that brought this method to our attention relied upon older methods). In the analysis using this method, following Knittel *et al*. and Kjellstrom *et al*. (2018), daily mean and max surface air temperature and daily mean relative humidity were used to represent the wet bulb globe temperature (WGBT) or heat index using the following equation:

$$\text{WBGT} = 0.567{\times}\text{T} + 0.393{\times}\text{Vapour} + 3.94$$

with T as either the daily mean, daily max or the average of those (daily halfmeanmax) 2-metre air temperature, in ºC, and Vapour as the water vapour partial pressure in kilopascals[9]. This equation is representative for light wind conditions and moderately high heat radiation levels typically experienced by outdoor workers. The WBGT minus 4 is used to represent conditions experienced by indoor workers (Knittel *et al*. 2020).

Vapour was calculated using the daily means of relative humidity (RH) and T using:

$$Vapour = \frac{RH}{100}{\times}6.105 {\times}\exp\left(\frac{17.27{\times}Tavg}{237.7{\times}Tavg}\right)$$

The WBGT was then related to work ability (WA) following Knittel *et al*. (2020) based on the work of Bröde *et al*. (2017) and Kjellstrom et al. (2014):

$$WA = 0.1 + 0.9/(1+(WBGT/α1)^{α2})$$

where and are unitless coefficients derived for the three different work intensity categories: light, 24.64 and 22.72; medium, 32.98 and 17.81; and heavy work, 30.94 and 16.64. Light work includes all the service sectors, such as retail sales, wholesale trade, hotels and restaurants, post and telecoms, financial services and insurance, and public administration, and is assumed to be indoors. Medium work includes such sectors as food, textile and wood industries, machinery and electronic equipment, and transport and is

9. Kilopascal = 1000 pascals

likewise assumed to be indoors (i.e. in a shaded or air conditioned space rather than direct sunlight). Heavy work includes the agriculture, forestry and fishery, extraction and construction sectors and is assumed to be outdoors.

Work ability is assumed to be limited to 0.1 to 0.9 (in portion of an hour) to allow for some minimal work and acknowledge that breaks are needed even under optimal conditions. The calculated fractional work loss, WL=1-WA, is then multiplied by the working population, adults aged 15–64, in each country in each work category to get the annual total labour loss due to heat. The lost hours are based on 12 months multiplied by 30 days per month multiplied by 12 hours per day, with a distribution of work that has 4 hours each at daily maximum, daily half mean max and daily mean temperatures; these assumptions have been shown to provide a good approximation of the hourly temperature distribution during the day (Kjellstrom *et al.* 2018). This leads to 4 320 potential work hours per year. The country-specific working population in 2018 for each labour category was based on data from the International Labour Organization (ILO), which includes gender-specific information (ILO, 2020). As in Knittel *et al*. (2020) and Kjellstrom *et al.* (2018), the relationship between WA and WBGT is assumed to be applicable worldwide although the underlying data is largely from more developed nations.

3.4.3.2 MORBIDITY AND LABOUR PRODUCTIVITY RESULTS

The ozone decreases in response to reductions in methane emissions lead to an estimated reduction of 855 annual hospitalizations for persons aged 65+ per 10 Mt of methane in countries for which sufficient data is available. Among those nations, the largest values are seen in China, followed by the United States (Table 3.4; Figure 3.10). Effects are larger than in either of those nations, however, for Europe. Note that data is unavailable to allow these effects to be quantified outside of China, Europe and the United States. In addition, the overall uncertainty range for this impact is quite large, ±84 per cent, owing primarily to the uncertainty in the exposure–response relationship.

The ozone decreases in response to reductions in methane emissions also lead to a decrease in asthma-related accident and emergency department visits, with a response of 43050

fewer cases per 10 Mt methane emission cuts. Note that in comparison with respiratory hospitalizations, there is much more data available and so the impact on asthma-related accident and emergency department visits is quantified for many more nations (Table 3.5a; Figure 3.11). In addition, the epidemiological relationship has a much narrower uncertainty range, so that the overall uncertainty in the change in number of accident and emergency department visits is much smaller at ±37 per cent. Among the many countries for which impacts were estimated, benefits in India are far larger than in any other nation, with more than half the avoided cases taking place there. China ranks second and the benefits distinctly larger than in countries ranking third and lower. Several other countries do see substantial benefits, however, including both developed ones such as the Republic of Korea, Japan and the United States as well as developing countries including Brazil, Ethiopia and Nigeria, all of which see more than 500 fewer accident and emergency department visits per 10 Mt of methane emissions decrease.

As described above, the change in labour losses due to exposure to extreme heat was calculated for the United States only using the first method applied to multiple models. Based on the simulations of the climate response to methane emissions changes, the cooler climate resulting from the methane emission reduction between simulations C2 and C1 leads to 13.6 million (2.2–18.2; 95 per cent confidence interval) fewer lost work hours annually in the United States. This translates to approximately 1.0 (0.2–1.4) million hours per 10 Mt of methane.

The second method provided work loss estimates for most of the world, but in this case from a single model only. It is noted that the second method finds a much larger loss for the United States, namely 44 million fewer lost work hours annually in the United States. The second method is based on the temperature changes simulated in the GISS model and using the first method that model produced an estimate of just 4.8 million lost work hours rather than the 13.6 million lost work hours for the multi-model mean. Hence a multi-model mean with the second method would be likely to find larger impacts than the results based on the GISS model alone. Using the GISS climate simulations, the second method finds that the cooler climate resulting from the methane emission reduction between simulations C2 and C1 leads to 55 billion lost work hours annually (±38 billion based on the

GISS model's interannual variability over the 20 year simulation). Using this global method, effects tend to be greatest in low latitude, humid countries in which the daily heat index or WBGT frequently reaches high values (Table 3.5b; Figure 3.12). This corresponds to ~410 million lost work hours per million tonne of methane emitted, assuming responses are again quasi-linear. Employment within those sectors of the economy that are affected by heat exposure varies across gender, leading to disparities in the impacts for men and women in most countries. While in a few, such as Angola, Uganda, Cambodia, Viet Nam, Azerbaijan, Brazil and Kenya, there is nearly an even split between lost hours for men and women, in most the majority of the lost hours are for male labour, with female labour losses often accounting for only 20–35 per cent of the total (Table 3.5b). Nepal stands out as the only country with substantial losses, millions of hours lost in response to a 134 Mt decrease in emissions, for which the loss of labour is substantially higher amongst women, 59 per cent, while globally 66 per cent of impacts are felt by men and 34 per cent by women.

In a related analysis, the ILO reports that increased heat projected for 2030 could bring productivity losses equivalent to 80 million jobs (ILO 2019). Converting 80 million jobs to hours lost, assuming 50 weeks of 40 hours are worked per year, this translates to roughly 160 billion lost work hours annually. Their analysis hence similarly identifies the potential for large impacts. It also indicates substantial non-linearities in response, with impacts in 2030 nearly 10 times greater than those in 1995 despite 2030 warming being only roughly double the 1995 value. This makes it difficult to compare the results here directly with the ILO's, and also suggests that assuming a linear response as in this assessment provides only a very rough measure of impacts and that the non-linearity of this response merits further characterization.

Table 3.4 Respiratory hospital admissions due to ozone exposure per 10 Mt methane emissions for countries with available data

Note: other countries are likely have impacts as well, though these are not quantified here.

COUNTRY	CASES	COUNTRY	CASES
China	247	Norway	5.7
United States	145	Denmark	4.7
Italy	96	Czechia	4.5
Germany	78	Serbia and Montenegro	4.5
France	59	Slovakia	3.0
Spain	51	Finland	2.5
United Kingdom	45	Croatia	2.4
Poland	21	Slovenia	2.4
Greece	13	Ireland	2.1
Romania	9.9	Lithuania	1.2
Belgium	9.9	Estonia	0.9
Portugal	8.3	Cyprus	0.7
Sweden	8.1	Malta	0.5
Bulgaria	7.2	Luxembourg	0.3
Austria	7.2	Latvia	0.3
Netherlands	6.7	Iceland	0.2
Hungary	6.2	TOTAL	855

The uncertainty range is ±84 per cent.

Figure 3.10 Change in respiratory hospital admissions for people aged 65+ due to ozone exposure change resulting from a 134 Mt change in methane emissions, China, Europe and United States

Note: Based on the multi-model mean ozone change. Values are for China, the US, Europe and China only; although other countries are likely have impacts, these have not been quantified here due to data limitations – grey indicates no quantification.

Source: UNEP and CCAC
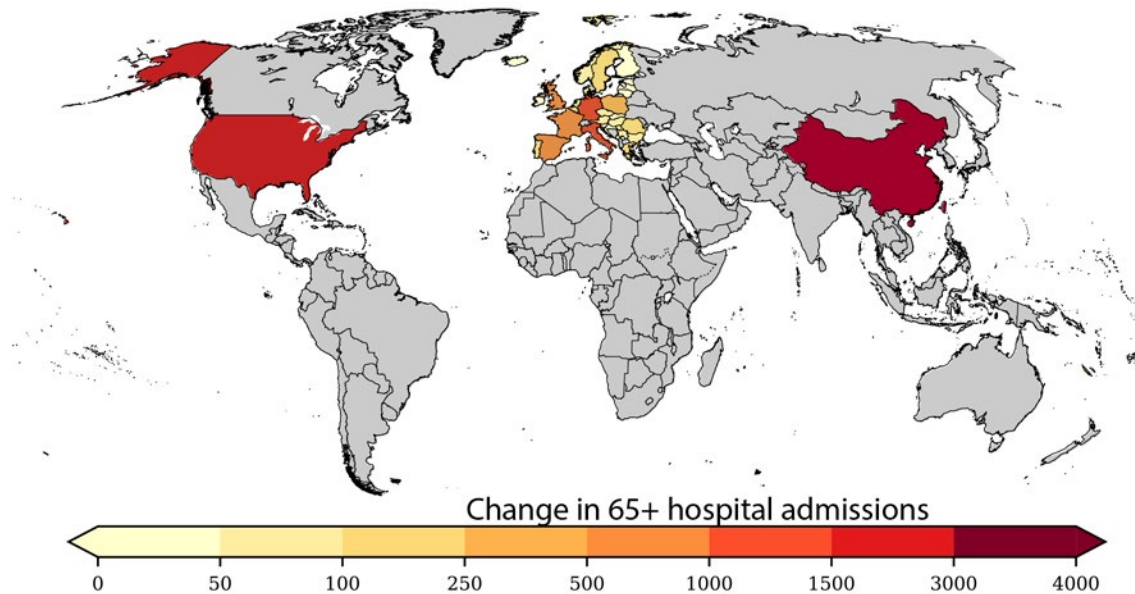
Figure 3.11 Change in asthma-related visits to accident and emergency departments due to ozone exposure change resulting from a 134 Mt increase in methane emissions, all ages, selected countries

Note: Based on the multi-model mean ozone change. Values given for countries with available underlying data – grey indicates no quantification.

Source: UNEP and CCAC
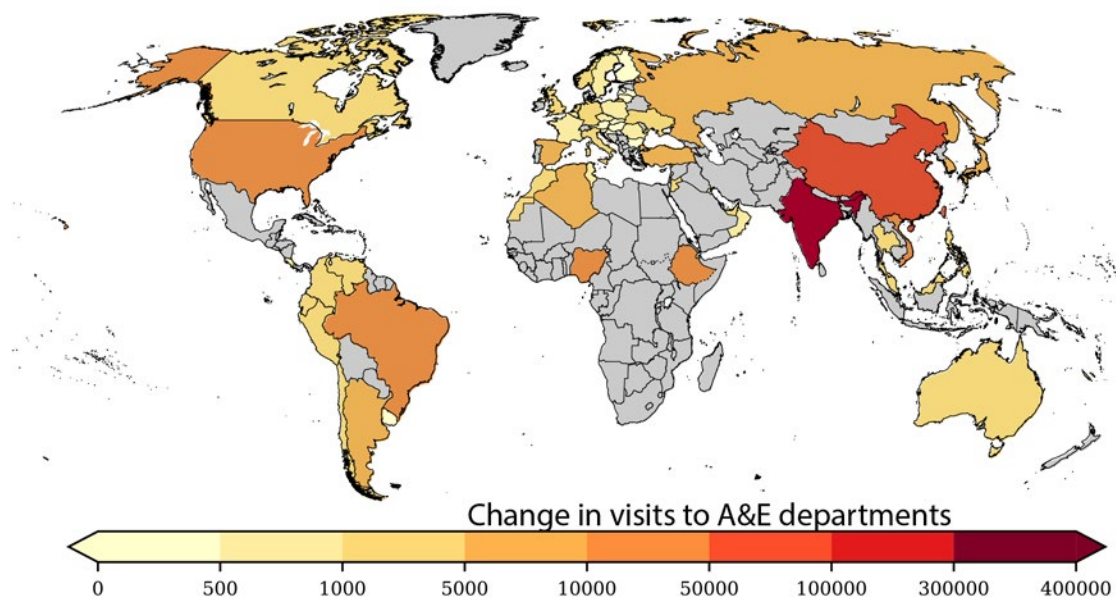
Figure 3.12 Change in lost labour hours due to heat exposure resulting from a 134 Mt increase in methane emissions, selected countries, million hours

Note: Values given for countries with available underlying data and statistically significant temperature responses – grey indicates no quantification.

Source: UNEP and CCAC
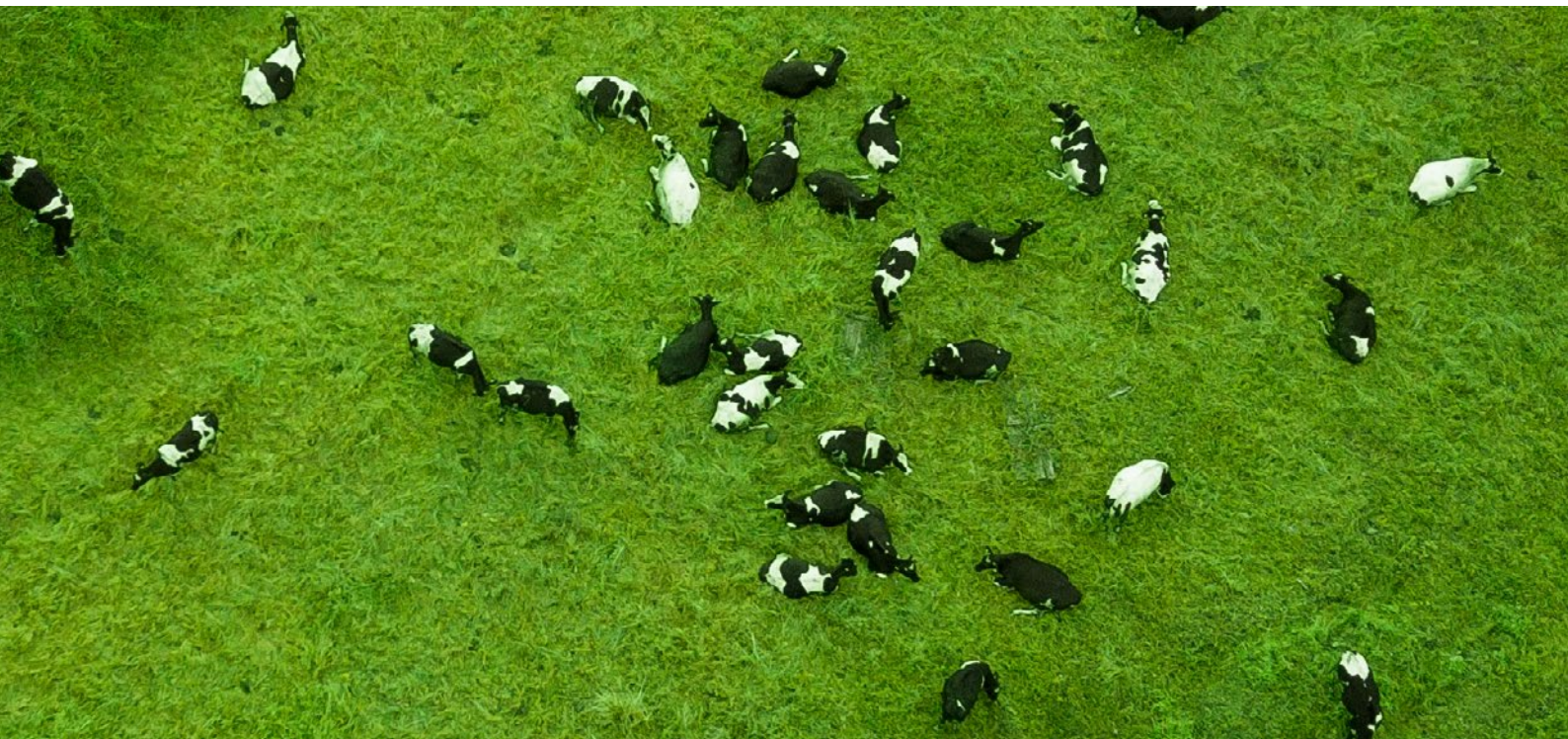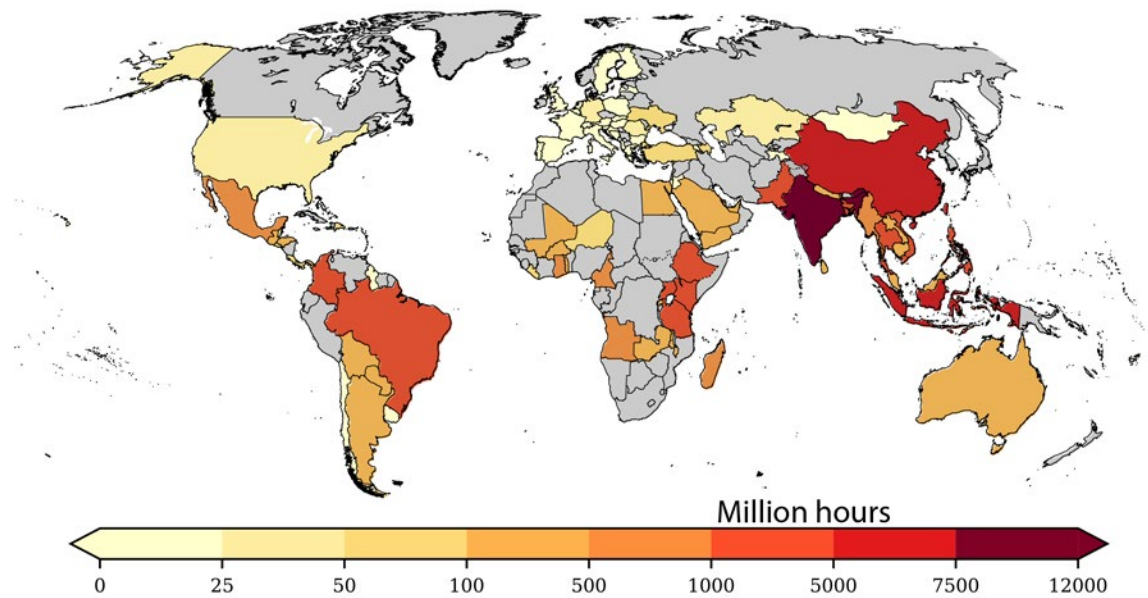
Table 3.5a. Asthma-related accident and emergency department visits due to ozone exposure, all age groups, per 10 Mt of methane emissions

COUNTRY	CASES	COUNTRY	CASES
India	23 000	Australia	110
China	7 200	Norway	108
United States	1 500	Jordan	95
Brazil	1 100	Italy	83
Ethiopia	1 100	United Arab Emirates	81
Nigeria	1 100	Poland	69
Viet Nam	860	Sweden	64
Turkey	580	Lebanon	63
Russia	570	France	63
Korea, Rep.	530	Costa Rica	56
Japan	510	Czechia	51
Argentina	410	Romania	47
Algeria	380	Oman	46
Spain	380	Belgium	46
Colombia	360	Tunisia	40
Thailand	345	Kuwait	38
Peru	308	Hungary	35
Morocco	261	Austria	26
Venezuela	246	Finland	23
Canada	224	Croatia	23
Ukraine	220	Uruguay	18
Philippines	161	Bulgaria	17
Germany	150	Singapore	17
Ecuador	133	Slovakia	15
United Kingdom	121	Latvia	12
Netherlands	114	Slovenia	12
Malaysia	113	Lithuania	10
Chile	111	**TOTAL**	**43 050**

The uncertainty range is ± 37 per cent.

Table 3.5b. Reduced labour losses due to heat exposure resulting from a 134 Mt decrease in methane emissions for the nations with the 15 largest number of hours lost

COUNTRY	LOST WORK HOURS (MILLION)	LOSSES FOR WOMEN (%)
India	12 000	22
China	6 700	39
Indonesia	5 900	32
Brazil	4 900	44
Viet Nam	2 300	45
Ethiopia	2 200	41
Philippines	1 700	19
Bangladesh	1 600	32
Thailand	1 400	42
Tanzania	1 200	47
Uganda	1 200	51
Pakistan	1 200	23
Colombia	1 100	36
Kenya	1 100	50
Mexico	800	17
GLOBAL TOTAL	55 000	34

The uncertainty range is ± 70 per cent.

3.5 CROP IMPACTS: METHODS AND RESULTS

Methane also plays a significant role in reducing crop yields and the quality of vegetation. Ozone exposure is estimated to result in yield losses in wheat, 7.1 per cent; soybean,12.4 per cent; maize, 6.1 per cent; and rice, 4.4 per cent for near present-day global totals (Mills *et al*. 2018; Shindell *et al*. 2016; Avnery *et al*. 2011a). Impacts on these four crops for which robust ozone concentration-response functions are available, were evaluated using an empirical crop model based on statistical relationships for the impacts of temperature, precipitation, carbon dioxide concentrations, and ozone, rather than plant level simulations (Shindell *et al*. 2019). Wheat, maize and rice responses to changes in meteorological variables are based on a meta-analysis of more

than 1 000 modelling studies (Challinor *et al*. 2014), incorporating relationships observed in field studies. Responses for soybeans to temperature are based upon a separate study (Zhao *et al*. 2017) as those were not included in the meta-analysis. Separate temperature response coefficients for wheat, maize, and rice are included according to temperate or tropical conditions. For ozone, the M7 and M12 exposure metrics, the mean 7- or 12-hour daylight exposure during the growing season, depending on the crop, are used. These affect yields based on the response reported in field studies (Wang and Mauzerall 2004), and have been used previously for global crop modelling (Van Dingenen *et al*. 2009). The growing season is locally defined based on Van Dingenen *et al*. (2009). Changes in temperature, precipitation

and ozone in response to methane emissions changes are taken from the simulations performed for this assessment. In addition, a small amount of carbon dioxide is formed when methane is oxidized. This carbon dioxide response fertilizes crop growth, especially for C3 plants such as wheat, soybeans and rice with only very small effects for maize, a C4 plant (C3 and C4 refer to the type of photosynthesis used by the plant to create energy, with the first carbon compound produced containing either 3 or 4 carbon atoms). These effects are included here based on relationships described previously (Tebaldi and Lobell 2018). Crop distributions for 2010 were taken from the Food and Agricultural Organization of the United Nations (FAO) data sets[10] and are maintained at those levels in all calculations of impacts – no projected changes in crop areas are included. It is noted that ozone has additional detrimental impacts on ecosystems, including the loss of protein content in grains, loss of forage quality in grasslands, and losses in forest productivity and carbon uptake.

The effects of ozone and temperature dominate the response, with only minimal impact from projected changes in precipitation or carbon dioxide at large scales, as in prior analyses (Shindell *et al*. 2019). The relative importance of temperature change versus ozone change varies across crops and locations. They are, for example, similar in importance for maize, but temperature has a much larger impact than ozone on tropical wheat, whereas ozone dominates for soybeans in most locations and is larger for rice in many nations. Based on the quasi-linearity of the responses of both ozone and temperature to methane emissions changes, the modelled impacts were converted to crop impacts per unit methane emission.

The global totals for a 50 reduction in anthropogenic-related methane increases, a 134 Mt decrease in methane emissions, are avoided yield losses of 7.46 Mt of wheat, 2.23 Mt of soybeans, 5.58 Mt of maize and 4.20 Mt of rice, with uncertainty ranges of roughly 36 per cent based on the Monte-Carlo sampling performed previously (Shindell *et al*. 2019). National level totals are reported in Tables 3.6a–3.6d and shown in Figure 3.13. Losses in terms of total tonnage are naturally heavily weighted towards nations with large baseline yields as those vary across countries much more than the relative yield changes due to methane emissions. Relative yield losses tend to be greatest in low latitude countries, predominantly those in South Asia, the Middle East and Africa.

The total effects reported here, avoided yield losses of ~20 Mt, are slightly smaller than the value of 27 Mt in response to a very similar methane emissions reduction that was reported in prior modelling using just two models (Shindell *et al*. 2012; UNEP 2011). This is at first somewhat surprising given that these new estimates include both ozone and climate whereas the earlier results were for ozone alone. As the ozone exposure–response functions have not changed, this suggests that the multi-model analysis has produced a slightly smaller crop-related ozone response (M7 or M12) than in the prior study. The range given in the prior work, however, was very large spanning 7–69 million tonnes, as the two models differed markedly. The prior studies used the GISS and ECHAM models, with nearly a factor of two larger response in the latter and the current analysis reporting a multi-model mean close to the earlier low-end model (GISS). Using several models this time, the current results provide a substantially better constrained value that is well within the large range in the earlier analysis. Differences may also stem in part from changes in background conditions in predominantly rural areas where crops are grown.

As with health-related impacts, the linearity of crop impacts was examined across the various prescribed changes in methane concentrations. Responses are again relatively linear in nearly all cases at the national level for countries with substantial impacts (Figure 3.14). Significant deviations are seen for maize in China and rice in Bangladesh, with weaker responses to an increase than a decrease in methane in the former and vice-versa in the latter. Even in these cases, however, a linear approximation yields a fairly close result over the 0–134 Mt decrease range. Hence as with health impacts, hereafter it is assumed that crop responses can be well approximated with a linear scaling of the multi-model mean response from the half anthropogenic methane simulations.

10. faostat.fao.org

Table 3.6a Total (Mt) and relative (per cent) losses in yield of maize per 134 Mt methane emissions for countries with losses greater than 0.040 Mt and the top 14 countries for relative yield losses

COUNTRY	YIELD LOSS (MT)	COUNTRY	YIELD LOSS (%)
United States	2.345	Bangladesh	3.1
China	1.554	Nepal	3.1
Brazil	0.214	Jordan	2.9
India	0.147	Tajikistan	2.9
Mexico	0.134	Iraq	2.8
Egypt	0.115	Pakistan	2.7
Italy	0.107	India	2.6
France	0.078	Iran	2.6
South Africa	0.060	Afghanistan	2.3
Argentina	0.059	Uzbekistan	2.2
Romania	0.050	Egypt	2.1
Hungary	0.047	Syria	2.0
Indonesia	0.043	Turkmenistan	2.0
Canada	0.040	Angola	1.8
GLOBAL	5.580	GLOBAL	1.2

The uncertainties are ~40 per cent.

Table 3.6b Total (Mt) and relative (%) losses in yield of wheat per 134 Mt methane emissions for countries losses greater than 0.075 Mt and the top 16 countries for relative yield losses

COUNTRY	YIELD LOSS (MT)	COUNTRY	YIELD LOSS (%)
India	2.700	United Arab Emirates	5.9
China	1.324	Saudi Arabia	5.8
Pakistan	0.556	Brazil	5.7
United States	0.449	Oman	5.2
France	0.203	Paraguay	5.1
Australia	0.200	Qatar	4.6
Turkey	0.186	Bahrain	4.6
Egypt	0.148	Bolivia	4.5
Iran	0.142	Madagascar	4.3
Germany	0.139	Yemen	4.2
Russia	0.115	India	4.2
Argentina	0.085	Sudan	4.1
Saudi Arabia	0.083	Eritrea	3.6
United Kingdom	0.076	Tanzania	3.5
Canada	0.076	Niger	3.5
Ukraine	0.075	Myanmar	3.3
GLOBAL	7.460	GLOBAL	1.7

The uncertainties are ~30 per cent.

Table 3.6c Total (Mt) and relative (%) losses in yield of rice per 134 Mt methane emissions (for countries with losses greater than 0.020 Mt and the top 16 countries for relative yield losses

COUNTRY	YIELD LOSS (MT)	COUNTRY	YIELD LOSS (%)
India	1.432	Uzbekistan	1.8
China	1.252	Nepal	1.7
Bangladesh	0.360	Tajikistan	1.7
Indonesia	0.173	Afghanistan	1.6
Myanmar	0.119	Iraq	1.5
Thailand	0.102	Kyrgyzstan	1.4
United States	0.085	Bhutan	1.4
Viet Nam	0.075	Pakistan	1.3
Pakistan	0.071	Turkmenistan	1.3
Japan	0.071	Kazakhstan	1.2
Korea, Rep.	0.061	India	1.2
Nepal	0.053	Bangladesh	1.1
Egypt	0.053	United States	1.1
Brazil	0.038	Iran	1.1
Philippines	0.038	Australia	1.0
Angola	0.027	Rwanda	1.0
GLOBAL	4.202	GLOBAL	0.8

The uncertainties are ~40 per cent.

Table 3.6d Total (Mt) and relative (%) losses in yield of soy per 134 Mt methane emission for countries with losses greater than 0.010 Mt and the top 11 countries for relative yield losses

COUNTRY	YIELD LOSS (MT)	COUNTRY	YIELD LOSS (%)
United States	1.054	Iran	3.4
Brazil	0.412	Iraq	3.3
Argentina	0.231	Nepal	2.8
Congo, Dem. Rep.	0.182	India	2.8
India	0.077	Zambia	2.7
Australia	0.061	Tanzania	2.6
China	0.047	Kazakhstan	2.5
Paraguay	0.030	Korea, Rep.	2.4
Gabon	0.016	Zimbabwe	2.3
Canada	0.012	Angola	2.2
Italy	0.010	Mozambique	2.2
GLOBAL	2.232	GLOBAL	1.7

The uncertainties are ~40 per cent.
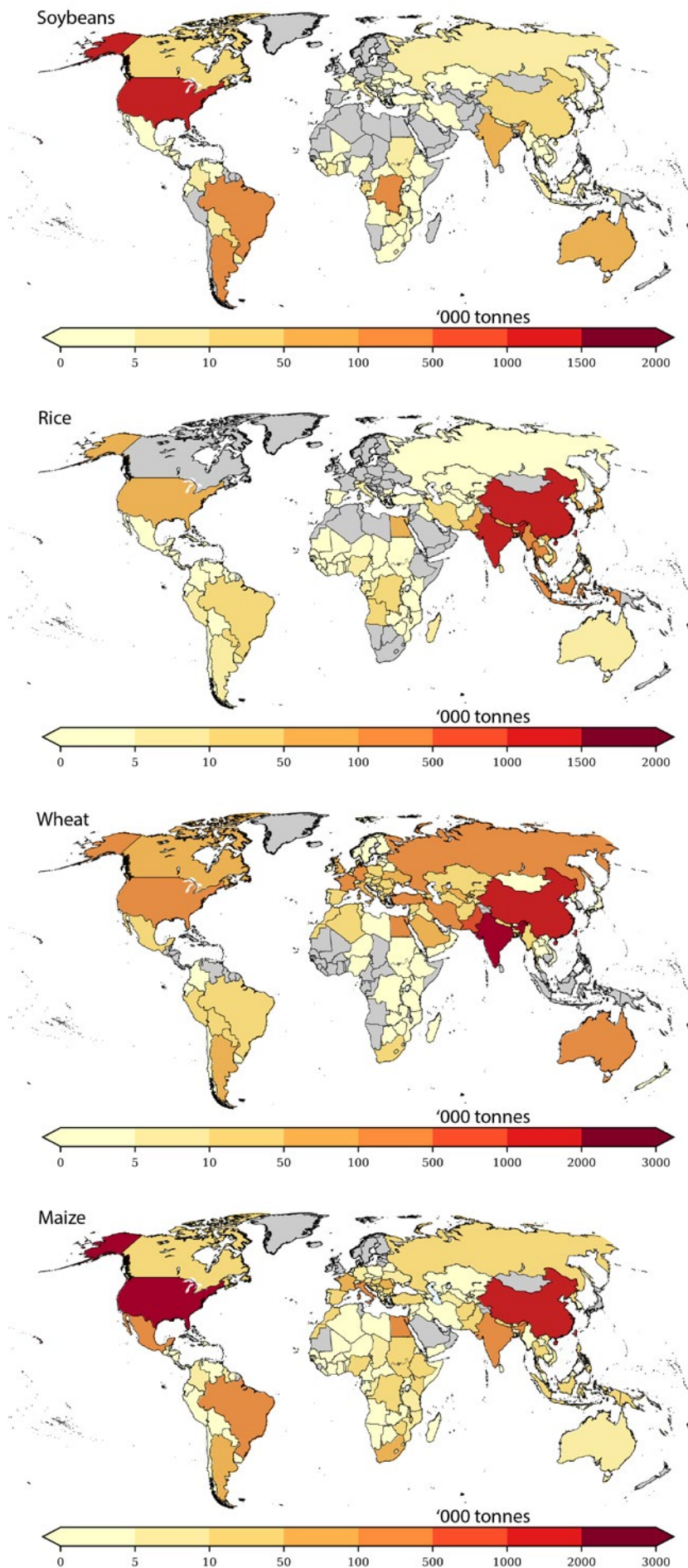
Figure 3.13 Annual change in soybean, rice, wheat and maize yields due to ozone exposure, climate and carbon dioxide changes resulting from a 134 Mt change in methane emissions, thousand tonnes

Note: Based on the multi-model mean changes – grey indicates no quantification.

Source: UNEP and CCAC
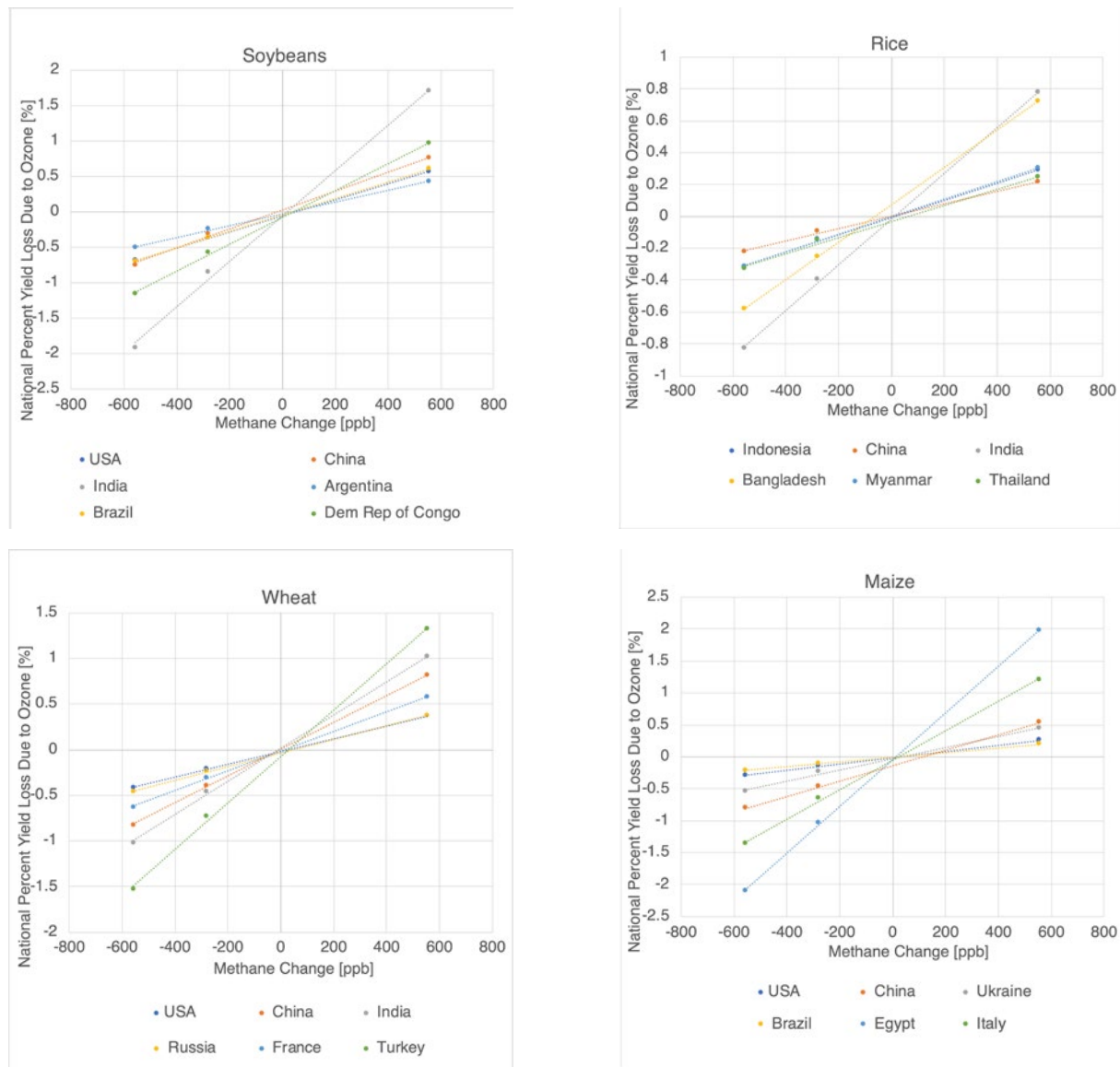
Figure 3.14 Change in wheat, soybean, maize and rice yields versus change in methane amounts, selected countries, per cent

Note: Responses are shown for countries with the largest impacts for each crop based on GISS-E2 simulations. The charts include points from individual simulations along with linear fits for each country. Negative losses represent gains.

Source: UNEP and CCAC

3.6 MONETIZATION OF IMPACTS: METHODS AND RESULTS

Both market and non-market costs associated with the impacts described above are evaluated. All values are in constant 2018 US dollars. Non-market values include those associated with premature death and many of the effects of climate change. Market costs include direct spending on health care and the effects of environmental changes on labour productivity.

Monetized benefits associated with avoided mortality are evaluated using a willingness-to-pay (WTP) measure of the value societies place upon reduced risk of premature death. This measure is often referred to as the value of a statistical life (VSL) though it is in fact an expression of the value that people affix to small changes in mortality risks in monetary terms rather than the value of any individual's life. Health literature often uses disability adjusted life years (DALYs), which are arguably more informative since they incorporate the age of the affected individuals and years with disabilities as well as premature deaths. Monetization is virtually always based on VSL, however, which is a better-established metric in the economics literature (Viscusi and Aldy 2003). Here the societal willingness-to-pay based is evaluated on national level gross domestic product (GDP) using data from the World Bank based upon national accounts data (World Bank, 2019). Gross domestic product values are used for 2018 except in the few cases for which they are unavailable in which case the most recent year is used – 2017 for Iran and 2011 for Eritrea. The WTP here is based on the mean of 26 peer-reviewed studies evaluated by the United States Environmental Protection Agency (US EPA 1997) and used by that agency to derive its official recommended VSL of US$ 7.4 million in 2006 US dollars. That value is then inflated to represent the year 2018 using an economic growth rate of 2.6 per cent per year and an elasticity for WTP with income growth for any specific country of 0.4, as in prior studies (Shindell *et al*. 2012; UNEP 2011). To account for the fact that WTP is a function of income across countries, monetized benefits are evaluated using both the same elasticity of 0.4, a value typically used to account for differential income levels within a country or region, and also using an elasticity of 1.0 as recommended by Hammitt and Robinson (2011) for across country analyses and used in the work of OECD (2018) and the World Bank and the Institute for Health Metrics and Evaluation (IHME) (2016) for both high-to-low income and low-to-high income comparisons. In other words, in this analysis, for country a,

$$VSL_a = VSL_{US} \times (Income_a/Income_{US})^\beta$$

where ß is either 1.0 or 0.4. Both sets of values are presented (Tables 3.7a and 3.7b).

The results for ozone-related deaths show that national level values are greatest for countries with either or both large populations and high per person GDP, including China, India, Japan and the United States (Table 3.7 and Figure 3.15). It is important to emphasize that the WTP does not reflect an ethical judgement about the comparative value of the life of any individual, but simply that the willingness to pay to reduce risk is naturally a function of income. Hence the larger valuation associated with lives lost in wealthier nations merely reflects their wealth and does not imply a greater value for their citizens.

Values in countries with lower per person income are larger with the smaller value of income elasticity, as is the global total for ozone-related deaths which is approximately US$ 2500 (US$ 600–4 300; 95 per cent confidence interval here and hereafter) per tonne of methane emitted for an across country income elasticity of 1.0 and US$ 5 300 (US$ 1 200–9 100) per tonne for across country income elasticity of 0.4. Additional mortality-related benefits owing to reduced heat-related deaths are US$ 110 (US$ 75–150) for impacts in the United States, and US$ 120 (US$ 75–160) for China with income elasticity of 1.0 and US$ 360 (US$ 230–490) for China with income elasticity of 0.4. Using the results from the national-average seasonal-mean method to evaluate a broader set of countries (Section 3.4.2), the valuation rises to US$ 700 (US$ 200–1 100) per tonne for an elasticity of 1.0 and US$ 1 400 (US$ 300–2 500) per tonne for an elasticity of 0.4 and adopting the better characterized uncertainty range associated with ozone-related mortalities. These values are used hereafter, noting again that they do not include South Asia or Africa and are hence conservative. The total worldwide mortality valuation of all quantified impacts using an income elasticity of 1.0 is thus US$ 3 200 (US$ 800–5 400) per tonne of methane.

As described in the previous section, several additional impacts that can be readily monetized, including health morbidity outcomes, labour productivity in the United States, and crop yield changes have been quantified. First, morbidity changes associated with ozone exposure, for which values are calculated for two health impacts: hospital admissions and asthma-related accident and emergency department visits. For both end points, valuations are calculated only

for countries where baseline hospital admission data for respiratory conditions are available – China, Europe and the United States – or accident and emergency department visits – a broader set of countries.

First, the unit costs associated with each type of morbidity burdens are estimated. However, unit cost data is limited, as a result of which the cost estimation involves data collection and imputation, the latter for cases when actual data are not available. In the data collection, one important source was compiled by the CaRBonH calculation tool (Spadaro 2018). It estimated unit costs of several major morbidity endpoints for 53 countries, mostly in Europe. Since the target pollutant for CaRBonH was PM instead of ozone, the unit costs of morbidity endpoints studied were not, however, immediately usable in this project. CaRBonH reported country-specific average costs of cardiovascular and respiratory hospital admissions, for example, rather than reporting respiratory hospital admission separately. In addition, it reported the unit cost of each asthma symptom day for those between the ages of 5–20, rather than costs for asthma accident and emergency department visits for all age groups. This analysis took advantage of the broad coverage of CaRBonH's country-level data but made several adjustments to obtain estimates for unit costs of ozone-related morbidity.

For hospital admissions, most countries for which morbidity burdens could be estimated are in Europe, due to the availability of baseline hospitalization rates, except for China and the United States and China. Thus the average unit costs of hospital admissions for cardiovascular (ICD-9 codes 390–459; ICD-10 codes I00–I99) and respiratory (ICD-9 codes 460–519; ICD-10 codes J00–J99) concerns were collected for all age groups from CaRBonH for all the European countries in this analysis' morbidity estimates, and adjusted for respiratory issues as a single cause, and for the post-65 age group. Detailed cost information was used from the Healthcare Cost and Utilization Project (HCUP) for the United States to make the adjustment – the HCUP's dataset is the most comprehensive for inpatients in the United States. The same ICD-9 codes from CaRBonH were used to locate the diseases in HCUP dataset. The ratio of the mean hospital costs for all (age) discharges between cardiovascular and respiratory diseases, were found to be 1.43, and the ratio of the mean hospital costs for respiratory diseases between those aged 65+ and all age groups was 0.98. The unit costs for European countries were adjusted using a scaling factor of 0.69 (= 0.98/1.43), to

obtain the estimated unit costs for respiratory hospital admissions of those aged 65+. The unit cost from HCUP for the United States was used directly. To estimate the unit cost for China, the average costs were calculated for three respiratory diseases reported in China's 2016 *Health and Family Planning Statistical Yearbook*, weighted by the number of hospitalizations for each disease. This estimate was not strictly equivalent to all respiratory diseases considered for other countries and was not specific to the 65+ population. Nonetheless, it is likely to be a good approximation, since the three most prevalent respiratory diseases in China were selected, and the ratio between those aged 65+ and all age groups from HCUP, 0.98, indicated that the hospitalization costs were likely to be very similar between the two age-groups.

For the cost of visits to accident and emergency departments for asthma, it was first note that there is a highly linear relationship (R-square = 0.96) between the cost of asthma symptom days and of income per person across the 53 countries in CaRBonH. The cost of asthma symptom days of children aged 5–19 analyzed in CaRBonH is based upon health treatment expenditures. Hence, here both the different age groups were considered for the impact and the difference between accident and emergency department visits and general health treatment for asthma. Since the cost for an accident and emergency department visit is a proportion of all treatment expenditure, it was assumed that there was also a good correlation between the cost of an accident and emergency department visit and income per person worldwide. Secondly, it was assumed that the correlation for children aged 5–19 holds for all age groups. Thus the cost estimate utilized for each asthma accident and emergency department visit for all age groups in the United States, US$ 1 501 in 2008 US dollars (Wang *et al*. 2014). As with mortality valuations, income comparisons are made based on:

$$\text{Cost}_a = \text{Cost}_{US} \times (\text{Income}_a/\text{Income}_{US})^{\beta}$$

In this case, the income elasticity (ß) follows that used in CaRBonH, which is 0.8, 0.9, and 1.0 for high, upper-middle, and lower-middle income countries, respectively. Income data was obtained from the World Bank (World Bank 2020).

For respiratory hospital admissions, the largest economic impact is in the United States, followed by Germany, Italy, France and China within the relatively limited set of countries (Table 3.8). The

total across all countries for which estimates were made is US$ 0.36 per tonne. Values are generally larger for the healthcare costs of asthma-related accident and emergency department visits, with highest expenditures in the United States, Japan, India and China, respectively (Table 3.9; Figure 3.16). The total across all countries for which estimates were made is US$ 0.92 per tonne. Hence, as expected, these healthcare expenditures are comparatively small relative to mortality-related valuations.

As previously discussed, labour losses due to exposure to extreme heat were calculated using two distinct methodologies. The first was applied only for the United States and, using this method, a 50 per cent reduction in anthropogenic methane concentrations led to a reduction in lost labour of 13.6 million work hours. To estimate the value associated with the time lost, 2016 county-level annual employment for those of working ages, 15–64 year-olds, and annual average weekly wages from the Quarterly Census of Employment and Wages (U.S. Bureau of Labor Statistics 2020a; accessed 10 January 2019) were used. The following North American Industry Classification System (NAICS) codes were used to determine the number of workers in high-risk industries/sectors: NAICS 11 for agriculture, forestry, fishing and hunting; NAICS 23 for construction; NAICS 31-33 for manufacturing; NAICS 21 for mining; NAICS 48–49 for transport, and NAICS 22 for utilities (U.S. Bureau of Labor Statistics 2020b; accessed 10 January 2019). The 2016 fraction of workers in high-risk industries was used for each county. National average wages range from US$ 19.0 per hour for agriculture to US$ 44.90 per hour for utilities and are spatially heterogeneous across the United States. Accounting for the affected economic sectors, largely manufacturing and construction, these losses are valued at US$ 449 (73–601; 95 per cent confidence interval) million. At the state level, the largest impacts are in Texas, US$ 141 million; Arizona, US$ 32 million; and Florida, US$ 24 million, with impacts generally larger in warmer states.

The second method for estimating of labour losses due to extreme heat was applied globally. Hours of reduced work availability calculated using this method were valued based on hourly wage data for the affected work areas from the ILO (ILO 2020; accessed 2 September 2020). This dataset provided enough detail to attribute wages to the three labour categories described previously (light, medium and heavy) for 131

countries. The hourly wage data provided by ILO varies from country to country, ranging from 2014 to 2018, and were converted to US dollars based on national purchasing power parity. For the United States, the latest year, 2015, as reported by ILO was used, adjusted to 2018 US dollars. For the United States, the labour loss reductions from a 50 per cent decrease in anthropogenic methane concentrations were 44.1 million hours. These losses are valued at US$ 531 million per year (360–702; 95 per cent confidence interval), similar to the results using the first method. This similarity, however, is largely coincidental as the labour losses are much larger in the second method but that is offset by markedly lower hourly wages across all sectors in the United States in the ILO dataset relative to government statistics. There are also differences in the employment sectors affected. The strongest effects in the first method are in the manufacturing, construction and transport sectors. In the second method, there are again significant impacts in construction which is considered part of the heavy outdoor work category, the category that represents the vast majority of impacts, but there are no impacts on manufacturing or transport due to the assumption of a lower WBGT for these sectors as they are considered indoor medium work. Hence the labour loss results are quite sensitive to the wage dataset used and the methodology employed.

The global total using this second method was a value of US$ 8.5 billion (3.1–13.8; 95 per cent confidence interval) for the half anthropogenic methane reduction, corresponding to value of US$ 63 per tonne of methane (US$ 23–103 per tonne). Effects are large in both hot and humid countries where the hours lost are greatest such as Brazil, China, India and Indonesia, but also in some less sensitive but wealthier countries such as Australia, the United States and the United Arab Emirates (Table 3.10; Figure 3.17). The total is substantially larger than valuations associated with ozone-related morbidity outcomes across all countries with estimates of accident and emergency department visits for asthma and hospital admissions but is similarly much less than the value associated with ozone-related or heat-related mortalities. There would be differences in the valuation of the lost labour for men and women, as was seen for the labour hours lost (Table 3.5b). These are not quantified here as the ILO dataset underlying these calculations does not include wage differences by gender.

For changes in crop production, valuation is based upon yield changes multiplied by the 2018 global market prices per tonne from the

United States Department of Agriculture (USDA) and World Bank[11] which gives US$ 210 for wheat, US$ 394 for soybeans, US$ 164 for maize and US$ 421 for rice. This provides a fairly simplistic measure of the value of yield changes, as it clearly does not account for benefits such as those to subsistence farmers or national food security. The valuation per tonne of methane is then US$ 11.7 for wheat, US$ 6.6 for soybeans, US$ 6.8 for maize and US$ 13.2 for rice leading to a valuation summing over these four crops of just more than US$ 38 per tonne of methane. For comparison, in prior studies that only accounted for the effects of ozone on yields, the value was US$ 29 per tonne of methane (Shindell *et al*. 2012; UNEP 2011). As climate impacts, predominantly from temperature change, are now included it seems reasonable that the new values is roughly one third larger. While at the global level valuation of reduced risk of premature death dominates all other impacts, crop changes can be of comparable magnitude in some areas depending on the income elasticity used to account for differential income levels across countries. Using an elasticity of 1.0, for example, leads to agricultural impacts in India having a larger valuation than that of the reduced risk of premature death, and a valuation for Brazil that is more than half that of the reduced risk of premature death (Figures 3.15 and 3.18). It should be note that there are additional potential effects from air quality that were not included here, such as changes in forestry yields, tourism or depreciation of man-made materials. The valuation of the impacts of ozone resulting from methane emissions on forestry have been evaluated as ~US$ 20 per tonne of methane, based on a global extrapolation of a United States analysis (West and Fiore 2005).

Finally, the effects of climate change using a social cost framework was assessed. Social costs of climate change attempt to account for all the effects of climate, including both market and non-market costs, but ignore the effects of air pollution. This makes it challenging to compare with the values in this analysis as the agricultural impacts included, for example, are the result of both climate and air pollution changes. There was a clear rationale for excluding air pollution in the original development of social costs for carbon dioxide given that emissions of carbon dioxide and co-emitted air pollutants are not necessarily correlated. For example, two similar coal-fired power plants or motor vehicles (with internal combustion engines) could have quite

different air pollutant emissions depending on the efficiency of any applied pollution controls such as scrubbers or catalytic converters. Hence conventional practice has been to include the response of air pollutants such as ozone to carbon dioxide emissions when this takes place due to climate change but to exclude the response to co-emissions that takes place via atmospheric chemistry. This has extended not only to social costs, but to broader evaluations of the societal impacts of greenhouse gas emissions such as the US EPA's Climate Change Impacts and Risk Analysis project (US EPA 2015a). With methane, however, this rationale breaks down as methane affects ozone both via climate change and atmospheric chemistry. Following conventional practice and leaving out atmospheric chemical responses therefore means that an intrinsic effect of methane emissions themselves is neglected rather than an effect of a potentially co-emitted pollutant.

Prior analyses of the climate impacts of methane yield a per tonne social cost of US$ 810 (Marten and Newbold 2012) or US$ 910 (Shindell 2015) in 2007 US dollars and using a 3 per cent economic discount rate. Values without discounting, as in the VSL analyses here, would of course be larger but are not standard in the existing literature. The largest climate-related impact in the analysis was the finding that the reduced risk of heat-related premature mortalities in China and the United States alone were valued at ~US$ 230 per tonne, and that a rough estimate of the worldwide valuation was US$ 700 per tonne. Applying 3 per cent discounting to that estimate would reduce the US$ 700 per tonne to US$ 580 per tonne. This analysis therefore suggests that prior estimates of the climate-only social cost of methane are potentially too low. As such, this analysis includes the valuation of heat-related health impacts along with these social costs as they account for damage associated with all other impacts and appear to underestimate the effects of climate change on human health (Carleton *et al*. 2020; Shindell 2015). Here, the mean of the studies mentioned above is used, which is US$ 1 100 per tonne converted to 2018 US dollars and rounded to the nearest hundred. Note that values for fossil methane are slightly higher, by ~US$ 150 per tonne with a 3 per cent discount rate (Shindell *et al*. 2017), due to the climate impacts of the carbon dioxide that is eventually produced by the oxidation of the carbon within the emitted methane.

11. indexmundi.com/commodities

The total valuation per tonne of methane for all market and non-market impacts assessed here is roughly US$ 4 300 using a cross-nation income elasticity for WTP of 1.0 and US$ 7 900 using an elasticity of 0.4 (Figure 3.19) – values are ~US$ 150 per tonne larger for fossil-related emissions. This value is dominated by mortality effects, of which US$ 2 500 are due to ozone and ~US$ 700 are due to heat using the more conservative 500 deaths per million tonnes of methane of this analysis' two global-scale estimates and a WTP income elasticity of 1.0, followed by climate impacts. These numbers are comparable to those reported previously using a social cost framework that incorporated both climate and air pollution related impacts (Shindell *et al*. 2017), though slightly larger as a result of the updated epidemiology underlying the estimates of ozone-attributable premature deaths. Given the dominance of ozone-related impacts that occur immediately in response to methane changes, decaying thereafter with the residence time of methane, these impacts are only weakly sensitive to discounting. For example, the ozone-related impacts over the first 25 years following methane emissions, using 5 per cent annual discounting, are 83 per cent of the value using 2 per cent discounting and the value is 80 per cent over the first 50 years. In contrast, the valuation of a specific impact 25 years in the future using 5 per cent discounting is only 50 per cent of the value using 2 per cent discounting, a proportionality more applicable to the effect of temperature change based on the evaluation of the response averaged over 10–40 years after emissions. Hence roughly two thirds of the total valuation has minimal sensitivity to discounting whereas the remainder would be substantially affected were future benefits to be discounted at a rate other than the 3 per cent assumed here for climate, which is the dominant contributor to the third of impacts sensitive to discounting. Using a discount rate of 5 per cent, for example, the value of benefits would be ~US$ 700 less whereas using a discount rate of 1.4 per cent it would be ~US$ 700 greater.

The total market costs are comparatively small at ~US$ 122 per tonne and stem predominantly from labour losses, agricultural yield changes and forestry losses. In contrast, healthcare costs related to morbidity effects associated with ozone were relatively small, about US$ 1 per tonne, though there are likely to be additional non-fatal health outcomes associated with ozone. It was noted that although discounting is conventionally applied to estimates of mitigation costs (Section 5), the valuation of impacts does not discount future benefits. This is consistent with the usage of impact valuations to assess effects on future generations, especially in the case of climate change related impacts that occur over many decades, and the desire to value welfare of future generations similarly to that of today's population, which implies a near-zero discount rate. This is in contrast to the use of mitigation costs to compare options for the use of capital that employ a variety of discount rates that are not near zero. This issue is discussed further in Section 5. As the valuation of benefits is dominated by the effects of air pollution, and this responds immediately to changes in methane emissions, with impacts tapering off according to the ~12-year methane residence time, these benefits are in any case much less sensitive to the choice of discounting rate than are climate-related benefits.

A prior valuation of the impacts of methane through ozone on agriculture, forestry, and non-fatal health endpoints found a monetized impact of ~US$ 80 per tonne (West and Fiore 2005). This resulted from estimated impacts of roughly US$ 30 per tonne due to both agricultural losses and non-fatal human health effects, along with the ~US$ 20 per tonne due to forestry losses. The agricultural impacts shown in this analysis are larger, consistent with the prior study not including climate impacts – it should also be noted that West and Fiore (2005) also extrapolated globally from limited regional studies in the United States, Europe and East Asia. Their valuation of non-mortality human health effects is markedly greater, however. They again extrapolated from limited studies, in this case in the United States and Europe only, but more importantly included different impacts, namely avoided minor restricted activity days and worker productivity changes in the United States and morbidity impacts in Europe associated with ozone exposure, for both of which there is some, but limited, evidence. Hence the results here are larger for market valuations because this analysis found larger impacts for crops and included impacts on labour, which had a larger influence than not including several of the impacts that contributed most strongly in West and Fiore's 2005 analysis.

Table 3.7a Value of reduced risk of ozone-related deaths per tonne of methane for countries with values greater US$ 10*

COUNTRY	US$ (MILLION)	LOW	HIGH
United States	639	159	1 077
China	390	95	653
Japan	210	57	346
Germany	161	38	278
United Kingdom	133	32	229
India	85	13	149
Italy	74	18	126
Russia	74	18	127
France	72	16	124
Spain	59	14	100
Canada	39	10	67
Netherlands	32	7	56
Brazil	30	6	53
Australia	27	6	48
Korea, Rep.	27	7	45
Belgium	23	5	40
Poland	21	5	37
Indonesia	19	3	35
Mexico	18	4	31
Switzerland	17	4	29
Sweden	17	4	30
Turkey	15	4	25
Argentina	14	3	25
Saudi Arabia	14	4	23
Denmark	14	3	23
Norway	13	3	22
Austria	13	3	22
Portugal	12	3	21
Romania	12	3	21
Greece	11	3	18
Ireland	10	2	17
Czechia	10	2	17
GLOBAL	2 511	598	4 264

Note: income elasticity of 1.0 across countries

Table 3.7b Value of reduced risk of ozone-related deaths per tonne of methane for countries with values greater than US$ 10*

COUNTRY	US$ (MILLION)	LOW	HIGH	COUNTRY	US$ (MILLION)	LOW	HIGH
China	1 189	291	1 994	Belgium	27	6	47
India	671	100	1 179	Saudi Arabia	25	6	42
United States	639	159	1 077	South Africa	25	6	43
Japan	278	75	459	Portugal	22	5	38
Russia	206	49	354	Morocco and Western Sahara	22	5	37
Germany	191	45	328	Greece	21	5	35
United Kingdom	168	40	288	Sweden	19	4	32
Italy	107	26	180	Czechia	18	4	31
Indonesia	103	14	185	Kazakhstan	18	4	30
Brazil	98	21	172	Malaysia	17	3	31
France	92	21	159	Myanmar	17	4	29
Spain	91	22	154	Algeria	16	4	28
Pakistan	72	14	124	Uzbekistan	16	4	26
Egypt	64	17	106	Hungary	16	4	27
Ukraine	57	13	98	Nigeria	15	2	27
Mexico	56	13	94	Switzerland	15	4	25
Poland	49	11	85	Austria	14	3	24
Canada	47	12	80	Denmark	14	3	24
Turkey	47	12	79	Serbia and Montenegro	14	3	23
Korea, Rep.	41	11	68	Cuba	14	3	24
Philippines	41	9	72	Bulgaria	13	3	22
Argentina	39	9	69	Sri Lanka	13	2	23
Iran, Islamic Rep.	36	10	60	Chile	12	3	21
Netherlands	36	8	62	Ethiopia	12	2	22
Bangladesh	35	7	59	Peru	12	2	22
Romania	32	7	55	Belarus	11	3	20
Viet Nam	30	6	51	Norway	11	3	19
Australia	29	6	51	Israel	11	2	18
Thailand	28	5	50	**GLOBAL**	**5 315**	**1 193**	**9 073**

Note: income elasticity of 0.4 across countries

Table 3.8 Country-specific cost of respiratory hospital admissions attributable to ozone exposure, 2018 US$ per '000 tonnes, 65+ age group

COUNTRY	COST (2018 US$)
United States	83
Germany	54
Italy	46
France	37
China	31
United Kingdom	26
Spain	25
Belgium	6.2
Greece	5.5
Netherlands	5.4
Austria	5.3
Poland	5.2
Norway	4.9
Sweden	4.8
Portugal	3.6
Denmark	3.1
Hungary	1.6
Czechia	1.5
Ireland	1.4
Finland	1.3
Bulgaria	1.2
Romania	1.1
Slovakia	1.0
Slovenia	1.0
Croatia	0.6
Serbia and Montenegro	0.4
Luxembourg	0.3
Lithuania	0.3
Estonia	0.2
Cyprus	0.2
Malta	0.2
Iceland	0.1
Latvia	0.05
TOTAL	358

The uncertainty range is ± 84 per cent.

Table 3.9 Cost of asthma-related accident and emergency department visits attributable to ozone exposure, US$ per '000 tonnes for countries with values greater than US$ 5 per '000 tones, all age groups

COUNTRY	US$ PER '000 TONNES
United States	278
Japan	78
India	66
China	52
Spain	49
Korea, Rep.	41
Norway	39
Canada	33
Germany	26
Netherlands	24
Brazil	22
United Kingdom	19
Turkey	18
Australia	15
Sweden	14
United Arab Emirates	13
Russian	13
Italy	12
France	11
Argentina	8.6
Belgium	8.4
Kuwait	5.6
Venezuela	5.5
Colombia	5.1
Austria	5.0
TOTAL	924

The uncertainty range is ± 37 per cent.

Table 3.10 Value of labour losses due to heat exposure, 2018 US$, top 15 countries

COUNTRY	COST PER TONNE (2018 US$)
China	32.7
Brazil	5.3
Australia	4.7
United States	3.7
India	2.4
Indonesia	1.7
Viet Nam	1.4
United Arab Emirates	1.1
Philippines	1.0
Thailand	0.8
Qatar	0.6
Malaysia	0.5
Mexico	0.5
Pakistan	0.5
Saudi Arabia	0.5
Global	63

The uncertainty range is ± 62 per cent.
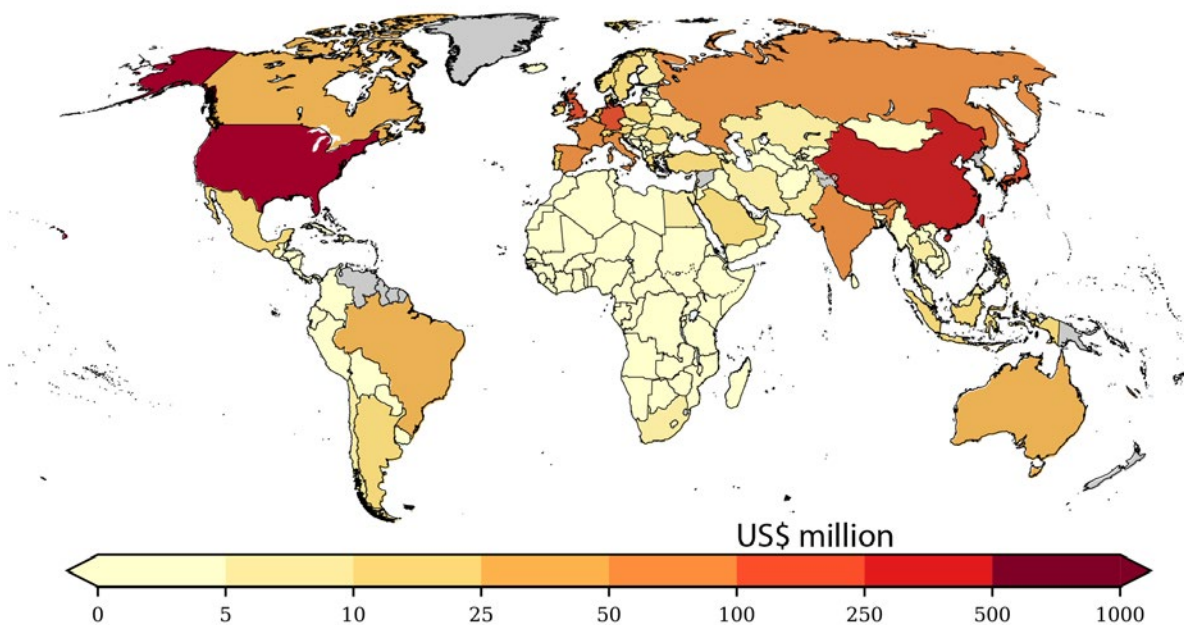
Figure 3.15 Valuation of reduced risk of premature death due to respiratory and cardiovascular illnesses caused by ozone, people aged 30+ per million tonnes of methane emission, US$ millions

Note: Grey indicates no quantification.

Source: UNEP and CCAC

US$ '000

| 0 | 2 | 5 | 10 | 25 | 50 | 100 | 200 | 300 |
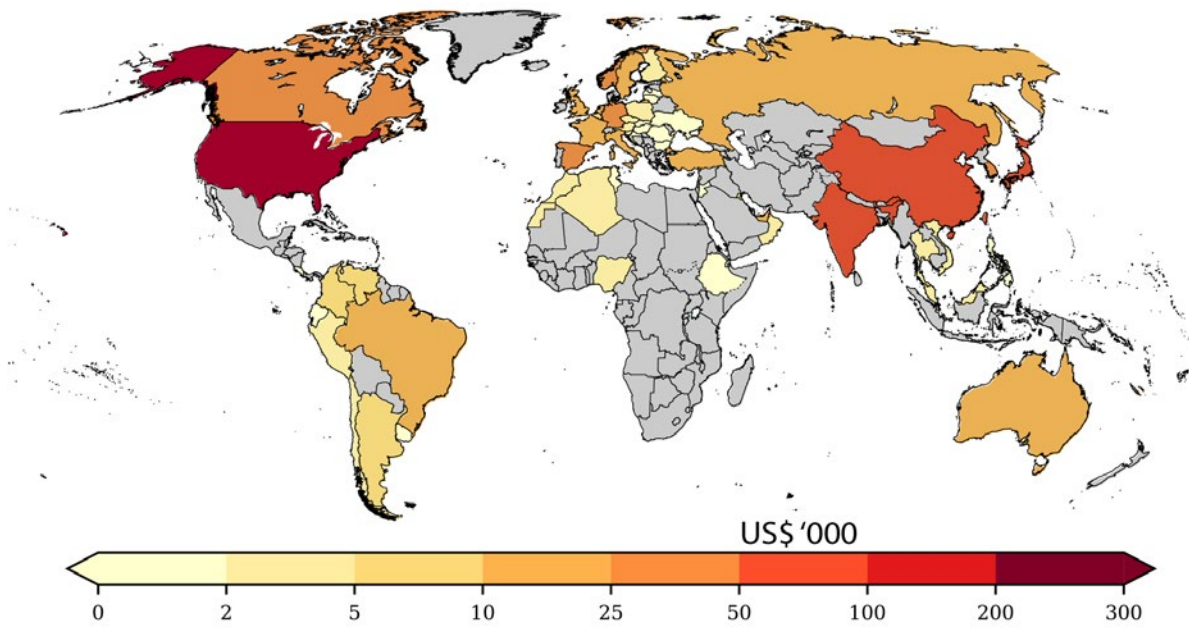
Figure 3.16 Valuation of the change in asthma-related accident and emergency department visits due to ozone exposure change per million tonne increase in methane emissions, 2018 US$ '000

Note: Based on the scaled multi-model mean ozone change. Grey indicates no quantification.

Source: UNEP and CCAC

US$ '000

| 0.00 | 0.25 | 0.50 | 0.75 | 1.00 | 2.00 | 5.00 | 10.00 | 15.00 |
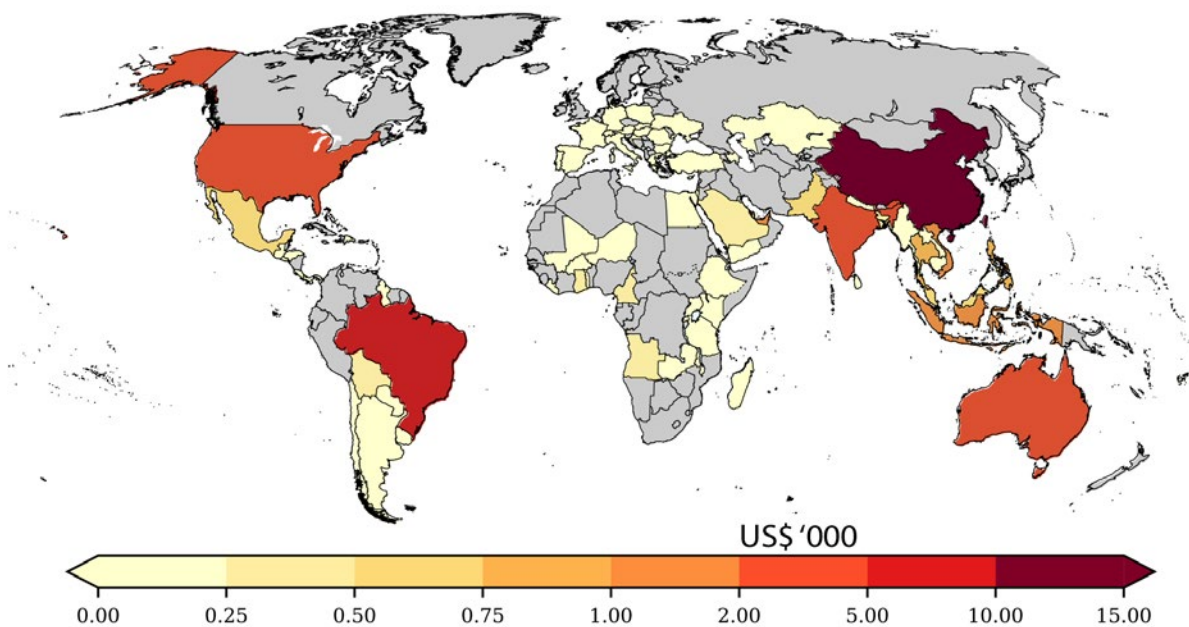
Figure 3.17 Valuation of labour productivity gains due to reduced heat exposure per million tonne reduction in methane emissions, 2018 US$ '000

Note: Grey indicates no quantification.

Source: UNEP and CCAC
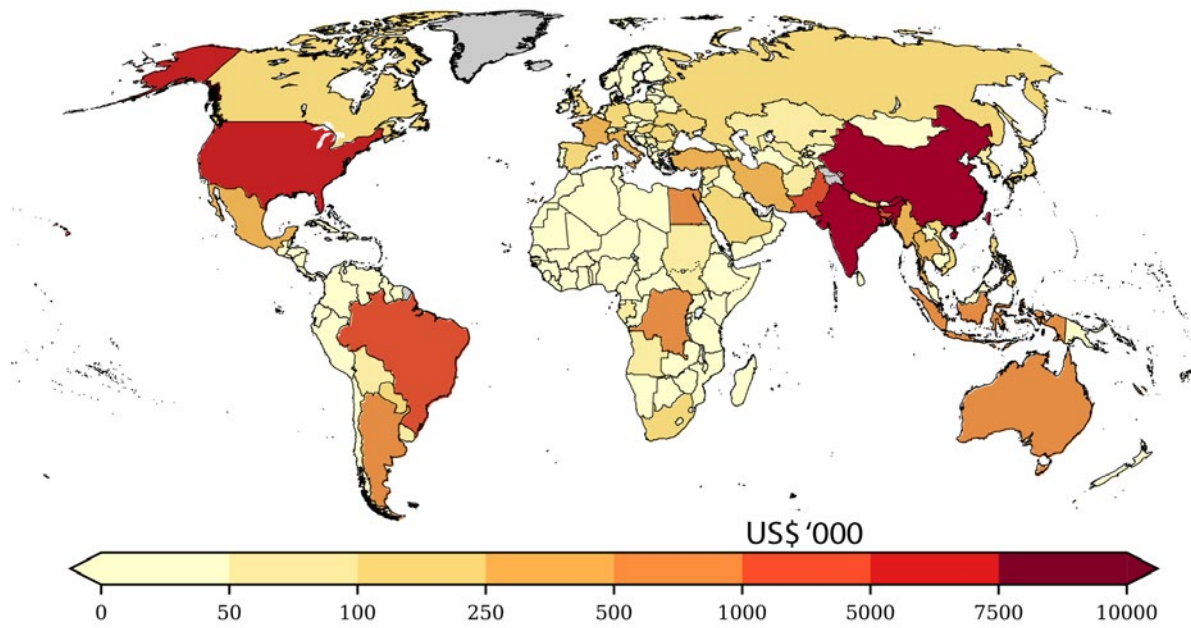
Figure 3.18 Valuation of the avoided yield losses of soybeans rice, wheat and maize per million tonne reduction in methane emissions, 2018 US$ '000

Note: Grey indicates no quantification.

Source: UNEP and CCAC
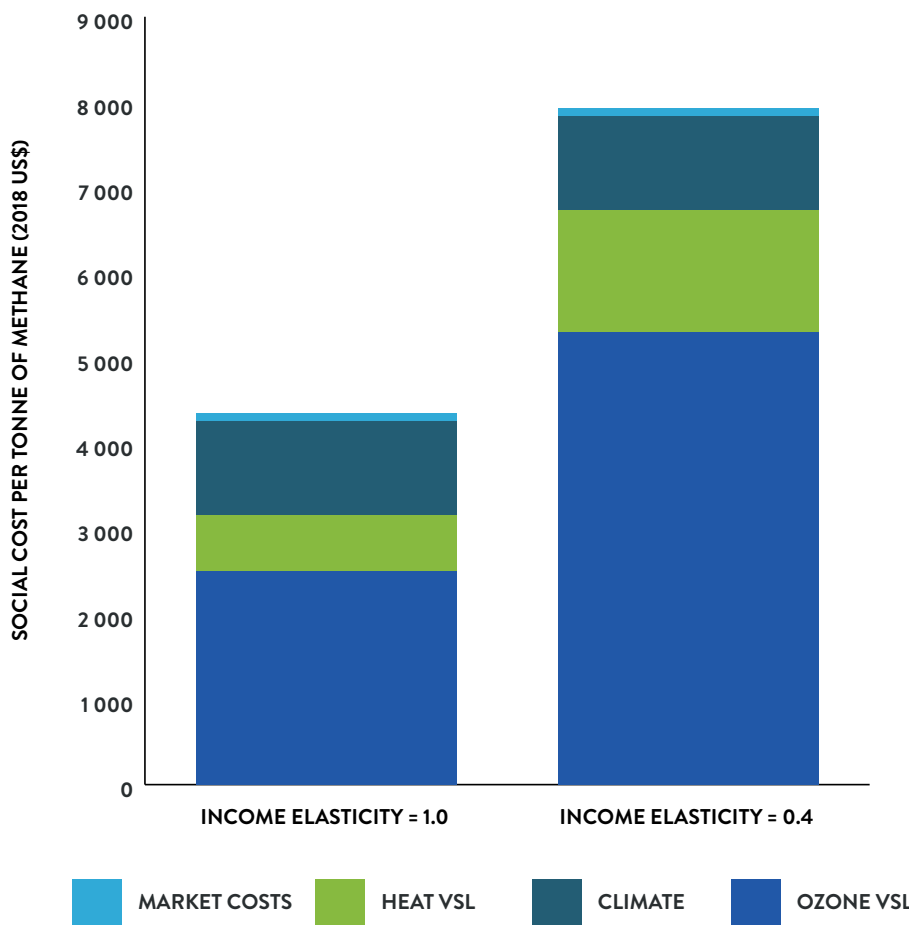
Figure 3.19. Valuation per tonne of emitted methane apportioned to the various impacts quantified in this assessment for the indicated elasticity in cross-nation income comparisons, 2018 US$

Note: Heat VSL and climate impacts are strongly sensitive to the assumed discount rate. Market costs are dominated by agricultural and labour impacts, which are moderately sensitive to discounting.

Source: UNEP and CCAC

4. METHANE EMISSIONS MITIGATION

CHAPTER FINDINGS

- In the absence of additional policies, methane emissions are projected to continue to rise through at least 2040 with emissions at the end of the century higher than at present in all but one socio-economic pathway.

- In modelled scenarios consistent with keeping global mean temperatures below the 1.5ºC target, methane emissions are reduced in response to targeted and additional measures by around 100–150 Mt/yr from the fossil fuel and waste sectors combined and by about 30–80 Mt/yr from the agricultural sector in 2030 relative to reference case emissions, with a substantial range across models and across baseline socio-economic pathways.

- Analysis of the technical potential to mitigate methane from four separate studies shows that for 2030, reductions of 29–57 Mt/yr could be made in the oil and gas subsector, 12–25 Mt/yr from coal mining, 29–36 Mt/yr in the waste sector and 6–9 Mt/yr from rice cultivation. Values for the livestock subsector are less consistent, ranging from 4–42 Mt/yr. Average cost estimates vary greatly across the analyses, not only in amounts but even as to whether they are net expenditures or savings for some sectors.

- Targeted abatement measures with a negative cost could reduce total emissions by ~40 Mt/yr with the greatest potential for abatement coming from the oil and gas subsector and the waste sector. Considering only low-cost targeted controls, defined here as less than US$ 600 per tonne of methane, abatement potentials still typically represent a substantial fraction of the total potential, from 60–80 per cent for oil and gas in three of the four analyses, but 36 per cent in the fourth which does not consider negative costs, from 55–98 per cent for coal, and from ~30–60 per cent in the waste sector.

- Considering the potential for mitigation in different sectors and regions, the largest potential in Europe and India is in the waste sector, in China from coal production followed by livestock, in Africa from livestock followed by oil and gas, in the Asia-Pacific region, excluding China and India, from the coal subsector and the waste sector, in the Middle East, North America and Former Soviet Union it is from the oil and gas subsector, and in Latin America from the livestock subsector. A majority of these major abatement potentials can be achieved at low cost, less than US$ 600 per tonne of methane, especially in the waste sector and coal subsector in most regions and for the oil and gas subsector in North America.

- Within the oil and gas subsector, across available analyses mitigation potentials are greatest for oil production, followed by natural gas production and then downstream gas. With regard to reducing emissions from the waste sector, most of the potential is from changes in the treatment and disposal of solid waste.

- Achieving climate stabilization at levels that avoid dangerous anthropogenic interference with the climate requires the decarbonizing of economies, which will affect methane emissions. Decarbonization of the economy results in only about 30 per cent of the methane abatement seen under a broad multi-pollutant, multi-policy 2°C scenario in 2050, however, highlighting the role of methane-specific policies.

- By 2050, emissions from enteric fermentation, especially from cattle, are by far the dominant remaining source of methane emissions in under 2°C scenarios produced by IAMs as emissions from other sources have been substantially reduced.

- There are numerous financial, legislative and regulatory mechanisms available to support implementation of the identified targeted and additional measures at scale. One commonly employed in IAMs is the imposition of a fairly modest methane tax, which could lead to rapid and substantial decreases in methane emissions, especially from coal, gas and landfills, with abatement of livestock-related emissions highly model-dependent.

- Given the limited technical potential to address agricultural sector methane emissions, behavioural change and policy innovation are particularly important for this sector.

- A relatively robust evidence base indicates that three behavioural changes, reduced food waste and loss, improved livestock management, and adoption of healthier diets, have the potential to reduce methane emissions by 65–80 Mt/yr over the next few decades.

- A web-based decision support tool has been created that allows users to input a level of methane emissions mitigation or select from the analyzed abatement options and view the national and global values for all impacts included in this assessment.

As discussed in Chapter 3, the modelling performed for this assessment quantifies many physical and societal impacts associated with potential changes in methane concentrations. Those changes are evaluated in terms of the corresponding change in emissions using the well-established relationship between methane emissions and concentrations, and the analysis presented in Chapter 3 shows that the impacts are generally well-represented by assuming a linear relationship between emissions changes and impact responses. This chapter examines changes in methane emissions both in scenarios consistent with low warming targets and in response to specific methane reduction policies or technologies. The impacts analyzed in Chapter 3 can then be related to the methane abatement potentials explored here, as is primarily done in Chapter 5.

4.1 METHANE EMISSIONS UNDER BASELINE AND ALL-SECTOR ALL-POLLUTANT MITIGATION SCENARIOS

There are a multitude of internally consistent projections of future methane emissions. Among those, the SSPs that are the result of a coordinated effort by the research community to generate consistent future scenarios that span a broad range of possible societal developments with a variety of IAMs are emphasized (Riahi *et al*. 2016). The underlying storylines include developments in socioeconomics, demographics, technology, lifestyle, policy and institutions. They consist of five distinct narratives, referred to as sustainability (SSP1), middle-of-the-road (SSP2), regional rivalry (SSP3), inequality (SSP4), and fossil-fueled development (SSP5). These scenarios are intended to span a range of challenge levels for both mitigation and adaptation. For mitigation, challenges are rated as relatively small for SSP1 and SSP4, medium for SSP2, and high for SSP3 and SSP5. Each scenario includes a baseline case as well as scenarios with increasingly stringent climate change mitigation goals. To examine the question of how much methane mitigation is achievable and how much is consistent with worldwide targets for climate change mitigation, this analysis is particularly interested in scenarios consistent with the 1.5°C target as assessed in the 2018 IPCC *Special Report on Global Warming of 1.5°C* (IPCC 2018; Rogelj *et al*. 2018). Here those scenarios classified by IPCC as either having at least a 50 per cent likelihood of keeping temperatures below 1.5°C throughout the 21st century and those with a median temperature below 1.5°C in 2100 but with a 50–66 per cent change of overshooting that value during the century, typically by no more than 0.1°C, are considered. Many, but not all, of these scenarios were generated within the SSP framework.

Given the wide range of socio-economic assumptions, it is not surprising that projected methane emissions over the remainder of this century vary markedly across the baseline cases for the SSPs (Figure 4.1). Through 2060, emissions are greatest for SSP3 and SSP5, but from 2070 onward they are largest in SSP3 as emissions in some regions continue to grow rapidly throughout the century. This increase is largely driven by agriculture as food demands increase with an ever-growing population that exceeds 12 billion by 2100. Under SSP3, no models were able to produce a 1.5°C scenario. Models were able to generate 1.5°C and 2°C

scenarios for the other four SSPs, though not all models could. Given the difference in baseline emissions across those four SSPs, evaluation of methane mitigation under the 1.5°C or 2°C scenarios as a fraction of projected emissions therefore depends greatly on the reference pathway. Even for 2030, there are substantial differences across the baselines with SSP4 and SSP5 having emissions of about 490–500 Mt/yr whereas SSP1 and SSP2 have emissions of about 390 Mt/yr. It should be noted that these also diverge by around 40 Mt/yr in 2020, reflecting uncertainties in current methane sources, as discussed in Chapter 2, and that the divergence is substantially larger in 2030.

Most 1.5°C scenarios are in agreement with recent observations for methane amounts (Figure 4.2). This is in contrast to the older representative concentration pathways (RCPs) that do not capture recent trends (Nisbet *et al*. 2020), with the better performance of the SSPs unsurprising as they were created later when these observations were known. This analysis has screened out the few scenarios that do not agree with observations made in the past decade for methane. The scenarios included in this assessment come from seven distinct IAMs, though not all provided all diagnostic outputs.

The 1.5°C scenarios show marked declines in methane amounts over the coming 20 years (Figure 4.2). These are achieved by lowering emissions in the current decade from the agriculture, forestry and other land-use category, the waste sector and especially the energy sector (Figure 4.3). All decrease energy- and waste-related emissions and all but one decrease emissions from agriculture, forestry and other land-use. In all three sectors there are large variation across models and scenarios. For the agriculture, forestry and other land-use, the average reduction in emissions in 2030 is 22 per cent compared with 2020, with a standard deviation of 18 per cent across models and a full range of 0–51 per cent. For the energy sector, the average reduction of emissions in 2030 is much larger at 59 per cent relative to 2020, with a smaller standard deviation of 14 per cent across models and a full range of -29 per cent to -82 per cent. For the waste sector, the average reduction of emissions in 2030 is between the other two at 34 per cent relative to 2020, with a substantial standard deviation of 23 per cent across models and a full range of -6 per cent to -78 per cent. The average reduction in the total from these three sectors is 37 per cent reduction in anthropogenic methane emissions in 2030 relative to 2020. Hence the 1.5°C

scenarios provide a wide range of estimates of potential methane mitigation relative to the present. Assuming the relative mitigation across subsectors is similar to that reported for most of these same IAMs under 2°C scenarios in 2050, this translates to average 2030 reductions of about 20 per cent for enteric fermentation, 22 per cent for manure management and 30 per cent for rice cultivation. For energy and waste, estimated reductions are about 75 per cent for coal mining related emissions, 60 per cent for oil and natural gas, 65 per cent for landfills and 45 per cent for sewage.

Analysis of the SSPs, which include some 1.5°C scenarios but not the full dataset shown in Figures 4.2 and 4.3, provides estimates of mitigation potential in a given future year relative to the reference case emissions for that year. Despite reference emissions varying greatly across the SSPs, mitigation in 2030 is fairly consistent across them (Figure 4.4). Examining the mean across IAMs, excepting SSP4, for which there is only one model that produced a 1.5°C scenario and that model's results also do not vary greatly across SSPs, methane abatement is around 50–70 Mt/yr- for land-use, primarily agriculture, and around 120–130 Mt/yr for the energy and waste sectors combined. There is a large range of results across the different IAMs, however, which show mitigation levels that differ by up to a factor of about seven in land-use and about two and a half in the energy and waste sectors combined. For SSP1 and SSP2, for which at least four models produced 1.5°C scenarios, the range for land-use mitigation in 2030 is in the range of 17–125 Mt/yr whereas for the energy and waste sectors combined the range is 69–192 Mt/yr.

Fuel switching plays an important role in the decreases in methane emissions from the energy sector in most of the IAMs. Transitioning to renewables, for example, would in the long term remove the bulk of methane emissions, and is what happens in most IAMs in order to achieve stringent mitigation targets. This does not happen, however, in all pathways consistent with low warming targets. The scenarios examined in 2018 IPCC *Special Report on Global Warming of 1.5°C* and classified as having no or limited overshoot, for example, found the 25th percentile showed a decrease of 26 per cent in primary energy from gas whereas the 75th percentile suggested an increase of 21 per cent in 2030 relative to 2010 (IPCC 2018). The full range across those scenarios shows a median decrease of 15 per cent in primary energy from gas between 2020 and 2030, but the range is extremely broad, expanding from 105–153 exajoules (EJ) in 2020 to 17–174 EJ in

2030 (Rogelj *et al*. 2018). As a result, there is a possibility that the use of gas, and hence fugitive methane emissions from the gas subsector as well as emissions associated with its extraction, will increase even under aggressive climate change mitigation policies. This is quite distinct from the use of coal or oil, which drop much more uniformly across all potential scenarios. Most of the scenarios that include increases in gas use over the next decades maintain consistency with the stringent climate targets by relying on large-scale negative-emissions technologies in the future to compensate for their high early emissions. This is primarily biofuel energy with carbon capture and storage (BECCS), which does not currently exist at scale, is currently quite expensive though the models project that it might be inexpensive many decades into the future, and requires converting large areas of land to growing biofuel crops rather than food with associated issues around food security, water usage, fertilizer application and biodiversity, which has led to popular protests against even the limited current deployment of biofuel plants without carbon capture and storage. Biofuel energy with carbon capture and storage is also not carbon negative in the short-term and can in fact lead to temporarily increased carbon, when, for example, a forest is cut down for biofuel use (Sterman *et al*. 2018; Holtsmark 2012). Many of these barriers also exist for the carbon capture and storage portion alone, as it similarly does not currently exist at scale and remains expensive. Hence there are multiple risks that this technology will not work, will be too expensive, and/or will have so many side effects that society will not want to use it. Those scenarios also generally overshoot the 1.5°C target substantially, only returning to an appropriate level towards the very end of this century.

Scenarios that do not overshoot the target or rely heavily on biofuel energy with carbon capture and storage generally feature a shift away from gas to renewables, but in a small number of those use of gas goes up over the current decade as well. In those pathways, afforestation can be very large and carbon capture and storage is eventually applied to natural gas plants, turning them in to approximately carbon neutral power sources. This technology does not raise the issues of water and land use associated with biofuel energy with carbon capture and storage, but does still assume that carbon capture and storage technology drops dramatically in price so that it becomes fairly inexpensive to have gas with carbon capture and storage before mid-century. Thus, there is still a range from

steep declines in gas usage for primary energy to substantial increases through 2030, though the typical values across those scenarios are decreases of ~15–30 per cent, with the largest decreases being about 85 per cent. When the analysis is restricted to only those scenarios in which the average 2040-2060 BECCS and afforestation values are fairly low (less than 5.0 Gt CO_2/yr and 3.6 Gt CO_2/yr, respectively), global production of gas has to decline annually by ~3% over 2020-2030 to be consistent with a 1.5°C pathway (SEI *et al.* 2020). This corresponds to a decrease in gas usage by roughly one-third by 2030, whereas current plans and projections are for an increase of ~20 per cent relative to 2020 usage (SEI *et al.* 2020).

It is worth emphasizing the dramatic changes required in scenarios that do not rely on large-scale future deployment of carbon capture and storage, whether for bio or fossil fuels. Analyses show that without large amounts of carbon removal, given the large reduction in gas usage required under low warming pathways even the current fossil fuel infrastructure is incompatible

with the world's climate targets, with the situation much worse when planned additional fossil fuel energy sector infrastructure is also considered (Shearer *et al*. 2020; Pfeiffer *et al*. 2018). This implies that use of current power plants would have to be curtailed either by early retirement or a reduction in usage and construction of additional fossil capacity halted in the absence of large-scale carbon removal in order to meet the well-below 2°C target.

In addition, a transition away from fossil fuels could still leave abandoned infrastructure. There were more than 3.2 million abandoned oil and gas wells in the United States alone in 2018, which emit ~0.3 Mt/yr of methane according to the US EPA (US EPA report to UNFCCC; 2020). That agency acknowledges that this figure is likely a large underestimate due to incomplete data. Similarly, The International Institute for Applied Systems Analysis (IIASA) estimates that 2020 emissions of methane from abandoned coal mines around the world are just over 3.5 Mt/yr (Höglund-Isaksson 2020).
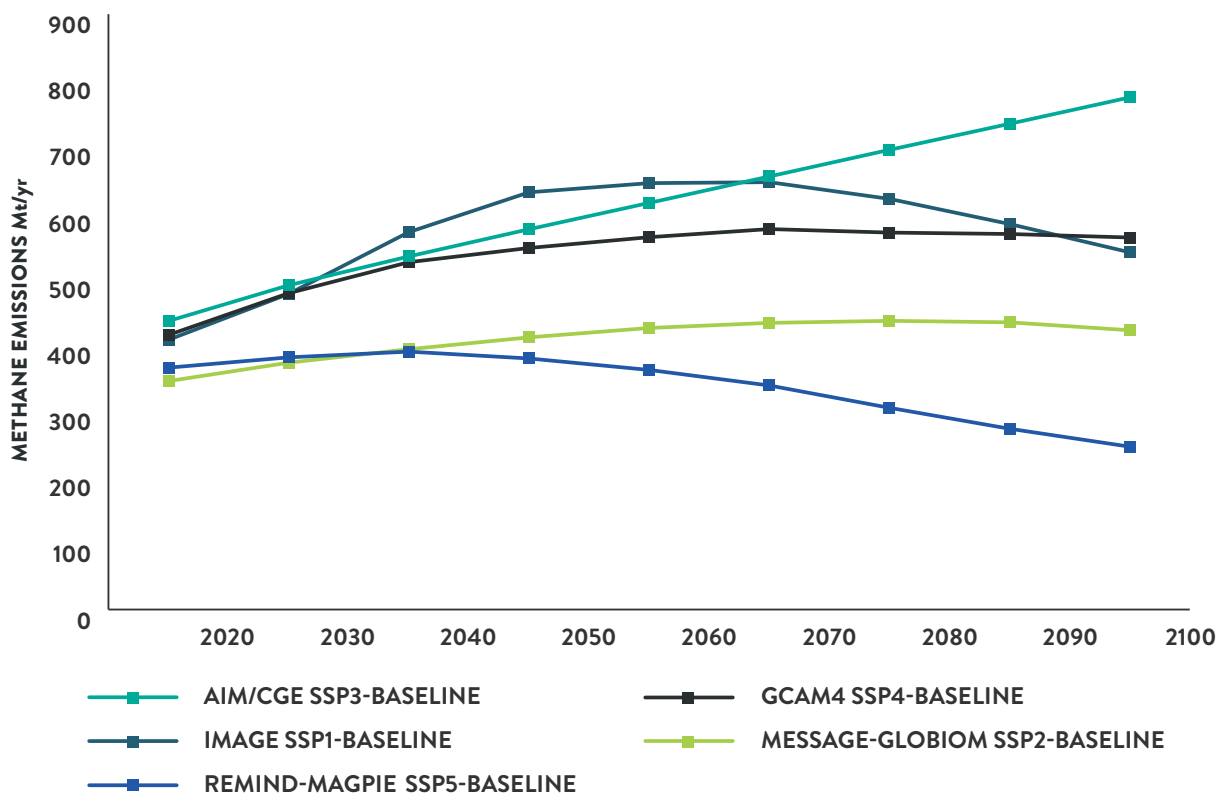
Figure 4.1 Estimated global total anthropogenic methane emissions under the five shared socioeconomic pathway baseline scenarios, 2020–2100, million tonnes per year

Values are shown for the marker scenario with a particular integrated assessment model's results chosen as a representative example for each shared socioeconomic pathway.

Source: UNEP and CCAC
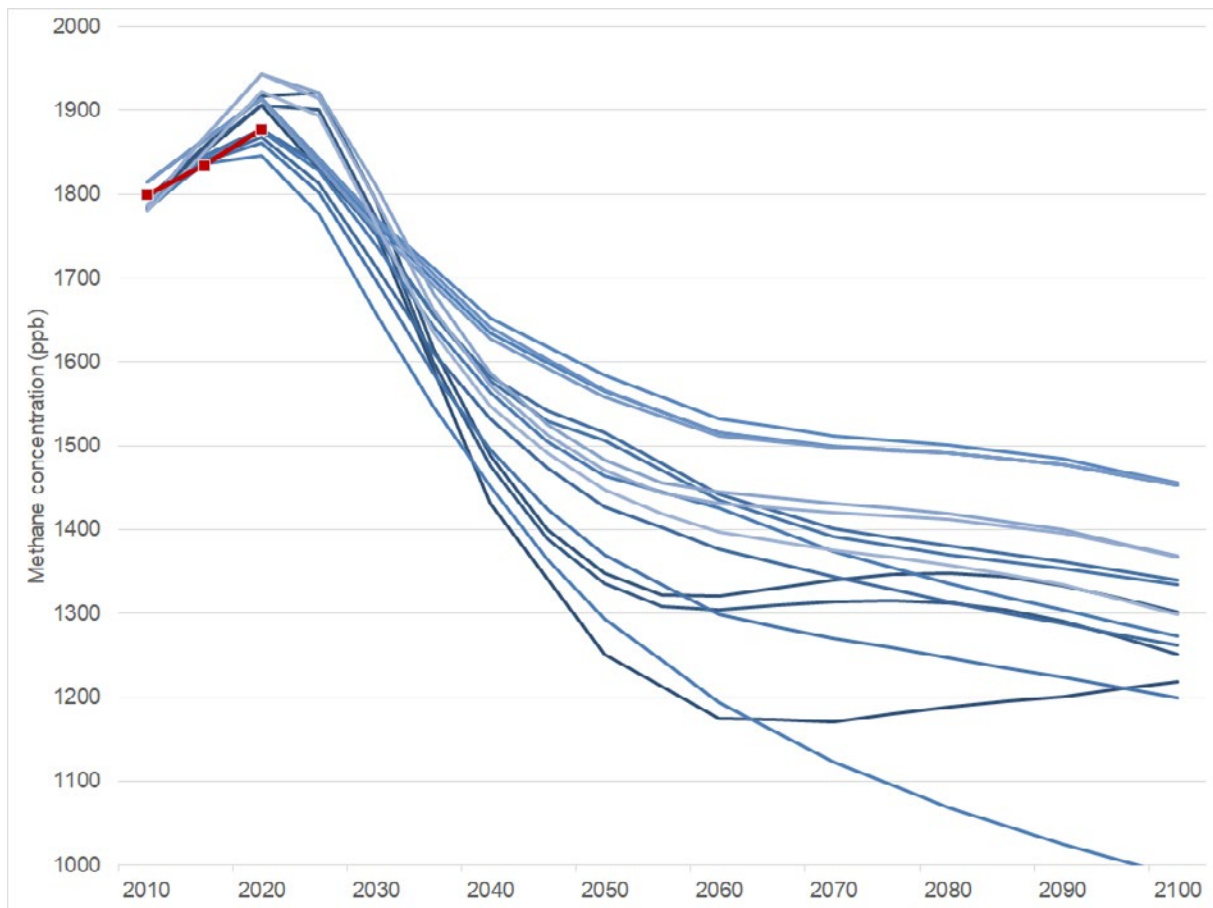
Figure 4.2 Estimated global average methane amounts under scenarios consistent with 1.5ºC, and as observed for 2010–2020, parts per billion

Source: UNEP and CCAC
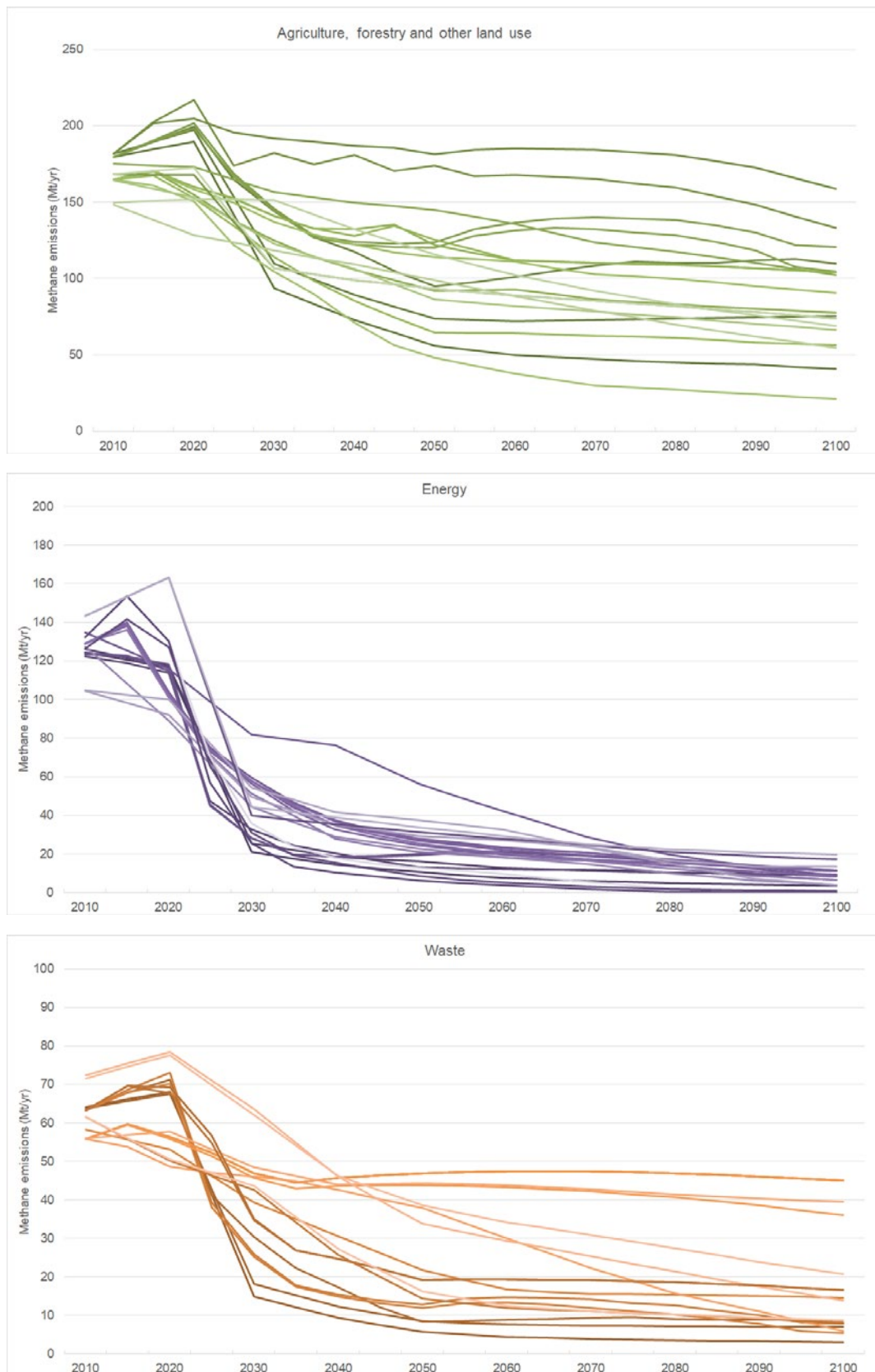
Figure 4.3 Estimated total global anthropogenic methane emissions under scenarios consistent with 1.5°C from the land-use (top), energy (middle) and waste (bottom) sectors, 2010–2100, million tonnes per year

Note: All available scenarios that included all three sectors are shown.

Source: UNEP and CCAC

AGRICULTURE, FORESTRY AND OTHER LAND USE
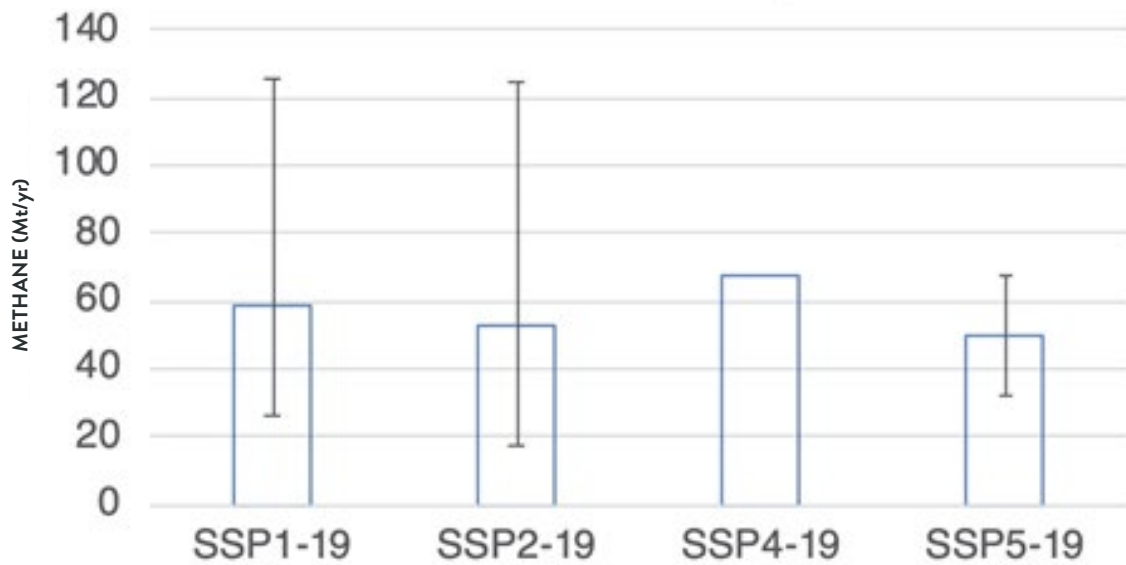
ENERGY AND WASTE
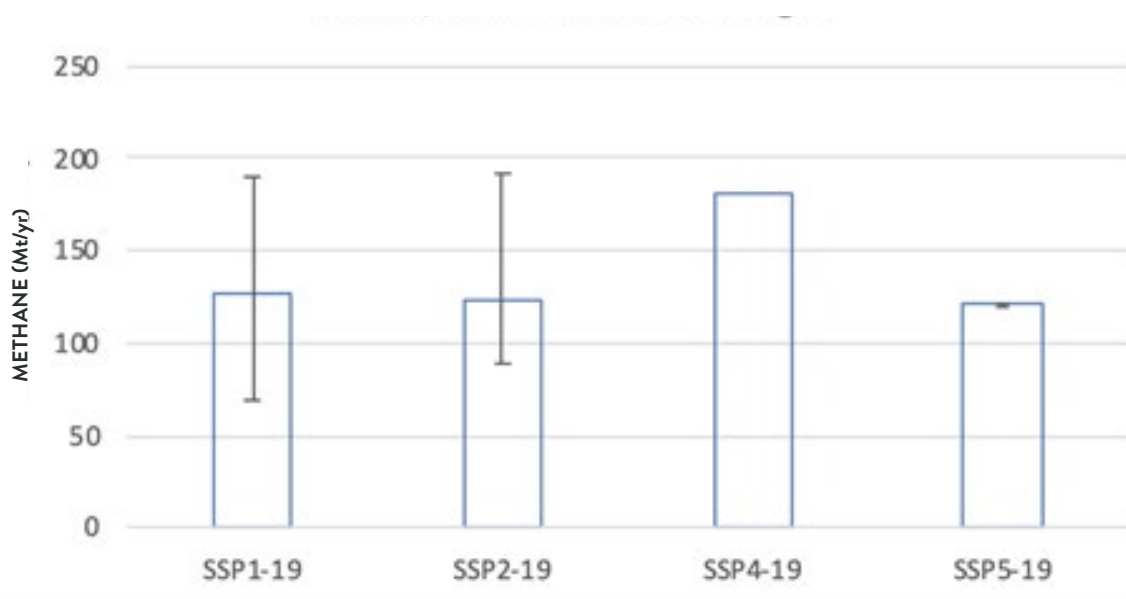
Figure 4.4 Estimates of methane mitigation potential for the land-use (top) and the energy and waste (bottom) sectors under the four shared socioeconomic pathways for which at least one model produced a 1.5°C scenario, 2030, million tonnes of methane per year

Note: Bars show the mean across integrated assessment models and ranges indicate maximum and minimum values – there is no range for SSP4 as only one produced a 1.5°C scenario under that pathway. Similarly, the range is very small for SSP5 as only two models produced a 1.5° C scenario. Agriculture, forestry and other land use includes biomass burning. Energy and Waste includes small contributions from biofuels and transportation.

Source: UNEP and CCAC

4.2 MARGINAL ABATEMENT POTENTIALS AND COSTS BY SECTOR

The methane abatement that takes place in the all-sector all-pollutant climate change mitigation scenarios discussed in Section 4.1 is based in part on abatement cost curves that are incorporated within the IAMs. These encompass methane mitigation opportunities in multiple sectors at a variety of costs, which are examined in detail in this section. Abatement potentials have been analyzed by several teams, including IIASA, US EPA, the International Energy Agency (IEA) and in a literature review by Harmsen *et al*. (2019). These analyses are similar in their aims but differ in coverage and methodology. In particular, the IEA analysis includes only the oil and gas subsector and analyzes present-day abatement potentials associated with targeted control measures (IEA 2020). In contrast, the IIASA analysis covers all sectors and include time-dependent estimates of both changes in baseline emissions and mitigation in which the latter include sector-specific assumptions about technology turnover times, based on the literature, improvements in technology over time and the achievable pace of regulations (Höglund-Isaksson 2020). The IIASA analysis, furthermore, includes discount rates of 4 and 10 per cent in their cost evaluation and extends to 2050. The US EPA produced analyses in 2019 that similarly include projected changes in baseline emissions, extend to 2050, and use a discount rate of 10 per cent in cost estimates (US EPA 2019). Finally, the Harmsen *et al*. (2019) analysis covers all sectors, includes estimates of technology development and the removal of implementation barriers through 2050 as implemented in the Integrated Model to Assess the Global Environment (IMAGE) IAM following SSP2, and uses a discount rate of 5 per cent. This analysis is not entirely independent of the others as it relies upon IIASA data for the fossil fuel sector and earlier US EPA data (US EPA 2013) for the waste sector but implements different projections of future development and so obtains different results even in those sectors as well as in the agricultural sector for which it provides an independent analysis. Note that the IEA documentation does not describe the discount rate used in its analysis.

To create compatible regional analyses, the following changes were made relative to regional results reported by these groups: for the IIASA analyses, Oceanian OECD, China, India, and the rest of Southeast Asia were added to create an Asia-Pacific group; for the IEA analyses, Ukraine was moved from Europe to Russia and the Former

Soviet Union and Mexico was moved from North America to Latin and Central America. The data from Harmsen *et al*. and the US EPA was provided at relatively high resolution, allowing its (re)assembly into the regions used in this assessment. Total anthropogenic emissions are estimated to be around 364–380 Mt/yr based on the central values of bottom-up and top-down estimates (Chapter 2). The IEA analysis does not have total baseline emissions as it does not include all sectors. The Harmsen analysis, using the IMAGE model with all sectors, has a value ~390 Mt/yr, similar to the Chapter 2 estimates. The IIASA analyses, without emissions from forest fires and savannah burning or transport, has baseline emissions of ~345 Mt/yr, similar to the analogous value of ~355 Mt/yr based on the source estimates described in Chapter 2. The US EPA baseline emissions, with the same sectors as IIASA, other than the very small source from agricultural waste burning, are substantially lower at ~325 Mt/yr. This value is based on national reporting to the UNFCCC, supplemented with IPCC Tier 1 methods, and this methodological difference is likely the main driver of this much lower baseline. In order to increase comparability across the mitigation analyses and to bring the US EPA estimates in line with the source estimates of Chapter 2, the US EPA baseline and mitigation has been scaled up by 7 per cent uniformly across all sectors, which brings the total to the same amount as the IIASA analysis, the next lowest baseline. Given the large uncertainties in emission source strengths discussed in Chapter 2, it is difficult to classify a particular baseline as inconsistent with observations however, and so this should be regarded as primarily a method to enhance comparability across the analyses. Based on the findings of potential underestimates of fossil-related methane sources based on ice cores discussed in Chapter 2 (Hmiel *et al*. 2020), it is noted that even the scaled US EPA baseline estimates and the IIASA baseline estimates may be biased low, with similar biases carrying over to mitigation.

4.2.1 BROAD SECTORAL ANALYSES

To analyze the abatement potential across broad sectors, these are grouped into five categories for ease of visualization: all oil and gas, coal, all livestock, rice, and all waste. Groups beginning with *all* include multiple subsectors, whereas rice is self standing and coal is related to mining alone, though some analyses do divide this by active and abandoned coal mines. These groupings

are somewhat arbitrary and were chosen in part to reflect data availability – the IEA, for example, does not include coal, precluding their inclusion in a fossil fuel sector. Analysis of results within these groupings is presented in Section 4.2.2.

At the global scale and considering abatement measures regardless of costs, the four analyses all find the greatest potential within the oil and gas subsector, for which 2030 (2020 for IEA) the maximum abatement range is 29–57 Mt/yr. There is greater divergence in the cost estimates than in the mitigation potential, with the average abatement cost being around US$ 1 000 per tonne of methane in the Harmsen analyses, near zero in the IEA analysis, and having a net negative cost of roughly US$ 700 per tonne methane in the IIASA analysis. The average cost in the US EPA analysis is nearly US$ 30 000 per tonne of methane, but this very high value results from a small number of very expensive measures. Restricting the analysis to those measures with costs of less than US$ 25 000 (2018 US dollars) per tonne of methane, which would be US$ 1 000 per tonne carbon dioxide equivalent if using a global warming potential over 100 years (GWP100) of 25, as in the US EPA analysis, reveals 85 per cent of the total abatement potential is available at an average cost of US$2 300 per tonne of methane (Figure 4.5). Though this cost is much lower, it is still higher than those of the other three analyses, which do not incorporate abatement measures costing more than US$ 25 000 per tonne of methane.

The three analyses that included the waste sector find very similar mitigation potentials of 29–36 Mt/yr but very different cost estimates that range from the most expensive (Harmsen) to the largest net negative costs (IIASA), for which there are several reasons. Firstly, IIASA's mitigation potential considers almost full source separation of organic waste with recycling or energy recovery possible globally. US EPA assumes a gradual shift away from open dumps in developing countries but this appears to be at a slower rate than in the IIASA analysis. Secondly, in the cost estimates, IIASA considers the cost-savings from recycling, energy recovery and use, and the opportunity cost of avoided landfilling. The cost-savings are subtracted from the investment and maintenance costs to arrive at net costs. Average world market prices for recycled materials are used to value cost savings of recycling and expected future gas and electricity prices from IEA are used to reflect the benefit of energy recovery in the waste sector. The US EPA uses generally similar methods, but

the larger discount rate in their analysis would make net costs higher. Note that the range quoted above is for all measures regardless of costs, but, as with the oil and gas subsector, the US EPA analysis includes a small number of very expensive measures in the wastewater subsector. When these are excluded, the mitigation potential in that analysis decreases from 36 to 32 Mt/yr and the costs become similar to the other analyses for the waste sector (Figure 4.5).

As a result of the above, extremely large discrepancies in the cost estimates result from the use of differing boundaries within the sector, different assumptions about global capacities, potentially different timescales for phasing in mitigation measures, and the inclusion of a small set of extremely expensive controls. It should also be noted that in the case of paper recycling, in the IIASA estimate this is reflected as a gain based the average global market price of recycled paper, but this may inflate the benefits because the market price of recycled paper is often distorted by the pulp and paper industry intervening in the market to keep the price of both recycled and virgin pulp high and stable, at least in some regions. The US EPA analysis also includes a price for scrap paper of US$ 140 per tonne.

In contrast, estimates of mitigation options for livestock are in fairly good agreement as to the costs but differ markedly in magnitude. In the Harmsen analysis, the mitigation potential is 42 Mt/yr, making it the second largest potential, the IIASA analysis is only 4 Mt/yr making it the group with the smallest potential among the five considered here, the US EPA analysis is in between at 12 Mt/yr (Figure 4.5). Average costs are similar at ~US$ 600 (IIASA) or ~US$ 1 000 (Harmsen and US EPA) per tonne of methane. Results for abatement from coal mining are relatively similar across the analyses in both potential and costs, with values of 12–25 Mt/yr[1] and average costs of ~US$ 100–700 per tonne. Finally, the mitigation potential is similar in the three analyses for rice cultivation at 6–9 Mt/yr but, as with waste, costs diverge greatly with the average value being ~US$ 150 per tonne in the IIASA analysis and about 20 times that, ~US$ 3 000 per tonne of methane, in the Harmsen analysis and the US EPA in between at US$ 1 700 per tonne.

The analysis of abatement potential available at all costs is a useful way of characterizing the maximum potential through targeted measures. These results can be highly influenced by a

small subset of very expensive measures, however, as noted previously for the US EPA's oil and gas subsector and wastewater results, and as such it is also useful to examine those measures that can be put into place at a low cost, which is defined here as less than US$ 600 per tonne methane, which would correspond to ~US$ 21 per tonne of carbon dioxide equivalent if converted using the IPCC Fifth Assessment Report's GWP100 value of 28 that excludes carbon-cycle feedbacks.

The abatement potential of low-cost controls is naturally smaller than the all-cost potential, but the difference varies by source group and across the four analyses. For oil and gas subsector, the low-cost measures make up ~80 per cent of the all-cost measures in the IIASA analyses, but only ~60 per cent in the US EPA and IEA analysis and just 36% in the Harmsen analysis. This leads to a large range of mitigation potentials, as in the all-cost case, with low-cost abatement in oil and gas ranging from 18 to 32 Mt/yr. Average costs remain positive in the Harmsen analysis despite the imposition of a low-cost threshold that removes the most abatement, which presumably largely accounts for its much smaller fraction of the total abatement potential falling within the low-cost threshold for the average costs. Average costs are slightly negative in the US EPA and IEA analyses, with IEA having the largest mitigation potential, and strongly negative for the IIASA analysis (Figure 4.6). Around 10–20 Mt/yr in the waste sector can be abated at low cost, though, as with all costs, the differences in scope lead to a large divergence in average costs across the analyses. They are, however, consistent in finding that most coal-related methane emissions abatement comes at low cost, though the values range from 55 to 98 per cent of the total potential. In contrast, the divergence between the three analyses expands for the mitigation potential for livestock when a low-cost threshold is imposed. Computing the mean across the available analyses for each subsector, the total mitigation potential available at low cost is estimated to be about 73 Mt/yr. This is a large fraction of the ~120 Mt/yr available at all costs.

Including only those abatement measures with negative costs reveals that the greatest potential for net economic benefits without accounting for environmental impacts comes from mitigating emissions from the oil and gas subsector and the waste sector (Figure 4.7). This is unsurprising given that many of the control measures for these two sources consist of capture and use of natural gas. Potentials are

smaller in the coal, rice and livestock subsectors and as noted previously, divergences in average cost estimates are large for livestock.

Analysis of the nine regions used in this assessment shows marked differences in mitigation potentials. For the all-cost analysis, the largest abatement potentials are as follows: for Europe and India in the waste sector; for China in the coal subsector, followed by livestock; for Africa livestock, followed by oil and gas; for Asia Pacific, excluding China and India, the coal subsector and the waste sector, for the Middle East, North America and Russia/Former Soviet Union (FSU) the oil and gas subsector; and for Latin America the livestock subsector. As with the global analysis, a large majority of these major abatement potentials can generally be achieved at low cost. This is especially the case for waste and the coal subsector, whereas for livestock the costs are quite dependent on the abatement analysis. The bulk of the abatement in the oil and gas subsector can also be achieved at low cost for North America in all four analyses, but for Russia and the Former Soviet Union this is the case in three of the four with one finding only about a third of all cost mitigation is available at low cost. For the Middle East, two of the analyses found 70–80 per cent of mitigation is available at low cost whereas the other two found less than half was available. Hence there are varying degrees of consistency across the analyses, but in most regions, it is clear where the largest methane abatement potential lies.

The total mitigation potentials analyzed here are a large fraction of the total emissions. For waste, the ~30 Mt/yr all-cost reductions represent roughly 40 per cent of the estimated 2030 emissions. For fossil fuels, the ~60 Mt/yr all-cost mitigation potential is likewise about 40 per cent of the estimated 2030 total. For agriculture, however, targeted measures make a smaller and less robust percentage contribution, with the analyses providing estimates of about 10, 15 and 35 per cent of estimated 2030 emissions from this sector (~10–50 M/yr).

This assessment focuses on the abatement potential for methane in 2030. The mitigation potential analyses of IIASA, Harmsen and the US EPA extend further into the future, and we also compare worldwide potentials in 2030 with those estimated for 2050. Though all three analyses include projected changes in baseline emissions and technological progress, there are much larger differences in 2050 values relative to their 2030 equivalents in the IIASA analysis than

in the Harmsen or US EPA analyses (Figure 4.8). The greatest differences are seen in the waste sector, in which, in particular for solid waste, the IIASA analysis reports a more than three-fold growth in low cost abatement potential between 2030 and 2050, whereas the growth is only 18 per cent in the Harmsen analysis that is based on the 2013 US EPA estimates and 41 per cent in the 2019 US EPA estimates. As noted previously, this is primarily related to the assumption that regions outside of Europe will continue to landfill waste rather than use source separation. For fossil fuels, there is again an 18 per cent growth in the estimated low-cost abatement potential over between 2030 and 2050 in the Harmsen analysis and a similar 17 per cent growth in the US EPA analysis whereas the growth is 67 per cent in the IIASA analysis.

The IIASA analysis also includes more than a tripling of the all-cost agricultural sector abatement potential between 2030 and 2050, which instead decreases slightly in the Harmsen and US EPA analyses, bringing the results of the IIASA and Harmsen analyses for this sector closer together in 2050. The three analyses still diverge substantially – 20 Mt in the US EPA analysis, 35 Mt of methane according to IIASA and 68 Mt according to Harmsen. They are closer for rice cultivation with 8 Mt in the US EPA analysis, 15 Mt in Harmsen, and 16 Mt in IIASA, but there are large differences in the abatement of livestock emissions; 11 Mt in the US EPA and 16 Mt in IIASA while Harmsen suggests 53 Mt. The difference is in the assessment of the feasible abatement potential for enteric fermentation in ruminants. While Harmsen sees

a large potential from replacing low-productivity indigenous cows and cattle globally with imported highly productive breeds, the other analyses only see this as a feasible solution for large industrial farms. For smallholder farmers in Africa and Southeast Asia, they do not see this as a feasible targeted solution without first implementing institutional and social reforms. This is because of the important role that keeping livestock plays in poor farmers' risk management; as assets when access to credits and health insurance schemes is missing.

Changes in average abatement costs for the low-cost measures are small over the 2030–2050 period in all three analyses for the fossil fuel and waste sectors, as well as their underlying subsectors. Projected changes in low-cost abatement potentials are substantial in the agricultural sector in the IIASA analysis while they are small for the other two, but costs in this sector are also not projected to change greatly over time. The large divergence in costs therefore remains with the average costs of low-cost measures across all sectors having fairly small positive values, from US$ 15–200 per tonne of methane, in the Harmsen study which had a minimum cost of zero whereas they are negative in the IIASA and US EPA analyses in which the range is about -US$ 1 000–10 000 per tonne for the global sectoral averages for waste, fossil fuels and agriculture. In 2050, the total low-cost abatement potential is estimated to be about 110 Mt/yr for the average of the three analyses, roughly 50 per cent larger than the 2030 potential.
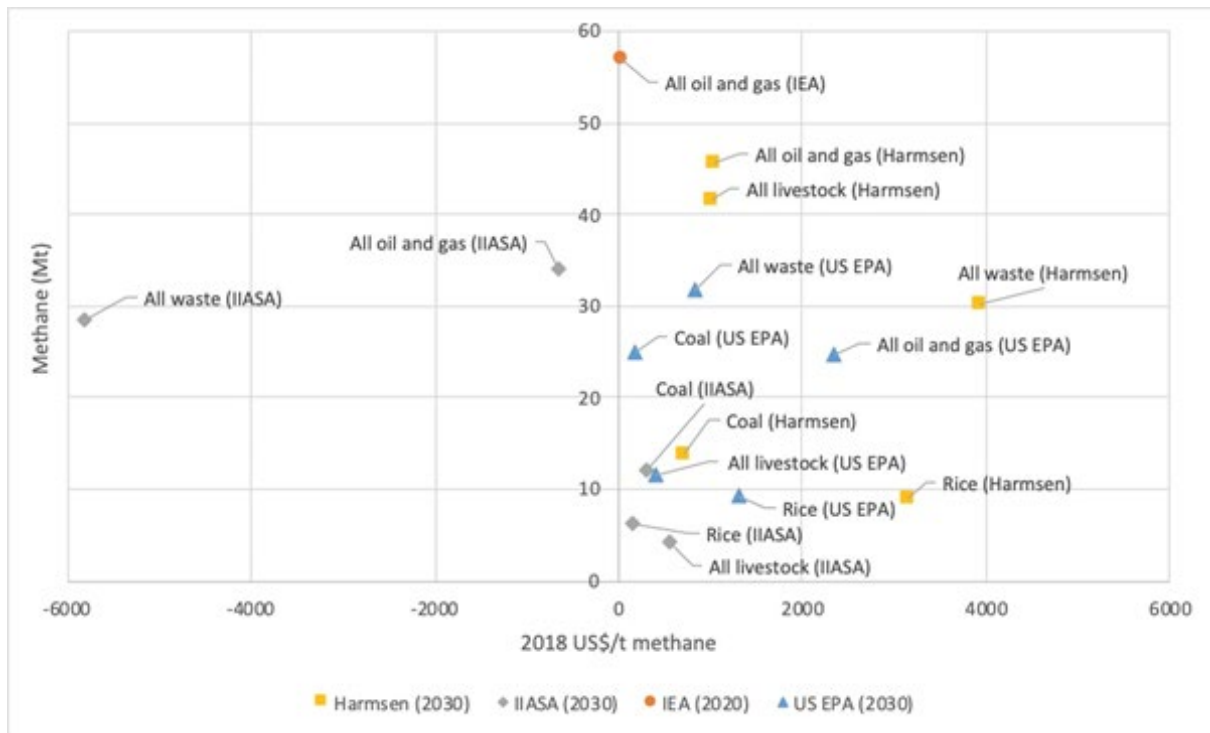
Figure 4.5 Worldwide methane mitigation potential by sector, million tonnes, versus average mitigation cost, 2018 US$ per tonne, from the indicated analyses

Note: All costs of mitigation are included below a US$ 25 000 per tonne of methane exclusion threshold.

Source: UNEP and CCAC
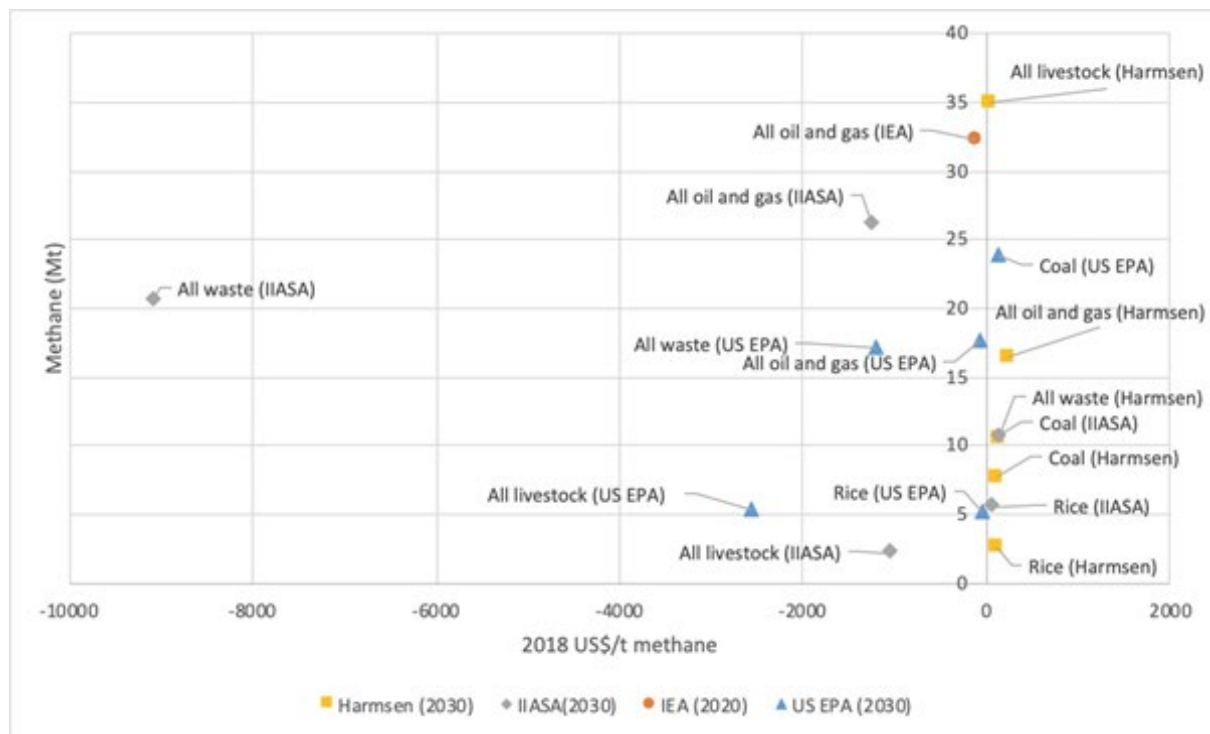
Figure 4.6 Worldwide methane mitigation potential by sector, million tonnes, versus average mitigation cost, 2018 US$ per tonne, from the indicated analyses

Note: Only includes abatement measures that cost less than 2018 US$ 600 per tonne of methane.

Source: UNEP and CCAC
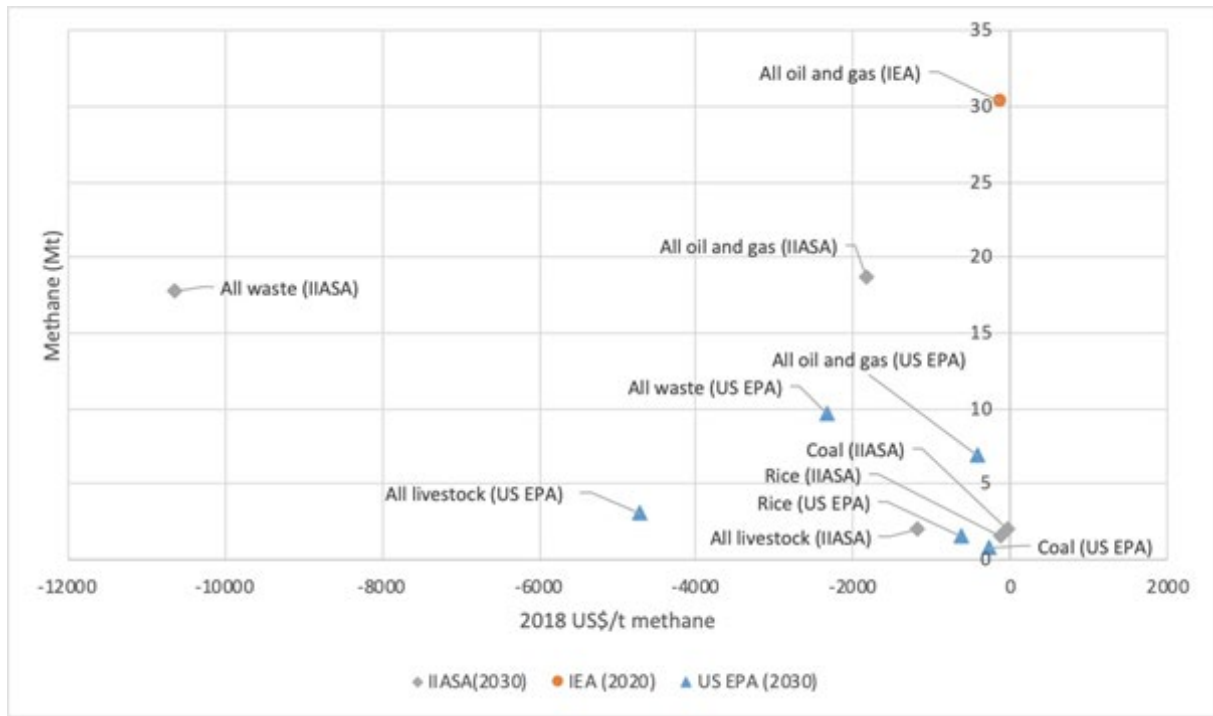
Figure 4.7 Worldwide methane mitigation potential by sector, million tonnes, versus average mitigation cost, 2018 US$ per tonne, from the indicated analyses

Note: Only includes abatement measures with negative net costs.

Source: UNEP and CCAC
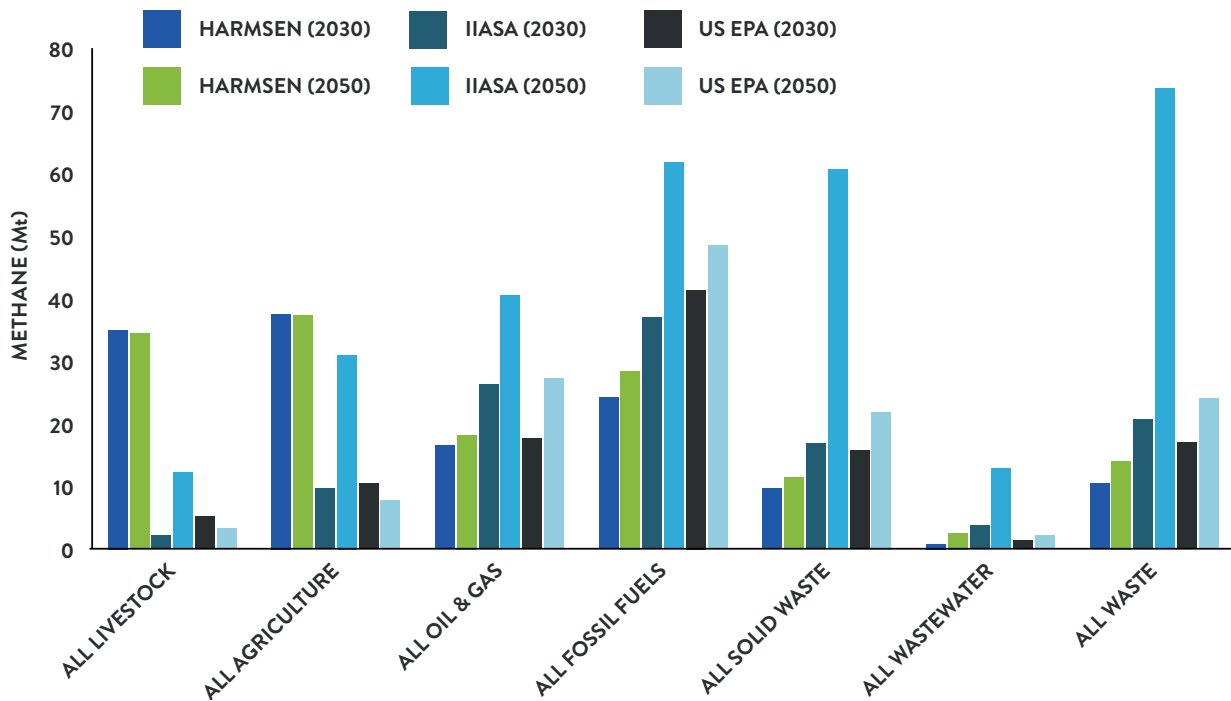
Figure 4.8 Comparison of mitigation potentials in the Harmsen, IIASA and US EPA analyses by sector for measures costing less than 2018 US$ 600 per tonne methane, 2030 and 2050

Source: UNEP and CCAC

4.2.2 DETAILED SUBSECTOR ANALYSES

Within the three of the five categories examined in the previous section, all oil and gas, all livestock, and all waste, there are several subsectors with different abatement potential, techniques and costs. These are explored here, beginning with oil and gas, putting this into context with the fossil sector as a whole, followed by waste and then livestock, similarly putting this into context with the agricultural sector as a whole.

The IEA analysis, which is only available for the oil and gas subsector, estimates that the full application of best available abatement technologies could reduce the oil and gas subsector's methane emissions by approximately 57 Mt annually, 72 per cent of its current emissions. These results are similar to those reported in the Harmsen study with substantially lower potential according to the IIASA and US EPA analyses (Figure 4.9). Within the oil and gas subsector, the IEA analysis finds larger potential in gas whereas the Harmsen and IIASA analyses find larger potential in oil, in the Harmsen case substantially so. The US EPA analysis does not separate oil and gas.

In comparison, mitigation options in the coal sector are slightly smaller than in either the oil or gas subsectors in the IIASA and Harmsen analyses, but the coal subsector potential is larger in the US EPA analysis than in either of those studies. The average of these leads to roughly comparable contributions from oil, gas and coal in the total abatement potential. The total fossil fuel mitigation potential is fairly robust across the three analyses, with the full range captured as 53 ± 7 Mt/yr. The average of the three coal subsector mitigation analyses and the four oil and gas analyses is higher at 58 Mt/yr. This represents from roughly 30 per cent to just over half of projected 2030 emissions from this sector. Looking at only the low-cost measures, the total fossil fuel abatement potential differs more sharply across the three analyses, with values of 24–42 Mt/yr (Figure 4.10) and an average based on the three coal subsector mitigation analyses and the four oil and gas analyses of 37 Mt/yr. Again, it seems that the abatement potential for the low-cost subset of all controls is similar for the three fossil fuels, except in the Harmsen analysis which includes little low-cost abatement within the oil subsector. Specific controls for all sectors applied in the various analyses are listed in Table 4.1.

The IEA, IIASA and US EPA analyses, but not the Harmsen study, all analyzed the portion of identified emissions reductions that could be achieved at a net cost savings. These are particularly large for the oil and gas subsector in which there is a net saving to operators through reduced losses. For this subsector, the portion of total reductions (Figure 4.9) that can be realized at negative cost is 53 per cent in the IEA analysis, 55 per cent in the IIASA analysis, and 25 per cent in the US EPA analysis for the global total in 2030. Though the IEA and IIASA analyses are similar for the global total, they vary substantially for some regions. In Europe, for example, the portion of abatement available at negative cost is only 31 per cent in the IEA analysis, but 87 per cent in IIASA's analysis. The spread is also large for North America, with values of 56 per cent in the IEA analysis and 92 per cent in the IIASA analysis. Russia and the Former Soviet Union has a generally smaller percentage of abatement potential with negative costs, 45–59 per cent, whereas all other regions have more than 70 per cent of emissions abatable at negative costs in at least one analysis. For the coal subsector, IIASA and US EPA, the two analyses with results for the subsector, find that 3 (US EPA) to 17 (IIASA) per cent of identified global emissions reductions can be achieved at negative costs, and again results are more variable at the regional level. For the waste sector, these two analyses differ considerably, with 27 per cent of global emissions reductions having negative costs according to the US EPA analysis and 62 per cent in the IIASA analysis, due to the differing scope of their economic analysis previously discussed.

Additional detail is provided for the oil and gas subsector within both the IEA and IIASA analyses. As shown in Figure 4.9, the IIASA analysis finds substantially less mitigation potential in the oil and gas subsector than the other three analyses, including the IEA. Examination of the components of this subsector shows that the differences are consistent across the components, but the relative differences are largest for natural gas production and smallest for oil production with downstream gas in the middle (Figure 4.11). Some of this discrepancy comes from the inclusion of technology turnover times by the IIASA that is not included in the IEA analysis, as can be seen by examining the IIASA abatement potential in 2050 which is substantially larger as roughly two thirds of the total mitigation potential in that analysis takes place in the 2030s with only on third in the 2020s. The difference between the oil and gas totals in the IIASA and US EPA results relative to the Harmsen results may also be linked to

turnover times, as the Harmsen analyses are based on assessments that are 5–10 years older than the IIASA and US EPA assessments. Harmsen is a review of assessments produced around 2012–2016 while the US EPA and IIASA studies were for 2019 to 2020. This leaves only a ~10-year horizon until 2030 in those analyses versus 15–18 years in the Harmsen study.

Individual abatement technologies were examined at a very detailed level in the IEA analysis. The IEA classifies all emissions from production, gathering and processing of fuels as upstream and all emissions from refining, transmission and distribution as downstream. Their analysis shows that the category with the largest mitigation potential, upstream leak detection and repair (LDAR), is also the cheapest. The bulk of the negative cost benefits are obtained from five abatement technologies, each of which contributes substantial health and climate benefits while simultaneously leading to economic gains even when the value of the environmental impacts is not included (Figure 4.12). The majority of the negative cost options occur in four source categories, onshore conventional oil and gas and offshore oil and gas, whereas abatement within the unconventional oil and gas and downstream categories typically have positive costs. Full application of all abatement technology in the offshore and onshore conventional categories, including individual applications with positive costs, would result in abatement of ~40 Mt/yr of methane emissions, leading to a reduction in global mean surface warming of ~0.05 C and ~45 000 avoided premature deaths annually with an overall negative cost for each of these four production sources – Chapter 5 includes more discussion of socio-economic impacts of abatement. Accounting for the environmental benefits of emissions reductions, all the identified IEA targeted measures have negative net costs. It should be note, however, that the most costly of the measures analyzed by IEA, the installation of flares, would likely lead to increased emissions of black carbon that would have damaging health and climate impacts (Stohl *et al*. 2015).

Within the waste sector, all cost abatement potential is concentrated within the solid waste subsector which has three to six times the potential found in the wastewater (sewage) subsector (Figure 4.9). Totals in the three available analyses are very similar for the full waste sector, so that the full range is captured by 32 ± 4 Mt/yr. Hence this sector has about half the potential of the fossil sector for all cost measures and a much narrower uncertainty range. Evaluating this mitigation potential as a share of projected 2030 waste sector emissions is complicated by a large divergence between them, which were ~70 Mt/yr in the Harmsen and US EPA analyses, whereas there was a much larger value of 114 Mt/yr in the IIASA analysis. Hence although all the studies find similar abatement potential, the share of 2030 emissions from waste estimated to be abatable ranges from just 25 per cent in the IIASA analysis to ~40-50 per cent in the US EPA and Harmsen analyses. For low-cost measures in the waste sector, the analyses are again fairly consistent with all falling within the range 16 ±5 Mt/yr.

Within the waste sector, the IIASA analysis provides additional detail on specific measures. The largest abatement within the analysis is for municipal waste, for which the separation and treatment of biodegradable municipal waste with no biodegradable waste being sent to landfill forms the primary component of the estimated potential abatement. The separation of biodegradable waste is another measure with a negative cost, even without accounting for environmental impacts, with an estimated average value per tonne of methane of ~US$ 8 500 per tonne methane and a global mitigation potential of ~16 Mt/yr. Industrial solid waste also shows significant potential for abatement, ~5 Mt/yr, with again a large majority of that able to be achieved at zero or net negative costs – the average cost is -US$ 6 800 per tonne of methane. It should be noted that, in the IIASA analysis, the vast majority of the waste sector's methane emissions, other than the relatively small subsector of domestic wastewater, can be eliminated by targeted control measures by 2040. The US EPA analysis categorizes waste sector measures differently, but similarly finds many with negative cost. The largest mitigation potential with a negative net cost is nearly 9 Mt/yr for gas capture and usage for electricity generation at an average cost -US$ 1 750 per tonne methane. The largest of the negative costs is for landfill gas recovery for direct use, with an average value of -US$ 3 100 per tonne and an estimated mitigation potential of 2.2 Mt/yr. Among other waste sector measures in the US EPA analysis, flaring of landfill gas and composting are on average low-cost measures, whereas anaerobic digestion, waste to energy, mechanical biological treatment and paper recycling all have average costs higher than this assessment's low cost threshold.

Three of the analyses included the agriculture sector, and as noted previously they differ greatly

from one another. These large differences stem from livestock, as the analyses are in fairly close agreement with mitigation potentials for rice of 6, 9 and 9 Mt/yr for the all-cost abatement potential (Figure 4.9), corresponding to ~20–30 per cent of emissions from this subsector. The analyses differ markedly on the costs associated with rice methane mitigation measures, however, with nearly all the identified potential achievable at low cost in the IIASA analysis, 55 per cent in the US EPA analysis, and less than a third of them in the Harmsen analysis (Figure 4.10). For livestock, the all-cost emissions reductions represent 3 per cent of that subsector's projected 2030 emissions in the IIASA analysis, 8 per cent in the US EPA analysis and 30 per cent in Harmsen's (Figure 4.9), with the differences arising primarily from differing assumptions about the previously discussed plausibility of introducing high productivity breeds to Africa and Southeast Asia as for both rice and livestock the three analyses project similar 2030 baseline emissions. For the small agricultural waste-burning subsector within agriculture, targeted measures are estimated to be able to eliminate emissions completely at no cost in the IIASA analysis, but they will require regulation and enforcement.

Within the livestock subsector, the analyses include changes in management practices and in animal feed. Changes in management may include improving herd health, breeding for improved productivity, and shifts from pastoral to intensive systems for cattle. In the last, additional impacts on biodiversity, those living near intensive operations, and the treatment of the animals themselves need to be considered and are likely to be highly regionally dependent (Gerber *et al*. 2013). In the case of animal feed, options include processing feed grain to improve digestibility and feed supplements including nitrate and tannins (as antimethanogens). Additional feed supplements offer potential for reducing methane emissions from the livestock sector but are currently considered experimental and are therefore not included in most abatement potential analyses. In one study, an artificial supplement given to dairy cows reduces methane production from enteric fermentation by 30 per cent with no adverse effects on milk production and a gain in overall cattle growth (Hristov *et al*., 2015). Widespread application of this practice could lead to significant abatement of methane, potentially of up to 20 Mt/yr (Shindell *et al*. 2017), though the supplement has thus far been tested in only a single small herd. Adding small quantities of the seaweed *Asparagopsis taxiformis*, potentially in combination with *Oedogonium* sp., to ruminant feed has also been found to greatly reduce methane production from enteric fermentation, with decreases of 80 per cent in sheep and up to 99 per cent in cows based on *in vitro* trials (Roque *et al*. 2021; Abbott *et al*. 2020; Vijn *et al*. 2020; Kinley *et al*., 2016; Li *et al*., 2016; Machado *et al*., 2016; 2018). In both cases, further studies are needed to confirm benefits and explore the potential for scaling up these practices as well as fully characterizing potential effects on animal health and the long-term persistence of the identified potential benefits.

All three mitigation analyses for the livestock sector include methane emissions abatement through improved manure management. The primary policy in this area is the adoption of farm-scale anaerobic digesters for manure from cattle and pigs. There have also been analyses of the potential of additives mixed into the manure slurry ponds to reduce emissions, with both widely available acids such as sulfuric or lactic acid (Sokolov *et al*. 2019; Sommer *et al*. 2017; Petersen *et al*. 2014) and commercial products (Peterson *et al*. 2020; Borgonovo *et al*. 2019) having been explored. Both seem to offer the potential to greatly reduce both methane and ammonia emissions based on field studies and sulfuric acidification has been widely used in Denmark primarily to control ammonia. In the rest of the world, however, there has been limited use of such techniques, primarily owing to concerns over the safe handling of the acids and uncertainty regarding the long-term impacts on soils. In terms of mitigation potential, it appears that such practices are likely to achieve roughly the same methane reductions as the application of well-managed anaerobic digestion with biogas recovery that is included in current mitigation analyses. These are therefore not included as separate measures in the IIASA analysis, although they are included in the Harmsen analysis, along with anaerobic digesters, decreased manure storage time, improved manure storage covering and improved housing systems and bedding (Table 4.1).

It is noted that many emissions abatement measures are expected to affect methane while leaving other emissions virtually unchanged; such measures include capture of fugitive emissions or controls on landfills, use of anaerobic digestion for manure, and introducing intermittent irrigation practices for rice. Other measures, however, in particular those that affect people's diets or, especially, livestock are likely to affect emissions of carbon dioxide and nitrous oxide, both greenhouse gases – for example,

the slurry acidification of manure discussed previously may increase nitrous oxide emissions. The impacts of those additional greenhouse gas emissions on global climate could be accounted for fairly easily based on prior modelling of the response to well-mixed greenhouse gases. Changes such as fuel switching or efficiency increases would also affect multiple pollutant emissions, and hence are typically studies with IAMs rather than using MAC curve analyses – efficiency is discussed further in Section 4.3.1. In addition to methane, fuel switching from coal or increasing energy efficiency would reduce carbon dioxide and volatile organic compound emissions and air pollution, switching away from gas would reduce carbon dioxide and volatile organic compound emissions (Fann et al. 2018), and reducing consumption of cattle-based foods would be likely to reduce both carbon dioxide emissions by reducing deforestation, and nitrous oxide emissions through reducing fertilizer use, and hence all these measures would be expected to yield addition benefits through non-methane emissions changes rather than having additional impacts that offset some of those related to planetary warming described in Chapter 3.
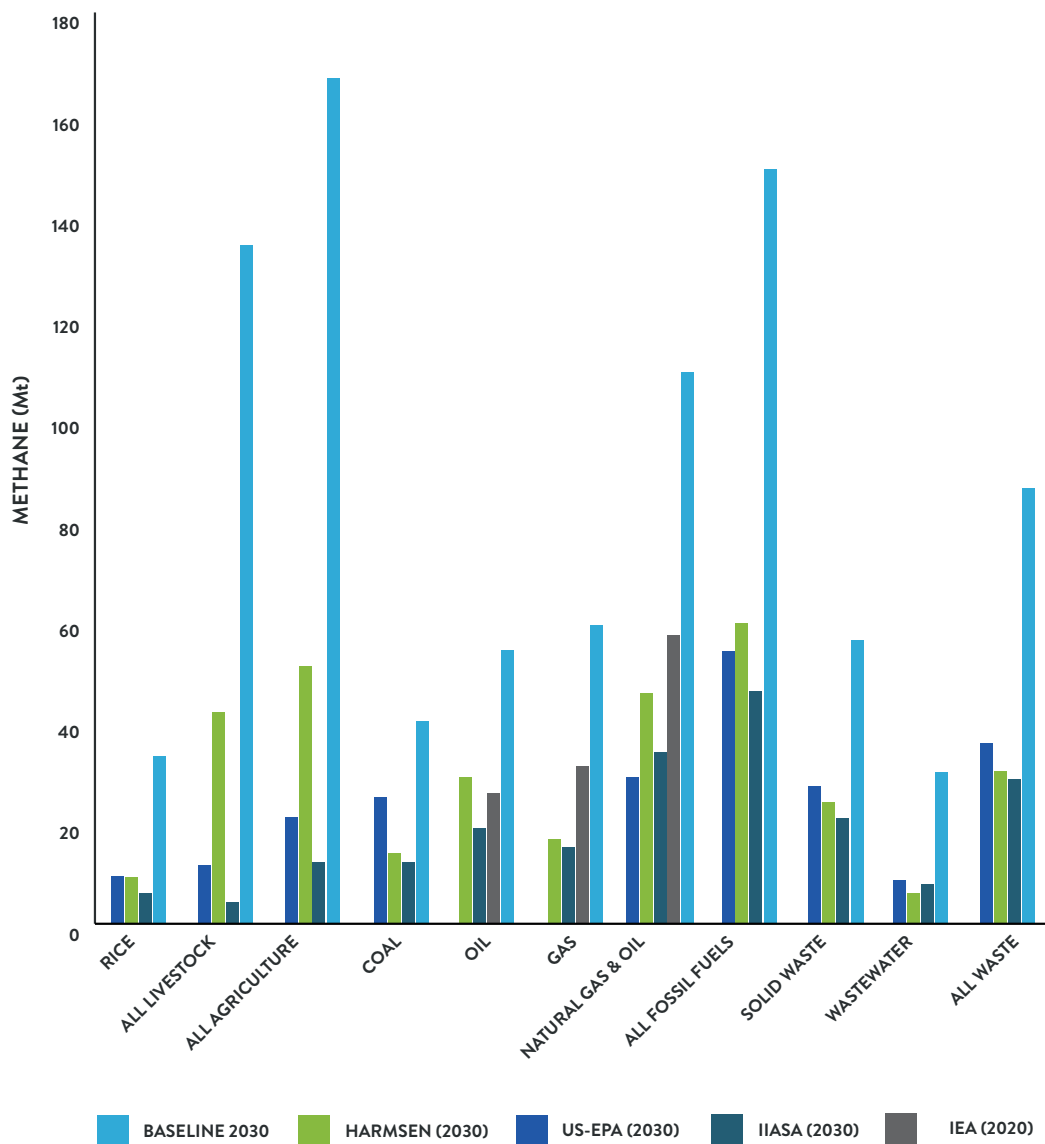
Figure 4.9 Methane emissions mitigation potentials for 2020 for the IEA analysis and 2030 in the Harmsen, IIASA and US EPA analyses including all cost measures as well as the average baseline 2030 emission projected in the IIASA, Harmsen and US EPA analyses

Note: The potential in the IIASA and US EPA studies is based on a 10 year time horizon whereas the Harmsen study has an ~15 year horizon.

Source: UNEP and CCAC

Figure 4.10 Methane emissions mitigation potentials for 2020 for the IEA analysis and 2030 in the Harmsen, IIASA and US EPA analyses for measures costing less than 2018 US$ 600 per tonne of methane

Source: UNEP and CCAC
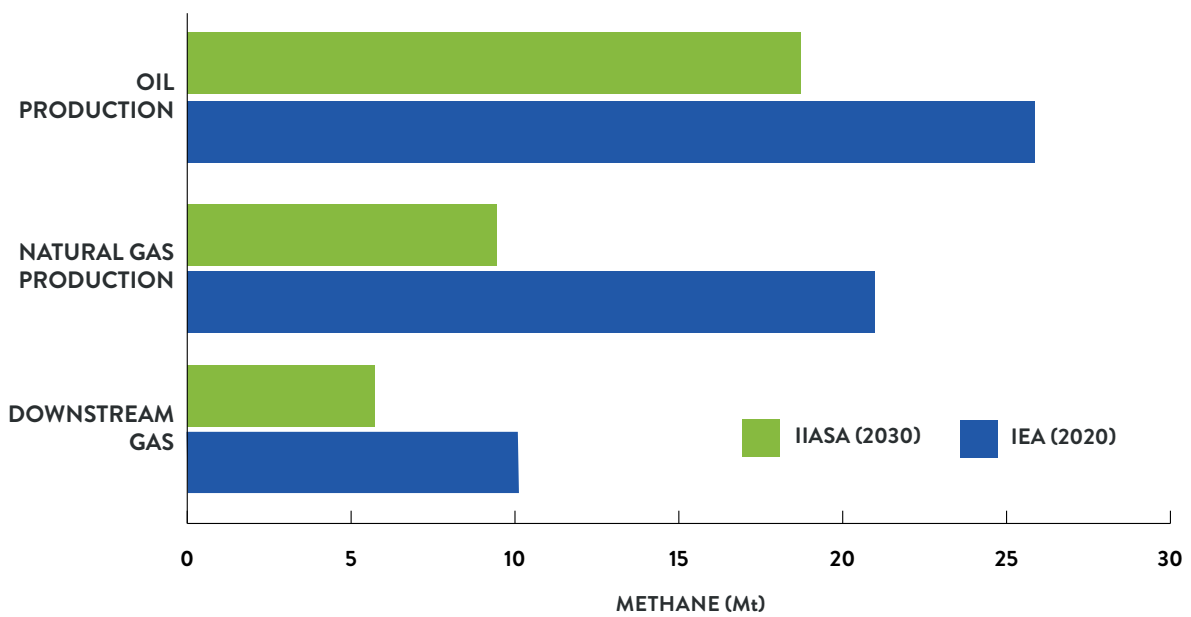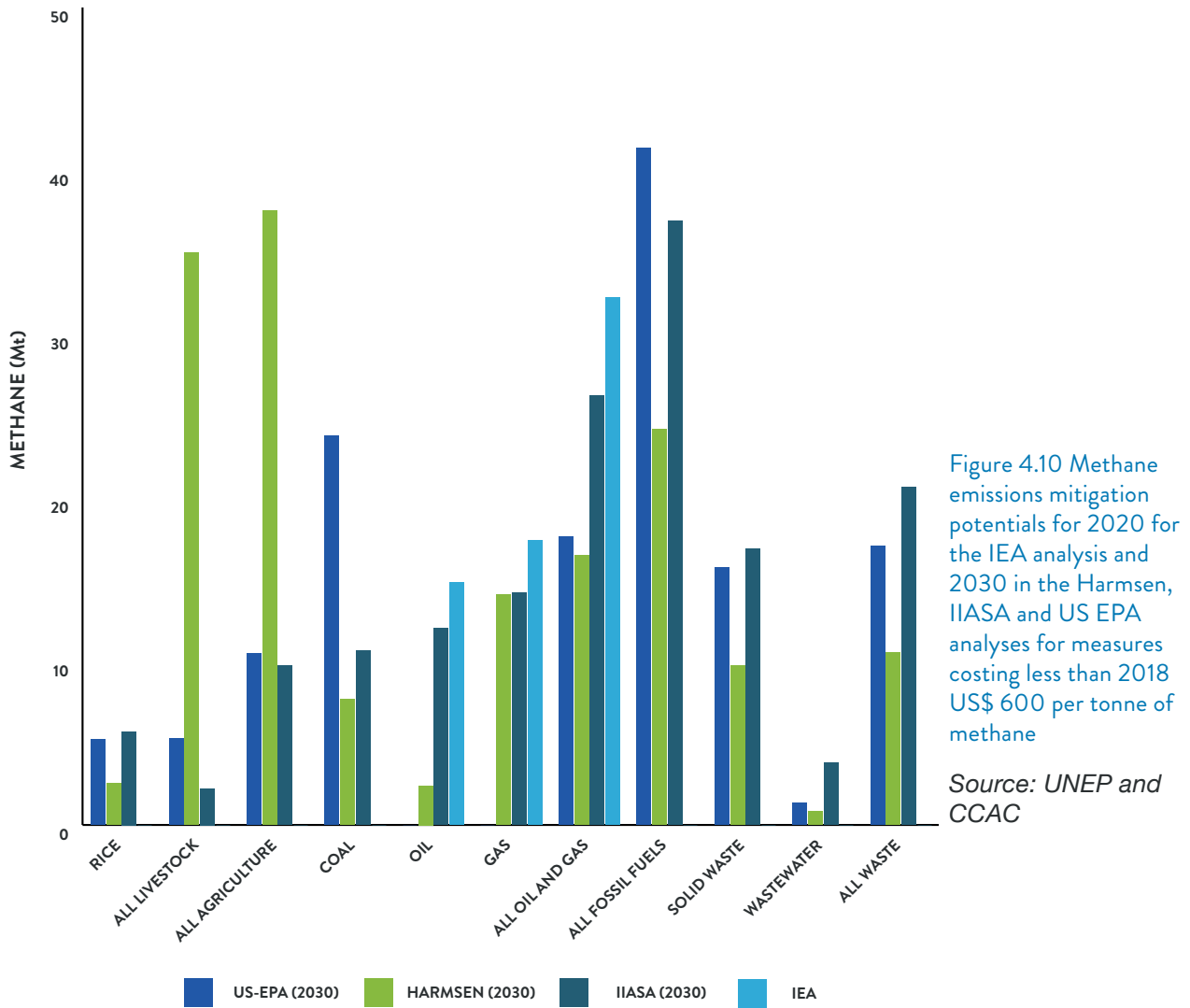
Figure 4.11 IEA estimated mitigation potentials in the oil and gas sectors, million tonnes of methane

Note: IEA potentials are estimated for 2020 while the IIASA values are shown for 2030.

Source: UNEP and CCAC
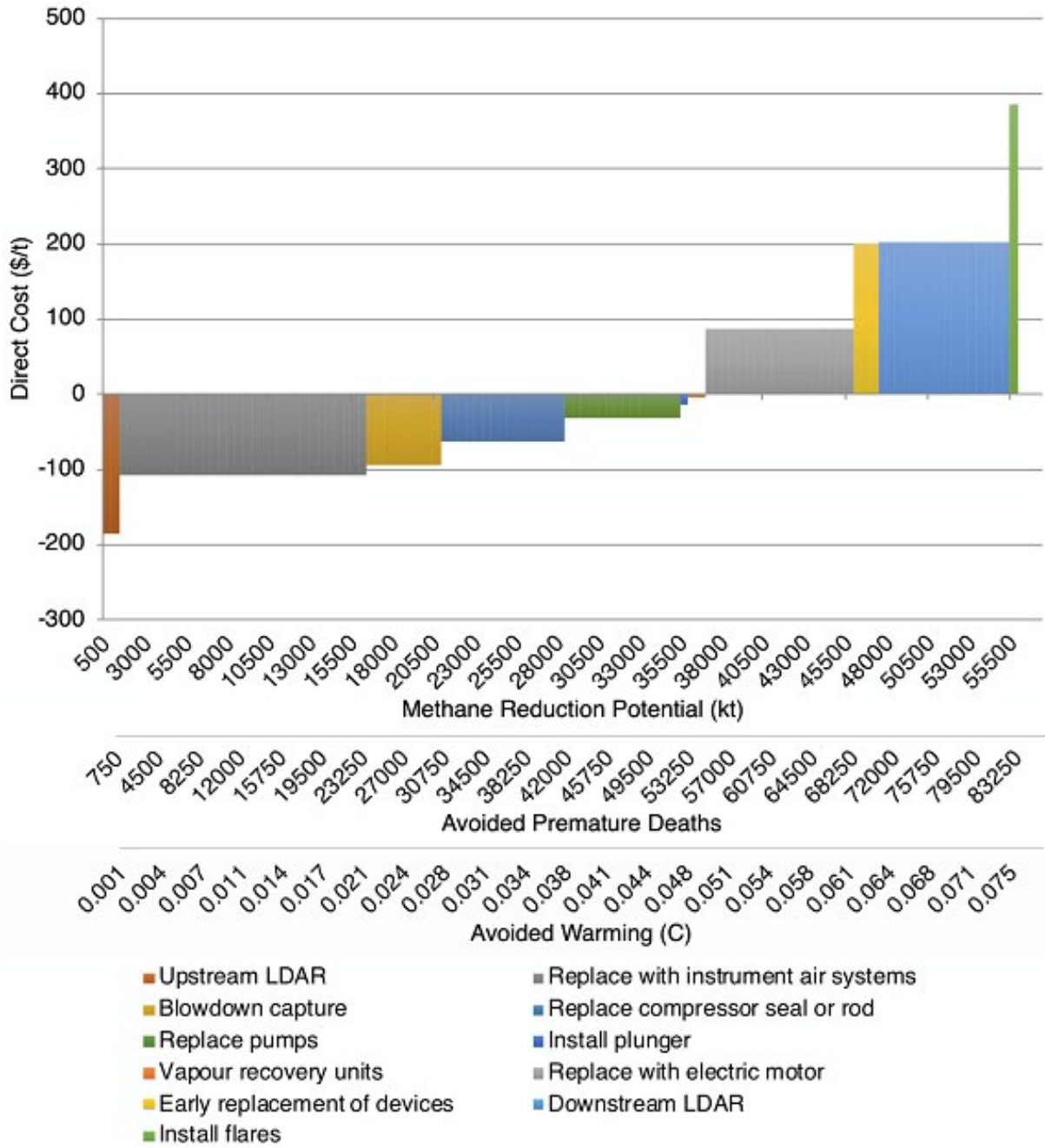
Figure 4.12 Relative savings/costs (2018 US$ per tonne) of targeted methane abatement measures in the oil and gas sector identified by the IEA showing the reduction potential, '000 tonnes; impacts on premature deaths and global mean surface temperature, degrees Centigrade

Source: UNEP and CCAC

Table 4.1 Emissions control measures included in at least one of the mitigation analyses

TECHNICAL CONTROLS		
FOSSIL FUELS	**WASTE**	**AGRICULTURE**
Oil and gas: upstream and downstream leak detection and repair (LDAR).	Municipal solid waste: source separation with recycling/reuse; no landfill of organic waste; treatment with energy recovery or collection and flaring of landfill gas.	Cattle, sheep and other ruminants through enteric fermentation: feed changes and supplements; breeding to improve productivity and animal health/fertility.
Oil and gas: blowdown capture; recovery and utilization of vented gas with vapour recovery units and well plungers; installation of flares.	Industrial solid waste: recycling or treatment with energy recovery; no landfill of organic waste.	Ruminants and pigs through manure management: treatment in biogas digesters; decreased manure storage time; improved manure storage covering; improved housing systems and bedding; manure acidification.
Oil and gas by existing devices: replace pressurized gas pumps and controllers with electric or air systems; replace gas-powered pneumatic devices and gasoline or diesel engines with electric motors; early replacement of devices with lower-release versions; replace compressor seals or rods; cap unused wells.	Residential wastewater: upgrade of primary treatment to secondary/tertiary anaerobic treatment with biogas recovery and utilization. Wastewater treatment plants instead of latrines and disposal.	Rice cultivation: improved water management or alternate flooding/drainage wetland rice; direct wet seeding; phosphogypsum and sulphate addition to inhibit methanogenesis; composting rice straw; use of alternative hybrids.
Coal mining: pre-mining degasification; air methane oxidation with improved ventilation.	Industrial wastewater: upgrade of treatment to two-stage treatment, i.e., anaerobic treatment with biogas recovery followed by aerobic treatment.	Agricultural waste burning: ban and enforcement of existing bans.
Coal mining: flooding abandoned mines.		
BEHAVIOURAL AND TECHNOLOGICAL CHANGES		
FOSSIL FUELS	**WASTE**	**AGRICULTURE**
Fuel switching from fossil fuels to renewables/nuclear.		Reduced food waste.
Energy demand management.		Dietary change.
Energy efficiency improvement.		
Emissions pricing.	Emissions pricing.	Emissions pricing.

4.3 ABATEMENT IN RESPONSE TO METHANE-SPECIFIC POLICIES

4.3.1 MULTIPLE INTEGRATED ASSESSMENT MODEL 2050 ANALYSES

The IAMs used to generate scenarios consistent with particular warming targets are designed to achieve those targets at the lowest possible cost considering all sectors, usually all pollutants, and all mitigation options including targeted controls, behavioural changes and directed policies such as taxes. They therefore include many methane abatement measures, as discussed in Section 4.1. Here the methane abatement in those scenarios are compared with the total potential from the analyses discussed in Section 4.2 and with the response seen in IAMs to methane-specific policies.

An analysis of nine IAMs has probed their changes in methane emissions in response to various policies, focusing on the year 2050 (Harmsen *et al*. 2019b), and here the impact of low carbon scenarios on methane in 2050 is also discussed. In the reference cases used in the Harmsen *et al*. (2019b) study, which follow SSP2, anthropogenic emissions are projected to rise from 2010 levels of about 360 Mt/yr to about 460 Mt/yr in 2050. Transitioning to the least-cost mitigation pathway consistent with the 2°C climate target in those models leads to a decrease in emissions to about 185 Mt/yr in 2050 to, a reduction of about 275 Mt/yr, 60 per cent. This is towards the high end of the emissions consistent with 1.5°C scenarios shown in Section 4.1, which range from about 60 to 200 Mt/yr in 2050. In contrast, were a climate policy to consider mitigation of carbon dioxide alone, i.e. following a 2°C-like scenario but imposing an emissions price only on carbon dioxide, the reduction would be only about 80 Mt/yr. Comparison of these results demonstrates that the bulk of the methane reductions under a 2°C scenario come about from policies targeted directly at methane as opposed to being merely a co-benefit of a strategy focused of carbon dioxide. This highlights that general measures to decarbonize the economy result in only a modest reduction in methane emissions over the near term. In the case of SSP2, the carbon dioxide focused mitigation policies lead to only ~30 per cent of the methane abatement in 2050 seen under a broad 2°C scenario, and a similar fraction over the longer term with values of 22–48 per cent of the 2°C abatement in 2100 (Harmsen *et al*. 2019b). This stems from the limited impact of carbon dioxide-focussed mitigation policies on waste and agricultural sector methane emissions as a whole and on end-of-pipe controls for methane on remaining fossil fuel use within the energy sector.

Across sectors, under a 2°C climate policy the models produce reductions in methane emissions from fossil fuels that are essentially as large as their maximum reduction potential. In contrast, reductions in emissions from agricultural subsectors – manure, enteric fermentation and rice cultivation – are lower than the maximum potential, whereas those for waste – sewage and landfills – are at the maximum in some models but lower in others. Reductions are typically greater than 50 per cent for fossil fuels and landfills, and they extend as high as 95 per cent, but smaller for other sectors, with 25–55 per cent for manure, 15–80 per cent for sewage, 25–65 per cent for rice and about 15–45 per cent for enteric fermentation. Along with these percentage changes, it is important to consider the overall magnitude of each source. Along a 2°C pathway in the IAMs, emissions from manure, oil, coal and landfills are nearly always 20 Mt/yr or less each by 2050, and emissions from sewage, rice and natural gas are nearly always 35 Mt/yr or less respectively, whereas emissions from enteric fermentation primarily range from about 80 to 140 Mt/yr. Hence enteric fermentation, especially from cattle, becomes by far the dominant remaining source of methane emissions in the IAMs under 2°C scenarios, even in those with the largest estimates of reduction in that sector – emissions in the very lowest emission example for this sub-sector are slightly more than 60 Mt/yr.

The analysis of methane emissions in IAMs not only explored the response in least-cost multi-pollutant pathways and in the carbon dioxide tax only pathways, but also examined the role of a cross-sector focus on methane (Harmsen *et al*. 2019b). This was accomplished by imposing an economy-wide tax on methane emissions and examining how the models responded. In principle, this is similar to imposing a cap on methane and allowing markets to find the least-cost way of staying within that cap. The tax was imposed from 2020 at a value of 2018 US\$ 2 100 × 1.05 to the power of (year-2040) per tonne of methane. This leads to ~US\$ 790 in 2020 and ~US\$ 1 300 in 2030 greater than the low-cost threshold. Hence these analyses encompass reductions larger than those included in these analyses of marginal abatement potential available at low cost and that covering all costs reported in Section 4.2.

The results show that the models generally respond to a methane tax by most strongly reducing emissions from the energy sector, followed by

land use, largely agriculture, and lastly the waste sector (Figure 4.13, top). Differences between the models are very large, however, especially for the land-use and waste sectors. Delving more deeply into the IAM responses to a methane tax shows that the models typically produce the largest total abatement from the coal subsector, followed, in order, by enteric fermentation, landfills, gas, sewage, rice and oil (Figure 4.13, bottom). Contributions from reductions in energy demand, manure management and agricultural waste burning are small in nearly all models. Model-to-model differences are considerable, however, especially for the fossil fuel subsectors, enteric fermentation and sewage. The AIM model is particularly distinct, with far larger mitigation,

~20–30 Mt/yr in the enteric fermentation, sewage, oil and agricultural waste burning subsectors than any other IAM.

Across sectors, the models on average reduce 2050 emissions by a total of 209 Mt/yr in response to the imposed tax, representing a reduction of about 50–75 per cent in the projected 2050 emissions. The upper end of this range is consistent with the methane reductions in 2°C pathways in these same models, though on average the tax produces a smaller reduction than that which occurs in the 2°C pathways. Naturally these results would be sensitive to the level of the tax imposed in the models, though it is expected that the relative sectoral contributions are fairly robust to the level of the tax.
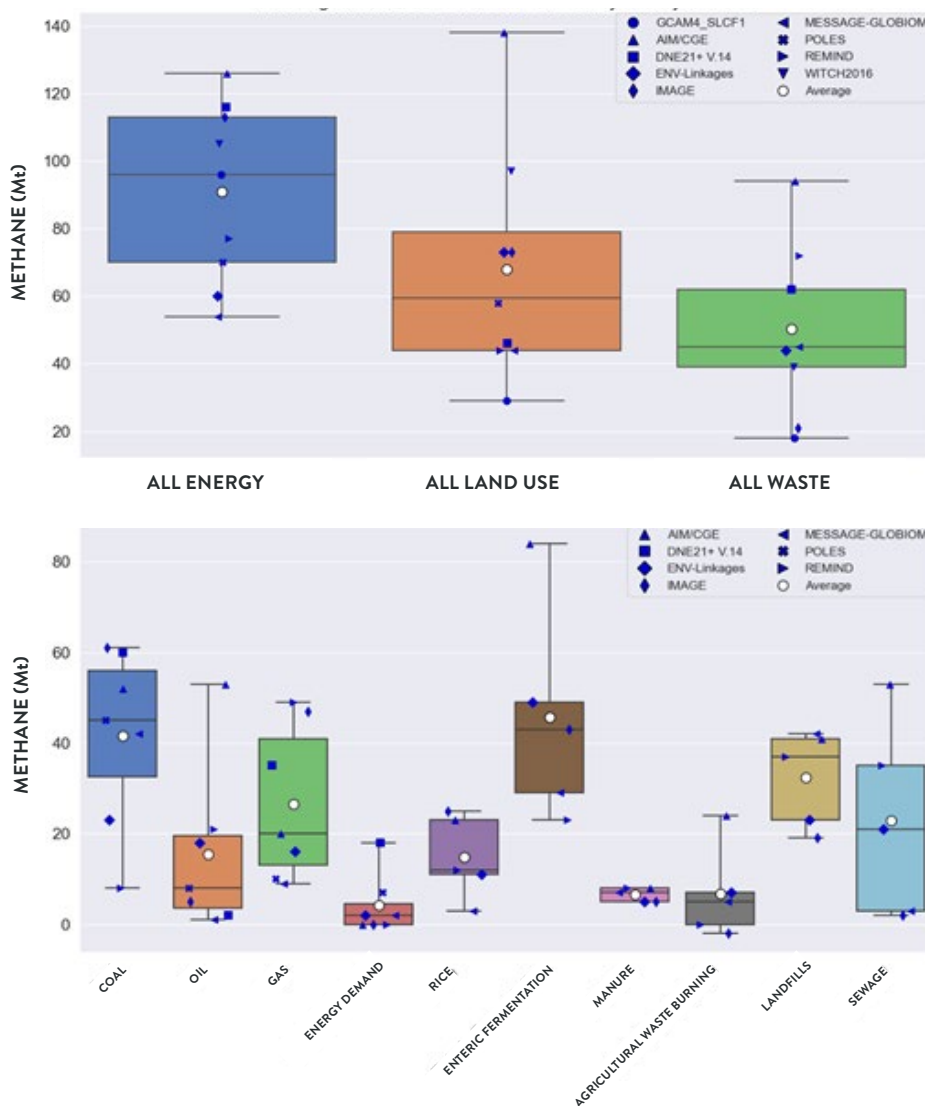
Figure 4.13 Abatement in 2050, relative to the baseline, by sector in integrated assessment model simulations that imposed a methane tax, million tonnes of methane

Note: The horizontal lines within each box are the median values, open circles are average values, filled symbols are individual integrated assessment model results, and the box and uncertainty bar show the 25–75th percentile and full range, respectively.

Source: UNEP and CCAC

4.3.2 2030 ANALYSIS USING THE GLOBAL CHANGE ASSESSMENT MODEL

Though the use of multiple IAMs in Harmsen *et al*. (2019b) provides valuable information about the relative ease of reducing methane emissions from different sectors, that analysis is restricted to 2050 and 2100 and only explored SSP2. Here, additional analyses were therefore performed using an updated version of one of the IAMs included in that study, the Global Change Assessment Model (GCAM), to examine the response in 2030 across multiple SSPs for consistency with the mitigation potential analyses. The GCAM is an IAM that is capable of simulating the dynamics of human-Earth systems and how those systems respond to global changes, such as in population, economic output, energy resource availability, technology performance and climate. The version used was GCAM5.2, as opposed to the version in Harmsen *et al*., GCAM4, that was also used to generate SSPs. The GCAM5.2 is an updated version of GCAM5.1, described in Calvin *et al*. (2019). While earlier versions of the GCAM model focussed more heavily on the energy sector, GCAM 5.2 contains additional detail in other sectors and can better reflect the reality of human-Earth systems. Compared to GCAM4, GCAM5.2 includes a new climate model, new land region and new representations of water supply and demand, regional agricultural markets, and depletable energy resources.

In this study, the environmental and socioeconomic impacts of a global tax on methane are explored. Two baseline scenarios that assume no specific climate policy is in effect were simulated, as well as versions of those scenarios in which the same global methane tax as in Harmsen *et al*. (2019b) is imposed. The differences between baseline and tax scenarios show the effects of the imposed tax for each baseline. The first baseline scenario follows the second shared socioeconomics pathway (SSP2), as in the IAM simulations in Harmsen *et al*. (2019b). No major changes from historical patterns in social, economic and technological trends are assumed in SSP2. To examine the sensitivity to the choice of baseline scenario, the second baseline follows SSP1, a sustainability scenario.

Differing from many other climate policy scenarios that either impose a tax on carbon dioxide or carbon dioxide equivalent, the methane policy scenario involves a global tax specifically on methane that increases by 5 per cent annually. The GCAM separates methane emissions into three categories:

1. methane emissions from agricultural production, including but not limited to rice cultivation and livestock;

2. methane emissions from agricultural waste, including the burning of crop residues; and

3. a general category which covers all other methane emissions.

The methane tax is applied to all three categories simultaneously. The GCAM includes marginal abatement curves for many methane sources, allowing the methane emission factor to be reduced as a function of the magnitude of the methane tax. It also has an option that allows the effectiveness of controls to improve time, representing technological improvement. This analysis opted not to use this option as the resulting removal efficiencies for some control options approached 100 per cent for future years, exceeding what was believed to be reasonable. As a result, it is expected that the scenarios used here may have underestimated methane mitigation potential and overestimated costs. To analyze the results, methane emissions were aggregated into seven groups: agriculture, fossil-fuel extraction, buildings, electricity, industry, transportation and waste, allowing the exploration of the tax's effect on different sectors.

It was found that implementing the methane tax described above (2018 US\$ 2 100 rising by 5 per cent a year up to 2040 per tonne of methane) in GCAM to represent a policy specifically designed to reduce methane emissions causes an immediate drop in anthropogenic methane emissions in the implementation year, 2025, and, under the conditions of SSP2, a fairly constant emission rate thereafter (Figure 4.14). As emissions continue to grow in the reference case, the influence of the tax grows with time, so that anthropogenic emissions are reduced by 20 per cent in 2030, 25 per cent in 2050 and 40 per cent in 2100.

The abatement in response to the economy-wide methane tax under SSP2 comes primarily from the fossil-fuel sector in the GCAM (Figure 4.15). Within this sector, abatement through 2030 is largely achieved by reductions in emissions related to coal which provide 43 Mt/yr of abatement relative to 15 Mt/yr for gas and 6 Mt/yr for oil. Reductions in emissions in the agricultural and waste sectors are also substantial, though smaller. Within agriculture, these come primarily from abatement of emissions related to rice cultivation, 10 Mt/yr of abatement, with an additional 7 Mt/yr from cattle and 4 Mt/yr each from smaller ruminants –pigs, sheep and goats.

The waste sector has a total reduction of 9 Mt/yr entirely from municipal landfills. An additional minor contribution of less than 1 Mt/yr globally in 2030, comes from reductions in the building sector. The total drop in 2030 in response to the tax is 92 Mt/yr. Examining the regional breakdown of responses to the tax, the largest share of the reductions takes place in China, 24 per cent; and Russia and the Former Soviet Union, 24 per cent; followed by Europe, 20 per cent. In contrast, 4 per cent or less each of the reductions come from North America, South and Central America, India and the Middle East, with Africa and Asia Pacific in between at 11 per cent and 12 per cent, respectively.

In contrast, under SSP1, emissions of methane are markedly lower in the baseline scenario and the imposition of the methane-specific tax has less impact on the emissions, decreasing them by 70 Mt/yr in 2030. Under SSP1, the majority of the emissions reductions again come from the fossil-fuel sector, which provides 58 Mt/yr of the 70 Mt/yr reduction. This is 91 per cent of the reduction under SSP2 but represents 83 per cent of the total reductions, a larger fraction than the 70 per cent contribution from the fossil sector under SSP2. The larger fraction of the total coming from the fossil-fuel sector under SSP1 largely stems from the greater baseline reductions in the agricultural sector under that scenario. Those remove nearly all the methane abatement potential in that sector that responded to the methane tax under SSP2, i.e. the rice and livestock abatement, so that under SSP1 the agricultural sector emissions are largely unchanged by the imposition of the methane tax (Figure 4.15). Note that the methane reduction under the baseline SSP1 scenario in the GCAM is slightly greater than that in the SSP1 marker scenario (Figure 4.1), but only marginally so. Methane emissions reductions in the waste sector in response to the tax are 9 Mt/yr- in 2030 under SSP1, equal to those under SSP2.

For comparison with the analysis from Harmsen *et al*. (2019b), presented in Section 4.3.1, the sectoral contributions in 2050 were also examined. Under SSP2, GCAM5.2 produces methane emissions abatements of 81 Mt/yr in the fossil fuel sector, 32 Mt/yr- in the agricultural sector and 15 Mt/yr in the waste sector. In response to the same tax and using the same SSP2 baseline, GCAM4 produced abatement values of 96, 29 and 18 Mt/yr in the fossil-fuel, agriculture and waste sectors, respectively. Hence overall the updated version of GCAM behaves fairly similarly to the prior version, though GCAM4 appears to have included more

use of coal in its baseline scenario. As shown in Figure 4.13, the abatement within the fossil fuel sector in response to a methane tax in the GCAM is right in the middle of that obtained across the many IAMs that performed these simulations. In 2050, the abatement within the fossil-fuel subsectors is 58 Mt/yr from coal, 16 Mt/yr from gas and 6 Mt/yr from oil, the latter two being almost the same as the 2030 values. In comparison with other IAMs, these results put GCAM5.2 towards the high-end for coal abatement but at the low end for the other fuels. The abatement in the agricultural. Land-use and waste sectors, however, is the lowest of all the participating models with a value roughly half the multi-model mean and less than a quarter of the highest value. Still examining 2050, GCAM5.2 produces an abatement of emissions in response to the methane tax of 85 Mt/yr under SSP1, only two thirds of that seen under SSP2. Hence, unsurprisingly, the influence of the baseline scenario becomes progressively more important over time.

In addition to evaluating the emission impacts of a global methane tax, the control cost of the policy in each model year was also evaluated. The GCAM reports the marginal cost of control, which is equivalent to the tax. Many of the resulting emission reductions, however, may have been achieved for less. Therefore, to estimate the policy cost in a particular year, five additional scenarios were created with taxes that were 10, 20, 40, 60, and 80 per cent of the original methane tax trajectory. Integrating these under the resulting curve for a particular year produced an estimate of the control cost for that year. Note that the control cost is not intended to represent the overall policy cost, the calculation of which would include economic feedbacks.

Analysis of the costs in GCAM5.2 show that measures considered low cost, less than US$ 600 per tonne of methane, in this assessment can abate roughly 72 Mt/yr (Figure 4.16), which corresponds to about 16 per cent of anthropogenic methane emissions under SSP2. Under SSP1, the abatement is reduced to ~54 Mt/yr, though this represents a fairly similar 15 per cent of anthropogenic methane emissions as those are reduced relative to SSP2 under that scenario's baseline. These values are fairly similar to the sum of the low-cost sectoral abatement potential estimated in the analyses by Harmsen *et al*., IIASA and the US EPA (Figure 4.10). The mitigation across sectors, however, being heavily weighted towards abatement within the fossil-fuel sector, is similar only to that in the US EPA analysis and differs substantially

from the other two. With the full tax implemented in 2030, ~US$ 1 300 per tonne of methane, roughly 21 per cent or 91 Mt/yr of emissions are abated under SSP2, a value again fairly similar to that found in the US EPA analysis (Figure 4.9). Within the fossil-fuel subsectors, however, the GCAM's abatement is overwhelmingly in coal whereas the Harmsen *et al*., IIASA and the US EPA analyses all show greater abatement potential within oil and gas than within coal.

Overall, there is broad consistency in the proportion of anthropogenic emissions that can be abated by targeted measures in approximately a decade between GCAM5.2 and the bottom-up sectoral analyses of abatement potentials. There are marked differences in the proportion within

each of the three main anthropogenic methane emission sectors, and indeed the GCAM is an outlier within IAMs in producing minimal abatement within the agricultural and waste sectors. In addition, the balance of abatement potential across the three main fossil fuels is quite different in GCAM5.2 with respect to the abatement potential analyses of the Harmsen *et al*., IIASA and the US EPA. Nonetheless, all these analyses indicate that roughly 20 per cent of anthropogenic emissions could be eliminated through targeted control measures that cost less than ~US$ 1 200 per tonne of methane, a value less than a third the societal benefit of ~US$ 4 300 per tonne based on the evaluation in Section 3.5.
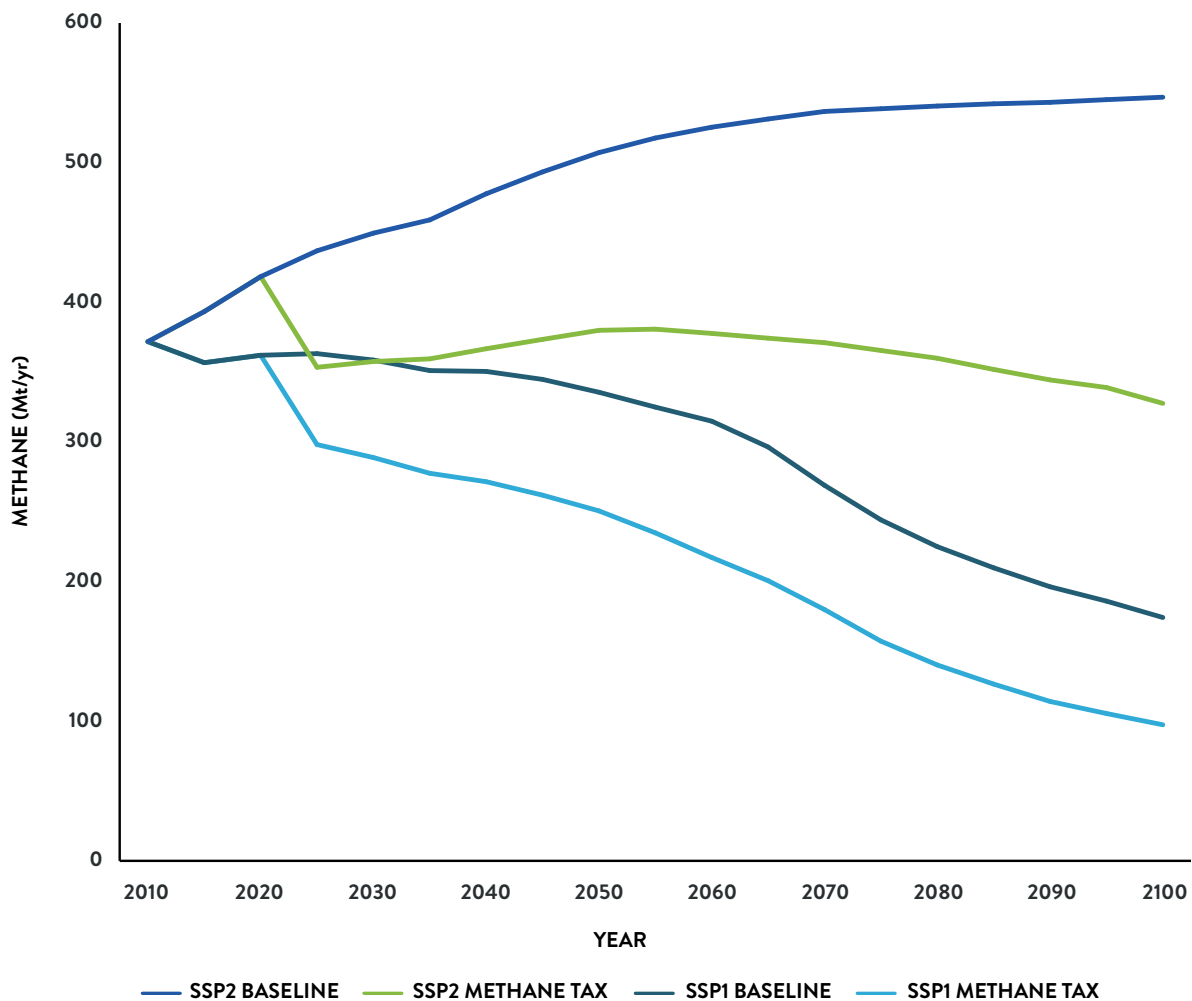
Figure 4.14 Anthropogenic methane emissions in Global Change Assessment Model 5.2, in baseline shared socioeconomic pathways 1 and 2 simulations and in the same simulations but with an economy-wide methane tax of 2018 US$ 2 100 per tonne of methane, increasing annually by 5 per cent to 2040, 2010–2100, million tonnes

Source: UNEP and CCAC
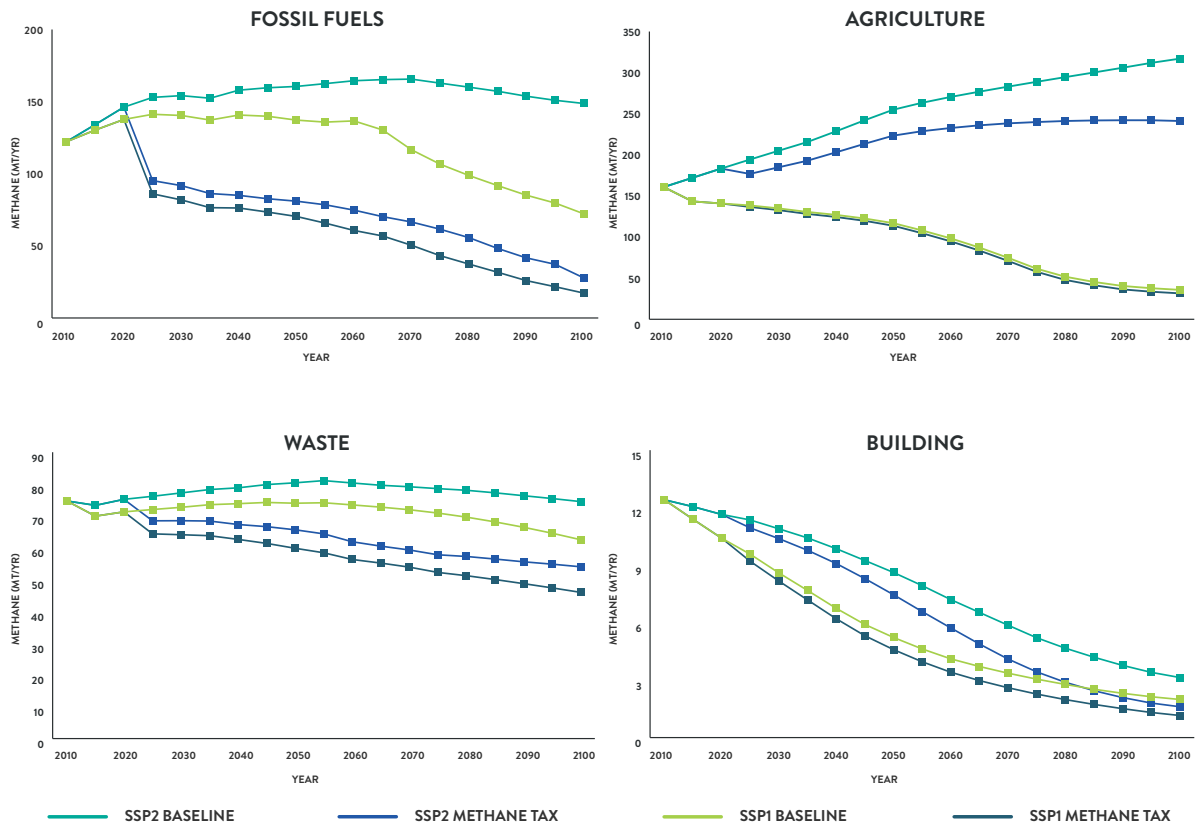
Figure 4.15 Methane emissions in Global Change Assessment Model 5.2 as in Figure 4.14 but by sector, 2010–2100, million tonnes

Source: UNEP and CCAC
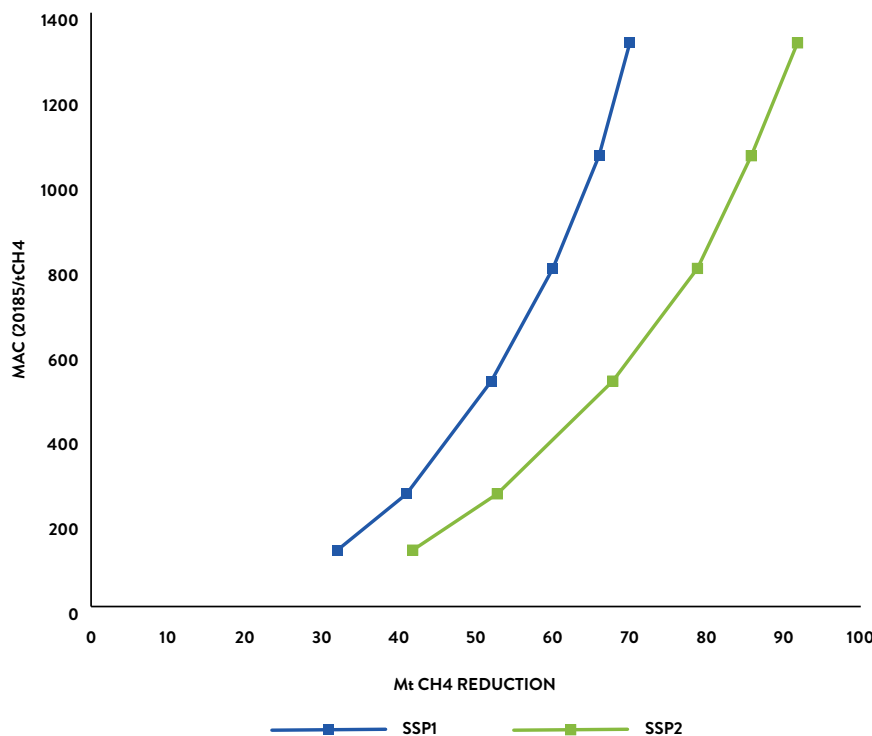
Figure 4.16 Marginal abatement cost for economy-wide methane reductions relative to the percentage of anthropogenic emissions abated in 2030, 2018 US$ per tonne of methane.

Note: The Global Change Assessment Model 5.2 under a shared socioeconomic pathway 1 and 2 projections

Source: UNEP and CCAC

4.4 METHANE MITIGATION AND FOOD

Behavioural changes are an important component of climate change mitigation according to the IPCC (Mbow *et al*. 2019; Field *et al*. 2014), though solutions presented in the literature are overwhelmingly focused on their technological aspects (van de Ven *et al*. 2017). Along with options such as fuel switching and increased efficiency discussed in the previous section, demand management can play a substantial role and may be especially relevant in the agricultural sector in which targeted mitigation options leave a large share of methane emissions unabated (Sections 4.2 and 4.3). This section therefore focuses on those options that are directly relevant to methane emissions from the food supply chain. Values quoted in this analysis are largely based on the FAO's GLEAM dataset (Gerber *et al*. 2013). This includes methane emissions associated with enteric fermentation and manure management, as well as a small component from animal feed, primarily for pigs and chickens.

4.4.1 REDUCING FOOD WASTE

Food loss and waste (FLW) is linked to environmental, social and economic impacts (FAO, 2019; Ishangulyyev *et al*. 2019; Mbow *et al*. 2019; Abiad *et al*. 2018; FUSIONS 2016) including substantial methane emissions. According to the FAO (2019) food loss is defined as loss occurring in the food supply chain from harvest up to, but not including, the retail level, while food waste is defined as loss occurring at the retail and consumption levels (FAO, 2019). There is no consensus to-date, however, on separate definitions of food loss and food waste (Ishangulyyev *et al*. 2019; Abdelradi *et al*. 2018). Food that ends up in landfills with other municipal solid waste is a source of methane.

While it occurs at various points along the supply chain there are differences in food loss and waste produced at different points between developing and developed countries. In developing regions most food waste occurs on-farm and during distribution while in developed countries, food is much more likely to be wasted because certain foods are unappealing to consumers or because they have passed their use-by dates (Porter *et al*. 2018; Garrone *et al*. 2014; Parfitt *et al*. 2010).

While more than 10 per cent of the global population lives in hunger (FAO 2017) roughly a third of all food produced for human consumption turns into lost or wasted at some point along the food supply chain (Porter *et al*. 2018; Gustavsson *et al*. 2011). Many studies highlight the mitigation benefits of reducing this large volume and indicate that the potential reductions of emissions can be substantial but also diverse (FAO 2019; Springmann *et al*. 2018; Wollenberg *et al*. 2015; Bajželi *et al*. 2014). Most of these provide both base case emissions and emissions reductions estimates only in terms of carbon dioxide equivalent rather than separating the various greenhouse gases. For example, an FAO report (2019) suggests that the global carbon footprint of food loss and waste, excluding emissions from land-use change, is 3.3 gigatonnes[12] of carbon dioxide equivalent (Gt CO_2e). Similarly, an earlier report from the FAO estimated total emissions related to food loss and waste of 2.7 Gt CO_2e (FAO, 2014). Based on the source data reported in Chapter 2, methane emissions from ruminants and rice cultivation are ~145 Mt/yr. Hence if it is assumed here that loss and waste in these two categories is similar to the total across all food types, methane emissions associated with food loss and waste would be nearly 50 Mt/yr.

A prior study explored the implications of reducing food loss and waste to reduce total agricultural losses by 15 per cent by 2030, representing roughly a 50–75 per cent decrease in food loss and waste (Stehfest *et al*. 2013). Using two models, the study found that this led to a reduction in ruminant products of ~3–4 per cent and in crops of ~6–9 per cent. These values are lower than the theoretical maximum as prices decline for these commodities with increased supply, leading to a rebound effect that offsets some of the 15 per cent reduction in food loss and waste. Such decreases would lead to an abatement of ~5–7 Mt/yr of methane emissions. Larger reductions could potentially be achieved with policies focussed on preventing loss and waste of cattle products, potentially including price adjustments to prevent the rebound effects, as these have the largest associated methane emissions. Food loss and waste reductions would provide additional benefits through reductions in carbon dioxide and nitrous oxide emissions, though prior valuation of the benefits of food loss and waste reductions found that approximately two-thirds of the benefits of such agricultural sector changes are attributable to methane (Shindell *et al*. 2017) – including the updates presented in Chapter 3 the portion attributable to methane would be even higher. Similarly, another study estimated a 2.2

12. Gigatonne = 109 tonnes

per cent reduction in 2020 total greenhouse gas emissions could be achieved by reducing food waste (van de Ven *et al*. 2017). This translates to about 1.3 Gt CO_2e or about 40–50 per cent of the food loss and waste total. Based on the 50 Mt/yr of methane associated with food loss and waste, this suggests reductions of as high as ~20 Mt/yr.

There are many potential strategies to reduce food loss and waste for the different stages of production, handling and storage, processing and packaging, distribution and marketing, and consumption. Table 4.2 presents a list of strategies related to the distribution and marketing, and consumption stages (Ishangulyyev *et al*. 2019). Targeting behavioural change to women is particularly important for the consumption stage since women generally bear primary responsibility for food purchase and preparation. Reductions in food loss and waste can also come in part from improvements in the cold food chain – storage and transport – which not only influences methane emissions but includes opportunities to mitigate climate change by replacement of hydrofluorocarbons with more climate friendly substances.

Table 4.2 Potential strategies for reductions in food loss and waste

DISTRIBUTION AND MARKETING	CONSUMPTION
Improve inventory systems	
Establish online marketplaces to facilitate sale (donation) of perishable products	Facilitate increased donation of unsold foods from cafeterias and restaurants
Change food date labelling practices and in-store promotions	Implement consumer education and campaigns, both nationally and regionally
Improve institutions related to this stage	Reduce portion sizes
Improve distribution vehicles	Provide education about home economics in educational institutions and communities
Provide guidance on storage and preparation of food to consumers	Involve women in food safe campaigns
Improve the knowledge and ability of workers	Effective use of leftovers
Improve marketplaces – storage, covered areas	Training for restaurant, cafeteria, and supermarket management to forecast customer demand and reflect demand in food purchasing to avoid bulk purchases
Deevelop links with research institutions to predict consumer demand changes	Implement good storage practices
Improve the cold-storage food chain	Correctly interpret label dates
	Distribution of excess food to charitable groups

4.4.2 IMPROVING LIVESTOCK MANAGEMENT

Farm management practices vary widely around the world, and hence in regions with greater emissions per unit of animal protein produced there are substantial mitigation opportunities through the adoption of best practices. This issue was recently assessed by the FAO (Gerber *et al*. 2013), which reported wide disparities in emissions per kilogram of protein using the Global Livestock Environmental Assessment Model (GLEAM) framework. That dataset was analyzed to explore the abatement potential if the livestock production chain worldwide were to match the practices of the most efficient producers, where the latter were assessed based on the 10th percentile of the lowest emission intensity – i.e. a high-performing value, but not an extreme case. In such an instance, methane emissions from ruminants could be reduced by ~31 Mt/yr. By far the largest share of this abatement would come from cattle, which contribute ~28 Mt/yr- – ~20 Mt/yr from meat and ~8 Mt/yr from dairy. Another 5 Mt/yr might be abated by the adoption of best management practices for buffalo, which were not included in this analysis due to a lack of data specifying the 10th percentile of emissions per kilogram of protein in the FAO dataset.

Achieving very low emissions per kilogram of protein may involve large-scale industrialized agriculture, which can have other social and environmental impacts beyond greenhouse gas emissions and hence such policies need to be considered with care. It should also be noted that improved livestock management is sometimes considered in the targeted mitigation options discussed previously (Section 4.2), though clearly some of those analyses estimate much lower potential for this as they find less total mitigation potential across the entire agricultural sector than that estimated here for livestock management alone. In addition, changes to livestock feed are commonly included in the targeted analyses (Section 4.2) and constitute another component of livestock management.

4.4.3 DIETARY CHANGE

According to the FAO (2019) between 2007–2016 current food consumption patterns were responsible for 21–37 per cent of total greenhouse gas emissions. The FAO furthermore estimates that the world will need to produce about 50 percent more food by 2050 to feed the growing world population (FAO 2017). Unless current dietary patterns and food

systems change, this would result in significant increases in greenhouse gas emissions (Drew *et al*. 2020; FAO 2019; Poore and Nemecek 2018; Alexandrowicz *et al*. 2016).

As described in Chapter 2, both rice cultivation and especially ruminant animals are large sources of methane emissions. It is therefore not surprising that several studies suggest that dietary shifts could significantly contribute to reducing greenhouse gas emissions, including methane (Clark *et al*. 2019; Springmann *et al*. 2018; Bryngelson *et al*. 2016; Springmann *et al*. 2016; Bajželj *et al*. 2014; Hedenus *et al*. 2014; Pradhan *et al*. 2013).

Poor diet is also itself a major global health concern, resulting in an estimated 11 million premature deaths in 2017. Consequently, setting dietary and nutritional goals would have great benefits for human health through reducing the incidence of non-communicable diseases such as type 2 diabetes and cardiovascular disease (Afhsin *et al*. 2019). It is important, however, to mention that setting both dietary and nutritional goals without considering the environmental cost associated with them could in fact result in an increase of greenhouse gas emissions (Torero 2020). Recent studies also demonstrate the multiple benefits of healthier and more sustainable diets, including benefits to human health and land use (Gao *et al*., 2018; Springmann *et al*., 2016; Tilman *et al*. 2014; Popp *et al*. 2010; Stehfest *et al*. 2009). The IPCC Synthesis Report provides further detailed analysis in relation to food systems, food security, greenhouse gas emissions, and land degradation (Pauchari *et al*. 2014).

There are three types of diets described by the FAO in terms of the nutrients received by each diet:

1. energy sufficient diet: provides adequate calories for energy balance for work each day;

2. nutrient adequate diet: provides adequate calories and relevant nutrient intake values;

3. healthy diet: provides adequate calories and nutrients, but also includes a more diverse intake of foods from several different food groups.

While each of these diets comes with a climate-related cost, a critical point presented in the FAO report (2020) is that not all healthy diets are sustainable and not all diets designed for sustainability are always healthy. The FAO highlights, "this important nuance is not well understood and is missing from ongoing

discussions and debates on the potential contribution of healthy diets to environmental *sustainability*" (FAO 2020).

Policies that integrate and combine environmental and nutritional priorities are limited (Aleksandrowicz *et al*. 2016; Watts *et al*. 2015). Furthermore, as is highlighted in Gao *et al*. (2018), several studies suggest that combining health, air pollution and greenhouse gas benefits can lead to more attractive strategies that encourage implementation of mitigation measures related to dietary choices (Gao *et al*. 2018; Watts *et al*. 2017; Edenhofer *et al*. 2014; Field *et al*. 2014; Haines *et al*. 2012; Shindell *et al*. 2012; Chae *et al*. 2011; Watts *et al*. 2009; Aunan *et al*. 2006; Cifuentes *et al*. 2001).

As with food waste reduction, most of the studies of dietary change provide emissions reductions estimates only in terms of carbon dioxide equivalent rather than separating out the various greenhouse gases. Several, however, provide estimates of the change in consumption of cattle-based foods, for which the impact on methane emissions can readily be evaluated. For example, a study of diets in the United Kingdom explored how alterations could both optimize nutrition and maximize greenhouse gas reductions without drastically changing overall dietary patterns. This study found that a reduction of 34 per cent in the consumption of both beef and dairy products (average for men and women) was ideal (Green *et al*. 2015). If extended across the European Union, and assuming a similar percentage decrease was ideal across that region, this would lead to a reduction in methane emissions of ~6 Mt/yr based on the full lifecycle emissions associated with livestock (Weiss and Leip 2012).

In a broader study, it was estimated that the adoption of healthy diets globally would entail approximately a 50 per cent reduction in beef consumption in 2050 (Stehfest *et al*. 2009). Accomplishing such as shift in the near term would lead to a reduction in methane emissions from beef cattle of ~14 Mt/yr based on current consumption. As demand for red meat is projected to roughly double by the middle of this century, the overall benefits in the future would be larger, though obviously they would depend on a reduction that could be achieved by a target year such as 2030. Including such a dietary shift in climate change mitigation policies is also estimated to greatly reduce the costs of achieving low-warming targets (Stehfest *et al*. 2009). These results seem generally comparable to the overall greenhouse gas reductions estimated for dietary change, which are in the range of 4.4 per cent for healthy diets and ~6–7 per cent for vegetarian or vegan diets in 2030 (van de Ven *et al*. 2017). Given that livestock accounts for roughly 18 per cent of total greenhouse gas emissions (Stehfest *et al*. 2009), the healthy diet reductions translate to a decrease in livestock-related emissions of about 25 per cent. Based on total ruminant emissions of 115 Mt/yr of methane (Chapter 2), this corresponds to diet-related reductions of ~29 Mt/yr of methane if the reductions are comparable across consumption of the various potential animal products.

These estimates provide a rough idea of the emissions reductions that could be achieved by a reduction in the consumption of ruminant-based foods, primarily from cattle through the adoption of either healthy or vegetarian/vegan diets. Reductions associated with healthy diets are likely to represent the majority of those that would come from vegetarian diets, with lower barriers to adoption. Healthy diets might achieve reductions in methane emissions in the range of 15–30 Mt/yr, with additional climate benefits from reductions in carbon dioxide and nitrous oxide – the IPCC, for example, estimates a total mitigation potential from healthier and more sustainable diets of 0.7-8.0 Gt CO_2e/yr by 2050 (Mbow *et al*. 2019).

4.4.4 CONCLUSION ON METHANE MITIGATION AND FOOD

Additional possibilities for mitigation of the large methane emissions from agriculture, especially livestock, exist and some cannot be easily characterized as solely targeted or additional. For instance, substitution of cultured meat for traditional livestock products could substantially reduce associated greenhouse gas emissions, especially methane (Post 2012; Tuomisto and Teixeira de Mattos 2011). Such technologies are not yet commercially viable, however, and may not gain widespread consumer acceptance.

Overall, while individual behaviour cannot address the scale of greenhouse gas emissions, literature suggests that including behavioural change in a broad portfolio of policies could help address and mitigate emissions and also support top-down policies (IPCC 2018; van de Ven *et al*. 2017; Watts *et al*. 2015; Gilligan *et al*. 2010). Implementing these changes, however, may be challenging for several reasons. There will be a clear discrepancy in the priorities, needs and abilities of different national governments to assist with these changes. Taking the example

of diets, many developed countries have an obesity epidemic, while in some developing ones, hunger and malnutrition, through having too little or not enough of the right types of food, is a severe problem. Switching diet to more sustainable sources will have co-benefits for reducing greenhouse gas emissions, particularly methane, and improving health (Willet *et al*. 2019). Implement structural and long-lasting changes in individual dietary intake, however, will likely require strong intervention, mitigation and incentivisation by governments through innovative policies. Social influence approaches can be an effective way of encouraging resource conservation (Camilleri *et al*. 2019; Abrahamse and Steg 2013), as part of either government or non-governmental programmes. Similarly, interventions in livestock management practices or efforts to reduce food loss and waste face considerable barriers in terms of institutional capacity, education and societal reluctance to change traditional habits as well as economic barriers. Nevertheless, given that the impact of the three elements with the strongest evidence base – reduced food loss and waste, improved livestock management, and change to healthier diets – is estimated here to have the potential to reduce methane emissions by up to 65–80 Mt/yr over the next few decades, the impact of behavioural change and innovative policies on agricultural methane emissions should not be ignored. The full abatement potential identified here for these elements is unlikely to be realized by 2030, so that abatement at these levels is perhaps an appropriate target for 2050.

4.5 WEB-BASED DECISION SUPPORT TOOL

A web-based decision support tool that allows users to input a level of methane emissions mitigation and easily determine the national values for the response of all impacts included in this analysis has been developed. This can be used to evaluate the benefits to climate, health and, through environmental changes, the economy of a wide range of action, ranging from individual mitigation projects to national pledges

under the Paris Agreement or international targets for methane controls.

The tool also allows the user to view the impacts of methane mitigation options based on the four mitigation potential analyses described in this assessment – Harmsen *et al*., IEA, IIASA, and the US EPA. The user can select broad sectors or more detailed subsectors and can choose to view impacts of worldwide or regional mitigation.

For example, a user wanting to examine mitigation potential of methane emissions from the fossil-fuel sector based on the IIASA analysis, can select low-cost measures only, and the global total, and get the impact on respiratory health from the associated methane emissions reductions. By placing the cursor over a country a panel will pop up showing the reduction in national-level deaths per million persons and the numerical value for that country's results will be displayed. Worldwide totals and the associated mitigation costs and benefits will be displayed below the interactive maps.

Note that the temperature responses in the tool include the estimated carbon cycle response enhancement of 10 per cent (Section 3.3), though this has not been applied to heat-related labour productivity changes, for which a 10 per cent change would be far less than the associated 70 per cent uncertainty. This tool can be found at: http://shindellgroup.rc.duke.edu/apps/methane/

An archive of the hourly ozone produced by the modelling described in Chapter 3 has also been created. This will allow calculation of any new health or agriculture metrics should the finding for which metric is most appropriate change again. This repository is available at https://doi.org/10.7924/r4qn65b0z and can be cited as:

Shindell, D., Zhang, Y., Seltzer, K., Faluvegi, G., Naik, V., Horowitz, L., He, J., Lamarque, J.-F., Sudo, K., and Collins, B. 2020. *Data from modelling in support of the Global Methane Assessment*, UN Environment and Duke Research Data Repository. https://doi.org/10.7924/r4qn65b0z

5. CONCLUSIONS: MITIGATION OPPORTUNITIES, IMPACTS AND UNCERTAINTIES

CHAPTER FINDINGS

- Implementation of identified targeted control measures with costs less than the estimated societal benefits could abate ~100 Mt/yr of methane emissions by 2030 and provide benefits including reducing global warming by ~0.15ºC over the 2040–2070 period, and by ~0.2º C over the longer term (2070–2100); preventing premature deaths due to ozone exposure immediately with annual totals reaching ~140 000 per year in 2030; preventing ~40 billion lost work hours annually due to heat exposure annually by ~2045; and preventing ~15 Mt tonnes of crop losses due primarily to ozone exposure each year by 2030. The crop yield increases would be worth approximately US$ 4 billion per year, the increased labour productivity about US$ 6.3 billion per year, and the valuation of the reduced risk of premature deaths is ~US$ 250 billion (US$60–420; 95 per cent confidence interval).

- The greatest targeted abatement potential very likely lies within the fossil-fuel sector, for which average mitigation costs range from a high of ~US$1 250 per tonne of methane in the US EPA analysis to a net savings of ~US$ 400 per tonne in the IIASA analysis, with values in between those for the Harmsen and IEA analyses, the latter of which only considers the oil and gas subsectors. All these average costs are much lower than the per tonne societal benefits.

- Examining only targeted controls in the relatively robustly characterized fossil-fuel and waste sectors that cost less than the estimated societal benefits per tonne, the abatement potential is about 75 ±2 Mt/yr. Benefits from this level of abatement include ~0.13ºC warming avoided in the 2040–2070 period, ~105 000 avoided premature deaths due to ozone exposure annually by 2030, and 11 Mt of avoided crop losses due primarily to ozone exposure each year. The benefits of the annually avoided premature deaths alone are estimated at US$ 190 billion (US$ 40–310 billion; 95 per cent confidence interval).

- Targeted measures alone are not enough to reach emissions levels seen in 1.5ºC scenarios over the next several decades, which require both targeted and additional measures to achieve ~180 Mt/yr of methane abatement by 2030. Behavioural measures include fuel switching, energy efficiency, improved waste separation, reducing food waste, dietary change and transport demand management. Both targeted and additional measures face implementation barriers including financing, a lack of awareness/ education, governance and consumer preferences.

- Uncertainties exist along the entire chain from mitigation potential through physical responses to societal impacts. Overall uncertainties are likely to be primarily driven by limited understanding of climate sensitivity and of the effects of ozone exposure on human health, with generally small contributions from incomplete knowledge of mitigation potentials or in an understanding of the ozone response to methane emissions reductions. In some specific sectors or regions, however, limited knowledge of current emissions is probably a major driver of uncertainties in benefit-potential estimates.

It has been clear to the scientific community for some time that reducing methane emissions would contribute to both improved air quality and climate change mitigation (Shindell *et al*. 2012; UNEP 2011; UNEP/WMO 2011; Fiore *et al*. 2002). There are substantial uncertainties, however, in the characterization of each step along the pathway from mitigation to impacts, including the methane emissions themselves, the responses of the physical system to changes in emissions, and the potential for emissions reductions in the various sectors that emit large amounts of methane. Prior analyses have typical relied on the results of one or two models for physical responses, used a single set of emissions data and a single set of mitigation potentials. This assessment, however, provides a more thorough analysis of robustness for each step by analyzing results from multiple models of the composition-climate system, multiple models of the energy-economy-land system, and multiple analyses of methane mitigation potentials. It also incorporates recent advances in understanding of the societal impacts of physical system responses to methane emissions, including not only climate and composition responses of the physical system, but many downstream impacts of both ozone and climate change on human health and crops. This provides a robust characterization of the overall societal costs and benefits of methane mitigation.

The analysis shows that there is great potential to mitigate methane emissions over the current decade, 2020–2030, using existing targeted control measures. Such measures could abate roughly 125 Mt/yr of methane emissions, about 30 per cent of the projected 2030 anthropogenic emissions. Taking the average across the various available analyses of abatement potentials and costs, targeted control measures with costs of less than the estimated societal benefits could abate 101 Mt/yr of methane emissions by 2030 and achieving such abatement would have enormous societal benefits. These include climate-related benefits of reducing warming by ~0.15°C by 2040, with a value of 0.2°C over the longer term (~2070–2100), and the associated prevention of ~40 billion lost work hours, roughly 30 per cent of which are for women and 70 per cent for men, due to heat exposure annually, starting around 2040. They also include air pollution-related benefits starting immediately after emissions are reduced and continuing each year thereafter. Increasing through the 2020s, benefits for 2030 and subsequent years include preventing annually ~140 000 premature deaths

due to ozone exposure, ~430 000 accident and emergency department visits due to asthma and ~9 000 hospitalizations of elderly people due to ozone, and ~15 Mt of crop losses due to ozone exposure. The crop yield increases would be worth approximately US$ 4 billion per year, the increased labour productivity about US$ 6.4 billion per year, while the valuation of the reduced risk of premature deaths is ~US$ 250 billion annually (US$ 60–420; 95 per cent confidence interval).

The discussion of climate change responses to methane mitigation in Chapter 3 focussed on the response averaged over 1–3 decades after potential cuts. It is useful to also characterize the potential impact of methane mitigation on global mean temperature as a function of time. Therefore the response was evaluated using absolute global temperature potentials (AGTPs), as in prior Assessments (UNEP 2017; UNEP/WMO 2011). In brief, the yearly AGTPs represent the global mean temperature change per kilogram of emission each year subsequent to those emissions based on an impulse-response function for the climate system, as is used in IPCC for selected example years, for example, AGTP50 or AGTP100 (Myhre *et al*. 2013). In the calculations in this assessment, the transient climate response is based on analysis of the last generation of climate models (CMIP5) (Geoffroy *et al*. 2013). The AGTPs include the carbon-cycle response to the temperature change induced by the emitted species including the impact of ozone generated by methane on carbon uptake (Gasser *et al*. 2017; Collins *et al*. 2010) as described in Shindell *et al*. (2017). Temperature responses are also provided averaged over latitude bands based on analogous absolute regional temperature potentials (Collins *et al*. 2013; Shindell 2012). To take advantage of the new results from simulations in support of this assessment, the responses have been calibrated to match the global climate impacts reported in Chapter 3, including the estimated carbon cycle response enhancement of 10 per cent (Section 3.3), though this changes the AGTPs only minimally.

To illustrate the evolution of temperature responses over time, the temperature response to the methane mitigation seen in 1.5°C scenarios is evaluated, based on IAMs that included targeted controls, behavioural change, emissions pricing and other developments such as decarbonization. The average mitigation across the available scenarios is 180 Mt/yr in 2030, 240 Mt/yr in 2040 and 280 Mt/yr in 2050. Avoided warming reaches 0.3°C towards the

end of the 2040s in response to those emissions reductions (Figure 5.1). In comparison with prior studies, the 2050 value of 0.32°C is slightly greater than the impact of methane mitigation estimated in Shindell *et al*. (2012)/ UNEP/WMO (2011) for 2050, 0.28°C, but is substantially so when comparing both results for period 30 years after abatement begins – 2040 in the earlier scenarios, for which time the response was 0.24°C in response to abatement of 139 Mt yr in 2030. The greater 2050 value in this analysis stems primarily from the greater abatement amounts which have a larger impact than the later start of abatement. The Arctic response is 60 per cent larger than the global mean value, in good agreement with the results found here in the full climate model simulations (Chapter 3; Table 3.2).

Comparisons are also drawn with the 2017 UNEP *Emissions Gap Report* that estimated that the response to the full application of targeted methane mitigation options identified by IIASA would lead to avoided warming of 0.09°C in 2030 and 0.30±0.12°C in 2050 using a similar method to that used here (UNEP 2017). Methane mitigation analyzed in that report was 152 Mt/yr by 2030 and 171 Mt/yr in 2050. Those are greater values for 2030 than reported here from the IIASA bottom-up analyses as the older ones used in the UNEP report had an earlier abatement starting date. The results presented here exhibit a slightly smaller response per million tonnes of emissions mitigation based upon the latest climate modelling, though well within the

uncertainty range. Of note is that, based on both the new modelling and updated constraints on climate sensitivity, the uncertainty ranges are slightly reduced in the new analyses: 95 per cent confidence intervals were 40 per cent in the 2017 UNEP report and 36 per cent in Shindell *et al*. (2012)/UNEP/WMO (2011), whereas now they are estimated at 33 per cent (Chapter 3).

In addition to this analysis of the impact of emissions changes through 2050, the impact of methane emissions changes through 2100 were also explored, again using AGTP. In 1.5° C scenarios generated by IAMs, methane emissions fall rapidly in the first half of the century but thereafter decline only modestly through 2100 (Rogelj *et al*. 2018). As discussed in Chapter 4, this is primarily due to emissions from agriculture which are not abated given the cost curves, abatement options and pricing mechanisms used in most of the IAMs. As such, the longer-term climate impact of aggressive methane abatement becomes highly dependent upon the reference case against which the fairly steady post-2050 are compared (Figure 4.1). Relative to the high baseline methane emissions under SSP3's marker scenario, the 2100 impact of 1.5° C methane reductions is a reduction in warming of 0.77° C. Relative to the lower baseline emissions of SSP1's marker scenario, the reduction is much less at -0.42° C, with the mid-range (for methane) SSP4 and SSP5 having value of about -0.6° C.
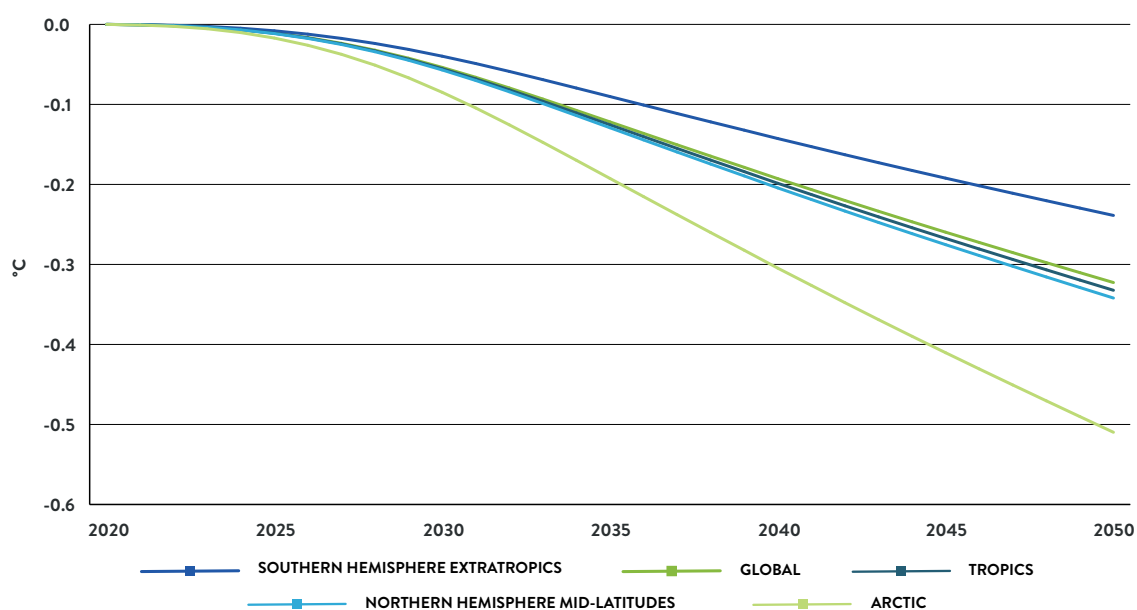
Figure 5.1. Temperature response to methane abatement from 2020–2050 based on mitigation levels consistent with 1.5° C scenarios, 2020–2050, degrees centigrade

Note: In addition to global mean responses, values are given for the southern hemisphere extratropics (90–28° S), the tropics (28° S–28° N), the northern hemisphere mid-latitudes (28–60° N) and the Arctic (60–90° N).

Source: UNEP and CCAC

The identified targeted abatement measures reduce emissions in the fossil fuel sector by ~58 ±12 Mt/yr and those in the waste sector by ~32 ±4 Mt/yr when examining all controls regardless of cost for 2030. The targeted abatement potential within the agricultural sector is not as robustly characterized as the estimates are very different at ~10, 20 and 50 Mt/yr. Hence this analysis reveals that the greatest targeted potential very likely lies within the fossil-fuel sector, whereas there is the greatest agreement on the abatement potential in the waste sector. Delving further into the emission sources, this assessment finds that within the fossil-fuel sector there is a comparable magnitude abatement potential in each the three subsectors coal, gas and oil. In contrast, within the waste sector the abatement potential is largely concentrated within the solid waste subsector with a relatively small amount within the wastewater subsector. These results consider all abatement measures regardless of cost and show substantial differences in the average value, weighted by mitigation potential at each cost value, across the various analyses. For the fossil-fuel sector, average mitigation costs range from a high of US$1 240 in the US EPA analysis for measures costing less than US$ 25 000 per tonne of methane), a middle value of US$ 960 per tonne of methane in the Harmsen *et al.* analysis to -US$ 400 in the IIASA analysis, with values in between those from IEA, US$ 10 for the oil and gas subsectors only. Although the mitigation potential for the waste sector is more consistent across the various analyses, the costs are more divergent, with an average cost range of US$ 3 930 per tonne of methane in the Harmsen *et al*. analysis, $840 in the US EPA analysis for measures costing less than US$ 25 000 per tonne of methane, to -US$ 5 800 in the IIASA analysis. In comparison, average costs for the agricultural sector are more consistent at US$ 1 390 in Harmsen *et al*., US$ 800 in the US EPA analysis and US$ 270 in IIASA, despite the large divergence in the abatement potential itself for this sector. As discussed in Section 4.2.1, abatement potentials vary greatly across regions. The largest potential in the waste sector is for Europe and India; the coal subsector followed by livestock for China; in livestock for Africa, followed by oil and gas, in the coal subsector and the waste sector for Asia and the Pacific (excluding China and India); in the oil and gas subsector for the Middle East, North America, and Russia and the Former Soviet Union; and in the livestock subsector for Latin America.

The targeted mitigation potential was examined for only those measures with costs of less than the US$ 4 300 per tonne of methane in estimated societal benefits found in Chapter 3. The total abatement potential in the three cross-sector analyses are 85 Mt/yr in IIASA, 93 Mt/yr in US EPA and 121 Mt/yr in Harmsen *et al*., for an average of 100 Mt/yr. In that same order, potentials are 46, 44, and 59 Mt/yr for the fossil-fuel sector, 27, 30 and 18 Mt/y for the waste sector, and 12, 19 and 44 Mt/yr for the agricultural sector. Hence the totals across the more robust fossil-fuel and waste sectors are 73, 74 and 77 Mt/yr, for a range of 75 ±2 Mt/yr. The benefits from this level of abatement (75 Mt/yr) are also substantial: just over 0.1°C of warming avoided a decade after these reductions are achieved, and benefits immediately following reductions, and continuing each year thereafter, that include about 105 000 avoided premature deaths due to ozone exposure, about 325 000 fewer accident and emergency department visits due to asthma, and ~11 Mt of crop losses due to avoided ozone exposure. The benefits of the avoided premature deaths alone are estimated at US$ 190 billion per year. It is emphasized that these benefits all come at a net gain to society as even the most expensive controls within this analysis have costs of less than the societal benefits, and hence the average costs of controls are far less than the average benefit per tonne of emissions abatement.

It is also informative to examine the total cost of implementing all targeted methane measures. The IEA analysis is excluded here as it does not encompass the full fossil-fuel sector, and the IIASA and US EPA analyses are relied on since the Harmen *et al.* analysis does not include negative costs. For the fossil fuel sector, the total cost based on the US EPA analysis is US$ 62 billion for measures costing less than US$ 25 000 per tonne of methane, whereas the total is a savings of US$ 18 billion in the IIASA analysis. Similarly for waste, the total cost based on the US EPA analysis is US$ 27 billion whereas the total is a saving of US$ 166 billion in the IIASA analysis. The differences in both sectors are partly attributable to the much higher discount rate used in the US EPA analysis –10 per cent versus 4 per cent in the IIASA analysis – which greatly reduces the value of gas that is captured and utilized – net costs will also depend on the estimated future price of natural gas. In the waste sector, the inclusion of substantial revenue from recycled paper in the IIASA waste

analysis, as discussed in Chapter 4, is another major source of differences. Hence the total cost for all targeted measures across these two sectors ranges from ~US$ 90 billion to a savings of ~US$ 185 billion. For the agricultural sector, the total cost based on the IIASA analysis is US$ 3 billion whereas the total is US$ 17 billion in the US EPA analysis. Thus the spending in the agricultural sector is more consistent, even though the mitigation potential differs strongly – see Chapter 4 for further discussion on the agricultural sector in these two analyses. This is likely due to the reduced influence of the discount rate differences as less of the methane abatement is used in this sector. Hence it is very difficult to estimate the total spending required to implement the targeted measures. Averaging across these two analyses for all three sectors, the total spending is negative. In all sectors the total cost seems likely to be relatively small or negative but will depend on the chosen discount rate and prices of natural gas. As the total costs include both measures with net savings and those with net costs, sometimes large costs, it is important to keep in mind that even when total costs are large, they are sensitive to the costs of the most expensive measures along the cost curves. Thus the conclusions regarding the portion of targeted measures available at negative or low costs are typically emphasized in this assessment.

The uncertainty in the fossil-fuel plus waste sector, the methane mitigation potential is about 17–20 per cent, though it is larger for some subsectors within those general sectors. Considering the all-cost measures, the uncertainty is about 25 per cent for the total from fossil fuels and about 10 per cent for the total from waste. The variation in these mitigation potentials can be compared with the uncertainties in climate, health and crop responses. For climate, there is about a 34 per cent uncertainty in the global mean temperature change, based on current understanding of climate sensitivity, with a slightly smaller value for the tropics and a larger one for the Arctic, here 60–90° N, where the response is largest. For premature deaths, uncertainties for those related to respiratory effects are ~35 per cent and those for cardiovascular-related effects are ~65 per cent, both for the 95 per cent confidence interval. Uncertainties in heat-related deaths, for China and the United States only, are about 48 per cent with a 95 per cent confidence interval, whereas those for crop yield impacts are roughly 36 per cent. These impact uncertainties reflect the fact that the temperature response to methane emissions

changes, ~34 per cent, is more uncertain than the ozone response, ~24 per cent. In general, it was found that uncertainties in the impacts of methane mitigation are likely to be driven most strongly by uncertainties in climate sensitivity and in the effects of ozone exposure on human health, with relatively small contributions from uncertainties in the mitigation potential or ozone response to methane emissions reductions. It is also noted that there likely are additional effects of ozone on human health, as recent research indicates that exposure to air pollution affects nearly every organ in the human body (Andrade *et al*., 2019), and hence additional impacts are likely to be present beyond those quantified here, so that health benefits of mitigation should be considered conservative.

Considering the low-cost measures, defined here as those costing less than US$ 600 per tonne of methane, the different analyses vary more as they are sensitive to the use of a cost threshold at this level since it falls within a range encompassing many mitigation measures. For mitigation within the fossil-fuel sector, low-cost mitigation potentials range from 32 to 66 Mt/yr in the two analyses finding that the average cost of the low-cost measures is negative, -US$ 120 and -US$ 851 per tonne of methane in the IEA and IIASA analyses, respectively. The Harmsen *et al*. and US EPA analyses, however, find low-cost potentials of 24 and 42 Mt/yr and average costs that are positive at US$ 182 and US$ 38 per tonne of methane, respectively. For the waste and agricultural sectors, the average costs of the low-cost measures is negative in some analyses and very low in others, always less than US$ 140 per tonne of methane and typically less than US$ 60 per tonne of methane. Magnitudes vary by nearly a factor of two in the waste sector, 11–21 Mt/yr, and nearly a factor of four in the agricultural sector, 10 to 38 Mt/yr. Hence the low-cost measures are generally beneficial from an economic standpoint even without accounting for the environmental benefits, or when only accounting for market costs, primarily crop yield and labour productivity increases, when evaluating environmental impacts, but the potential available at these low costs is quite sensitive to the particular analysis used. As discussed previously, when environmental benefits are accounted for, slightly more than 80 per cent of identified targeted potential for methane controls lead to net societal benefits.

Though significant, a reduction of either ~100 or ~125 Mt/yr, which represents ~25 or 30 per cent in anthropogenic methane emissions by 2030 is less than that seen in 1.5°C scenarios.

Examining estimated targeted mitigation potential over a longer timescale provides valuable insights into the potential for targeted controls to provide abatement consistent with low warming scenarios. Looking at the total assessed mitigation potential across all sectors, IIASA concluded that maximum feasible reductions would reduce 2050 methane emissions by 242 Mt/yr whereas Harmsen *et al.* found a 2050 total abatement potential of 185 Mt/yr. These analyses account for the time required for technological turnover and for phasing in new regulations, and also include changes in baseline emissions based on projected energy demand and population growth, which affects generation of waste and food production. Baseline 2050 anthropogenic emissions were projected to be 450 Mt/yr in the IIASA analysis, a large increase over the 355 Mt/yr in 2020 in its model. The reduction of 242 Mt/yr thus represents a decrease of 54 per cent. The reduction is similar in the Harmsen *et al.* analysis at 47 per cent despite the smaller abatement as that analysis had a smaller projected growth in baseline methane emissions. An equivalent percentage reduction today would translate to about 190 Mt/yr of methane mitigation. That level of reduction would be almost exactly equal to the mean methane mitigation in 2030 seen in 1.5ºC scenarios. On the one hand, this indicates that full implementation of targeted mitigation measures in a single decade could potentially lead to methane reductions consistent with the magnitude required in 2030 for such a low warming pathway. On the other hand, this indicates that were targeted measures to be the only policies employed, full application of all technologies, even those with very high mitigation costs, would be required at an exceptionally fast rate of deployment and that even with targeted measures across the full cost range, the additional methane mitigation after 2030 needed to stay on a 1.5ºC pathway would require additional measures which contribute to other priority development goals with benefits for methane. The additional measures examined in this assessment include several that might be widely considered part of climate policy, such as switching to renewable energy, and others that might not, such as reducing food waste or improving waste separation. Such categorizations are highly subjective, but in general the additional measures in the fossil-fuel sector are more closely aligned with policies commonly viewed as part of a climate portfolio. Those constitute roughly 40 per cent of the additional measures included in this assessment. Roughly 43 per cent come from changes in the agricultural sector and

17 per cent from the waste sector, both of which include measures associated with consumption or disposal practices that are less consistently currently viewed as part of climate policies.

Behavioural changes have the potential to substantially augment targeted methane controls. These are especially important for the agricultural sector, where targeted measures have the smallest relative impact. The analysis presented here suggests that behavioural changes, reducing food loss and waste, improving livestock management and shifting to healthier diets that at the global level include reduced consumption of ruminant-based foods, have the potential to provide up to 65–80 Mt/yr of additional methane emissions mitigation. Though these face substantial structural barriers, widespread adoption of such measures alongside targeted controls could bring anthropogenic methane emissions in line with those in 1.5ºC scenarios. Additional progress in targeted measures including feed supplements for livestock and alternatives to animal protein (Section 4.4.4) as well as diverting organic material that would otherwise lead to methane release from landfills to make useful products also have potential if they prove economically feasible and societally acceptable, and hence can be scaled up.

Policy ambition to date has thus far fallen short of mitigation consistent with 1.5ºC scenarios, and, as discussed in Chapter 1, atmospheric methane amounts are continuing to increase. Some steps have been taken, however. The countries of North America pledged to reduced methane emissions from oil and gas by 45 per cent by 2025, and the Climate and Clean Air Coalition (CCAC) Mineral Methane Initiative is aiming for a reduction of 60–75 per cent from the oil and gas subsector by 2030 among participants. These would provide substantial sector and region-specific mitigation. For example, were the low end of the 2030 Oil and Gas Initiative goal to be achieved across all CCAC partner countries, that would correspond to mitigation of about 30 Mt/yr of methane emissions based on projected 2030 baseline emissions, or ~28 Mt/yr based upon current 2020 emissions. Several sub-national jurisdictions have also put ambitious methane reduction laws into place. These include the US states of California and New York, with a 40 per cent reduction from 2013 methane emissions by 2030 in the former and a 40 per cent reduction from 1990 emissions by 2030 in the latter for all greenhouse gases including methane – using a 20-year methane global warming potential to emphasize the importance of reducing this gas as outlined in the New York's Methane Reduction Plan. Such steps are, however, only a partial recipe for achieving a 1.5ºC pathway.

Achieving a 1.5°C pathway would require not only reversing the current rising trend in methane emissions but also greatly reducing anthropogenic methane emissions by 2030. This could be accomplished by policies targeted at implementing targeted controls on specific sectors, policies to bring about behavioural change, policies to bring about broad, cross-sectoral emissions reductions such as ambitious international agreements, following, for example, the pattern of the Kigali Amendments to reduce hydrofluorocarbon emissions, imposition of emissions caps or taxes, such as in the modelling presented in Section 4.3, or a combination of such policies. Implemented policies should be gender responsive, especially those promoting behavioural change. Achieving methane reductions also requires increased education and information about the economic and societal impacts of mitigation, something this assessment aims to provide, along with additional infrastructure to make use of abated emissions in some sectors and a change in economic incentives that may be misaligned and prevent even action with overall negative costs from being taken up (IEA 2020). It is also worth pointing out that due to the removal of co-emitted aerosols that accompanies a realistically paced phase-out of fossil fuels, even aggressive decarbonization will tend to have minimal net impacts on near-term, the first 20 years, temperatures. (Shindell and Smith, 2019). Prior research has therefore pointed out that the only plausible way of decreasing warming relative to the reference case during the next 20 years is through reductions in greenhouse gases from non-fossil sources including methane and nitrous oxide from agriculture and waste as well as fluorinated gases (Shindell and Smith 2019).

Prior analyses have shown the multiple benefits of reducing methane emissions (Shindell *et al*. 2012; UNEP/WMO 2011). This work adds to those prior analyses by both including more modelling to better characterize robustness and analyses of additional impacts, and also by greatly extending the scope of the associated economic analysis. A prior economic analysis by UNEP (UNEP 2011) included results from a single analysis of mitigation costs, whereas this study includes multiple such analyses and finds that the variation across them of mitigation potentials is large, leading to greater uncertainty than in the analyses of physical system responses, especially for the agricultural sector. Results are relatively robust for the fossil fuel and waste sectors and indicate clearly that there is an enormous potential for methane emissions mitigation with benefits that greatly outweigh implementation costs.

6. REFERENCES

Abbott, D.W., Aasen, I.M., Beauchemin, K.A., Grondahl, F., Gruninger, R., Hayes, M., Huws, S., Kenny, D.A., Krizsan, S.J., Kirwan, S.F., Lind, V., Meyer, U., Ramin, M., Theodoridou, K., von Soosten, D., Walsh, P.J., Waters, S., and Xing, X. (2020) Seaweed and Seaweed Bioactives for Mitigation of Enteric Methane: Challenges and Opportunities. *Animals*, 10(12), 2432.

Abdelradi, F. (2018). Food waste behaviour at the household level: A conceptual framework. *Waste Manag*., 71, 485-493.

Abiad M.G. and Meho L.I. (2018). Food loss and food waste research in the Arab world: A systematic review. *Food Security*, 1–12.

Abrahamse, W. and Steg, L. (2013). Social influence approaches to encourage resource conservation: A meta-analysis. *Global Environ. Change*, 23, 1773–85.

Academy of Science of South Africa, Brazilian Academy of Sciences, German National Academy of Sciences Leopoldina, U.S. National Academy of Medicine and U.S. National Academy of Sciences. (2019). Air Pollution and Health – A Science-Policy Initiative. *Annals of Global Health*, 85, 140, 1-9.

Afhsin, A., et al. (2017). Health effects of dietary risks in 195 countries, 1990–2017: a systematic analysis for the Global Burden of Disease Study. *The Lancet*, 393, 1958-1972.

Alexandrowicz, L., Green, R., Joy. E.J.M., Smith, P. and Haines, A. (2016). The Impacts of Dietary Change on Greenhouse Gas Emissions, Land Use, Water Use, and Health: A Systematic Review. *PloS ONE*, 11(11): e0165797.

Alexe, M., Bergamaschi, P., Segers, A., Detmers, R., Butz, A., Hasekamp, O., Guerlet, S., Parker, R., Boesch, H., Frankenberg, C., Scheepmaker, R.A., Dlugokencky, E., Sweeney, C., Wofsy, S.C., and Kort, E.A. (2015). Inverse modelling of CH_4 emissions for 2010–2011 using different satellite retrieval products from GOSAT and SCIAMACHY. *Atmos. Chem. Phys*., 15, 113–133, doi:10.5194/acp-15-113-2015.

Alvarez, R.A., Zavala-Araiza, D., Lyon, D.R., Allen, D.T., Barkley, Z.R., Brandt, A.R., Davis, K.J., Herndon, S.C., Jacob, D.J., Karion, A. and Kort, E.A. (2018). Assessment of methane emissions from the US oil and gas supply chain. *Science*, 361, 186-188.

Anderson, G.B., Oleson, K.W., Jones, B. and Peng, R.D. (2018). Projected trends in high-mortality heatwaves under different scenarios of climate, population, and adaptation in 82 US communities. *Climatic Change*, 146, 455–470.

Anenberg, S.C., Horowitz, L.W., Tong, D.Q. and West J.J. (2010). An estimate of the global burden of anthropogenic ozone and fine particulate matter on premature human Mortality using atmospheric modeling. *Env. Health Persp*., 118, 1189–1195.

Anenberg, S.C., Henze, D.K., Tinney, V., Kinney, P.L., Raich, W., Fann, N., Malley, C.S., Roman, H., Lamsal, L., Duncan, B. and Martin, R.V. (2018). Estimates of the global burden of ambient PM 2.5, ozone, and NO2 on asthma incidence and emergency room visits. *Environmental Health Perspectives*, 126(10), p.107004.

Anthony, K.W., von Deimling, T.S., Nitze, I., Frolking, S., Emond, A., Daanen, R., Anthony, P., Lindgren, P., Jones, B. and Grosse, G. (2018). 21st-century modeled permafrost carbon emissions accelerated by abrupt thaw beneath lakes. *Nature Communications*, 9, 1-11.

Archibald, A., O'Connor, F., Archer-Nicholls, S., Chipperfield, M., Dalvi, M., Folberth, G., Dennison, F., Dhomse, S., Griffiths, P., Hardacre, C., Hewitt, A., Hill, R., Johnson, C., Keeble, J., Köhler, M., Morgenstern, O., Mulchay, J., Ordóñez, C., Pope, R., Rumbold, S., Russo, M., Savage, N., Sellar, A., Stringer, M., Turnock, S., Wild, O. and Zeng, G. (2019). Description and evaluation of the UKCA stratosphere-troposphere chemistry scheme (StratTrop vn 1.0) implemented in UKESM1. *Geosci. Model Dev. Discuss*., doi:10.5194/gmd-2019-246.

Armstrong, B., Sera, F., Vicedo-Cabrera, A.M., Abrutzky, R., Åström, D.O., Bell, M.L.,

Chen, B-Y., de Sousa Zanotti Stagliorio Coelho, M., Correa, P.M., Dang, T.N., Diaz, M.H., Dung,

D.V., Forsberg, B., Goodman, P., Guo, Y-L.L., Guo, Y., Hashizume, M., Honda, Y., Indermitte, E., Íñiguez, C., Kan, H., Kim, H., Kyselý, J., Lavigne, E., Michelozzi, P., Orru, H., Ortega, N.V., Pascal, M., Ragettli, M.S., Saldiva, P.H.N., Schwartz, J., Scortichini, M., Seposo, X., Tobias, A., Tong, S., Urban, A., De la Cruz Valencia, C., Zanobetti, A., Zeka, A. and Gasparrini, A. (2019). The role of humidity in associations of high temperature with mortality: a multicountry, multicity study. *Environmental Health Perspectives*, 127(9), 097007.

Aunan, K., Fang, J., Hu, T., Seip, H.M., and Vennemo, H. (2006). Climate change and air quality-measures with co-benefits in China. *Environ. Sci. Technol*., 40, 4822-4829.

Avnery, S., Mauzerall, D.L., Liu, J. and Horowitz, L.W. (2011). Global crop yield reductions due to surface ozone exposure: 1. Year 2000 crop production losses and economic damage, *Atmospheric Environment*, 45, 2284-2296.

Bajželj, B., Richards, K.S., Allwood, J.M., Smith, P., Dennis, J.S., Curmi, E. and Gilligan, C.A. (2014). Importance of food-demand management for climate mitigation. *Nature Climate Change*, 4, 924–929.

Baray, S., Darlington, A., Gordon, M., Hayden, K.L., Leithead, A., Li, S.M., Liu, P.S.K., Mittermeier, R.L., Moussa, S.G., O'Brien, J., Staebler, R., Wolde, M., Worthy, D., McLaren, R. (2018). Quantification of Methane Sources in the Athabasca Oil Sands Region of Alberta by Aircraft Mass Balance. *Atmos. Chem. Phys*., 18, 7361– 7378.

Bauer, N., Calvin, K., Emmerling, J., Fricko, O., Fujimori, S., Hilaire, J., Eom, J., Krey, V., Kriegler, E., Mouratiadou, I. and de Boer, H.S. (2017). Shared socio-economic pathways of the energy sector–quantifying the narratives. *Global Environmental Change*, 42, pp.316-330.

Bender, M., Sowers, T. and Brook, E. (1997). Ice core isotope data constrain methane emissions. *Proceedings of the National Academy of Sciences*, 94 (16), 8343-8349.

Benmergui, J.S. (2019). *Innovations in Modeling and Statistical Analysis for Greenhouse Gas Flux Monitoring*. Doctoral dissertation, Harvard University, Graduate School of Arts & Sciences.

Bentayeb, M., Wagner, V., Stempfelet, M., Zins, M., Goldberg, M., Pascal, M., Larrieu, S., Beaudeau, P., Cassadou, S., Eilstein, D., Filleul, L., Le Tertre, A., Medinaa, S., Pascal, L., Prouvost, H., Quénel, P., Zeghnoun, A. and Lefranc, A. (2015). Association between long-term exposure to air pollution and mortality in France: a 25-year follow-up study. *Environ Int*., 85, 5–14.

Bergamaschi, P., Frankenberg, C., Meirink, J.F., Krol, M., Dentener, F., Wagner, T., Platt, U., Kaplan, J.O., Körner, S., Heimann, M., Dlugokencky, E.J. and Goede, A. (2007). Satellite chartography of atmospheric CH_4 from SCIAMACHY on board ENVISAT: 2. Evaluation based on inverse model simulations. *J. Geophys. Res.-Atmos*., 112, D02304.

Bergamaschi, P., Frankenberg, C., Meirink, J.F., Krol, M., Villani, M.G., Houweling, S., Dentener, F., Dlugokencky, E.J., Miller, J.B., Gatti, L.V., Engel, A., and Levin, I. (2009). Inverse modeling of global and regional CH_4 emissions using SCIAMACHY satellite retrievals. *J. Geophys. Res*., 114, D22301.

Bergamaschi, P., Houweling, S., Segers, A., Krol, M., Frankenberg, C., Scheepmaker, R.A., Dlugokencky, E., Wofsy, S.C., Kort, E.A., Sweeney, C., Schuck, T., Brenninkmeijer, C., Chen, H., Beck, V. and Gerbig, C. (2013). Atmospheric CH_4 in the first decade of the 21st century: Inverse modeling analysis using SCIAMACHY satellite retrievals and NOAA surface measurements. *J. Geophys. Res.-Atmos*., 118, 7350–7369.

Bignell, D.E., Eggleton, P., Nunes, L., Thomas, K.L. (2017). Termites as mediators of carbon fluxes in tropical forest: Budgets for carbon dioxide and methane emissions. In Watt, A.D., Stork, N.E. and Hunter, M.D. (eds.). *Forests and Insects*. Chapman & Hall, London, UK.

Blake, D.R., Mayer, E.W., Tyler, S.C., Makide, Y., Montague, D.C. and Rowland, F.S. (1982). Global increase in atmospheric methane concentrations between 1978 and 1980. *Geophys. Res. Lett*., 9: 477-480.

Bock, M., Schmitt, J., Beck, J., Seth, B., Chappellaz, J. and Fischer, H. (2017). Glacial/interglacial wetland, biomass burning, and geologic methane emissions constrained by dual stable isotopic

CH_4 ice core records. *Proceedings of the National Academy of Sciences*, 114 (29) E5778-E5786.

Borgonovo, F., Conti, C., Lovarelli, D., Ferrante, V. and Guarino, M. (2019). Improving the sustainability of dairy slurry by a commercial additive treatment. *Sustainability*, 11, 4998.

Brandt, A.R., Heath, G.A., Kort, E.A., O'Sullivan, F., Pétron, G., Jordaan, S.M., Tans, P., Wilcox, J., Gopstein, A.M., Arent, D., Wofsy, S., Brown, N.J., Bradley, R., Stucky, G.D., Eardley, D. and Harriss, R. (2014). Methane Leaks from North American Natural Gas Systems, *Science*, 343, 733–735.

Bröde, P., Fiala, D., Lemke, B. and Kjellstrom, T. (2017). Estimated work ability in warm outdoor environments depends on the chosen heat stress assessment metric. *Int J Biometeorol*. https://doi.org/10.1007/s00484-017-1346-9 (accessed 6 March 2021).

Brune, A. (2010). Methanogenesis in the digestive tracts of insects. In Timmis, K.N. (ed.). *Handbook of Hydrocarbon and Lipid Microbiology, Vol 8*. Springer Verlag, Berlin, Germany.

Bryngelsson, D., Wirsenius, S., Hedenus, F. and Sonesson, U. (2016). How can the EU climate targets be met? A combined analysis of technological and demand-side changes in food and agriculture. *Food Policy*, 59, 152–164.

Buchwitz, M., Schneising, O., Reuter, M., Heymann, J., Krautwurst, S., Bovensmann, H., Burrows, J.P., Boesch, H., Parker, R.J., Somkuti, P. and Detmers, R.G. (2017). Satellite-derived methane hotspot emission estimates using a fast data-driven method. *Atmospheric Chemistry and Physics*, 17, 5751.

Buzan, J.R. and Huber, M. (2020). Moist heat stress on a hotter Earth. *Annual Review of Earth and Planetary Sciences*, 48.

Calvin, K.V., Patel, P.L., Clarke, L.E., Asrar, G.R., Bond-Lamberty, B., Cui, Y., Di Vittorio, A., Dorheim, K.R., Edmonds, J.A., (2019). GCAM v5.1: Representing the linkages between energy, water, land, climate, and economic systems. *Geoscientific Model Development*, 12, 1–22.

Cambaliza, M.O.L., Bogner, J.E., Green, R.B., Shepson, P.B., Harvey, T.A., Spokas. K.A., Stirm, B.H., Corcoran, M., Hartin, C., Hejazi, M., Horowitz, R., Iyer. G., Kyle, P., Kim, S., Link, R., McJeon, H., Smith, S.J., Snyder, A., Waldhoff, S. and Wise, M. (2017). Field measurements and modeling to resolve m2 to km2 CH_4 emissions for a complex urban source: An Indiana landfill study, *Elementa: Science of the Anthropocene*, 5(36).

Camilleri, A.R., Larrick, R.P., Hossain, S. and Patino-Echeverri, D. (2017). Consumers underestimate the emissions associated with food but are aided by labels. *Nat. Clim. Change*, 9, 53–8.

Carey, I.M., Atkinson, R.W., Kent, A.J., van Staa, T., Cook, D.G. and Anderson, H.R. (2013). Mortality Associations with Long-Term Exposure to Outdoor Air Pollution in a National English Cohort. *Am J Respir Crit Care Med*., 187, 1226–123.

Carleton, T.A., Jina, A., Delgado, M.T., Greenstone, M., Houser, T., Hsiang, S.M., Hultgren, A., Kopp, R.E., McCusker, K.E., Nath, I.B., Rising, J., Rode, A., Seo, H.K., Viaene, A., Yuan, J, and Zhang, A.T. (2020). *Valuing the Global Mortality Consequences of Climate Change Accounting for Adaptation Costs and Benefits*. NBER Working Paper No. 27599. National Bureau of Economc Research, Cambridge, MA, US. http://www.nber.org/papers/w27599 (accessed 6 March 2020)

Carmichael, M.J., Bernhardt, E.S., Bräuer, S.L. and Smith, W.K. (2014). The role of vegetation in methane flux to the atmosphere: should vegetation be included as a distinct category in the global methane budget? *Biogeochemistry*, 119(1-3), 1-24.

Center for International Earth Science Information Network, Columbia University, Food and Agriculture Programme of the United Nations, and Centro Internacional de Agricultura Tropical (2016). *Gridded Population of the World, Version 4 (GPWv4): Population Count Grid*. NASA Socioeconomic Data and Applications Center (SEDAC), Palisades, NY, US.

Chae, Y. and J. Park. (2011). Quantifying costs and benefits of integrated environmental strategies of air quality management and greenhouse gas reduction in the Seoul Metropolitan Area. *Energy Policy*, 39, 5296-5308.

Challinor, A.J., Watson, J., Lobell, D.B., Howden, S.M., Smith, D.R. and Chhetri, N. (2014). A meta-analysis of crop yield under climate change and adaptation. *Nature Climate Change*, 4, 287–291.

Chappellaz J., Raynaud D., Blunier T. and Stauffer B. (2000) The Ice Core Record of Atmospheric Methane. In Khalil M.A.K. (ed.). *Atmospheric Methane*. Springer Verlag, Berlin, Germany.

Chappellaz, J., Barnola, J., Raynaud, D., Korotkevich, Y.S. and Lorius, C. (1990). Ice-core record of atmospheric methane over the past 160,000 years. *Nature*, 345, 127–131.

Chan, E., Worthy, D.E., Chan, D., Ishizawa, M., Moran, M.D., Delcloo, A. and Vogel, F. (2020). Eight-Year Estimates of Methane Emissions from Oil and Gas Operations in Western Canada are Nearly Twice those Reported in Inventories. *Environmental Science & Technology*, 54, 23, 14899–14909.

Cifuentes, L., Borja-Aburto, V.H., Gouveia, N., Thurston, G. and Davis, D.L. (2001). Hidden health benefits of greenhouse gas mitigation. *Science*, 293.

Clark, M.A., Springmann, M., Hill, J. and Tilman, D. (2019). Multiple health and environmental impacts of foods, *Proceedings of the National Academy of Sciences*, 116(46), 23357–23362.

Collins, W.J., Sitch, S. and Boucher, O. (2010). How vegetation impacts affect climate metrics for ozone precursors. *J. Geophys. Res*., 115, D23308.

Collins, M., Knutti, R., Arblaster, J., Dufresne, J.-L., Fichefet, T., Friedlingstein, P., Gao, X., Gutowski, W.J., Johns, T., Krinner, G., Shongwe, M., Tebaldi, C., Weaver, A.J. and Wehner, M. (2013). Long-term Climate Change: Projections, Commitments and Irreversibility. In Stocker, T.F., Qin, D.. Plattner, G.-K., Tignor, M., Allen, S.K., Boschung, J., Nauels, A., Xia, Y., Bex, V. and Midgley, P.M. (eds.). Climate Change 2013: *The Physical Science Basis*. Contribution of Working Group I to the Fifth Assessment Report of the Intergovernmental Panel on Climate Change. Cambridge University Press, Cambridge, UK.

Collins, W.J., Fry, M.M., Yu, H., Fuglestvedt, J.S., Shindell, D.T. and West, J.J. (2013). Global and regional temperature-change potentials for near-term climate forcers. *Atmos. Chem. Phys*., 13, 2471–2485.

Collins, W.J., Webber, C.P., Cox, P.M., Huntingford, C., Lowe, J., Sitch, S., Chadburn, S.E., Comyn-Platt, E., Harper, A.B., Hayman, G. and Powell, T. (2018). Increased importance of methane reduction for a 1.5 degree target. *Environmental Research Letters*, 13, 054003.

Conley, A.J., Westervelt, D.M., Lamarque, J.-F., Fiore, A.M., Shindell, D., Correa, G., Faluvegi, G. and Horowitz, L.W. (2018). Multimodel surface temperature responses to removal of U.S. sulfur dioxide emissions. *J. Geophys. Res*., 123, 2773–2796.

Conley, S., Faloona, I., Mehrotra, S., Suard, M., Lenschow, D.H., Sweeney, C., Herndon, S., Schwietzke, S., Pétron, G., Pifer, J. and Kort, E.A. (2017). Application of Gauss's theorem to quantify localized surface emissions from airborne measurements of wind and trace gases. *Atmospheric Measurement Techniques*, 10(9).

Cooper, M.D., Estop-Aragonés, C., Fisher, J.P., Thierry, A., Garnett, M.H., Charman, D.J., Murton, J.B., Phoenix, G.K., Treharne, R., Kokelj, S.V. and Wolfe, S.A. (2017). Limited contribution of permafrost carbon to methane release from thawing peatlands. *Nature Climate Change*, 7, 507-511.

Crouse, D.L., Peters, P.A., Hystad, P., Brook, J.R., van Donkelaar, A., Martin, R.V.,

Villeneuve, P.J., Jerrett, M., Goldberg, M.S., Arden Pope III, C., Brauer, M., Robert D. Brook, R.D., Robichaud, A., Richard Menard, R. and Burnett, R.T. (2015). Ambient PM2.5, O3, and NO2 exposures and associations with mortality over 16 years of follow-up in the Canadian Census Health and Environment Cohort (CanCHEC). *Environ. Health Persp*., 123, 1180–1186.

Danabasoglu, G., Lamarque, J.-F., Bacmeister, J., Bailey, D.A., DuVivier, A.K., Edwards, J., Emmons, L., Fasullo, J., Garcia, R., Gettelman, A., Hannay, C., Holland, M.M., Large, W.G., Lawrence, D., Lenaerts, J., Lindsay, K., Lipscomb, W., Lofverstrom, M., Mills, M., Neale, R., Oleson, K., Otto-Bleisner, B., Phillips, A., Sacks, W., Tilmes, S., Vertenstein, M., Bertini, A., Deser, C., Fox-Kemper, B., Kay, J.E., Kushner, P., Long, M.C., Mickelson, S., Moore, J.K., Nienhouse, E., Polvani, L., Rasch,

P.J., and Strand, W.G. (2020). The Community Earth System Model version 2 (CESM2). Accepted for publication in *JAMES*.

Dean, J.F., Middelburg, J.J., Röckmann, T., Aerts, R., Blauw, L.G., Egger, M., Jetten, M.S., de Jong, A.E., Meisel, O.H., Rasigraf, O. and Slomp, C.P. (2018). Methane feedbacks to the global climate system in a warmer world. *Reviews of Geophysics*, 56, 207-250.

Di, Q., Wang, Y., Zanobetti, A., Wang, Y., Koutrakis, P., Choirat C., Dominici, F. and Schwartz, J.D. (2017). Air pollution and mortality in the Medicare population, *N Engl J Med*., 376, 2513–2522.

Dlugokencky E. and Houweling S. (2015). *Chemistry of the Atmosphere: Methane, In Encyclopedia of Atmospheric Sciences*, 2nd. Edition. Academic Press, Cambridge, MA, US.

Drew, J., Cleghorn, C., Macmillan, A. and Mizdrak, A. (2020). Healthy and Climate-Friendly Eating Patterns in the New Zealand Context. *Environmental Health Perspectives*, 128,1, 17007.

Dunne, J.P., Horowitz, L.W., Adcroft, A.J., Ginoux, P., Held, I.M., John, J.G., Krasting, J.P., Malyshev, S., Naik, V., Paulot, F., Shevliakova, E., Stock, C. A., Zadeh, N., Balaji, V., Blanton, C., Dunne, K.A., Dupuis, C., Durachta, J., Dussin, R., Gauthier, P.P.G., Griffies, S.M., Guo, H., Hallberg, R.W., Harrison, M., He, J., Hurlin, W., McHugh, C., Menzel, R., Milly, P.C.D., Nikonov, S., Paynter, D. J., Ploshay, J., Radhakrishnan, A., Rand, K., Reichl, B.G., Robinson, T., Schwarzkopf, D.M., Sentman, L.T., Underwood, S., Vahlenkamp, H., Winton, M., Wittenberg, A.T., Wyman, B., Zeng, Y. and Zhao, M. (2020). The GFDL Earth System Model version 4.1 (GFDL-ESM4.1): Model description and simulation characteristics. *J. Adv. Modeling Earth Sys*. https://doi.org/10.1029/2019MS002015 (accessed 6 March 2021).

Duren, R.M., Thorpe, A.K., Foster, K.T., Rafiq, T., Hopkins, F.M., Yadav, V., Bue, B.D..Thimpson, D.R., Conley, S., Colombi, N.K., Frankenberg, C., McCubbin, I.B., Eastwood, M.L. Falk, M., Herner, J.D., Croes, B.E., Green, R.D. and Miller, C.E. (2019). California's methane super-emitters. *Nature,* 575, 180-185.

Edenhofer, O., Pichs-Madruga, R., Sokona, Y., Farahani, E., Kadner, S., Seyboth, K. Adler, A., Baum, I., Brunner, S., Eikemeier, P., Kriemann, B., Savolainen, J., Schlömer, S., von Stechow, C. and Zwickel, T. (2014). *Climate Change 2014: Mitigation of Climate Change*. Contribution of Working Group III to the Fifth Assessment Report of the Intergovernmental Panel on Climate Change. Cambridge University Press, Cambridge, UK.

Etheridge, D.M., Steele, L.P., Francey, R.J. and Langenfeld, R.L. (1998). Atmospheric methane between 1000 A.D. and present: Evidence of anthropogenic emissions and climatic variability. *J. Geophys. Res*., 103, D13, 15,979-15,993.

Etiope, G. and Schwietzke, S. (2019). Global geological methane emissions: an update of top-down and bottom-up estimates. *Elem. Sci. Anth*., 7, 47.

Etminan, M., Myhre, G., Highwood, E.J. and Shine, K.P. (2016). Radiative forcing of carbon dioxide, methane, and nitrous oxide: A significant revision of the methane radiative forcing. *Geophysical Research Letters*, 43, 12-614.

EUROSTAT. (2016). *Hospital discharges by diagnosis*. Publications Office of the European Union, Luxembourg.

Fann, N., Coffman, E., Timin, B. and Kelly, J.T. (2018). The estimated change in the level and distribution of PM2.5-attributable health impacts in the United States: 2005-2014. *Environ Res.*, 167, 506-514.

Fann, N., Baker, K.R., Chan, E.A.W., Eyth, A., Macpherson, A., Miller, E. and Snyder, J. (2018) Assessing Human Health PM 2.5 and Ozone Impacts from U.S. Oil and Natural Gas Sector Emissions in 2025. *Environ. Sci. Technol., 52, 8095*–8103.

Food and Agriculture Organization (2014). *Food wastage footprint: Full cost accounting*. Food and Agriculture Organization of the United Nations, Rome, Italy.

Food and Agriculture Organization of the United Nations (2017). *Global Livestock Environmental Assessment Model (GLEAM)*. Food and Agriculture Organization of the United Nations, Rome, Italy. www.fao.org/gleam/en/ (accessed 6 March 2021).

Food and Agriculture Organization of the United Nations (2019). *State of Food and Agriculture (SOFA), 2019*. Food and Agriculture Organization of the United Nations, Rome, Italy. http://www.fao.org/state-of-food-agriculture/2019/en/ (accessed 6 March 2021)

Food and Agriculture Organization of the United Nations, International Fund for Agricultural Development, United Nations Children's Fund, World Food Programme and World Health Organization (2017). *The State of Food Security and Nutrition in the World: Building Resilience for Peace and Food Security*. Food and Agriculture Organization of the United Nations, Rome, Italy.

Food and Agriculture Organization of the United Nations, International Fund for Agricultural Development, United Nations Children's Fund, World Food Programme and World Health Organization (2020). *The State of Food Security and Nutrition in the World 2020. Transforming food systems for affordable healthy diets*. Food and Agriculture Organization of the United Nations, Rome, Italy. https://doi.org/10.4060/ca9692en (accessed 6 March 2021).

Field, C.B., Barros, V.R., Dokken, D.J., Mach, K.J., Mastrandrea, M.D., Bilir, T.E.

Chatterjee, M., Ebi, K.L., Estrada, Y.O., Genova, R.C., Girma, B., Kissel, E.S., Levy, A.N.. MacCracken, S., Mastrandrea, P.R. and White, L.L. (eds.). (2014). *Climate Change 2014: Impacts, Adaptation, and Vulnerability. Part A: Global and Sectoral Aspects*. Contribution of Working Group II to the Fifth Assessment Report of the Intergovernmental Panel on Climate Change. Cambridge University Press, Cambridge, UK.

Fiore, A.M., Jacob, D.J., Field, B.D., Streets, D.G., Fernandes, S.D. and Jang, C. (2002). Linking ozone pollution and climate change: The case for controlling methane. *Geophysical Research Letters*, 29, 25-1.

Fiore, A.M., West, J.J., Horowitz, L.W., Naik, V. and Schwarzkopf, M.D. (2008). Characterizing the tropospheric ozone response to methane emission controls and the benefits to climate and air quality. *J. Geophys. Res*., 113, 1–16.

Frankenberg, C., Meiring, J.F., Bergamaschi, P., Goede, A.P.H., Heimann, M., Korner, S., Platt, U., van Weele, M., and Wagner, T. (2006). Satellite chartography of atmospheric methane from SCIAMACHY on board ENVISAT: Analysis of the years 2003 and 2004. *JGR: Atmospheres*. Doi:10.1029/2005JD006235.

Frankenberg, C., Thorpe, A.K., Thompson, D.R., Hulley, G., Kort, E.A., Vance, N., Borchardt, J., Krings, T., Gerilowski, K., Sweeney, C., Conley, S., Bue, B.D., Aubrey, A.D., Hook, S. and Green, R.O. (2016). Airborne methane remote measurements reveal heavy-tail flux

distribution in Four Corners region. *Proc. Natl Acad. Sci*., 113, 9734–9739.

Fu, B., Gasser, T., Li, B. and Tao, S. (2020) Short-lived climate forcers have long-term climate impacts via the carbon–climate feedback. *Nat. Clim. Chang*., 10, 851–855.

Fujimori, S., Hasegawa, T., Masui, T., Takahashi, K., Herran, D. S., Dai, H., Hijioka, Y. and Kainuma, M. (2017). SSP3: AIM implementation of Shared Socioeconomic Pathways. *Global Environmental Change*, 42, 268–283.

FUSIONS. (2016). *Estimates of European food waste levels*. IVL Swedish Environmental Research Institute, Stockholm, Sweden. http://www.eu-fusions.org/phocadownload/Publications/Estimates%20of%20European%20food%20waste%20levels.pdf (accessed 6 March 2021).

Gao, J., Kovats, S., Vardoulakis, S., Wilkinson, P., Woodward, A., Li, J., Gu, S., Liu, X., Wu, H., Wang, J., Song, X., Zhai, Y., Zhao, J. and Liu, Q. (2018). Public health co-benefits of greenhouse gas emissions reduction: A systematic review. *Science of the Total Environment*, 627, 388-402.

Garrone, P., Melacini, M. and Perego, A. (2014). Opening the black box of food waste reduction. *Food Pol*., 46, 129-139.

Gasbarra, D., Toscano, P., Famulari, D., Finardi, S., Di Tommasi, P., Zaldei, A., Carlucci, P., Magliulo, E. and Gioli, B. (2019). Locating and quantifying multiple landfills methane emissions using aircraft data. *Environmental Pollution*, 254, Part B, 112987, ISSN 0269-7491.

Gasser, T., Peters, G.P., Fuglestvedt, J.S., Collins, W.J., Shindell, D.T. and Ciais, P. (2017). Accounting for the climate-carbon feedback in emission metrics. *Earth System Dynamics*, 8(2), 235-253.

Gasparrini, A., Guo, Y.M., Hashizume, M., Lavigne, E., Zanobetti, A., Schwartz, J., Tobias, A., Tong, S.L., Rocklov, J., Forsberg, B., Leone, M., De Sario, M., Bell, M.L., Guo, Y.L.L., Wu, C.F., Kan, H., Yi, S.M., Coelho, M., Saldiva, P.H.N., Honda, Y., Kim, H. and Armstrong, B. (2015). Mortality risk attributable to high and low ambient temperature: a multicountry observational study. *The Lancet*, 386, 369–375.

Gedney, N., Cox, P.M. and Huntingford, C. (2004). Climate feedback from wetland methane emissions. *Geophysical Research Letters*, 31(20).

Geoffroy, O., Saint-Martin, D., Bellon, G., Voldoire, A., Olivié, D.J.L. and Tytéca, S. (2013). Transient climate response in a two-layer energy-balance model. Part II: Representation of the efficacy of deep-ocean heat uptake and validation for CMIP5 AOGCMs. *J. Climate*., 26, 1859-1876.

Gerber, P.J., Steinfeld, H., Henderson, B., Mottet, A., Opio, C., Dijkman, J., Falcucci, A. and Tempio, G. (2013). *Tackling climate change through livestock – A global assessment of emissions and mitigation opportunities*. Food and Agriculture Organization of the United Nations, Rome, Italy.

Gettelman, A., Mills, M.J., Kinnison, D.E., Garcia, R.R., Smith, A.K., Marsh, D.R., Tilmes, S., Vitt, F., Bardeen, C.G., McInerny, J., Liu, H.-L., Solomon, S.C., Polvani, L.M., Emmons, L.K., Lamarque, J.-F., Richter, J.H., Glanville, A.S., Bacmeister, J.T., Phillips, A.S., Neale, R.B., Simpson, I.R., DuVivier, A.K., Hodzic, A. and Randel, W.J. (2019). The Whole Atmosphere Community Climate Model Version 6 (WACCM6). *J. Geophys. Res*. https://doi.org/10.1029/2019JD030943 (accessed 6 March 2021).

Gillett, N.P., Kirchmeier-Young, M., Ribes, A., Shiogama, H., Hegerl, G.C., Knutti, R., Gastineau, G., John, J.G., Li, L., Larissa Nazarenko, L., Rosenbloom, N., Seland, Ø., Wu, T., Yukimoto, S. and Ziehn, T. 2021. Constraining human contributions to observed warming since the pre-industrial period. *Nature Climate Change*. https://doi.org/10.1038/s41558-020-00965-9 (accessed 19 Feb. 2021).

Gilligan, J., Dietz, T., Gardner, G., Stern, P. and Vandenbergh, M. (2010). The behavioural wedge. *Significance*, 7: 17–20.

Global Burden of Disease Collaborative Network. (2017). *Global Burden of Disease Study 2017 (GBD 2017) Results*. The Institute for Health Metrics and Evaluation, Seattle, WA, US.

Gorchov Negron, A.M., Kort, E.A., Conley, S.A. and Smith, M.L. (2020). Airborne Assessment of Methane Emissions from Offshore Platforms in the US Gulf of Mexico. *Environmental Science & Technology*, 54, 5112–5120.

Graff Zivin, J. and Neidell, M. (2014). Temperature and the Allocation of Time: Implications for Climate Change. *J. Labor Econ*., 32(1), 1–26.

Green, R., Milner, J., Dangour, A.D. and Haines, A. (2015). The potential to reduce greenhouse gas emissions in the UK through healthy and realistic dietary change. *Climatic Change*, 129, 253.

Gustavsson, J., Cederberg, C., Sonesson, U., van Otterdijk, R. and Meybeck, A. (2011). *Global Food Losses and Food Waste – Extent, Causes and Prevention*. Food and Agriculture Organization of the United Nations, Rome, Italy.

Gvakharia, A., Kort, E.A., Brandt, A., Peischl, J., Ryerson, T.B., Schwarz, J.P., Smith. M.L. and Sweeney, C. (2017). Methane, black carbon, and ethane emissions from natural gas flares in the Bakken Shale, North Dakota. *Environmental Science & Technology*, 51(9), 5317–5325.

Haines, A. (2012). Health benefits of a low carbon economy. *Public Health*, 126 (Suppl. 1), pp. S33-9.

Haines, A., Amann, M., Borgford-Parnell, N., Leonard, S., Kuylenstierna, J.C.I. and Shindell, D. (2017). Short-lived climate pollutant mitigation and the sustainable development goals. *Nature Climate*

Change, 7, 863–869.

Hammitt, J.K. and Robinson, L.A. (2011). The income elasticity of the value per statistical life: transferring estimates between high and low income populations. *Journal of Benefit-Cost Analysis*, 2(1), 1–29.

Hansen, J., Sato, M., Ruedy, R., Nazarenko, L., Lacis, A., Schmidt, G.A., Russell, G., Aleinov, I., Bauer, M., Bauer, S.E., Bell, N., Cairns, B., Canuto, V., Chandler, M., Cheng, Y., Del Genio, N., Faluvegi, G., Fleming, E., Friend, A., Hall, T., Jackman, H., Kelley, M., Kiang, N., Koch, D., Lean, J., Lo, K., Menn, S., Miller, R.L., Minnis, P., Novakov, T., Oinas, V., Perlwitz, Ja., Rind, D., Romanou, A., Shindell, D., Stone, P., Sun, S., Tausnev, N., Thresher, D., Wielieki, D., Wong, T., Yao, M. and Zhang, S. (2005). Efficacy of climate forcings. J. Geophys. Res., 110, D18104.

Harmsen, M.J.H.M., van Den Berg, M., Krey, V., Luderer, G., Marcucci, A., Strefler, J. and Van Vuuren, D.P. (2016). How climate metrics affect global mitigation strategies and costs: a multi-model study. *Climatic Change*, 136, 203–216.

Harmsen, M.J.H.M., van Vuuren, D.P., Nayak, D.R., Hof, A.F., Höglund-Isaksson, L., Lucas, P.L., Nielsen, J.B., Smith, P. and Stehfest, E., (2019). Long-term marginal abatement cost curves of non-CO_2 greenhouse gases. *Environmental Science & Policy*, 99, 136–149.

Harmsen, M.J.H.M., van Vuuren, D.P., Bodirsky B.L., Chateau, J., Durand-Lasserve, O., Drouet, L., Fricko, O., Fujimori, S., Gernaat, D.E.H.J., Hanaoka, T., Hilaire, J., Keramidas, K., Luderer, G., Moura, M.C.P., Sano, F., Smith, S.J. and Wada, K. (2019b). The role of methane in future climate strategies: mitigation potentials and climate impacts. *Climatic Change*, 163:1409–1425.

https://doi.org/10.1007/s10584-019-02437-2 (accessed 6 March 2021).

Hedenus, F., Wirsenius, S. and Johansson, D.J.A. (2014). The importance of reduced meat and dairy consumption for meeting stringent climate change targets. *Climatic Change*, 124(1–2): 79–91.

Héroux, M.E., Anderson, H.R., Atkinson, R., Brunekreef, B., Cohen, A., Forastiere, F., Hurley, F., Katsouyanni, K., Krewski, D., Krzyzanowski, M. and Künzli, N. (2015). Quantifying the health impacts of ambient air pollutants: recommendations of a WHO/Europe project. *Int J Public Health*, 60, 619–27.

Hmiel, B., Petrenko, V.V., Dyonisius, M.N., Buizert, C., Smith, A.M., Place, P.F., Harth, C., Beaudette, R., Hua, Q., Yang, B., Vimont, I., Michel, S.E., Severinghaus, J.P., Etheridge, D., Bromley, T., Schmitt, J., Faïn, X., Weiss, R.F. and Dlugokencky, E. (2020). Preindustrial 14 CH_4 indicates greater anthropogenic fossil CH_4 emissions. *Nature*, 578, 409–412.

Höglund-Isaksson, L., Gómez-Sanabria, A. Klimont, Z., Rafaj, P. and Schöpp, W. (2020). Technical potentials and costs for reducing global anthropogenic methane emissions in the 2050 timeframe –results from the GAINS model. *Environ. Res. Comm.*, 2, 025004.

Holtsmark, B. (2012). Harvesting in boreal forests and the biofuel carbon debt. *Climatic Change*, 112, 415–428.

Honda, Y., Kondo, M., McGregor, G., Kim, H., Guo, Y.L., Hijioka, Y., Yoshikawa, M., Oka, K., Takano, S., Hales, S. and Kovats, R. (2014). Heat-related mortality risk model for climate change impact projection. *Environmental Health and Preventive Medicine*, 19, 56–63.

Horowitz, L.W., Naik, V., Paulot, F., Ginoux, P.A., Dunne, J.P., Mao, J., Schnell, J., Chen, X., He, J., John, J.G. and Lin, M. (2020). The GFDL global atmospheric chemistry-climate model AM4. 1: Model description and simulation characteristics. *Journal of Advances in Modeling Earth Systems*, 12(10), e2019MS00203.

Hristov, A.N., Oh, J., Giallongo, F., Frederick, T.W., Harper, M.T., Weeks, H.L., Branco, A.F., Moate, P.J., Deighton, M.H., Williams, S.R.O. and Kindermann, M. (2015). An inhibitor persistently decreased enteric methane emission from dairy cows with no negative effect on milk production. *Proceedings of the National Academy of Sciences*, 112, 10663–10668.

Hsiang, S., Kopp, R., Jina, A., Hsiang, S., Kopp, R., Jina, A., Rising, A., Delgado, M., Mohan, S.,

Rasmussen, D.J., Muir-Wood, R., Wilson, P., Oppenheimer, M., Larsen, K. and Houser, T. (2017). Estimating economic damage from climate change in the United States. *Science*, 356(6345), 1362–1369.

International Energy Agency (2020). *Methane Tracker*. International Energy Agency, Paris, France. https://www.iea.org/reports/methane-tracker (accessed 6 March 2021).

International Labour Organization (2019). *Working on a warmer planet: The impact of heat stress on labour productivity and decent work*. International Labour Office, Geneva, Switzerland.

International Labour Organization (2020). *ILOSTAT explorer: Statutory nominal gross monthly minimum wage – Harmonized series – Annual, 2020*. International Labour Office, Geneva, Switzerland. https://www.ilo.org/shinyapps/bulkexplorer0/?lang=en&segment=indicator&id=EAR_4MMN_CUR_NB_A (accessed 6 March 2021).

International Futures (Ifs) modeling system, Version 7.58. Frederick S. Pardee Center for International Futures, Josef Korbel School of International Studies, University of Denver, Denver, CO. http://www.ifs.du.edu/ifs/frm_MainMenu.aspx (accessed 6 March 2021).

Intergovernmental Panel on Climate Change (2018). Summary for Policymakers. In Masson-Delmotte, V., Masson Delmotte, V., Zhai, P., Portner, H.O., Roberts, D.C., Skea, J., Shukla, P.R., Pirani, A., Mouffouma-Okia, W., Pean, C., Pidcock, R., Connors, S., Matthews, J.B.R., Chen, Y., Zhou, X., Gomis, M.I., Lonnoy, E., Maycock, T., Tignor, M. and Waterfield, T. (eds.). *Global warming of 1.5°C. An IPCC special report on the impacts of global warming of 1.5°C above pre-industrial levels and related global greenhouse gas emission pathways, in the context of strengthening the global response to the threat of climate change, sustainable development, and efforts to eradicate poverty*. World Meteorological Organisation, Geneva, Switzerland.

Ishangulyyev, R., Kim, S. and Lee, S.H. (2019). Understanding Food Loss and Waste-Why Are We Losing and Wasting Food? *Foods*, 8, 297.

Jackson, R.B., Saunois, M., Bousquet, P., Canadell, J.G., Poulter, B., Stavert, A.R., Bergamaschi, P., Niwa, Y., Segers, A. and Tsuruta, A. (2020). Increasing anthropogenic methane emissions arise equally from agricultural and fossil fuel sources. *Environ. Res. Lett*., 15, 071002.

Jackson R.B., Solomon E.I., Canadell J.G., Cargnello M. and Field C.B. (2019). Comment, Methane Removal and Atmospheric Restoration. *Nature Sustainability*, 2, 436–438.

Jackson R.B., Solomon E.I., Canadell J.G., Cargnello M., Field C.B. and Abernethy S. (2020). Reply to: Practical constraints on atmospheric methane removal. *Nature Sustainability*, 3, 358–359.

Jacob, D., Turner, A., Maasakkers, J., Sheng, J-X., Sun, K., Liu, X., Chance, K., Aben, I., McKeever, J. and Frankenberg, C. (2016). Satellite observations of atmospheric methane and their value for quantifying methane emissions. *Atmospheric Chemistry and Physics*, 16. 14371–14396. 10.5194/acp-16-14371-2016.

Jerrett, M., Burnett, R.T., Beckerman, B.S., Turner, M.C., Krewski, D., Thurston, G., Martin,R.V., van Donkelaar, A., Hughes, E., Shi, Y., Gapstur, S.M., Thun, M.J and Arden Pope III, C. (2013). Spatial analysis of air pollution and mortality in California. *Am J Respir Crit Care Med*., 188, 593–599.

Johnson, M.R., Tyner, D.R., Conley, S., Schwietzke, S. and Zavala-Araiza, D. (2017). Comparisons of Airborne Measurements and Inventory Estimates of Methane Emissions in the Alberta Upstream Oil and Gas Sector. *Environ. Sci. Technol*., 51, 13008–13017.

Karion, A., Sweeney, C., Pétron, G., Frost, G., Hardesty, R.M., Kofler, J., Miller, B.M., Newberger, T., Wolter, S., Banta, R., Brewer, A., Dlugokencky, E., Lang, P., Montzka, S.A., Schnell, R., Tans, P., Trainer, M., Zamora, R. and Conley, S. (2013). Methane emissions estimate from airborne measurements over a western United States natural gas field. *Geophys. Res. Lett*., 40, 4393–4397.

Karl, D.M., Beversdorf, L., Björkman, K.M., Church, M.J., Martinez, A. and Delong, E.F. (2008). Aerobic production of methane in the sea. *Nature Geosci*., 1, 473–478.

Katsouyanni, K., Samet, J.M., Anderson, H.R., Atkinson, R., Le, A.T., Medina, S., Samoli, E., Touloumi, G., Burnett, R.T., Krewski, D. and Ramsay, T. (2009). *Air pollution and health: a European and North American approach (APHENA)*. Research report. Health Effects Institute, Boston, MA, US.

Kelley, M., Schmidt, G.A., Nazarenko, L.S., Bauer, S.E., Ruedy, R., Russell, G.L., Ackerman, A.S., Aleinov, I., Bauer, M., Bleck, R., Canuto, V., Cesana, G., Cheng, Y., Clune, T.L., Cook, B.I., Cruz, C.A., Del Genio, A.D., Elsaesser, G.S., Faluvegi, G., Kiang, N.Y., Kim, D., Lacis, A.A., Leboissetier, A., LeGrande, A.N., Lo, K.K., Marshall, J., Matthews, E.E., McDermid, S., Mezuman, K., Miller, R.L., Murray, L.T., Oinas, V., Orbe, C., García-Pando, C.P., Perlwitz, J.P., Puma, M.J., Rind, D., Romanou, A., Shindell, D.T., Sun, S., Tausnev, N., Tsigaridis, K., Tselioudis, G., Weng, E., Wu, J. and Yao, M.S. (2020). GISS-E2.1: Configurations and Climatology. *J. Adv. Modeling Earth Sys*., 12(8), e2019MS002025.

Kelso, M. (2018). Pipeline Incidents Continue to Impact Residents. *Fractracker Alliance*, 7. https://www.fractracker.org/2018/12/pipeline-incidents-impact-residents/ (accessed 9 March 2021).

Keppler, F., Hamilton, J.T., Brass, M. and Röckmann, T. (2006). Methane emissions from terrestrial plants under aerobic conditions. *Nature*, 439,187–91.

Kinley, R.D., de Nys, R., Vucko, M.J., Machado, L. and Tomkins, N.W. (2016). The red macroalgae Asparagopsis taxiformis is a potent natural antimethanogenic that reduces methane production during in vitro fermentation with rumen fluid. *Animal Production Science*, 56, 282–289.

Kirschke, S., Bousquet, P., Ciais, P., Saunois, S., Canadell, J.G., Dlugokencky, E.J., Bergamaschi, P., Bergmann, D., Blake, D.R., Bruhwiler, L., Cameron-Smith, P., Castaldi, S., Chevallier, F., Feng, L., Fraser, A., Heimann, M., Hodson, E.L., Houweling, S., Josse, B., Fraser, P.J., Krummel, P.B., Lamarque, J-F., Langenfelds, R.L., Le Quéré, C., Naik, V., O'Doherty, S., Palmer, P.I., Pison, I., Plummer, D., Poulter, B., Prinn, R.G., Rigby, M., Ringeval, B., Santini, M., Schmidt, M., Shindell, D.T., Simpson, I.J., Spahni, R., Steele. L.P., Strode, S.A., Sudo, K., Szopa, S., van der Werf, G.R., Voulgarakis, A., van Weele, M., Weiss, R.F., Williams, J.E. and Zeng, G.(2013). Three decades of global methane sources and sinks. Nature Geoscience, 6, 813–823.

Kirtman, B., Power, S.B., Adedoyin, J.A., Boer, G.J., Bojariu, R., Camilloni, I., Doblas-Reyes, F.J., Fiore, A.M., Kimoto, M., Meehl, G.A., Prather, M., Sarr, A., Schär, C., Sutton, R., van Oldenborgh, G.J., Vecchi, G. and Wang, H.J. (2013). Near-term Climate Change: Projections and Predictability. In Stocker, T.F., Qin, D., Plattner, G.-K., Tignor, M., Allen, S.K., Boschung, J., Nauels, A., Xia, Y., Bex, V. and Midgley, P.M. (eds.). *Climate Change 2013: The Physical Science Basis*. Contribution of Working Group I to the Fifth Assessment Report of the Intergovernmental Panel on Climate Change. Cambridge University Press, Cambridge, U.K.

Kjellstrom, T., Freyberg, C., Lemke, B., Otto, M. and Briggs, D. (2018) Estimating population heat exposure and impacts on working people in conjunction with climate change. *Int J Biometeorol, 62, 291–306.*

Kjellstrom, T., Lemke, B., Otto, M., Hyatt, O. and Dear, K. (2014). Occupational Heat Stress. Contribution to WHO project on Global assessment of the health impacts of climate change. Technical Report 2014:4, 1–52. *Climate CHIP*.

Knittel, N., Jury, M.W., Bednar-Friedl, B., Bachner, G. and Steiner, A.K. (2020). A global analysis of heat-related labour productivity losses under climate change – implications for Germany's foreign trade. *Climatic Change*, 1–19.

Kort, E.A., Frankenberg, C., Costigan, K.R., Lindenmaier, R., Dubey, M.K. and Wunch, D. (2014). Four corners: The largest US methane anomaly viewed from space. *Geophys. Res. Lett*., 41, 6898–6903.

Lackner, K.S. (2020). Practical Constraints on Atmospheric Methane Removal. *Nature Sustainability*, 3, 357.

Lavoie, T. N., Paul B. Shepson, Maria O. L. Cambaliza, Brian H. Stirm, Stephen Conley, Shobhit Mehrotra, Ian C. Faloona, and David Lyon, Spatiotemporal Variability of Methane Emissions at Oil and Natural Gas Operations in the Eagle Ford Basin. *Environmental Science & Technology*, 51 (14), 8001-8009, 2017.

Lee, M., Nordio, F., Zanobetti, A., Kinney, P., Vautard, R. and Schwartz, J. (2014). Acclimatization across space and time in the effects of temperature on mortality: a time-series analysis. *Environmental Health*, 13, doi: 10.1186/1476-069x-13-89.

Lee, J.Y., Kim, H., Gasparrini, A., Armstrong, B., Bell, M.L., Lavigne, F.S.E., Abrutzky, R., Tong, S., de Sousa Zanotti Stagliorio Coelho, M., Hilario, P., Matus Correal Nicolas Valdes Ortega, N.S.P., Kan, H., Osorio Garcia., S., Kyselý, J., Urban,, A., Orru, H., Indermitte, E., Jaakkola, J.J.K., Ryti, N.R.I., Pascal, M., Goodman, P.G., Zeka, A., Michelozzi, P., Scortichini, M., Hashizume, M., Honda, Y., Hurtado, M., Cruz, J., Seposo., Nunes, B., Teixeira, J.P., Tobias, A., Íñiguez, C., Forsberg, B., Åström, C., Vicedo-Cabrera, A.M., Ragettli, M.S., Guo, Y-L,L, Chen, B-Y., Zanobetti, A., Schwartz, J., Dang, T.N., Van, D.D., Mayvaneh, F., Overcenco, A., Li, S. and Guo,, Y..(2019). Predicted temperature-increase-induced global health burden and its regional variability. *Env. Intl*., 131, 105027.

Lenhart, K., Klintzsch, T., Langer, G., Nehrke, G., Bunge, M., Schnell, S. and Keppler, F. (2016). Evidence for methane production by the marine algae Emiliania huxleyi. *Biogeosciences*, 13, 3163–3174.

Li, D., Yuan, J. and Kopp, R.B. (2020). Escalating global exposure to compound heat-humidity extremes with warming. *Environmental Research Letters*.

Li, X., Norman, H.C., Kinley, R.D., Laurence, M., Wilmot, M., Bender, H., de Nys, R. and Tomkins, N. (2016). Asparagopsis taxiformis decreases enteric methane production from sheep. *Animal Production Science*, 58, 681–688.

Luber, G. and McGeehin, M. (2008). Climate Change and Extreme Heat Events. *American Journal of Preventive Medicine*, 35, 429–435.

Ma, W., Chen, R. and Kan, H. (2014). Temperature-related mortality in 17 large Chinese cities: How heat and cold affect mortality in China. *Environmental Research*, 134, 127–133.

Maasakkers, J.D., Jacob, D., Sulprizio, M.P., Scarpelli, T.R., Nesser, H., Sheng, J.X., Zhang, Y., Hersher, M., Bloom, A.A., Bowman, K.W., Worden, J.R., Janssens-Maenhout, G. and Parker, R.J. (2019). Global distribution of methane emissions, emission trends, and OH concentrations and trends inferred from an inversion of GOSAT satellite data for 2010-2015. *Atmos. Chem. Phys*., 19, 7859–7881.

Machado, L., Magnusson, M., Paul, N.A., Kinley, R., de Nys, R. and Tomkins, N. (2016). Dose-response effects of Asparagopsis taxiformis and Oedogonium sp. On in vitro fermentation and methane production. *J Appl Phycol*., 28, 1443–1452.

Machado, L., Tomkins, N., Magnusson, M., Midgley, D.J., de Nys, R. and Rosewarne, C.P. (2018). In Vitro Response of Rumen Microbiota to the Antimethanogenic Red Macroalga Asparagopsis taxiformis, *Microb. Ecol*., 75, 811–818.

Malley, C.S., Henze, D.K., Kuylenstierna, J.C.I., Vallack, H.W., Davila, Y., Anenberg S.C., Turner, M.C. and Ashmore, M.R. (2017). Updated global estimates of respiratory mortality in adults ≥ 30 years of age attributable to long-term ozone exposure. *Env. Health Persp*., 125, 087021.

Marais, E.A., Jacob, D.J., Wecht, K., Lerot, C., Zhang, L., Yu, K., Kurosu, T.P., Chance, K., and Sauvage, B. (2014). Anthropogenic emissions in Nigeria and implications for ozone air quality: a view from space. *Atmos. Environ*., 99, 32–40.

Marten, A. and Newbold, S. (2012). Estimating the social cost of non-CO_2 GHG emissions: Methane and nitrous oxide. *Energy Policy*, 51, 957.

Mbow, C., Rosenzweig, C. ., Barioni, L.G., Benton, T.G., Herrero, M, Krishnapillai, M., Liwenga, E., Pradhan, P., Rivera-Ferre, M.G., Sapkota, T., Tubiello, F.N. and Xu, Y. (2019). Food Security. In Shukla, P.R., Skea, J., Calvo Buendia, E., Masson-Delmotte, V., Pörtner, H.-O., Roberts, D.C., Zhai, P., Slade, R., Connors, S., van Diemen, R., Ferrat, M., Haughey, E., Luz, S., Neogi, S., Pathak, M., Petzold, J., Portugal Pereira, J., Vyas, P., Huntley, E., Kissick, K., Belkacemi, M. and Malley, J. (eds.). *Climate Change and Land: an IPCC special report on climate change, desertification, land degradation, sustainable land management, food security,*

and greenhouse gas fluxes in terrestrial ecosystems. Intergovernmental Panel on Climate Change, Geneva, Switzerland.

Mehrotra, S., Faloona, I., Suard, M., Conley, S. and Fischer, M.L. (2017). Airborne methane emission measurements for selected oil and gas facilities across California. Environmental *Science & Technology*, 51, 12981–12987.

Meijer, Y. *et al*. (2019). Copernicus Mission Requirements Document, EOP-SM/3088/YM-ym, Issue 2.0.

Miller, S.M., Michalak, A.M., Detmers, R.G., Hasekamp, O.P., Bruhwiler, L.M.P., and Schwietzke, S. (2019). China's coal mine methane regulations have not curbed growing emissions. *Nature Communications*, doi:10.1038/s41467-018-07891-7.

Mills, G., Sharps, K., Simpson, D., Pleijel, H., Frei, M., Burkey, K., Emberson, L., Uddling, J., Broberg, M., Feng, Z., Kobayashi, K. and Agrawal, M. (2018). Closing the global ozone yield gap: Quantification and cobenefits for multistress tolerance. *Glob Change Biol*., 24, 4869–4893.

Monteil, G., Houweling, S., Butz, A., Guerlet, S., Schepers, D., Hasekamp, O., Frankenberg, C., Scheepmaker, R., Aben, I. and Röckmann, T. (2013). Comparison of CH_4 inversions based on 15 months of GOSAT and SCIAMACHY observations. *J. Geophys. Res.-Atmos*., 118, 11807–11823, doi:10.1002/2013JD019760.

Myhre, G., Shindell, D., Bréon, F.-M., Collins, W., Fuglestvedt, J., Huang, J., Koch, D., Lamarque, J.-F., Lee, ., Mendoza, B., Nakajima, T., Robock, A., Stephens, G., Takemura, T. and Zhang, H. (2013). Anthropogenic and Natural Radiative Forcing. In Stocker, T.F., Qin, D., Plattner, G.-K., Tignor, M., Allen, S.K., Boschung, J., Nauels, A., Xia, Y., Bex, V. Midgley, P.M. (eds.). *Climate Change 2013: The Physical Science Basis*. Contribution of Working Group I to the Fifth Assessment Report of the Intergovernmental Panel on Climate Change. Cambridge University Press, Cambridge, UK.

Naik, V., Voulgarakis, A., Fiore, A.M., Horowitz, L.W., Lamarque, J.-F., Lin, M., Prather, M.J., Young, P.J., Bergmann, D., Cameron-Smith, P.J., Cionni, I., Collins, W.J., Dalsøren, S. B., Doherty, R., Eyring, V., Faluvegi, G., Folberth, G.A., Josse, B., Lee, Y.H., MacKenzie, I. A., Nagashima, T., van Noije, T.P.C., Plummer, D.A., Righi, M., Rumbold, S.T., Skeie, R., Shindel, D.T., Stevenson, D.S., Strode, S., Sudo, K., Szopa, S. and Zeng, G. (2013). Preindustrial to present-day changes in tropospheric hydroxyl radical and methane lifetime from the Atmospheric Chemistry and Climate Model Intercomparison Project (ACCMIP). *Atmos. Chem. Phys*., 13, 5277–5298.

National Academies of Sciences, Engineering and Medicine. (2018). *Improving Characterization of Anthropogenic Methane Emissions in the United States*. National Academies Press, Washington, DC, U.S. https://www.ncbi.nlm.nih.gov/books/NBK519293/ (accessed 22 March 2021).

Nauer, P.A., Hutley, L.B. and Arndt, S.K. (2018). Termite mounds mitigate half of termite methane emissions. *Proceedings of the National Academy of Sciences*, 115, 13306–13311.

Nisbet, R.E., Fisher, R., Nimmo, R.H., Bendall, D.S., Crill, P.M., Gallego-Sala, A.V., Hornibrook, E.R., López-Juez, E., Lowry, D., Nisbet, P.B., Shuckburgh, E.F., Sriskantharajah, S., Howe, C.J. and Nisbet, E. G. (2009). Emission of methane from plants. *Proceedings Biological Sciences*, 276, 1347–1354.

Nisbet, E.G., Manning, M.R., Dlugokencky, E J., Fisher, R.E., Lowry, D., Michel, S.E., (2019). Very strong atmospheric methane growth in the 4 Years 2014–2017: Implications for the Paris Agreement. *Global Biogeochemical Cycles*, 33, 318–342.

Nisbet, E. G., Fisher, R. E., Lowry, D., France, J. L., Allen, G., Bakkaloglu, S., Lund Myhre, C., Platt, S.M., Allen, G., Bousquet, P., Brownlow, R., Cain, M., France, J.L., Hermansen, O., Hossaini, R., Jones, A.E., Levin, I., Manning, A.C., Myhre, G., Pyle, J.A., Vaughn, B.H., Warwick, N.J. and White, J.W.C. (2020). Methane mitigation: methods to reduce emissions, on the path to the Paris agreement. *Reviews of Geophysics*, 58, e2019RG000675.

National Health and Family Planning Commission (2016), *China health and family planning statistical yearbook*. Peking Union Medical College Publishing House, Beijing, China.

Organisation for Economic Co-operation and Development (2018). *Cost-Benefit Analysis and the*

Environment: Further Developments and Policy Use. Organisation for Economic Co-operation and Development Publishing, Paris, France. https://doi.org/10.1787/9789264085169-en (accessed 9 March 2021).

Oh, Y., Zhuang, Q., Liu, L., Welp, L.R., Lau, M.C.Y., Onstott, T.C., Medvigy, D., Bruhwiler, L., Dlugokencky, E.J., Hugelius, G., D'Imperio, L. and Elberling, B. (2020). Reduced net methane emissions due to microbial methane oxidation in a warmer Arctic, *Nat. Clim. Chang*. 10, 317–321, 2020.

Orellano, P., Quaranta, N., Reynoso, J., Balbi, B. and Vasquez, J. (2017). Effect of outdoor air pollution on asthma exacerbations in children and adults: Systematic review and multilevel meta-analysis. *PloS One*, 12, e0174050.

Pachauri, R.K., Allen, M.R., Barros, V.R., Broome, J., Cramer, W., Christ, R., Church, J.A., Clarke, L., Dahe, Q., Dasgupta, P., Dubash, N.K., Edenhofer, O., Elgizouli, I., Field, C.B., Forster, P., Friedlingstein, P., Fuglestvedt, J., Gomez-Echeverri, L., Hallegatte, S., Hegerl, G., Howden, M., Jiang, K., Jimenez Cisneros, B., Kattsov, V., Lee, H., Mach, K.J., Marotzke, J., Mastrandrea, M.D., Meyer, L., Minx, J., Mulugetta, Y., O'Brien, K., Oppenheimer, M., Pereira, J.J., Pichs-Madruga, R., Plattner, G-K., Pörtner, H-O., Power, S.B., Preston, B., Ravindranath, N.H., Reisinger,A., Riahi, K., Rusticucci, M., Scholes, R., Seyboth, K., Sokona, Y., Stavins, R., Stocker, T.F., Tschakert, P., van Vuuren, D. and van Ypersele, J-P. (2014). *Climate change 2014: synthesis report*. Contribution of Working Groups I, II and III to the fifth assessment report of the Intergovernmental Panel on Climate Change, Cambridge University Press, Cambridge, UK.

Pandey, S., Gautam, R., Houweling, S., van der Gon, H.D., Sadavarte, P., Borsdorff, T., Hasekamp, O., Landgraf, J., Tol, P., van Kempen, T., Hoogeveen, R., van Hees, R., Hamburg, S.P., Maasakkers, J.D., Aben, I. (2019) Satellite observations reveal extreme methane leakage from a natural gas well blowout. *Proc. National Acad. Sci*., 116, 26376–26381.

Parfitt, J., Barthel, M. and Macnaughton, S. (2010). Food waste within food supply chains: quantification and potential for change to 2050. *Philosophical Transactions of the Royal Society B: Biological Sciences*, 365, 3065–3081.

Petersen, S.O., Højberg, O., Poulsen, M., Schwab, C. and Eriksen, J. (2014). Methanogenic community changes, and emissions of methane and other gases, during storage of acidified and untreated pig slurry. *Journal of Applied Microbiology*, 117, 160–172.

Peterson, C.B., El Mashad, H.M., Zhao, Y., Pan, Y. and Mitloehner, F.M. (2020). Effects of SOP Lagoon Additive on Gaseous Emissions from Stored Liquid Dairy Manure. *Sustainability*, 12, 1393.

Pfeiffer, A., Hepburn, C., Vogt-Schilb, A. and Caldecott, B. (2018). Committed emissions from existing and planned power plants and asset stranding required to meet the Paris Agreement. *Environmental Research Letters*, 13(5), p.054019.

Poore, J., and Nemecek, T. (2018). Reducing food's environmental impacts through producers and consumers. *Science*, 360, 987–992.

Popp, A., Lotze-Campen, H. and Bodirsky, B. (2010). Food consumption, diet shifts and associated non-CO_2 greenhouse gases from agricultural production. *Global Environmental Change*, 20(3): 451–462.

Popp, A., Calvin, K., Fujimori, S., Havlik, P., Humpenöder, F., Stehfest, E., Bodirsky, B.L., Dietrich, J.P., Doelmann, J.C., Gusti, M. and Hasegawa, T. (2017). Land-use futures in the shared socio-economic pathways. *Global Environmental Change*, 42, 331–345.

Porter, S.D., Reay, D.S., Bomberg, E. and Higgins, P. (2018). Avoidable food losses and associated production-phase greenhouse gas emissions arising from application of cosmetic standards to fresh fruit and vegetables in Europe and the UK. *Journal of Cleaner Production*, 201, 869–878.

Post, M.J. (2012). Cultured meat from stem cells: Challenges and prospects. *Meat Science*, 92(3), 297–301.

Pradhan, P., Reusser, D.E. and Kropp, J.P. (2013). Embodied greenhouse gas emissions in diets. *PloS*

ONE, 8(5), e62228.

Prather, M.J., Holmes, C.D. and Hsu, J. (2012). Reactive greenhouse gas scenarios: Systematic exploration of uncertainties and the role of atmospheric chemistry. *Geophys. Res. Lett*., 39, L09803, doi:10.1029/2012gl051440.

Prinn, R.G., Weiss, R.F., Fraser, P.J., Simmonds, P.G., Cunnold, D.M., Alyea, F.N., O'Doherty, S., Salameh, P., Miller, B.R., Huang, J. and Wang, R.H.J. (2000). A history of chemically and radiatively important gases in air deduced from ALE/GAGE/AGAGE. *Journal of Geophysical Research: Atmospheres*, 105(D14), 17751–17792.

Ramanathan, V. and Xu, Y. (2010). The Copenhagen Accord for limiting global warming: Criteria, constraints, and available avenues. *Proc Natl Acad Sci USA*., 107, 8055–8062.

Reeburgh, W. S. (2007). Oceanic methane biogeochemistry. *Chemical Reviews*, 107, 486–513.

Riahi, K., van Vuuren, D.P., Kriegler, E., Edmonds, J., O'Neill, B., Fujimori, S., Bauer, N., Calvin, K., Dellink, R., Fricko, O., Lutz, W., Popp, A., Crespo Cuaresma, J., Samir, K. C., Leimback, M., Jiang, L., Kram, T., Rao, S., Emmerling, J., Ebi, K., Hasegawa, T., Havlik, P., Humpenöder, F., Da Silva, L.A., Smith, S., Stehfest, E., Bosetti, V., Eom, J., Gernaat, D., Masui, T., Rogelj, J., Strefler, J., Drouet, L., Krey, V., Luderer, G., Harmsen, M., Takahashi, K., Baumstark, L., Doelman, J., Kainuma, M., Klimont, Z., Marangoni, G., Lotze-Campen, H., Obersteiner, M., Tabeau, A. and Tavoni, M. (2016). Shared socioeconomic pathways: an overview. Global Environ. Change, 42, 153–168.

Robertson, A.M., Edie, R., Snare, D., Soltis, J., Field, R.A., Burkhart, M.D., Bell, C.S., Zimmerle, D. and Murphy, S.M. (2017). Variation in Methane Emission Rates from Well Pads in Four Oil and Gas Basins with Contrasting Production Volumes and Compositions. *Environmental Science & Technology*, 51, 8832–8840.

Rogelj, J., Shindell, D., Jiang, K., Fifita, S., Forster, P., Ginzburg, V., Handa, C., Kheshgi, H., Kobayashi, S., Kriegler, E., Mundaca, L., Séférian, R. and Vilariño, M.V. (2018). Mitigation pathways compatible with 1.5°C in the context of sustainable development. In Masson-Delmotte, V., Zhai, P., Pörtner, H.O., Roberts, D., Skea, J., Shukla, P.R., Pirani, A., Moufouma-Okia, W., Péan, C., Pidcock, R., Connors, S., Matthews, J.B.R., Chen, Y., Zhou, X., Gomis, M. I., Lonnoy, E., Maycock, T., Tignor, M. and Waterfield, T. (eds.). *Global warming of 1.5°C. An IPCC Special Report on the impacts of global warming of 1.5°C above pre-industrial levels and related global greenhouse gas emission pathways, in the context of strengthening the global response to the threat of climate change, sustainable development, and efforts to eradicate poverty*. Cambridge University Press, Cambridge, UK.

Roque, B.M., Venegas, M., Kinley, R.D., De Nys, R., Duarte, T.L., Yang, X., and Kebreab, E. (2021) Red seaweed (Asparagopsis taxiformis) supplementation reduces enteric methane by over 80 in beef steers, *PLoS One*, 16, e0247820.

Samir, K.C. and Lutz, W. (2017). The human core of the shared socioeconomic pathways: Population scenarios by age, sex and level of education for all countries to 2100. *Global Env. Change*, 42, 181–192.

Sarofim, M.C., Saha, S., Hawkins, M.D., Mills, D.M., Hess, J., Horton, R., Kinney, P., Schwartz, J. and St. Juliana, A. (2016). Temperature-Related Death and Illness, In Crimmins, A., Balbus, J., Gamble, J.L., Beard, C.B., Bell, J.E., Dodgen, D., Eisen, R.J., Fann, N., Hawkins, M.D., Herring, S.C., Jantarasami, L., Mills, D.M., Saha, S., Sarofim, M.C., Trtanj, J.and Ziska, L. (eds.). *The Impacts of Climate Change on Human Health in the United States: A Scientific Assessment*. US Global Change Research Program, Washington, DC, US.

Saunois, M., Bousquet, P., Poulter, B., Peregon, A., Ciais, P., Canadell, J.G., Dlugokencky, E.J., Etiope, G., Bastviken, D., Houweling, S., Janssens-Maenhout, G., Tubiello, F.N., Castaldi, S., Jackson, R.B., Alexe, M., Arora, V.K., Beerling, D.J., Bergamaschi, P., Blake, D.R., Brailsford, G., Brovkin, V., Bruhwiler, L., Crevoisier, C., Crill, P., Covey, K., Curry, C., Frankenberg, C., Gedney, N., Höglund-Isaksson, L., Ishizawa, M., Ito, A., Joos, F., Kim, H-S., Kleinen, T., Krummel, P., Lamarque, J-F., Langenfelds, R., Locatelli, R., Machida, T., Maksyutov, S., McDonald, K.C., Marshall, J., Melton, J.R., Morino, I., Naik, V., O'Doherty, S., Parmentier, F-J,W, Patra, P.K., Peng, C., Peng, S., Peters, G.P., Pison, I., Prigent, C., Prinn, R., Ramonet, M., Riley, W.J., Saito, M., Santini, M., Schroeder, R.,

Simpson, I.J., Spahni, R., Steele, P., Takizawa, A., Thornton, B. F., Tian, H., Tohjima, Y., Viovy, N., Voulgarakis, A., van Weele, M., van der Werf, G.R., Weiss, R., Wiedinmyer, C., Wilton, D.J., Wiltshire, A., Worthy, D., Wunch, D., Xu, X., Yoshida, Y., Zhang, B., Zhang, Z. and Zhu, Q. (2016). The global methane budget 2000–2012. *Earth System Science Data*, 8, 2.

Saunois, M., Stavert, A.R., Poulter, B., Bousquet, P., Canadell, J.G., Jackson, R.B., Raymond, P.A., Dlugokencky, E.J., Houweling, S., Patra, P.K., Ciais, P., Arora, V.K., Bastviken, D., Bergamaschi, P., Blake, D.R., Brailsford, G., Bruhwiler, L., Carlson, K.M., Carrol, M., Castaldi, S., Chandra, N., Crevoisier, C., Crill, P.M., Covey, K., Curry, C.L., Etiope, G., Frankenberg, C., Gedney, N., Hegglin, M.I., Höglund-Isaksson, L., Hugelius, G., Ishizawa, M., Ito, A., Janssens-Maenhout, G., Jensen, K.M., Joos, F., Kleinen, T., Krummel, P.B., Langenfelds, R.L., Laruelle, G.G., Liu, L., Machida, T., Maksyutov, S., McDonald, K. C., McNorton, J., Miller, P. A., Melton, J. R., Morino, I., Müller, J., Murguia-Flores, F., Naik, V., Niwa, Y., Noce, S., O'Doherty, S., Parker, R.J., Peng, C., Peng, S., Peters, G.P., Prigent, C., Prinn, R., Ramonet, M., Regnier, P., Riley, W.J., Rosentreter, J.A., Segers, A., Simpson, I.J., Shi, H., Smith, S.J., Steele, L.P., Thornton, B.F., Tian, H., Tohjima, Y., Tubiello, F.N., Tsuruta, A., Viovy, N., Voulgarakis, A., Weber, T.S., van Weele, M., van der Werf, G.R., Weiss, R.F., Worthy, D., Wunch, D., Yin, Y., Yoshida, Y., Zhang, W., Zhang, Z., Zhao, Y., Zheng, B., Zhu, Q., Zhu, Q., and Zhuang, Q. (2020). The Global Methane Budget 2000–2017, Earth Syst. Sci. Data, 12, 1561–1623.

Scarpelli, T.R., Jacob, D.J., Maasakkers, J.D., Sulprizio, M.P., Sheng, J-X., Rose, K., Romeo, L., Worden, J.R. and Janssens-Maenhout, G. (2020). A global gridded (0.1°×0.1°) inventory of methane emissions from oil, gas, and coal exploitation based on national reports to the United Nations Framework Convention on Climate Change. Earth Syst. Sci. Data, 12, 563–575.

Schneising, O., Burrows, J.P., Dickerson, R.R., Buchwitz, M., Reuter, M. and Bovensmann, H. (2014). Remote sensing of fugitive methane emissions from oil and gas production in North American tight geologic formations. *Earth's Future*, 2, 548–558.

Schneising, O., Buchwitz, M., Reuter, M., Vanselow, S., Bovensmann, H. and Burrows, J.P. (2020). Remote sensing of methane leakage from natural gas and petroleum systems revisited. *Atmos. Chem. Phys*., 20, 9169-9281.

Schuur, E.A., McGuire, A.D., Schädel, C., Grosse, G., Harden, J.W., Hayes, D.J., Hugelius, G., Koven, C.D., Kuhry, P., Lawrence, D.M. and Natali, S.M. (2015). Climate change and the permafrost carbon feedback. *Nature*, 520, 171–179.

Schwartz, J.D., Lee, M., Kinney, P.L., Yang, S.J., Mills, D., Sarofim, M.C., Jones, R., Streeter, R., St Juliana, A., Peers, J. and Horton, R.M. (2015). Projections of temperature-attributable premature deaths in 209 US cities using a cluster-based Poisson approach. *Environmental Health*, 14.

Stockholm Environment Institute, International Institute for Sustainable Development, Overseas Development Institute, E3G, and United Nations Environment Programme (2020). *The Production Gap Report: 2020 Special Report*. http://productiongap.org/2020report.

Sekiya, T., Miyazaki, K., Ogochi, K., Sudo, K. and Takigawa, M. (2018). Global high-resolution simulations of tropospheric nitrogen dioxide using CHASER V4. 0. *Geoscientific Model Development*, 11.

Sellar, A.A., Jones, C.G., Mulcahy, J., Tang, Y., Yool, A., Wiltshire, A., O'Connor, F.M., Stringer, M., Hill, R., Palmieri, J., Woodward, S., Mora, L., Kuhlbrodt, T., Rumbold, S., Kelley, D.I., Ellis, R., Johnson, C.E., Walton, J., Abraham, N.L., Andrews, M.B., Andrews, T., Archibald, A.T., Berthou, S., Burke, E., Blockley, E., Carslaw, K., Dalvi, M., Edwards, J., Folberth, G.A., Gedney, N., Griffiths, P.T., Harper, A.B., Hendry, M.A., Hewitt, A.J., Johnson, B., Jones, A., Jones, C.D., Keeble, J., Liddicoat, S., Morgenstern, O., Parker, R.J., Predoi, V., Robertson, E., Siahaan, A., Smith, R.S., Swaminathan, R., Woodhouse, M.T., Zeng, G. and Zerroukat, M. (2019). UKESM1: Description and evaluation of the UK Earth System Model. *J. Adv. Model. Earth Syst*., doi:10.1029/2019ms001739.

Seltzer, K., Shindell, D. and Malley, C. (2018). Measurement-based assessment of health burdens from long-term ozone exposure in the United States, Europe, and China. *Env. Res. Lett*., 13, 104018.

Shearer, C., Tong, D., Fofrich, R. and Davis, S.J. (2020). Committed emissions of the U.S. power sector, 2000–2018. *AGU Advances*, 1, e2020AV000162.

Sherwood, S., Webb, M.J., Annan, J.D., Armour, K.C., Forster, P.M., Hargreaves, J.C., Hegerl, G., Klein, S.A., Marvel, K.D., Rohling, E.J. and Watanabe, M. (2020). An assessment of Earth's climate sensitivity using multiple lines of evidence. *Reviews of Geophysics*, e2019RG000678.

Shindell, D.T. (2012). Evaluation of the Absolute Regional Temperature Potential. *Atmos. Chem. Phys*., 12, 7955–7960.

Shindell, D.T., Borgford-Parnell, N., Brauer, M., Haines, A., Kuylenstierna, J.C.I., Leonard, S.A., Ramanathan, V., Ravishankara, A., Amann, M. and Srivastava, L. (2017b). A climate policy pathway for near- and long-term benefits. *Science*, 356, 493–494.

Shindell, D., Faluvegi, G., Kasibhatla, P. and Van Dingenen, R. (2019). Spatial patterns of crop yield change by emitted pollutant. *Earth's Future*, 7, 101–112.

Shindell, D., Faluvegi, G., Seltzer, K. and Shindell, C. (2018). Quantified, localized health benefits of accelerated carbon dioxide emissions reductions. *Nat. Clim. Change*, 8, 291–295.

Shindell, D., Fuglestvedt, J.S. and Collins, W.J. (2017). The Social Cost of Methane: Theory and Applications. *Faraday Disc.,* 200, 429–451.

Shindell, D., Kuylenstierna, J.C.I., Vignati, E., Dingenen, R., Amann, M., Klimont, Z., Anenberg, S.C., Muller, N.., Janssens-Maenhout, G., Raes, F., Schwartz, J., Faluvegi, G., Pozzoli, L., Kupiainen, K., Höglund-Isaksson, L., Emberson, L., Streets, D., Ramanathan, V., Hicks, K., Oanh, K., Milly, G., Williams, M., Demkine, V. and Fowler, D. (2012). Simultaneously mitigating near-term climate change and improving human health and food security. *Science*, 335, 183–189.

Shindell, D. and Smith, C.J. (2019). Climate and air-quality benefits of a realistic phase-out of fossil fuels. *Nature*, 573, 408–411.

Shindell, D., Zhang, Y., Scott, M., Ru, M., Stark, K. and Ebi, K.L. (2020). The Effects of Heat Exposure on Human Mortality Throughout the US. *GeoHealth*, 3. https://doi.org/10.1029/ 2019GH000234 (accessed 22 March 2021).

Sjögersten, S., Siegenthaler, A., Lopez, O.R., Aplin, P., Turner, B. and Gauci, V. (2020). Methane emissions from tree stems in neotropical peatlands. *The New Phytologist*, 225,2, 769–781.

Skarke, A., Ruppel, C., Kodis, M., Brothers, D. and Lobecker, E.. (2014). Widespread methane leakage from the sea floor on the northern US Atlantic margin. *Nature Geosci.,* 7, 657–661.

Sokolov, V., VanderZaag, A., Habtewold, J., Dunfield, K., Wagner-Riddle, C., Venkiteswaran, J.J. and Gordon, R. (2019). Greenhouse gas mitigation through dairy manure acidification. *Journal of environmental quality*, 48, 1435–1443.

Sommer, S.G., Clough, T.J., Balaine, N., Hafner, S.D. and Cameron, K.C. (2017). Transformation of organic matter and the emissions of methane and ammonia during storage of liquid manure as affected by acidification. *Journal of Environmental Quality*, 46, 514–521.

Spadaro, J.V., Kendrovski, V. and Sanchez Martinez, G. (2018). *Achieving health benefits from carbon reductions: Manual for CaRBonH calculation tool*. World Health Organization, Geneva, Switzerland. https://core.ac.uk/reader/189891440 (accessed 9 March 2021).

Springmann, M., Clark, M., Mason-D'Croz, D., Wiebe, K., Bodirsky, B.L., Lassaletta, L., de Vries, W., Vermeulen, S.J., Herrero, M., Carlson, K.M., Jonell, M., Troell, M., DeClerck, F., Gordon, L.J., Zurayk, R., Scarborough, P., Rayner, M., Loken, B., Fanzo, J., Godfray, H.C.J., Tilman, D., Rockström, J. and Willett, W. (2018). Options for keeping the food system within environmental limits. *Nature*, 562, 519–525.

Springmann, M., Godfray, H.C.J., Rayner, M. and Scarborough, P. (2016). Analysis and valuation of the health and climate change cobenefits of dietary change. *Proceedings of the National Academy of Sciences*, 113(15), 4146–4151.

Stauffer, B., Fischer, G., Neftel, A. and Oeschger, H. (1985). Increase of Atmospheric Methane Recorded in Antarctic Ice Core. *Science*, 1386–1388.

Stehfest, E., Bouwman, L., Van Vuuren, D.P., Den Elzen, M.G.J., Eickhout, B. and Kabat, P. (2009). Climate benefits of changing diet. *Clim. Change*, 95, 83–102.

Stehfest, E., van den Berg, M., Woltjer, G. and Msangi, S. (2013). Options to reduce the environmental effects of livestock production – Comparison of two economic models. *Agr. Syst*., 114, 38–53.

Sterman J. D., Siegel, L. and Pooney-Varga, J.N. (2018). Does replacing coal with wood lower CO_2 emissions? Dynamic lifecycle analysis of wood bioenergy. *Env. Res. Lett*., 13, 1–10.

Stohl, A., Aamaas, B., Amann, M., Baker, L., Bellouin, N., Berntsen, T.K., Boucher, O., Cherian, R., Collins, W., Daskalakis, N. and Dusinska, M., Evaluating the climate and air quality impacts of short-lived pollutants, Atmos. Chem. Phy., 15,10529-10566, 2015.

Stolaroff J.K., Bhattacharyya S., Smith C.A., Bourcier W.L., Cameron-Smith P.J. and Aines R.D. (2012). Review of Methane Mitigation Technologies with Application to Rapid Release of Methane from the Arctic. *Env. Sci. Tech*., 46, 6455–6469.

Sudo, K., Takahashi, M., Kurokawa, J.-i., and Akimoto, H. (2002). CHASER: A global chemical model of the troposphere 1. Model description. *J. Geophys. Res*., 107, ACH–7.

Sweeney, C., Karion, A., Wolter, S., Newberger, T., Guenther, D., Higgs, J.A., Andrews, A.E., Lang, P.M., Neff, D., Dlugokencky, E., Miller, J.B., Montzka, S.A., Miller, J.B., Masarie, K.A., Biraud, S.C., Novelli, P.C., Crotwell, M., Crotwell, A.M., Thoning, K. and Tans, P.P. (2015).Seasonal climatology of CO_2 across North America from aircraft measurements in the NOAA/ESRL Global Greenhouse Gas Reference Network. *J. Geophys. Res. Atmos*., 120, 5155–5190.

Tebaldi, C. and Lobell, D. (2018). Estimated impacts of emission reductions on wheat and maize crops. *Climatic Change*, 146(3-4), 533–545.

Tilman, D. and Clark, M. (2014). Global diets link environmental sustainability and human health, *Nature*, 515, 518–522.

Torero, M. (2020). Without food, there can be no exit from the pandemic. *Nature*, 580, 588–589.

Tuomisto, H.L. and M.J. Teixeira de Mattos. (2011). Environmental Impacts of Cultured Meat Production. *Environmental Science & Technology*, 45(14), 6117–6123.

Turner, M.C., Jerrett, M., Pope, C.A., Krewski, D., Gapstur, S.M., Diver, W.R., Beckerman, B.S., Marshall, J.D., Su, J., Crouse, D.L. and Burnett, R.T. (2016). Long-term ozone exposure and mortality in a large prospective study. *Am. J. Respir. Crit. Care Med*., 193, 1134–42.

Turner, A.J., Jacob, D.J., Benmergui, J., Wofsy, S.C., Maasakkers, J.D., Butz, A., Hasekamp, O., Biraud, S.C. and Duglokencky, E. (2016). A large increase in US methane emissions over the past decade inferred from satellite data. *Geophys. Res. Lett*., 43, 2218–2224.

United Nations Environment Programme and World Meteorological Organization (2011). *Integrated Assessment of Black Carbon and Tropospheric Ozone*. United Nations Environment Programme, Nairobi, Kenya and World Meteorological Organization, Geneva, Switzerland.

United Nations Environment Programme (2011). *Near-term Climate Protection and Clean Air Benefits: Actions for Controlling Short-Lived Climate Forcers*. United Nations Environment Programme, Nairobi, Kenya.

United Nations Environment Programme (2017). *The Emissions Gap Report 2017*. United Nations Environment Programme, Nairobi, Kenya..

United States Bureau of Labor Statistics. (2020a). *Quarterly Census of Employment and Wages*. U.S. Bureau of Labor Statistics, Washington, DC, US. https://www.bls.gov/cew/datatoc.htm (accessed 9 March 2021).

United States Bureau of Labor Statistics. (2020b). *Quarterly Census of Employment and Wages: QCEW Industry Codes and Titles*. U.S. Bureau of Labor Statistics, Washington, DC, US. https://data.bls.gov/cew/doc/titles/industry/industry_titles.htm (accessed 9 March 2021).

United States Environmental Protection Agency. (1997). *The Benefits and Costs of the Clean Air Act 1970-1990. Prepared for Congress by Office of Air and Radiation and Office of Policy, Planning and Evaluation*. United States Environment Protection Agency, Washington, DC, US. https://www.epa.gov/environmental-economics/benefits-and-costs-clean-air-act-1970-1990-1997 (accessed 9 March 2021).

United States Environmental Protection Agency. (2013). *Global Mitigation of Non-CO$_2$ Greenhouse Gases: 2010-2030*. United States Environment Protection Agency, Washington, DC, US. EPA 430-R-13-011.

United States Environmental Protection Agency. (2015). *Environmental Benefits Mapping and Analysis Program–Community Edition (BenMAP-CE)*. United States Environment Protection Agency, Washington, DC, US.

United States Environmental Protection Agency (2015a) *Climate Change in the United States: Benefits of Global Action. United States Environmental Protection Agency, Office of Atmospheric Programs,* Washington, DC, US. EPA 430-R-15-001.

United States Environmental Protection Agency. (2017). *Multi-model framework for quantitative sectoral impacts analysis: A technical report for the Fourth National Climate Assessment*. United States Environment Protection Agency, Washington, DC, US.

United States Environmental Protection Agency (2019). *Global Non-CO$_2$ Greenhouse Gas Emission Projections & Mitigation Potential: 2015-2050*. United States Environment Protection Agency, Washington, DC, US. EPA 430-R-19-010.

United States Global Change Research Program (2018). *Climate Science Special Report: Fourth National Climate Assessment, Volume I*. Wuebbles, D.J., Fahey, D.W., Hibbard, K.A., Dokken, D.J., Stewart, B.C. and Maycock, T.K. (eds.). U.S. Global Change Research Program, Washington, DC, US.

Valentine, D.W., Holland, E.A. and Schimel, D.S. (1994). Ecosystem and physiological controls over methane production in northern wetlands. *J. Geophys. Res*., 99, 1563–1571.

van de Ven, D.-J., González-Eguino, M. and Arto, I. (2018). The potential of behavioural change for climate change mitigation: a case study for the European Union. *Mitigation and Adaptation Strategies for Global Change*, 23, 853–886.

Van Dingenen, R., Dentener, F.J., Raes, F., Krol, M.C., Emberson, L. and Cofala, J. (2009). The global impact of ozone on agricultural crop yields under current and future air quality legislation. *Atmospheric Environment*, 43, 604–618.

Varon, D.J., Jacob, D.J., McKeever, J., Jervis, D., Durak, B.O.A., Xia, Yan, and Huang, Y.,(2018) Quantifying methane point sources from fine-scale satellite observations of atmospheric methane plumes, *Atmos. Meas. Tech*., 11, 5673–5686.

Varon, D.J., McKeever, J., Jervis, D., Maasakkers, J.D., Pandey, S., Houweling, S., Aben, I., Scarpelli, T. and Jacob, D.J. (2019). Satellite discovery of anomalously large methane point sources from oil/gas production. *Geophysical Research Letters*, 46, 13507–13516.

Vaughn, T.L., Bell, C.C., Pickering, C.K., Schwietzke, S., Heath, G.A., Pétron, G., Zimmerle, D.J., Schnell, R.C. and Nummedal, D. (2018). Temporal variability largely explains top-down/bottom-up difference in methane emission estimates from a natural gas production region. *Proceedings of the National Academy of Sciences*, 115, 11712–11717.

Victor, D.G., Zaelke, D. and Ramanathan, V. (2015). Soot and short-lived pollutants provide political opportunity. *Nature Climate Change*, 5, 796–798.

Vijn, S., Compart D.P., Dutta, N., Foukis, A., Hess, M., Hristov, A.N., Kalscheur, K.F., Kebreab, E., Nuzhdin, S.V., Price, N.N., Sun, Y., Tricarico, J.M., Turzillo, A., Weisbjerg, W.R., Yarish, C., and Kurt, T.D. (2020) Key considerations for the Use of Seaweed to Reduce Enteric Methane Emissions From Cattle, *Front. Vet. Sci*., 7, 597430.

Viscusi, W.K. and Aldy, J.E. (2003). The Value of a Statistical Life: A Critical Review of Market Estimates Throughout the World. *J. Risk Uncert*., 27, 5–76.

Wania, R., Melton, J.R., Hodson, E.L., Poulter, B., Ringeval, B., Spahni, R., Bohn, T., Avis, C. A., Chen, G., Eliseev, A.V., Hopcroft, P.O., Riley, W.J., Subin, Z.M., Tian, H., van Bodegom, P.M., Kleinen, T., Yu, Z.C., Singarayer, J.S., Zürcher, S., Lettenmaier, D.P., Beerling, D.J., Denisov, S.N., Prigent, C., Papa, F. and Kaplan, J.O. (2013). Present state of global wetland extent and wetland methane modelling: methodology of a model inter-comparison project (WETCHIMP). *Geosci. Model Dev*., 6, 617–641.

Wang, Y., and Jacob, D.J. (1998). Anthropogenic forcing on tropospheric ozone and OH since preindustrial times. *J. Geophys. Res*., 103, 31123–31135.

Wang, X. and Mauzerall, D.L. (2004). Characterizing distributions of surface ozone and its impact on grain production in China, Japan and South Korea: 1990 and 2020. *Atmospheric Environment*, 38, 4383–4402.

Wang, T., Srebotnjak, T., Brownell, J. and Hsia, R.Y. (2014). Emergency department charges for asthma-related outpatient visits by insurance status, *J Health Care Poor Underserved*, 25, 396–405.

Wang, W-Q. and Shao, H. (2013). Azimuth-variant signal processing in high-altitude platform passive SAR with spaceborne/airborne transmitter. *Remote Sensing*, 5, 1292–1310.

Watanabe, S., Hajima, T., Sudo, K., Nagashima, T., Takemura, T., Okajima, H., Nozawa, T., Kawase, H., Abe, M., Yokohata, T., Ise (, T., Sato, H., Kato, E., Takata, K., Emori, S. and Kawamiya, M. (2011). MIROC-ESM 2010: Model description and basic results of CMIP5-20c3m experiments. *Geoscientific Model Development*, 4, 845.

Watts, G. (2009). *The Health Benefits of Tackling Climate Change: An Executive Summary*. The Lancet, London, UK.

Watts, N, Adger, W.N., Agnolucci, P., Blackstock, J., Byass, P., Cai, W., Chaytor, S., Colbourn, T., Collins, M., Cooper, A., Cox, P.M., Depledge, J., Drummond, P., Ekins, P., Galaz, V., Grace, D., Graham, H., Grubb, M., Haines, A., Hamilton, I., Hunter, A., Jiang, X., Li, M., Kelman, I., Liang, L., Lott, M., Lowe, R., Luo, Y., Mace, G., Maslin, M., Nilsson, M., Oreszczyn, T., Pye, S., Quinn, T., Svensdotter, M., Venevsky, S., Warner, K., Xu, B., Yang, J., Yin, Y., Yu, C., Zhang, Q., Gong, P., Montgomery, H. and Costello, A. (2015). Health and climate change: policy responses to protect public health. *The Lancet*, 386, 1861–914.

Watts, N., Amann, M., Ayeb-Karlsson, S., Belesova, K., Bouley, T., Boykoff, M., Byass, P., Cai, W., Campbell-Lendrum, D., Chambers, J., Cox, P.M., Daly, M., Dasandi, N., Davies, M., Depledge, M., Depoux, A., Dominguez-Salas, P., Drummond P., Ekins, P., Flahault, A., Frumkin, H., Georgeson, L., Ghanei, M., Grace, D., Graham, H., Grojsman, R., Haines, A., Hamilton, I., Hartinger, S., Johnson, A., Kelman, I., Kiesewetter, G., Kniveton, .C., 26, Liang, L., Lott, M., Lowe, R., Mace, G., Sewe, M.O., Maslin, M., Mikhaylov, S., Milner, J., Latifi, A.M., Moradi-Lakeh, M., Morrissey, K., Murray, K., Neville, T., Nilsson, M., Oreszczyn, T., Owfi, F., Pencheon, D., Pye, S., Rabbaniha, M., Robinson, E., Rocklöv, J., Schütte, S., Shumake-Guillemot, J., Steinbach, R., Tabatabaei, M., Wheeler, N., Wilkinson, P., Gong, P., Montgomery, H. and Costello, A. (2017). The Lancet Countdown on health and climate change: from 25 years of inaction to a global transformation for public health. *The Lancet*, pii: S0140-6736 (17), 32464–32469.

Weber, T., Wiseman, N.A. and Kock, A. (2019). Global ocean methane emissions dominated by shallow coastal waters. *Nat Commun*., 10, 4584.

Wecht, K.J., Jacob, D.J., Frankenberg, C., Jiang, Z. and Blake, D.R. (2014). Mapping of North America methane emissions with high spatial resolution by inversion of SCIAMACHY satellite data. *J. Geophys. Res*., 119, 7741–7756.

Weinberger, K.R., Haykin, L., Eliot, M.N., Schwartz, J.D., Gasparrini, A. and Wellenius, G.A. (2017). Projected temperature-related deaths in ten large US metropolitan areas under different climate change scenarios. *Environment International*, 107, 196–204.

Weiss, F. and Leip, A. (2012). Greenhouse gas emissions from the EU livestock sector: a life cycle assessment carried out with the CAPRI model. *Agriculture, Ecosystems & Environment*, 149, 124–134.

Wellenius, G.A., Eliot, M.N., Bush, K.F., Holt, D., Lincoln, R.A., Smith, A.E. and Gold, J. (2017). Heat-related morbidity and mortality in New England: Evidence for local policy. *Environmental Research*, 156, 845–853.

West, J.J. and Fiore, A.M. (2005). Management of tropospheric ozone by reducing methane emissions. *Environ. Sci. Technol*., 39, 4685.

West, J.J., Fiore, A.M., Horowitz, L.W. and Mauzerall, D.L. (2006). Global health benefits of mitigating ozone pollution with methane emission controls. *Proc. National Acad. Sci*., 103, 3988–3993.

Whalen, S.C. (2005). Biogeochemistry of Methane Exchange between Natural Wetlands and the Atmosphere. Environ. *Eng. Sci*., 22, 73–94.

Willett, W., Rockström, J., Loken, B., Springmann, M., Lang, T., Vermeulen, S., Garnett, T Tilman, D., DeClerck, F., Wood, A., Jonell, M., Clark, M., Gordon, L.J., Fanzo, J., Hawkes, C., Zurayk, R., Rivera, J.A., De Vries, W., Sibanda, L.M., Afshin, A., Chaudhary, A., Herrero, M., Agustina, R., Branca, F., Lartey, A., Fan, S., Crona, B., Fox, E., Bignet, V., Troell, M., Lindahl, T., Singh, S., Cornell, S.E., Reddy, K.S., Narain, S., Nishtar, S. and Murray, C.J.L.

(2019). Food in the Anthropocene: the EAT–Lancet Commission on healthy diets from sustainable food systems. *The Lancet*, 393, no. 10170, 447–492.

Wollenberg, E., Richards, M., Smith, P., Havlík, P., Obersteiner, M., Tubiello, F.N., Herold, M., Gerber, P., Carter, S., Reisinger, A., van Vuuren, D.P., Dickie, A., Neufeldt, H., Sander, B.O., Wassmann, R., Sommer, R., Amonette, J.E., Falcucci, A., Herrero, M., Opio, C., Roman-Cuesta, R.M., Stehfest, E., Westhoek, H., Ortiz-Monasterio, I., Sapkota, T., Rufino, M.C., Thornton, P.K., Verchot, L., West, P.C., Soussana, J.-F., Baedeker, T., Sadler, M., Vermeulen, S. and Campbell, B.M. (2016). Reducing emissions from agriculture to meet the 2 °C target. *Glob. Change Biol*., 22, 3859–3864.

Worden, J., Kulawik, S., Frankenberg, C., Payne, V., Bowman, K., Cady-Peirara, K., Wecht, K., Lee, J.-E. and Noone, D. (2012). Profiles of CH_4, HDO, H2O, and N2O with improved lower tropospheric vertical resolution from Aura TES radiances. *Atmospheric Measurement Techniques*, 5, 397–411.

World Health Organization (2013). *Health risks of air pollution in Europe—HRAPIE project recommendations for concentration–response functions for cost–benefit analysis of particulate matter, ozone and nitrogen dioxide*. World Health Organization, Copenhagen, Denmark.

World Health Organization (2014). *Quantitative risk assessment of the effects of climate change on selected causes of death, 2030s and 2050s*. World Health Organization, Geneva, Switzerland,

World Bank. 2020. *World Development Indicators*. The World Bank, Washington, DC, US. https://databank.worldbank.org/home.aspx (accessed 18 March 2020).

World Bank and Institute for Health Metrics and Evaluation (2016). *The Cost of Air Pollution: Strengthening the Economic Case for Action*. The World Bank, Washington, DC, US and Institute for Health Medicine, https://openknowledge.worldbank.org/handle/10986/25013 (accessed 10 March 2021).

Zavala-Araiza, D., Herndon, S.C., Roscioli, J.R., Yacovitch, T.I., Johnson, M.R., Tyner, D.R., Omara, M. and Knighton, B. (2018). Methane emissions from oil and gas production sites in Alberta, Canada. *Elem Sci Anth*., 6(1).

Zhang, S., Li, G., Tian, L., Guo, Q. and Pan, X. (2016). Short-term exposure to air pollution and morbidity of COPD and asthma in East Asian area: A systematic review and meta-analysis. *Environ Res*., 148, 15–23.

Zhang, Y., Gautam, R., Pandey, S., Omara, M., Maasakkers, J.D., Sadavarte, P., Lyon, D., Nesser, H., Sulprizio, M.P., Varon, D.J., Zhang, R., Houweling, S., Zavala-Araiza, D., Alvarez, R.A., Lorente, A., Hamburg, S.P., Aben, I. and Jacob, D. (2020). Quantifying methane emissions from the largest oil-producing basin in the United States from Space. *Science Advances*, doi:10.1126/sciadv.aaz5120.

Zhang, Z., Zimmermann, N.E., Stenke, A., Li, X., Hodson, E.L., Zhu, G., Huang, C. and Poulter, B. (2017). Emerging role of wetland methane emissions in driving 21st century climate change. *Proceedings of the National Academy of Sciences*, 114, 9647–9652.

Zhao, C., Liu, B., Piao, S., Wang, X., Lobell, D. B., Huang, Y., Huang, M., Yao, Y., Bassu, S., Ciais, P., Durand, J-L., Elliott, J., Ewert, F., Janssens, I.A., Li, T., Lin, E., Liu, Q., Martre, P., Müller, C., Peng, S., Peñuelas, J., Ruane, A.C., Wallach, D., Wang, T., Wu, D., Liu, Z., Zhu, Y., Zhu, Z. and Asseng, S. (2017). Temperature increase reduces global yields of major crops in four independent estimates. *Proceedings of the National Academy of Sciences*, 114, 9326–9331.

Zheng, X.Y., Ding, H., Jiang, L.N., Chen, S.W., Zheng, J.P., Qiu, M., Zhou, Y.X., Chen, Q. and Guan, W.J. (2015). Association between Air Pollutants and Asthma Emergency Room Visits and Hospital Admissions in Time Series Studies: A Systematic Review and Meta-Analysis. *PloS One*, 10, e0138146.

Zhu, Y., Purdy, K.J., Eyice, Ö. and Shen, L. (2020). Disproportionate increase in freshwater methane emissions induced by experimental warming. *Nat. Clim. Chang.*, 10, 685–690.

Zwiers, F.W and von Storch, H. (1995). Taking serial correlation into account in tests of the mean. *Journal of Climate*, 8, 336–351.

7. ABBREVIATIONS

A&E	Hospital accident and emergency departments
A&EV	Hospital accident and emergency department visits
ACS	American Cancer Society
AFOLU	Agriculture, forestry and other land use
AGAGE	Advanced Global Atmospheric Gases Experiment
AGTPs	Absolute global temperature potentials
AIM	Asia-Pacific Integrated Model
APHENA	Air Pollution and Health: a European and North American Approach
BC	Black carbon
BECCS	Biofuel energy with carbon capture and storage
C	centigrade
CaRBonH	Carbon reduction benefits on health
CCAC	Climate and Clean Air Coalition
CCS	Carbon capture and storage
CEDS	Community Emissions Data System
CESM	Community Earth System Model
CGE	Computable general equilibrium
C_2H_2	Acetylene
CH_4	Methane
CMIP	Coupled Model Intercomparison Project
CNES	Centre national d'études spatiales (French National Centre for Space Studies)
CO	Carbon monoxide
CO_2	Carbon dioxide
CO_2e	Carbon dioxide equivalent
DALY	Disability adjusted life year
DLR	Deutsches Zentrum für Luft- und Raumfahrt (German Aerospece Centre)
DRC	Democratic Republic of the Congo
EDF	Environmental Defense Fund
EDGAR	Emissions Database for Global Atmospheric Research
e.g.	*exempli gratia* (for example)
EJ	Exajoules (10^{18} joules)
EPA	Environment Protection Agency
ESA	European Space Agency
EU	European Union
FAO	Food and Agriculture Organization of the United Nations
FINN	Fire INventory from the National Center for Atmospheric Research
FLW	Food loss and waste

FSU	Former Soviet Union
GAINS	Greenhouse Gas – Air Pollution Interactions and Synergies
GBD	Global burden of disease
GCAM	Global Change Assessment Model
GDP	Gross domestic product
GFDL	Geophysical Fluid Dynamics Laboratory
GFED	Global Fire Emissions Database
GHG	Greenhouse gas
GISS	Goddard Institute of Space Studies
GLEAM	Global Livestock Environmental Assessment Model
GLOBIOM	Global Biosphere Management Model
GOSAT	Greenhouse Gases Observing Satellite
GPW	Gridded Population of the World
Gt	Gigatonne (10^9 tonnes)
GWP	Global warming potential
GWP100	Global warming potential over 100 years
HCUP	Healthcare Cost and Utilization Project
HCFC	Hydrochlorofluorocarbon
HFC	Hydrofluorocarbon
hrs/yr	Hours per year
IAM	Integrated assessment model
ICD	International Classification of Diseases
i.e.	*id est* (that is)
IEA	International Energy Agency
IGSD	Institute for Governance & Sustainable Development
IHME	Institute for Health Metrics and Evaluation
IIASA	International Institute for Applied Systems Analysis
ILO	International Labour Organization
IMAGE	Integrated Model to Assess the Global Environment
IPCC	Intergovernmental Panel on Climate Change
IPCC AR5	Intergovernmental Panel on Climate Change Fifth Assessment Report
JAMSTEC	Japan Agency for Marine-Earth Science and Technology
JAXA	Japan Aerospace Exploration Agency
kg	Kilogram
kt	Kilotonne (1 000 tonnes)
LDAR	Leak detection and repair
M	Metre

m^2	Square metre
mm	Millimetre
MAC	Marginal abatement cost
MDA	Maximum daily average
MDA8	Maximum daily 8-hour exposure averaged over the year
MESSAGE	Model of Energy Supply Systems and their General Environmental Impact
Met Office	The United Kingdom's Meteorological Office
MIROC	Model for Interdisciplinary Research on Climate
MMM	Multi-model mean
MST	Mean summer temperature
Mt	Million tonnes
Mt/yr	Million tonnes per year
mW	MilliWatts
N	North
NAICS	North American Industry Classification System
NASA	National Aeronautics and Space Administration
NCAR	National Center for Atmospheric Research
NH_3	Ammonia
NHml	Northern hemisphere mid-latitudes
NIES	National Institute for Environmental Studies, Japan
NMVOC	Non-methane volatile organic compound
NOAA	National Oceanic and Atmospheric Administration
NO_x	Nitrogen oxides
N_2O	Nitrous oxide
NTCF	Near-term climate forcers
NSO	Netherlands Space Organisation
O_3	Ozone
OC	Organic carbon
OECD	Organisation for Economic Co-operation and Development
OH	Hydroxide
PBL	Netherlands Environmental Assessment Agency
PM	Particulate matter
ppb	Parts per billion
ppbv	Parts per billion by volume
QFED	Quick Fire Emissions Dataset
RCP	Representative concentration pathway

REMIND	REgional *Model* of INvestments and Development
RR	Relative Risk
S	South
SCIAMACHY	Scanning Imaging Absorption Spectrometer for Atmospheric Cartography
SDG	Sustainable Development Goal
SEI	Stockholm Environment Institute
SHext	Southern hemisphere extratropics
SLCP	Short-lived climate pollutant
SO$_2$	Sulphur dioxide
SSP	Shared socioeconomic pathway
t	Tonne
Tg	Teragram (10^{12} grams)
TMREL	Theoretical minimum risk exposure level
TROPOMI	Tropospheric Monitoring Instrument
UK	United Kingdom
UKESM	United Kingdom Earth System Model
UN	United Nations
UNEP	United Nations Environment Program
UNFCCC	United Nations Framework Convention on Climate Change
US	United States of America
US$	United States dollar
USDA	United States Department of Agriculture
US EPA	United States Environmental Protection Agency
UV	Ultraviolet
VOC	Volatile organic compound
VSL	Value of statistical life
WA	Work availability
WBGT	Wet bulb globe temperature
WITCH	World Induced Technical Change Hybrid model
WL	Work loss
WMO	World Meteorological Organization
WTP	Willingness to pay
yr	Year

Note Throughout this assessment 1 billion = 1 000 000 000 (10^9)

8. ANNEX –
ADDITIONAL
FIGURES AND
TABLES

Figures A1 and A2 and Tables A1–A3 report values from the modelling performed in support of this assessment described in Chapter 3.
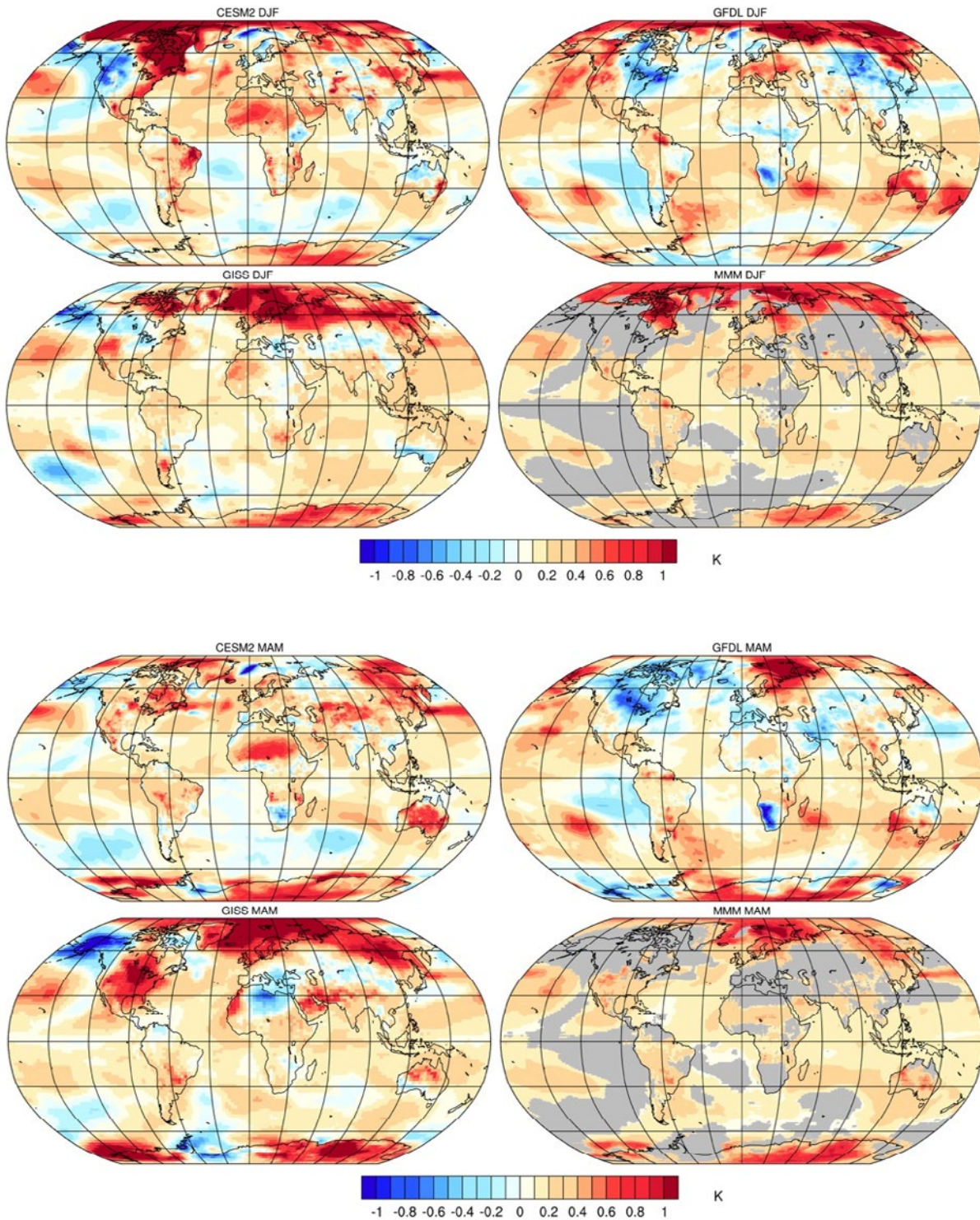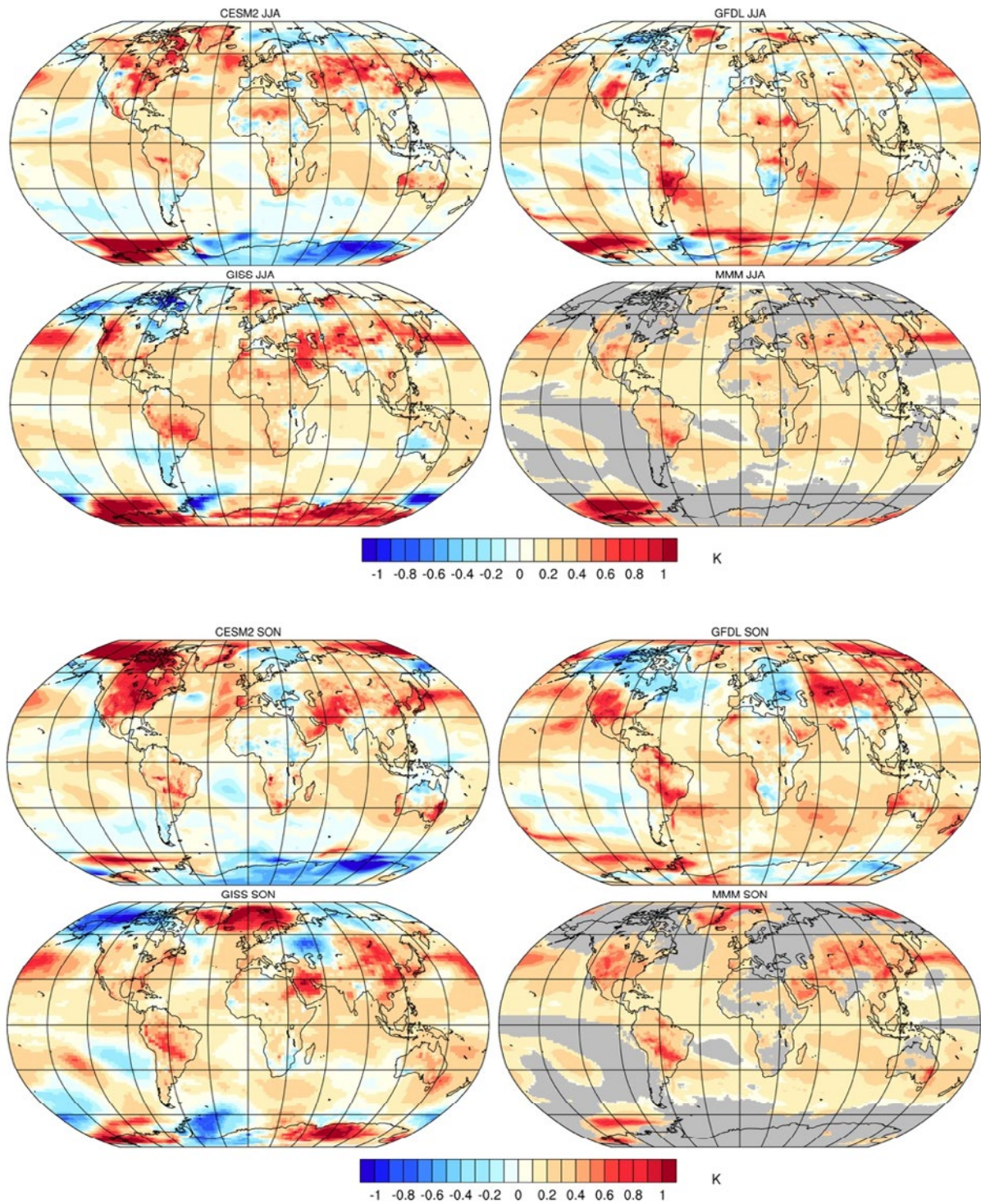
Figure A1 Average temperature responses to methane increase from one-half present methane to the present value, along with the ozone and stratospheric water vapour responses to that methane increase, for the indicated seasons, degrees Centigrade

Note: The multi-model mean is shown in the lower right map for each season, with values included only for areas in which the value is statistically significant – grey indicates no quantification.

Source: UNEP and CCAC
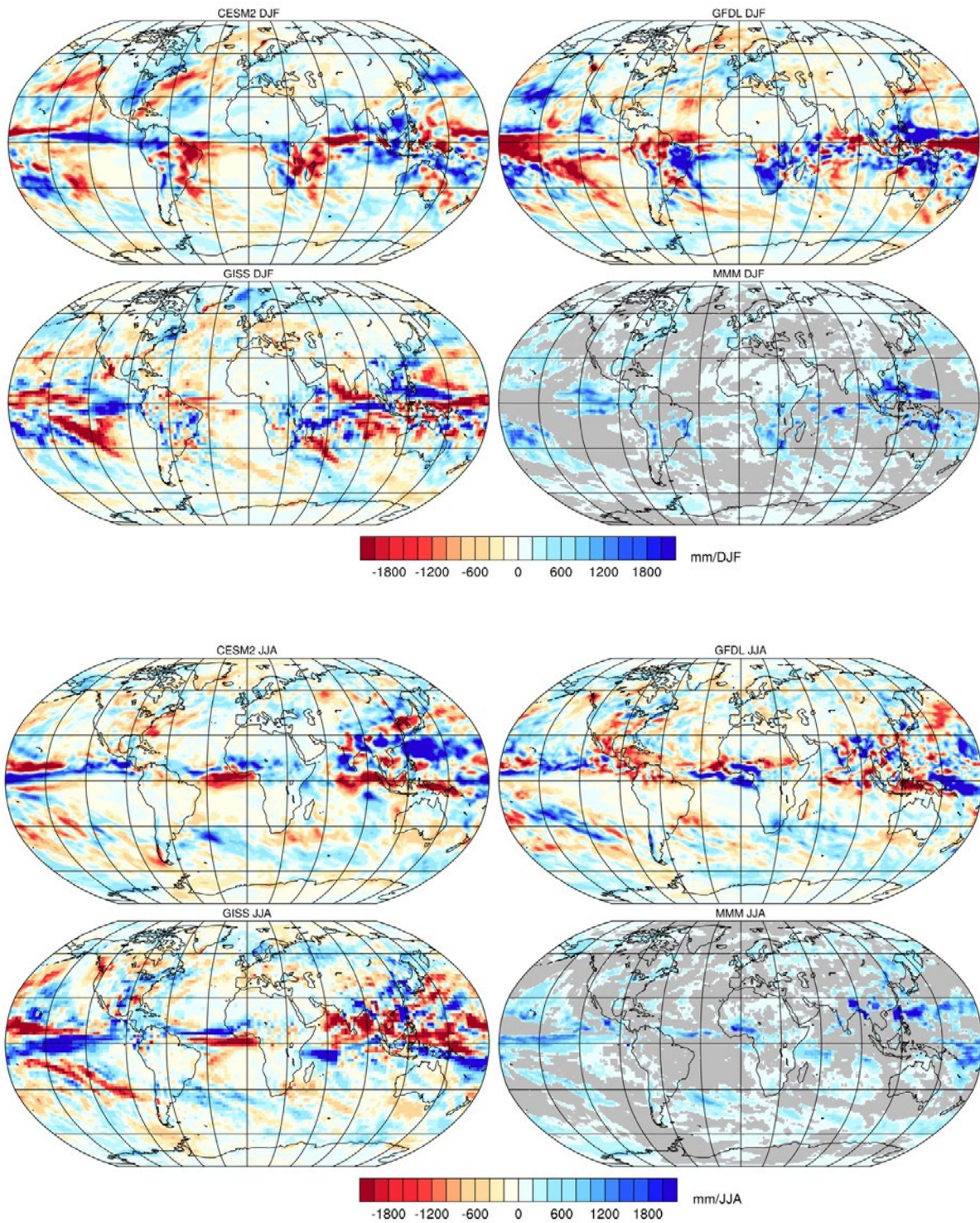
Figure A2 As Figure A1 but showing precipitation for solstice seasons only, millimetres

Note: The multi-model mean is shown in the lower right map for each season, with values included only for areas in which the value is statistically significant – grey indicates no quantification.

Source: UNEP and CCAC

Table A1 Total and per person respiratory deaths per 10 Mt of methane for all countries with non-zero values

COUNTRY	TOTAL	LOW	HIGH	COUNTRY	PER MILLION PEOPLE	LOW	HIGH
India	2 045	1 169	2 863	Lesotho	5	4	7
China	1 419	948	1 831	Korea, Dem People's Rep.	5	3	6
United States	428	287	553	Eritrea	4	2	6
Japan	251	176	316	United Kingdom	4	2	5
Brazil	160	100	216	India	4	2	5
Pakistan	159	98	215	Portugal	3	2	4
United Kingdom	157	102	207	São Tome and Principe	3	2	4
Indonesia	154	86	219	Guinea-Bissau	3	2	5
Germany	121	79	160	Zimbabwe	3	2	4
Russia	109	71	143	Denmark	3	2	4
Philippines	101	64	137	Belgium	3	2	4
Spain	89	59	116	Somalia	3	2	4
Bangladesh	82	51	111	Myanmar	3	2	4
Egypt	82	57	104	Nepal	3	2	4
Mexico	77	50	100	Argentina	3	2	4
Italy	74	49	96	Swaziland	3	2	4
Myanmar	72	45	97	Spain	3	2	4
France	69	45	92	Japan	3	2	3
Korea, Dem Peoples Rep.	64	45	80	Netherlands	3	2	4
Argentina	63	40	86	Gambia	3	1	4
Turkey	61	42	79	Chad	3	1	4
Viet Nam	61	38	82	Cuba	3	2	3
Ethiopia	58	35	80	Haiti	3	2	3
Thailand	52	31	72	Sri Lanka	3	1	4
South Africa	51	34	67	Philippines	2	2	3
Nigeria	42	22	61	Afghanistan	2	2	3
Korea, Rep.	39	27	49	Guinea	2	1	3
Iran, Islamic Rep.	38	27	47	Senegal	2	1	4
Poland	37	24	50	Djibouti	2	1	3
Canada	35	24	46	Grenada	2	2	3
DRC	34	21	46	Central African Rep.	2	1	3
Ukraine	33	21	44	Pakistan	2	1	3
Nepal	32	20	42	Niger	2	1	3
Netherlands	29	19	39	Mozambique	2	1	3
Sri Lanka	28	15	40	Barbados	2	1	3
Peru	27	15	37	Norway	2	1	3

COUNTRY	TOTAL	LOW	HIGH	COUNTRY	PER MILLION PEOPLE	LOW	HIGH
Malaysia	26	15	36	Uruguay	2	1	3
Kenya	25	15	36	United States	2	1	3
Tanzania	25	15	35	Greece	2	1	3
Portugal	23	15	31	Egypt	2	1	3
Morocco and Western Sahara	23	15	31	South Africa	2	1	3
Afghanistan	23	16	28	Cape Verde	2	1	3
Belgium	23	14	30	Germany	2	1	3
Australia	21	13	28	Israel	2	1	3
Romania	20	13	26	St. Lucia	2	1	3
Cuba	19	12	25	Malta	2	1	3
Sudan	18	11	25	Namibia	2	1	3
Mozambique	18	11	24	Mauritania	2	1	3
Ghana	18	9	26	Ireland	2	1	3
Greece	17	11	23	Burundi	2	1	3
Algeria	17	11	23	Puerto Rico and the Virgin Islands	2	1	3
Saudi Arabia	17	11	21	Ethiopia	2	1	3
Chile	16	11	21	Benin	2	1	3
Kazakhstan	15	10	19	Ghana	2	1	3
Zimbabwe	14	9	19	Cameroon	2	1	3
Colombia	14	8	19	Sweden	2	1	2
Uzbekistan	13	9	17	Malawi	2	1	3
Uganda	13	7	19	Peru	2	1	3
Venezuela	13	8	18	Malaysia	2	1	3
Cameroon	13	7	17	Georgia	2	1	2
Yemen	12	8	16	Armenia	2	1	2
Niger	12	6	17	Comoros	2	1	2
Czechia	12	8	15	Kenya	2	1	3
Sweden	12	8	15	El Salvador	2	1	2
Angola	12	7	15	Burkina Faso	2	1	3
Côte d'Ivoire	11	6	16	Italy	2	1	2
Denmark	11	7	15	Luxembourg	2	1	2
Somalia	11	7	15	Bahamas	2	1	2
Senegal	11	6	16	Sierra Leone	2	1	2
Hungary	10	7	14	China	2	1	2
Haiti	10	6	13	Zambia	2	1	2
Cambodia	10	6	13	Jamaica	2	1	2
Serbia and Montenegro	9	6	12	Tanzania	2	1	2

COUNTRY	TOTAL	LOW	HIGH	COUNTRY	PER MILLION PEOPLE	LOW	HIGH
Chad	9	5	13	France	2	1	2
Madagascar	9	0	0	Mali	2	1	3
Guinea	9	5	13	Kazakhstan	2	1	2
Israel	9	6	11	Côte d'Ivoire	2	1	2
Malawi	9	5	12	Bolivia	2	1	2
Burkina Faso	8	4	13	Timor-Leste	2	1	2
Guatemala	8	5	11	Bhutan	2	1	2
Mali	8	4	11	DRC	2	1	2
Syrian Arab Rep.	7	5	10	Czechia	2	1	2
Bulgaria	7	5	10	Chile	2	1	2
Switzerland	7	5	10	Botswana	2	1	2
Norway	7	5	10	Cyprus	2	1	2
Bolivia	7	5	9	Hungary	2	1	2
Zambia	7	5	10	St.Vincent and			
the Grenadines	2	1	2				
Austria	7	5	9	Turkey	2	1	2
Tunisia	7	5	9	Yemen	2	1	2
Ecuador	6	4	9	Cambodia	2	1	2
Benin	6	3	9	Angola	2	1	2
Dominican Rep.	6	4	8	Togo	2	1	2
Eritrea	6	4	8	Serbia and Montenegro	2	1	2
Ireland	6	4	8	Congo	2	1	2
Burundi	6	3	8	Iceland	2	1	2
Rwanda	5	3	8	Canada	2	1	2
Azerbaijan	5	4	7	Romania	2	1	2
Iraq	5	4	7	Guatemala	1	1	2
Singapore	5	3	7	Brazil	1	1	2
El Salvador	5	3	7	Bulgaria	1	1	2
Belarus	5	3	6	Poland	1	1	2
Georgia	4	3	6	Rwanda	1	1	2
Slovakia	4	3	6	Croatia	1	1	2
United Arab Emirates	4	3	6	Australia	1	1	2
Puerto Rico and the Virgin Islands	4	3	6	Morocco and Western Sahara	1	1	2
Uruguay	4	3	6	Antigua and Barbuda	1	1	2
Croatia	4	3	5	Lao People's Dem Rep.	1	1	2
Tajikistan	4	3	5	Singapore	1	1	2
Lebanon	4	2	5	Uganda	1	1	2

COUNTRY	TOTAL	LOW	HIGH	COUNTRY	PER MILLION PEOPLE	LOW	HIGH
Sierra Leone	4	2	5	Liberia	1	1	2
Lesotho	4	2	5	Lebanon	1	1	2
Togo	4	2	5	Tajikistan	1	1	2
Honduras	3	2	5	Switzerland	1	1	2
Finland	3	2	5	Mexico	1	1	2
Lao People's Dem Rep.	3	2	5	Bosnia and Herzegovina	1	1	2
Libyan Arab Jamahiriya	3	2	4	Slovenia	1	1	2
Central African Rep.	3	2	4	Dominican Rep.	1	1	2
Bosnia and Herzegovina	3	2	4	Viet Nam	1	1	2
Armenia	3	2	4	Indonesia	1	1	2
Kyrgyzstan	3	2	4	Gabon	1	1	2
Mauritania	3	2	4	Belize	1	1	2
Moldova	3	2	4	Slovakia	1	1	2
Jordan	2	2	3	Thailand	1	1	2
Congo	2	1	3	Kyrgyzstan	1	1	2
Jamaica	2	2	3	Madagascar	1	1	2
Costa Rica	2	1	3	Bangladesh	1	1	2
Lithuania	2	1	3	Tunisia	1	1	2
Nicaragua	2	1	3	Austria	1	1	2
Liberia	2	1	3	Lithuania	1	1	2
Slovenia	2	1	2	Russia	1	1	2
Paraguay	2	1	2	Sudan	1	1	2
Panama	2	1	2	Korea, Rep.	1	1	1
Guinea-Bissau	2	1	2	Libyan Arab Jamahiriya	1	1	1
Namibia	2	1	2	Syria	1	1	1
Albania	2	1	2	Moldova	1	1	1
Gambia	1	1	2	Ukraine	1	1	1
Botswana	1	1	2	Azerbaijan	1	1	1
Turkmenistan	1	1	2	Saudi Arabia	1	1	1
Latvia	1	1	2	Trinidad and Tobago	1	1	2
Oman	1	1	2	Honduras	1	1	1
Cyprus	1	1	1	Uzbekistan	1	1	1
Swaziland	1	1	1	Iran, Islamic Rep.	1	1	1
North Macedonia	1	1	1	Algeria	1	1	1
Gabon	1	1	1	Finland	1	1	1
Trinidad and Tobago	1	0	1	Equatorial Guinea	1	1	1
Djibouti	1	1	1	Albania	1	1	1
Estonia	1	0	1	Latvia	1	1	1
Kuwait	1	0	1	Costa Rica	1	1	1
Mongolia	1	0	1	Panama	1	1	1

COUNTRY	TOTAL	LOW	HIGH	COUNTRY	PER MILLION PEOPLE	LOW	HIGH
				Venezuela	1	1	1
				Maldives	1	1	1
				Estonia	1	1	1
				Ecuador	1	0	1
				Nigeria	1	0	1
				Nicaragua	1	1	1
				United Arab Emirates	1	1	1
				Belarus	1	0	1
				Jordan	1	0	1
				North Macedonia	1	0	1
				Brunei Darussalam	1	0	1
				Paraguay	1	0	1
				Oman	1	0	1
				Turkmenistan	1	0	1
				Colombia	1	0	1
				Mongolia	1	0	1

Table A2 Total and per person cardiovascular deaths per 10 Mt of methane for all countries with non-zero values

COUNTRY	TOTAL	LOW	HIGH	COUNTRY	PER MILLION PEOPLE	LOW	HIGH
China	1 566	502	2 522	Ukraine	7	2	11
India	1 122	297	1 844	Georgia	5	2	9
Russia	379	122	624	Uzbekistan	5	2	8
United States	333	108	540	Bulgaria	5	2	9
Pakistan	225	65	365	Egypt	5	2	8
Indonesia	219	57	368	Serbia and Montenegro	5	2	8
Egypt	194	64	310	Belarus	5	2	8
Ukraine	193	61	318	Lithuania	5	1	8
Japan	148	50	236	Latvia	4	1	7
Germany	133	42	218	Afghanistan	4	1	7
Brazil	95	29	159	Russia	4	1	7
Bangladesh	93	27	151	Romania	4	1	7
Italy	88	28	142	Armenia	4	1	6
United Kingdom	76	24	125	Azerbaijan	4	1	6
Iran, Islamic Rep.	76	25	120	Kyrgyzstan	4	1	6
Uzbekistan	70	23	112	Turkmenistan	4	1	6
Viet Nam	66	20	108	Bosnia and Herzegovina	4	1	6
Poland	65	21	108	Morocco and Western Sahara	4	1	6

COUNTRY	TOTAL	LOW	HIGH	COUNTRY	PER MILLION PEOPLE	LOW	HIGH
Mexico	63	20	103	Moldova	4	1	6
Morocco and Western Sahara	62	19	101	Croatia	4	1	6
Philippines	61	19	102	Kazakhstan	3	1	6
France	60	19	99	Yemen	3	1	5
Turkey	59	19	96	Pakistan	3	1	5
Spain	56	18	90	Hungary	3	1	5
Romania	53	17	87	Syria	3	1	5
Algeria	41	13	67	Albania	3	1	5
Afghanistan	40	13	63	North Macedonia	3	1	5
Sudan	39	11	65	Lebanon	3	1	5
Korea, Dem People's Rep.	34	11	54	Tajikistan	3	1	5
Kazakhstan	30	10	48	Slovakia	3	1	5
Belarus	29	9	48	Czechia	3	1	5
Serbia and Montenegro	29	9	48	Tunisia	3	1	5
Argentina	28	9	48	Greece	3	1	5
Canada	28	9	46	Malta	3	1	4
Thailand	28	8	46	Poland	3	1	4
Saudi Arabia	28	9	44	Haiti	3	1	4
Nigeria	27	7	46	Estonia	3	1	4
Ethiopia	27	8	44	Sudan	3	1	4
Bulgaria	26	8	43	Lesotho	2	1	4
Korea, Rep.	26	9	41	Korea, Dem People's Rep.	2	1	4
Yemen	25	8	41	Mongolia	2	1	4
South Africa	23	7	38	Cuba	2	1	4
Myanmar	22	7	36	Germany	2	1	4
Greece	22	7	35	Algeria	2	1	4
Hungary	22	7	35	Dominican Rep.	2	1	4
Iraq	21	7	33	Jamaica	2	1	4
Syria	21	7	33	Libyan Arab Jamahiriya	2	1	4
Czechia	21	7	34	Portugal	2	1	4
DRC	19	6	32	Italy	2	1	3
Azerbaijan	19	6	31	Eritrea	2	1	3
Nepal	19	6	30	Bahamas	2	1	3
Sri Lanka	18	5	30	Iran, Islamic Rep.	2	1	3
Cuba	17	5	28	Austria	2	1	3
Venezuela	17	5	28	India	2	1	3
Tunisia	17	5	27	Sweden	2	1	3
Netherlands	16	5	27	Finland	2	1	3

COUNTRY	TOTAL	LOW	HIGH	COUNTRY	PER MILLION PEOPLE	LOW	HIGH
Portugal	16	5	26	Grenada	2	1	3
Australia	15	5	25	China	2	1	3
Malaysia	15	4	25	St. Vincent and the Grenadines	2	1	3
Belgium	14	4	22	Belgium	2	1	3
Georgia	13	4	21	Guinea-Bissau	2	0	3
Tanzania	12	4	21	United Kingdom	2	1	3
Sweden	12	4	20	Indonesia	2	0	3
Mozambique	12	4	19	Iraq	2	1	3
Austria	11	4	19	Trinidad and Tobago	2	0	3
Kenya	11	3	18	Saudi Arabia	2	1	3
Dominican Rep.	10	3	17	United States	2	1	3
Slovakia	10	3	17	Barbados	2	1	3
Haiti	10	3	17	Slovenia	2	1	3
Croatia	10	3	16	Spain	2	1	3
Colombia	10	3	17	St. Lucia	2	1	3
Ghana	10	2	17	Cyprus	2	1	3
Chile	10	3	16	Nepal	2	1	3
Kyrgyzstan	9	3	15	Somalia	2	1	3
Moldova	9	3	15	Israel	2	1	3
Lithuania	9	3	15	Japan	2	1	3
Tajikistan	9	3	14	Sri Lanka	2	0	3
Turkmenistan	9	3	14	Gambia	2	0	3
Bosnia and Herzegovina	9	3	15	Djibouti	2	0	3
Lebanon	8	3	13	Cape Verde	2	0	3
Switzerland	8	3	13	Turkey	2	0	2
Peru	8	2	13	Timor-Leste	1	0	3
Côte d'Ivoire	7	2	12	Denmark	1	0	2
Finland	7	2	11	Netherlands	1	0	2
Israel	7	2	11	Philippines	1	0	2
Angola	6	2	11	Mozambique	1	0	2
Armenia	6	2	10	Switzerland	1	0	2
Uganda	6	1	11	Luxembourg	1	0	2
Somalia	6	2	10	France	1	0	2
Libyan Arab Jamahiriya	6	2	10	Norway	1	0	2
Cambodia	6	2	10	Central African Rep.	1	0	2
Zimbabwe	6	2	10	Oman	1	0	2
Latvia	6	2	10	Viet Nam	1	0	2
Senegal	6	1	10	Bangladesh	1	0	2

COUNTRY	TOTAL	LOW	HIGH	COUNTRY	PER MILLION PEOPLE	LOW	HIGH
Denmark	5	2	9	Jordan	1	0	2
Albania	5	2	9	Lao People's Dem Rep.	1	0	2
Niger	5	1	9	Iceland	1	0	2
Madagascar	5	1	9	Swaziland	1	0	2
Cameroon	5	1	8	Ireland	1	0	2
Guinea	5	1	8	Puerto Rico and the Virgin Islands	1	0	2
United Arab Emirates	5	1	8	Uruguay	1	0	2
Norway	5	1	8	Antigua and Barbuda	1	0	2
Mali	5	1	8	Guinea	1	0	2
Jordan	5	1	7	Senegal	1	0	2
Burkina Faso	5	1	8	Zimbabwe	1	0	2
Chad	4	1	7	Argentina	1	0	2
Honduras	4	1	7	Chad	1	0	2
Malawi	4	1	7	Honduras	1	0	2
Guatemala	4	1	7	El Salvador	1	0	2
North Macedonia	4	1	6	Canada	1	0	2
Ireland	4	1	6	Venezuela	1	0	2
Zambia	4	1	6	Mauritania	1	0	2
Bolivia	3	1	6	Mexico	1	0	2
Ecuador	3	1	6	São Tome and Principe	1	0	2
El Salvador	3	1	6	Ghana	1	0	2
Lao People's Dem Rep.	3	1	5	Malaysia	1	0	2
Jamaica	3	1	5	Bhutan	1	0	2
Mongolia	3	1	5	Niger	1	0	2
Eritrea	3	1	5	Australia	1	0	2
Puerto Rico and the Virgin Islands	3	1	5	Sierra Leone	1	0	2
Benin	3	1	5	Namibia	1	0	2
Singapore	3	1	5	Mali	1	0	2
Oman	3	1	4	Comoros	1	0	2
Burundi	3	1	4	Côte d'Ivoire	1	0	2
Uruguay	3	1	4	South Africa	1	0	2
Slovenia	2	1	4	Chile	1	0	2
Estonia	2	1	4	Cambodia	1	0	2
Sierra Leone	2	1	4	Burundi	1	0	2
Togo	2	0	4	Burkina Faso	1	0	2
Nicaragua	2	1	3	DRC	1	0	2
Costa Rica	2	1	3	Ethiopia	1	0	2

COUNTRY	TOTAL	LOW	HIGH	COUNTRY	PER MILLION PEOPLE	LOW	HIGH
Central African Rep.	2	1	3	Liberia	1	0	2
Rwanda	2	0	3	Myanmar	1	0	1
Paraguay	2	0	3	Togo	1	0	2
Lesotho	2	1	3	Malawi	1	0	1
Mauritania	2	0	3	Benin	1	0	2
Panama	1	0	2	Brazil	1	0	1
Congo	1	0	2	Angola	1	0	1
Trinidad and Tobago	1	0	2	Congo	1	0	1
Kuwait	1	0	2	Botswana	1	0	1
Liberia	1	0	2	Zambia	1	0	1
Cyprus	1	0	2	United Arab Emirates	1	0	1
Guinea-Bissau	1	0	2	Tanzania	1	0	1
Gambia	1	0	1	Bolivia	1	0	1
Namibia	1	0	1	Nicaragua	1	0	1
Botswana	1	0	1	Singapore	1	0	1
Malta	1	0	1	Kenya	1	0	1
				Korea, Rep.	1	0	1
				Costa Rica	1	0	1
				Belize	1	0	1
				Cameroon	1	0	1
				Maldives	1	0	1
				Panama	1	0	1
				Guatemala	1	0	1
				Gabon	1	0	1
				Madagascar	1	0	1
				Paraguay	1	0	1
				Thailand	1	0	1
				Uganda	1	0	1
				Bahrain	1	0	1
				Kuwait	1	0	1
				Peru	1	0	1
				Nigeria	1	0	1
				Rwanda	1	0	1

Table A3 Total and per person respiratory + cardiovascular deaths per 10 Mt of methane for all countries with non-zero values

COUNTRY	TOTAL	LOW	HIGH	COUNTRY	PER MILLION PEOPLE	LOW	HIGH
India	3 167	472	5 567	Ukraine	8	2	13
China	2 984	729	5 003	Lesotho	8	2	13
United States	761	189	1 284	Egypt	7	2	12
Russian	488	117	839	Georgia	7	2	12
Japan	399	108	659	Korea, Dem People's Rep.	7	2	11
Pakistan	384	74	659	Afghanistan	7	2	11
Indonesia	373	52	671	Bulgaria	7	2	12
Egypt	276	72	457	Serbia and Montenegro	6	2	11
Brazil	255	54	447	Uzbekistan	6	2	10
Germany	254	60	436	Eritrea	6	1	11
United Kingdom	233	55	400	Lithuania	6	1	10
Ukraine	226	51	390	Armenia	6	2	10
Bangladesh	176	34	300	United Kingdom	6	1	10
Philippines	162	35	285	Pakistan	6	1	10
Italy	162	39	273	Belarus	6	1	10
Spain	145	35	245	Romania	6	1	10
Mexico	140	33	237	India	5	1	10
France	130	29	223	Portugal	5	1	9
Viet Nam	127	27	219	Russia	5	1	9
Turkey	121	31	203	Latvia	5	1	9
Iran, Islamic Rep.	114	31	186	Morocco and Western Sahara	5	1	9
Poland	103	23	178	Bosnia and Herzegovina	5	1	9
Korea, Dem People's Rep.	97	27	160	Haiti	5	1	9
Myanmar	94	20	163	Kyrgyzstan	5	1	8
Argentina	92	20	161	Kazakhstan	5	1	9
Morocco and Western Sahara	85	19	145	Greece	5	1	8
Ethiopia	84	16	149	Guinea-Bissau	5	0	9
Uzbekistan	83	22	138	Azerbaijan	5	1	8
Thailand	80	14	141	Croatia	5	1	8
South Africa	75	18	127	Belgium	5	1	9
Romania	73	17	125	Moldova	5	1	8
Nigeria	69	8	128	Yemen	5	1	8
Korea, Rep.	65	17	107	Cuba	5	1	9
Canada	64	16	108	Hungary	5	1	8
Afghanistan	62	17	102	Malta	5	1	8
Algeria	58	14	99	Somalia	5	1	8
Sudan	57	10	102	Denmark	5	1	8

COUNTRY	TOTAL	LOW	HIGH	COUNTRY	PER MILLION PEOPLE	LOW	HIGH
DRC	54	10	94	Nepal	5	1	8
Nepal	50	11	84	Czechia	4	1	8
Netherlands	45	10	79	Germany	4	1	8
Sri Lanka	45	6	82	Spain	4	1	8
Saudi Arabia	44	11	74	Turkmenistan	4	1	7
Kazakhstan	44	11	75	Zimbabwe	4	1	8
Malaysia	40	6	72	Lebanon	4	1	7
Portugal	39	9	67	Tajikistan	4	1	7
Greece	39	9	66	Japan	4	1	7
Serbia and Montenegro	39	9	66	Syria	4	1	7
Tanzania	38	7	67	São Tome and Principe	4	1	7
Yemen	37	9	64	Grenada	4	1	7
Kenya	36	6	66	Slovakia	4	1	7
Belgium	36	8	63	Gambia	4	0	8
Cuba	36	7	63	Netherlands	4	1	7
Australia	36	8	63	Argentina	4	1	7
Peru	34	5	62	Swaziland	4	1	7
Belarus	34	8	59	Sri Lanka	4	1	7
Bulgaria	34	8	58	Poland	4	1	7
Czechia	32	7	56	Albania	4	1	7
Hungary	32	7	55	Tunisia	4	1	7
Venezuela	30	6	53	Barbados	4	1	7
Mozambique	29	7	51	Philippines	4	1	7
Syria	28	7	47	United States	4	1	7
Ghana	28	2	52	Djibouti	4	1	7
Iraq	26	7	43	Jamaica	4	1	7
Chile	26	6	44	Myanmar	4	1	7
Azerbaijan	24	6	41	Chad	4	1	7
Tunisia	24	5	40	St. Lucia	4	1	7
Sweden	24	6	41	Sweden	4	1	7
Colombia	24	4	43	Italy	4	1	6
Haiti	20	4	35	Mozambique	4	1	7
Zimbabwe	20	5	34	Central African Rep.	4	1	7
Uganda	19	2	36	Guinea	4	1	7
Austria	18	5	31	Israel	4	1	6
Côte d'Ivoire	18	3	33	Senegal	4	0	7
Angola	18	4	31	North Macedonia	4	1	6
Cameroon	18	3	31	Bahamas	4	1	6
Georgia	17	5	29	Sudan	4	1	7
Niger	17	2	32	Cape Verde	4	1	6
Somalia	17	3	30	Norway	4	1	6
Denmark	17	4	29	Dominican Rep.	4	1	6
Dominican Rep.	16	3	29	Uruguay	4	1	6

COUNTRY	TOTAL	LOW	HIGH	COUNTRY	PER MILLION PEOPLE	LOW	HIGH
Senegal	16	2	30	China	4	1	6
Switzerland	16	4	27	St. Vincent and the Grenadines	3	1	6
Cambodia	16	3	27	Estonia	3	1	6
Israel	15	3	26	Niger	3	0	6
Slovakia	15	3	26	Ireland	3	1	6
Madagascar	14	0	0	Puerto Rico and the Virgin Islands	3	1	6
Croatia	14	3	24	Libyan Arab Jamahiriya	3	1	6
Guinea	14	2	25	Cyprus	3	1	5
Chad	13	2	24	Algeria	3	1	6
Tajikistan	13	4	22	Mauritania	3	1	6
Burkina Faso	13	1	25	Luxembourg	3	1	6
Malawi	13	3	22	Timor-Leste	3	1	6
Guatemala	12	3	21	South Africa	3	1	5
Mali	12	1	23	Austria	3	1	5
Kyrgyzstan	12	3	20	France	3	1	5
Lebanon	12	3	20	Namibia	3	1	5
Moldova	12	3	21	Turkey	3	1	5
Bosnia and Herzegovina	12	3	20	Indonesia	3	0	6
Norway	12	3	20	Slovenia	3	1	5
Lithuania	11	3	20	El Salvador	3	1	5
Zambia	11	2	19	Ghana	3	0	6
Bolivia	11	3	18	Burundi	3	0	5
Turkmenistan	10	3	17	Iran, Islamic Rep.	3	1	5
Finland	10	2	18	Malaysia	3	0	5
Ecuador	10	2	18	Ethiopia	3	1	5
Ireland	10	2	16	Iceland	3	1	5
Armenia	9	3	16	Mongolia	3	1	5
Libyan Arab Jamahiriya	9	2	16	Trinidad and Tobago	3	0	5
United Arab Emirates	9	2	15	Saudi Arabia	3	1	5
Benin	9	1	17	Benin	3	0	5
Eritrea	9	2	16	Comoros	3	1	5
El Salvador	8	2	14	Finland	3	1	5
Burundi	8	1	15	Switzerland	3	1	5
Singapore	8	1	14	Lao People's Dem Rep.	3	1	5
Honduras	8	2	13	Malawi	3	1	5
Puerto Rico and the Virgin Islands	7	2	12	Canada	3	1	5
Rwanda	7	1	13	Antigua and Barbuda	3	1	5
Jordan	7	2	12	Sierra Leone	3	0	5
Latvia	7	2	12	Bhutan	3	1	4
Albania	7	2	12	Mali	3	0	5

COUNTRY	TOTAL	LOW	HIGH	COUNTRY	PER MILLION PEOPLE	LOW	HIGH
Uruguay	7	1	12	Viet Nam	3	1	5
Lao People's Dem Rep.	7	1	11	Côte d'Ivoire	3	0	5
Sierra Leone	6	1	10	Burkina Faso	3	0	5
Togo	6	0	11	Cameroon	3	0	5
Jamaica	5	1	9	Chile	3	1	4
Lesotho	5	1	9	Bangladesh	3	0	4
Central African Rep.	5	1	8	Kenya	3	0	5
North Macedonia	5	1	8	DRC	3	0	4
Slovenia	4	1	7	Cambodia	3	1	4
Mauritania	4	1	8	Zambia	3	1	4
Costa Rica	4	1	7	Tanzania	3	0	4
Nicaragua	4	1	7	Bolivia	2	1	4
Oman	4	1	7	Australia	2	1	4
Congo	4	1	7	Botswana	2	1	4
Mongolia	4	1	6	Togo	2	0	5
Paraguay	4	1	6	Angola	2	1	4
Liberia	3	1	5	Mexico	2	1	4
Panama	3	1	6	Congo	2	0	4
Estonia	3	1	5	Peru	2	0	4
Guinea-Bissau	3	0	5	Brazil	2	1	4
Namibia	2	1	4	Honduras	2	0	4
Gambia	2	0	4	Liberia	2	0	4
Trinidad and Tobago	2	0	4	Iraq	2	1	4
Cyprus	2	1	4	Guatemala	2	0	4
Kuwait	2	0	4	Singapore	2	0	4
Botswana	2	1	4	Jordan	2	1	4
Swaziland	2	0	3	Venezuela	2	0	4
Gabon	1	0	3	Uganda	2	0	4
Djibouti	1	0	2	Belize	2	0	4
Malta	1	0	2	Oman	2	0	3
Luxembourg	1	0	2	Rwanda	2	0	4
Timor-Leste	1	0	2	Gabon	2	0	4
Bhutan	1	0	1	Korea, Rep.	2	1	3
Qatar	1	0	1	Madagascar	2	0	0
Bahamas	1	0	1	Thailand	2	0	3
Bahrain	1	0	1	Costa Rica	2	0	3
Cape Verde	1	0	1	Panama	2	0	3
Barbados	1	0	1	Maldives	2	0	3
Comoros	1	0	1	United Arab Emirates	2	0	3
Iceland	1	0	1	Nicaragua	2	0	3
Mauritius	1	0	0	Ecuador	1	0	2
Equatorial Guinea	1	0	1	Equatorial Guinea	1	0	2
				Paraguay	1	0	2

Table A4 Methane measurement techniques, the methods used by each technique and the advantages and disadvantages of each method

Source: Methane Emission Measurement and Monitoring Methods, National Academies of Sciences, Engineering, and Medicine (2018)

TECHNIQUE	METHOD	ADVANTAGES	DISADVANTAGES
Ground-based measurements	Measurement of emissions from fixed points based on flow rate and methane composition.	Measures total methane emissions from individual point sources (e.g., stacks, animals).	Limited number of methane sources are emitted as point sources.
		Captures temporal trends if deployed for extended time periods.	Labour intensive to quantify spatial and temporal variability (requires a large number of individual measurements to capture variability).
			Often limited to measurements from normaloperations or where there are no safety concerns.
External tracer	Release of tracer gas (C2H2, N2O) at known rate from source area.	Measures total methane emissions from source area.	Difficult to isolate individual sources within source area depending on layout and meteorological conditions.
	Measurement of methane and tracer concentrations across well-mixed downwind plumes to derive emission rate.	Measures complex sources or quantifies the uncertainty in the emission estimate (multiple tracers).	Appropriate meteorological conditions are necessary for technique to work properly.
			Vulnerable to bias if the locations of tracer release differ significantly from the location of methane release.
			Labour intensive to measure the spatial and temporal variability of emissions over many sources.
			Difficult to isolate various sources within the source area depending on source layout and meteorological conditions.
Facility-scale in situ aircraft measurements	Multiple vertical measurements of atmospheric methane and wind-speed gradients above a source area to derive an emission rate.	Remotely measures total methane emissions from a source area/ facility regardless of the operational status or safety conditions at the facility.	Generally, cannot isolate individual sources within source area unless useful source-specific tracers can be co-quantified.
		Captures temporal trends with repeated overflights.	Appropriate meteorological conditions (sufficient vertical mixing of surface emissions at flyover elevations, typically midday conditions) are necessary.
			Requires multiple flights to capture temporal trends in emissions.
			Generally limited to higher-emitting sources (lower detection limits are much higher than point-source techniques).
			Labour intensive to measure the spatial and temporal variability of emissions over many sources.

Towers	Methane by infrared spectrometry at precise infrared wavelengths.	High precision.	Sparse spatial coverage, potential small-sensitivity footprint.
	Time-series measurements of concentrations, analyzed by eddy covariance or by inverse modeling.	Consistent measurements across multiple sites.	Methods are not fully developed.
		Long time series.	Challenging to apply to individual facilities and distinguish confounding sources.
Aircraft mass balance measurements	Measurements upwind and downwind of source region.	Ability to target specific emission source regions and obtain vertical profiles of methane concentrations.	Limited spatial coverage; temporal coverage limited to a snapshot.
	High time-resolution instruments.	Analyzed using simple flow-through models and/or sophisticated inversion modelling.	Challenging to account for transient plumes through the box.
	Infrared spectrometry at precise infrared wavelengths.		Labour intensive to measure the spatial and temporal variability of emissions.
Aircraft remote-sensing measurements	Absorption spectroscopy using reflected sunlight or thermal emissions.	Ability to map methane plumes at the 1–5 m scale, direct source attribution.	Limited spatial and temporal coverage.
			Not as accurate as in situ data.
Satellites – global coverage	Absorption spectroscopy using reflected sunlight (sensitive to entire atmospheric column) or thermal emissions (less sensitive to boundary layer).	Global, complete spatial coverage, frequent revisit time with a single instrument (e.g., TROPOMI, GOSAT).	Coarse spatial resolution with current instruments (~10 km).
			Not as accurate as in situ data, emissions not cleanly resolved.
			Limited to sunlit, cloud-free, snow-free scenes.
Satellites – targeted monitoring	Absorption spectroscopy using reflected sunlight (sensitive to entire atmospheric column) or thermal emissions (less sensitive to boundary layer).	Relatively high resolution (~50 m x 50 m) (e.g., GHGsat).	Limited spatial coverage (targeted facilities or locations).